The neurophysiology of sedation

Róisín Judith Ní Mhuircheartaigh

A thesis submitted in partial fulfillment of the requirements for the degree of Doctor of Philosophy at the University of Oxford

Green-Templeton College and the Centre for Functional MRI of the Brain
University of Oxford
Michaelmas Term 2011

Supervisor: Professor Irene Tracey

List of acronyms

ACh	Acetylcholine
AD	Alzheimer's disease
AE	Approximate entropy
AEP	Auditory evoked potential
AEP	Auditory evoked potentials
ARAS	Ascending reticular activating system
ASA	American Society of Anesthesiologists
BET	Brain extraction tool
BIS	Bispectral index
BOLD	Blood Oxygen Level Dependent
CBA	Cardioballistographic artifact
CBF	Cerebral blood flow
CBV	Cerebral blood volume
CNS	Central nervous system
COPE	Contrast of parameter estimates
CPEI	Composite PE index
CRS-R	Coma Recovery Scale-revised
CT	Computed tomography
DMN	Default node network
DOC	Disorders of consciousness
DRN	Dorsal raphe nucleus
ECG	Electrocardiogram
EEG	Electroencephalograph
EMG	Electromyograph
EPI	Echo planar imaging
EPSP	Excitatory post-synaptic potential
ERP	Event related potentials
ESC	Effect site concentration
FDG	Flurodeoxyglucose
FEAT	FMRI Expert Analysis Tool
FILM	FMRIB's Improved Linear Model
FLIRT	FMRIB's linear registration tool
FSL	FMRIB Software Library
FWHM	Full width half maximum
GABA	Gamma-amino-butyric-acid
GFP	Global field power
GLM	Generalized Linear Model
GP	Globus pallidus
HEOG	Horizontal eye movements
HFS	High frequency spindles
HRF	Haemodynamic response function
ICA	Independent component analysis
ICU	Intensive Care Unit
ILN	Substantia nigra
IPSP	Inhibitory post synaptic potential
LC	Locus coeruleus
LDT	Laterodorsal tegmental (nucleus)
LEP	Laser evoked potentials
LFS	Low frequency spindles

LIS	Locked-in syndrome
LMA	Laryngeal mask airway
LOBR	Loss of behavioural responsiveness
LTS	Low threshold spike
MAC	Minimum alveolar concentration
MCI	Mild cognitive impairment
MCS	Minimally conscious state
MMN	Persistent mismatch negativity
mPRF	Medial pontine reticular formation
MPTA	Mesopontine tegmental area
MRC	Medical Research Council?
MRI	Magnetic Resonance Imaging
NMDA	N-methyl-D-aspartate
NREM	Non rapid eye movement (sleep)
NRS	Numerical rating scale
OEF	Oxygen extraction factor
PCC	Posterior cingulate cortex
PE	Permutation entropy
pEEG	Processed EEG
PET	Positron emission tomography
PPN	Pedunculopontine (nucleus)
PrCC	Precuneus cortex
PTSD	Post-traumatic stress disorder
rCBF	Regional cerebral blood flow
rCBV	Regional cerebral blood volume
rCMRO	Regional cerebral metabolic rate
RE	Reticular nucleus of the thalamus
REM	Rapid eye movement
ROBR	Recovery of behavioural responsiveness
ROI	Region of interest
RSN	Resting-state networks
RSS	Ramsay sedation scale
S2	Secondary somatosensory cortex
SNc	Substantia nigra pars compacta
SNr	Substantia nigra pars reticulata
STN	Subthalamic nucleus
SWA	Slow wave activity
SWS	Slow wave sleep
TC	Thalamocortical
TCI	Target controlled infusion
TE	Echo time
TMN	Tubomamillary nucleus
TPJ	Temporo-parietal junction
TR	Repetition time
tROI	Temporal regions of interest
USB	Universal serial bus
VAS	Visual analogue rating scale
VBM	Voxel based morphometry
VEOG	Vertical eye movements
VLPO	Ventro-lateral preoptic nucleus
VS	Vegetative state

Table of Contents

Chapter 1: Background

Thesis Motivation

The objective of this thesis is to explore the pharmacological manipulations of consciousness, which occur every day in every hospital in the world, in an attempt to better understand the relationship between neurophysiological changes in the brain related to perception and what can be measured non-invasively during care.

1.1 Introduction

To mark the new millennium, an editorial in the New England Journal of Medicine considered the greatest achievements in medicine over the preceding thousand years [1]. Alongside the slow progressive journeys of broad disciplines including the elucidation of human physiology and biochemistry, the discovery of cells and x-rays and the application of statistics to health, stood a very specific, almost niche practice that had existed for less than 200 years and had been highly dangerous for almost a further hundred: anaesthesia. Yet by the turn of the millennium, this humanitarian transformation of care and the provision of safe hypnosis and analgesia, freeing patients from the horror of surgery, had become so ubiquitous as to be almost taken for granted. Its inclusion in the list was never in question.

Astonishingly, in spite of this, anaesthesia is still neither adequately defined nor understood and remains one of the few reverse-engineered practices in modern medicine. As a result, consciousness is the only systemic physiological process that anaesthetists actively manipulate without being able to measure. Circulation is manipulated according to monitors of blood pressure and perfusion, respiration is manipulated according to monitors of oxygenation and ventilation, while consciousness is manipulated on the basis of probability. To better inform ourselves about the state of the brain we look at the heart. There is no doubt that we can do better. There is no acceptable incidence of awareness for patients rendered vulnerable and incapable of communicating their distress, yet it does happen regularly in all operating theatres and intensive care units, not out of malice or negligence but because of the constraints imposed by ignorance. The desired state still cannot be reliably identified.

To place this work in context; a brief history of the brain and consciousness in medicine is first presented followed by a focused discussion of the architecture of the brain and the way its structure contributes to its function both in waking and in the other state, where it remains for almost one third of its existence, sleep. Current theories of consciousness are discussed before considering the clinical implications of deficits in current models. The evidence behind current hypotheses of mechanisms of actions of sedative anaesthetics is also reviewed.

1.1.1 The ancients' brains

The earliest written reference to the brain appeared almost 3,000 years ago in the Edwin Smith surgical papyrus, which describes the management and prognosis of cranial and spinal injuries [2]. At that time the brain was discarded during the mummification procedure and it was the heart in which the personality or intelligence was believed to reside. However, on some level an appreciation of the importance of the cranium, if not its contents, was emerging. In a fable from the 22nd century B.C., in which the parts of the body vie for superiority, the head claims "I am the basic foundation of the entire house….the ruler, because I am the one who gives life" [3].

The ancient Greeks regarded the mind and the soul as one and the same. Plato believed in the hierarchical co-existence of a soul for growth, shared with animals and plants, a soul for pain, pleasure and desire, shared with animals, and a soul for reason, unique to humanity. Aristotle shared this view but, in what could be regarded as an early attempt at physicalism, held that the soul perished with the body.

Descartes (1596-1650) argued that the mind and the body were fundamentally different and separate entities. Cartesian dualism is based on the assumption that subjective human experiences such as sensing colour, feeling pain, happiness, grief, pleasure, (i.e. qualia) cannot be reduced to component processes and therefore cannot have a physical basis. He maintained that there must be a non-physical entity, the mind, in which such qualia reside. Cartesian dualism does not adequately address the undeniable causal relationship between the physical and the mind. Descartes himself suggested that the interaction between his *res extensa*, or content of experience, and *res cogitans*, the associated or elicited thoughts, occurred in the pineal gland. While the pineal gland clearly plays no such role, he obviously recognised the need for "integration" in fashioning conscious experience from physical events [4].

A common, although often controversial, thread through the neuroscience of recent centuries has been the idea that rather than being a gift bestowed by a mysterious omnipotent being, consciousness, like life itself, may be dependent upon and be an emergent property of a definable physical process or processes. Both philosophy and neuroscience have moved inexorably towards a construct whereby separate facets of an event must be somehow comprehensively integrated into a whole for that experience to enter the realm of consciousness.

William James (1842-1910) furthered the concept of information integration being the key to conscious experience in the way he related emotion to physiology. He proposed that Cartesian qualia such as "fear" were the result of the combined experience of a physical stimulus (e.g. a sight or sound such as a gunshot), the associated threat based on memory or learning, the physical response to that threat (e.g. running away), and the physiological response to these (e.g. sympathetic nervous system activation and adrenaline release). This allows for the generation of conscious subjective experience from a combination of purely physical processes, without the need for any separate higher process or soul. James regarded consciousness not as a thing but as a process; "of which we know, as long as no-one asks us to define it" [5].

Thus with the declining influence of theological dogma in science, we have begun to describe how the brain might internally represent the surrounding environment as it is perceived. James, constrained by the limitations of the neuroscience of his day, spoke of consciousness as a function of the whole brain. We now know that specific parts of the brain, such as the thalamocortical and the mesencephalic reticular systems, are critical for consciousness while others are not. Current theories of consciousness have built on the foundations of James' principles, adding a neuroscientific perspective, rejecting the undefinable and adhering firmly instead to established biology and physics.

1.1.2 The cerebral cortex

The mammalian neocortex is perhaps the most complex structure in nature. It is extremely thin (3-4 mm) and while smooth in rodents and smaller mammals, is thrown into deep convolutions in the brains of higher mammals, allowing accommodation of the enormous surface area (approximately 2.6 m^2) within the constraints of the cranial vault. Broadly speaking there are two classes of cells, neurons and glia, present in equal numbers within the central nervous system (CNS). Glia fulfill a wide range of roles within the CNS including maintenance of the electrically insulating myelin sheath, production of cerebrospinal fluid, immunological protection and modulation of the neurochemical milieu. Neurons are electrically excitable cells that transmit signals through the rapid transmembrane flux of ions and molecules.

While cortical neurons may be classified in a number of ways, based for example on function, morphology, location or connections, a broad functional division exists between γ amino-butyric acid (GABA)-ergic interneurons and glutamatergic projection neurons. Interneurons make short-range connections locally within the neocortex whereas projection pyramidal neurons make long range connections with distant regions of the neocortex and subcortex [6]. In the early 20th century, the newly developed Golgi silver nitrate staining technique revealed the organisation of neural tissue within the brain and permitted the first steps to be taken towards understanding the relationship between structure and function in the brain [7,8].

Following the initial migration of primitive neurons in the developing forebrain, cellular differentiation leads to the emergence of a laminar arrangement of cells within the neocortex. Layers show commonalities of efferent and afferent connections. This six-layered arrangement is largely preserved across the neocortex and across species.

The development of glutamatergic pyramidal projection neurons and their synaptic connections precedes that of interneurons. In the embryonic central nervous system, developing neurons migrate along radial glial fibres with each of the laminae of the eventual cortical plate appearing in temporal sequence from deep (layer VI) to superficial (ayer II). Afferent, intrinsic and effernt patterns of connection are consistent within and specific to individual laminae [9].

Layer I contains the distal apical dendrites of pyramidal cells, axon terminations and a small number of inhibitory interneurons. This area receives feedback inputs from other cortical areas and direct inputs from

subcortical nuclei [6]. Associative and callosal neurons are found in layers II and III and project to other neocortical areas within the hemisphere (associative projection neurons) or the contralateral hemisphere (commissural or callosal projection neurons). Layer IV neurons receive sensory inputs from the thalamus. The motor cortex is therefore different to other neocortical areas in that there is no layer IV. Connections from one cortical area to another are regarded as ascending if they terminate in layer 4 and descending if they terminate in a layer other than layer 4. Neurons in layers V and VI are corticofugal with those in layer V projecting to subcerebral structures including the brainstem and spinal cord and those in layer VI projecting to the thalamus. The layered neocortex is also arranged into vertically interconnected minicolumns by virtue of the radial path of neuronal migration. This has been best described in the visual cortex but is also found in other neocortical areas. The final horizontal position of each neuron depends on its initial point of origin. Each mature minicolumn contains between 100 and 3,000 neurons that are then combined into functional columns or modules by horizontal synaptic connections. The surface area of the neocortex is determined by the number and not the size of columns [10]. In Chapter 3, pathways of activation involving different cortical layers are discussed, with particular reference to the role of this multi-layer arrangement, in which co-activation and corticothalamic feedback are the basis for co-ordinated activity within the brain's circuitry.

GABA-ergic inhibitory interneurons are fewer in number (approximately 20% of cortical neurons) but display enormous structural, functional and anatomical diversity [11]. Inhibition exerts essential control on the firing of pyramidal cells. Unimpeded feed-forward excitation would lead to instability, spreading excitation and error propagation. Feedback and feed forward inhibition narrow the temporal window for excitation and introduce functional complexity to a system which, if purely excitatory, would lead to the same deterministic outcome for every input. $GABA_A$ receptors are found at synapses, peri-synaptically and extra-synaptically. Synaptic and peri-synaptic $GABA_A$ receptors respond to transient high concentrations of GABA, producing an inhibitory post-synaptic potential and phasic (transient) inhibition of the target neuron. Extrasynaptic $GABA_A$ receptors on the other hand, have a high affinity for GABA and are activated by very low extracellular concentrations. This modulates the strength of a tonic current, causing the neuronal cell membrane to tend towards hyperpolarisation and reducing the probability of an excitatory post-synaptic potential (EPSP) leading to an action potential [12]. The resting membrane potential of interneurons is slightly less negative, and the threshold for firing lower, than that of pyramidal cells.

Cortical lamination and the columnar arrangement therefore constrain the ways in which neurons can influence one another, providing the architectural hardware underpinning neocortical function and subcortical-neocortical interactions. While pyramidal cells determine the spatial distribution of signals, interneurons govern signal processing in the temporal domain. Inhibitory interneurons modulate the context in which EPSPs occur, changing the probability that an afferent signal will lead to downstream transmission.

Microprocessors depend upon a clock, cycling slower than the longest propagation delay, to synchronise circuits. In the brain, it appears likely that balanced excitatory and inhibitory signals lead to a system of oscillators, temporal windows of activity that define the clock of internal brain dynamics. Systems oscillating slowly can involve large numbers of synchronised neurons while rapidly oscillating systems allow short-range local synchronisation. A group of neurons oscillating synchronously may form a more sophisticated collective than neurons firing in series. If signal processing within a network of nodes is bound into temporal windows, coincidence detection is possible, allowing the construction of a single percept [13]. In this thesis, oscillatory systems in the idling human brain, during cognition and during pharmacological manipulations of consciousness are explored using a range of noninvasive tools.

1.1.3 Theories of Consciousness

A satisfactory theory of consciousness would describe comprehensively how ion flux across plasma membranes, action potentials, synaptic transmission and subsequent activation or deactivation of a distributed array of neurons can form a subjective experience, an awareness of self or the environment, or an introspective rumination. Such a theory must explain how the same stimulus, eliciting the same basic series of action potentials may produce a different percept when input in a different context. While it has been said that "if the brain were simple enough for us to understand, we would be too simple to understand it"[13], neuroscience has advanced to a point where empirical theories of consciousness can be proposed based on the study of cell biology, sleep, traumatic brain injuries, psychiatric diseases and anaesthesia in humans as well as animals.

Current models of network activity within the central nervous system architecture are based on the airport hub-like "small world" construct, where activity in one node of a network may be modulated by activity in another node of another network with which the initial network can communicate, in spite of the two nodes in question not being in direct contact. Small world networks are dynamically coupled systems involving large numbers of clustered nodes. This is a highly efficient arrangement for rapid communication. Random graph theory shows that such networks result in the shortest path lengths between nodes, which is essential given spatial and metabolic limitations. Computational models based on this theory show that such networks can be highly synchronised [14].

Clustering in the cerebral cortex is extensive and most cortical connections are local. This allows for detailed topographic representation within clusters while at the same time, long-range connections to other cortical regions allow distributed activity to be synchronised across multiple clusters. Thus neuronal ensembles subserving specific tasks such as encoding of a colour or a face can process a specific fragment or aspect of a percept with conscious perception resulting from the integration of these fragments into a whole. Coherent activity in the gamma (> 30 Hz) frequency range has been postulated to underlie conscious awareness by binding neural activity across different parts of the brain. Phase-locked fast oscillations, with zero delay between distant cortical regions, have been described in the visual and auditory systems and are more prominent with selective attention [15]. The theory of "cognitive binding", integration of distributed information through temporally coherent oscillations, is often explored through the study of scenarios such as sleep and impaired consciousness, where the process of integration fails, described as "cognitive *un*binding"[16].

1.1.4 Sleep

The healthy brain can render itself unconscious, and does so every day. If it does not, it is damaged and its function impaired [17,18]. The relationship between natural sleep and pathological or pharmacological conditions resembling sleep is not straightforward. Culturally, sleep has positive connotations implying safety, comfort and recovery. Perhaps for this reason anaesthesia, coma and even death are often presented using sleep as a euphemism. However, these states are not the same as sleep. Describing the unknown (death) in terms of the commonplace (sleep) merely provides a familiar frame of reference. Those hearing an anaesthetist's reassurance that they are going "off to sleep now" do not really believe it but recognise and expect that their experience, whatever the mechanism, will be identical to their experience of sleep and that they will wake safely afterwards without any recall of what transpired. Nevertheless, this physiological "natural" unconsciousness does provide the opportunity to investigate the nature of consciousness and the changes underlying its impairment or loss.

The fundamental role of sleep in the maintenance of health was recognised by Hippocrates: "The patient should wake during the day and sleep during the night. If this rule be anywise altered it is so far worse….connected with sorrow or pain" (Hippocrates: The Book of Prognostics).

It may be said that the application of functional neuroimaging techniques, based on cerebral blood flow and metabolism, to the study of sleep is an extension of the ideas that were first recorded about 500 B.C., when Alcmaeon wrote that "sleep is produced by the withdrawal of the blood away from the surface of the body to the larger ('blood-flowing') vessels and we awake when the blood diffuses throughout the body again". Descartes' fixation upon the pineal gland again featured in his bizarre hydraulic theory of sleep, in which he described sleep as a state where neurons (which he described as fluid-carrying pipes) collapsed when the gland reduced its output of 'animal' spirits! Science returned from this diversion to the study of blood flow in the 19th century. Early theories still attempted to relate cerebral blood flow during sleep to the flux of Cartesian 'spirits', proposing that they were impeded by increased blood flow and associated raised intracranial pressure during sleep. These ideas finally gave way to scientific rigour when physicians such as Angelo Mosso (1846-1910) and Johann Friedrich Blumenbach (1752-1840), observing blood flow in the brains of injured patients noted that they were actually paler or less perfused during sleep than when awake [19].

In the early 20th century, physiological theories of sleep remained focused on cerebral blood flow changes as causal phenomena. Quickly however, a so-called psycho-biological theory of sleep gained ground. Édouard

Claparede (1873-1940) made several intriguing proposals in his *Enquisse d'une Theorie Biologique du Sommeil,* which have in many ways since been supported by experimental evidence. Proponents of the psycho-biological theory maintained that sleep was an active state, imposing disinterest or inattention and suppressing sensory functions. This, they maintained, provided an evolutionary advantage as these periods of inactivity allowed for greater activity during waking [20].

Sleep science could only make genuine progress however with the advent of the first modern "window on the brain", electroencephalography (EEG). In the 1930s, Alfred Loomis used the EEG techniques developed by Berger and others to study human physiological sleep and made a number of startling discoveries. He noted that the character of the EEG waves changed during sleep ("The impression was gained that a change in the level of consciousness was connected with this change in type of wave") and that waxing and waning waves of 10-14 cycles per second appeared during sleep. The Loomis group coined the term "spindles" to describe these phenomena. These experiments also revealed that sleep was not a homogenous state but cycled through stages of varying depth [21-23]. In 1953 another stage of sleep, rapid eye movement (REM) sleep, was described. The identification of periods of coincident eye movements, reduced skeletal muscle tone, increased autonomic activity and EEG transformation from sleep patterns to the desynchronisation seen in wakefulness [24] confirmed that sleep indeed was a highly active state rather than a passive 'off' period.

The first histological evidence that sleep and waking may be associated with specific loci of activity came from the study of a fatal post-viral vegetative state, encephalitis lethargica, by Constantin von Economo (1876-1831). Post-mortem studies of the brains of affected patients revealed neuronal loss in the hypothalamus and mesencephalic reticular formation. Later von Economo found cell loss in the anterior hypothalamus and basal forebrain of patients with chronic insomnia [25].

Moruzzi and Magoun found that lesions of the mesencephalic reticular formation could drive the entire cerebral cortex into the high amplitude low frequency oscillations of sleep. They also noted that stimulation of this region during sleep could desynchronise the EEG to a waking rhythm and would block high amplitude slow waves during anaesthesia [26]. The ascending reticular activating system (ARAS), which includes the cholinergic lateral dorsal tegmental (LDT) and pedunculopontine (PPN) nuclei and the noradrenergic locus coeruleus (LC), were thus recognised to be critical for the active maintenance of wakefulness. These nuclei project to and

modulate activity in the thalamus, hypothalamus, basal forebrain and spinal cord. Wakefulness-promoting outputs also project to cortical and subcortical areas from the serotonergic dorsal raphe nucleus (DRN), the subtantia nigra (SN) and ventral tegmental area (dopaminergic), the tubomamillary nucleus (TMN, histaminergic) and the anterior hypothalamus (orexinergic). A schematic outlining some of the main connections between sleep and wake-promoting centres is given in figure 1.1.

Sleep is an active, regulated, temporally structured process arising from the interplay of cyclical sleep and wake promoting systems. It is advantageous from an evolutionary perspective to have several systems promoting wakefulness. Arousal is central to survival and so redundancy is prudent. Current models of sleep-wake physiology propose two sleep promoting processes.

Process C describes the circadian modulation of arousal mediated through the GABA-ergic output of, as von Economo suspected, the ventro-lateral preoptic (VLPO) area of the the anterior hypothalamus. The GABA-ergic output of the VLPO is inhibitory to wake-promoting nuclei. VLPO neurons become disinhibited when output from the wake-promoting nuclei decreases, increasing GABA-ergic inhibition of the basal forebrain cholinergic output and the TMN, reducing the excitatory output of these key regions [27].

Process S may be described as metabolic debt, the exact mechanism of which has yet to be fully elucidated. At least two proposed mechanisms for Process S are supported by substantial evidence, adenosine accumulation and synaptic homeostasis.

Extracellular adenosine increases following neuronal activity. It accumulates with prolonged wakefulness and levels decrease during sleep. Caffeine, an adenosine antagonist, prolongs sleep latency. Genetic polymorphisms of adenosine deaminase, which result in delayed breakdown of adenosine to inosine and therefore locally increased adenosine levels, are associated with enhanced non-rapid eye movement (NREM) sleep and increased slow wave activity during sleep [28]. Adenosine acts on the A1 receptors of cholinergic neurons in the basal forebrain causing hyperpolarisation and reducing their excitatory output. This changes the balance of basal forebrain output, which projects to the striatum and cortex, from excitatory cholinergic to inhibitory GABA-ergic, thus promoting NREM sleep. Wake-promoting centres in the brainstem and hypothalamus project strongly to the basal forebrain, stimulating cholinergic activation, while GABA-ergic neurons in the basal

forebrain are inhibited by noradrenaline from the locus coeruleus via its activity on α_2 adrenoreceptors. While there is strong evidence for the role of adenosine in the homeostatic regulation of natural sleep, there is no evidence that adenosine metabolism plays any causal role in sedation or anaesthesia.

The synaptic homeostasis hypothesis has received increasing attention in recent years. This proposes that interaction with the environment during wakefulness increases the synaptic strength between neurons involved in those conscious experiences and in memory formation [29]. In fact there is now evidence in Drosophila of such activity dependent increases in synaptic strength [30]. It would be prohibitively expensive from a metabolic perspective to maintain an ever increasing number of synaptic links, therefore this increased synaptic strength must be returned to normal levels during sleep, with a new distribution of the total synaptic strength, enhancing pathways activated by the preceding waking experiences [31]. 40% of cortical grey matter metabolism supports synaptic activity and PET data in humans shows an 18% increase in cerebral blood flow (CBF) in the evening compared to the morning [32]. There is increasing evidence that the electrophysiological activity of neurons during sleep, dominated by low frequency activity, may be mechanistic in, or reflect the mechanisms of, this process of synaptic downscaling during sleep [33].

Sleep is driven by the neuronal activity underlying awareness and experience of the self and the environment, which has evolved to sustain the central nervous system over the course of the lifetime of an organism. Therefore, while there are behavioural similarities, the state is very different to the anaesthesia and disorders of consciousness (DOC) to which it is regularly compared. Consideration of sleep is nevertheless central to the investigation of disorders of consciousness, sedation and anaesthesia. Firstly, these states may involve abnormal function in sleep or wake-promoting centres or networks. Decades of evidence are converging on the probability that sedative anaesthetics produce their clinical effects through modulation of one or more components of the sleep/wake system rather than globally suppressing neuronal firing [34,35]. Stimulation can overcome, at least in part, the effects of injury to components of the sleep/wake system in specific cases of focal pathology [36,37]. Sedatives which produce states bearing a greater physiological resemblance to sleep appear to satisfy homeostatic drive [38-40] and may result in improved clinical outcomes in both surgical and intensive care patients. Finally, if sleep is an active co-ordinated process, then its occurrence shows some ordered cerebral function. The presence or recovery of spindles was shown to have prognostic implication for brain injured patients and spindle density increased in parallel with clinical recovery in patients following traumatic brain

injury [41]. The recovery of recognisable sleep architecture also has favourable prognostic implications in coma patients [42]. Consciousness and sleep are intimately related and the former cannot be studied in isolation from the latter.

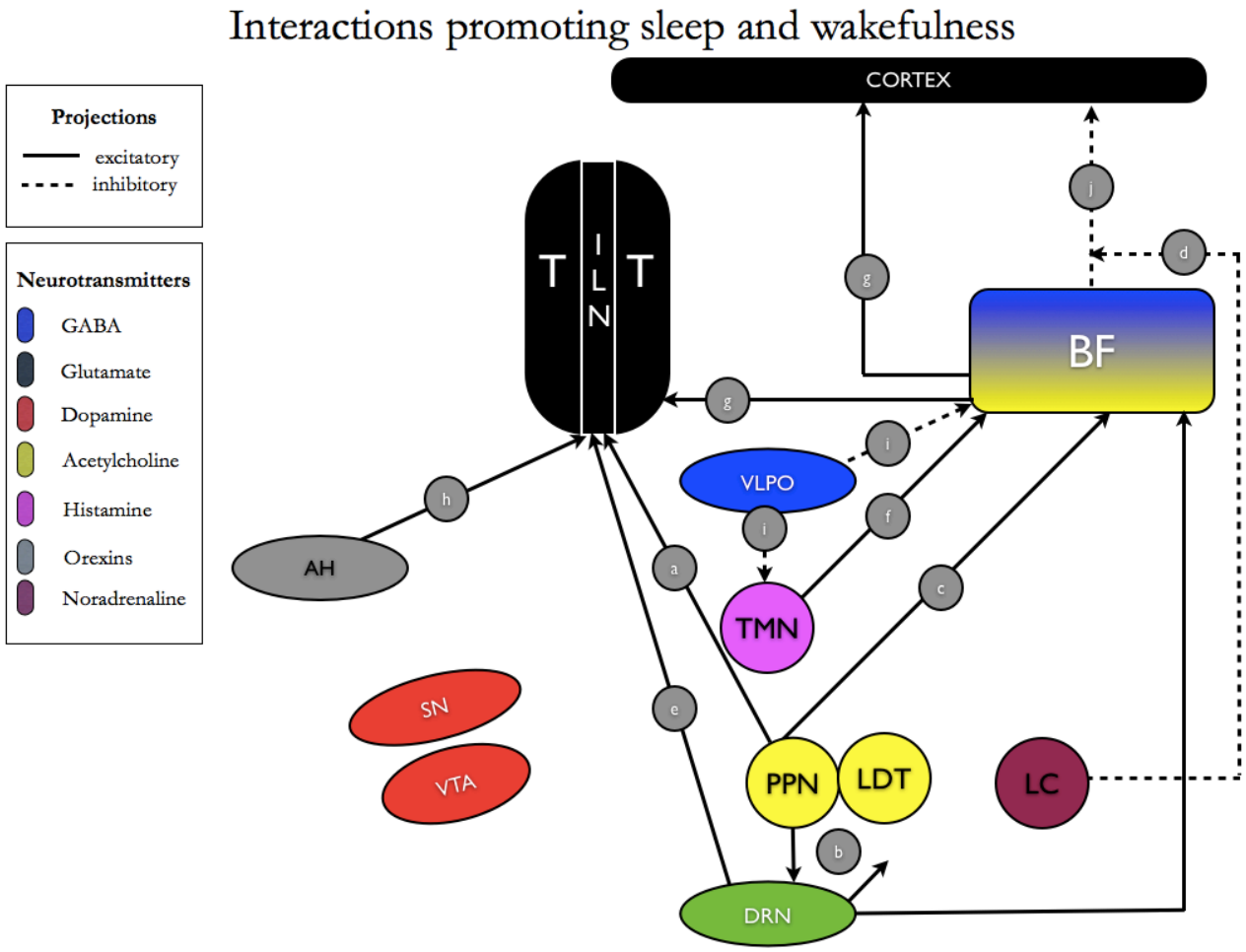

Figure 1.1 Schematic of the main pathways involved in sleep-wake regulation.

Arousal: Pontine cholinergic nuclei (PPN,LDT) project to the intralaminar thalamic nuclei (ILN) (a), other brainstem arousal nuclei (b) and the cholinergic BF (c). The noradrenergic locus coeruleus (LC) inhibits GABA-ergic output from the basal forebrain (BF) through its actions on local α_2 receptors (d), as well as innervating dorsal and non-specific thalamic nuclei (not shown). The serotonergic dorsal raphe nucleus (DRN) maintains arousal through projections to the cortex, ILN (e) and BF as well as local connections to other arousal nuclei (b). Orexinergic neurons in the lateral hypothalamus project widely to the sleep wake system, including the ILN (h) and the tubomamillary nucleus (TMN) has diffuse histaminergic projections including dense innervation of the cholinergic BF (f). Dopaminergic neurons in the substantia nigra (SN) and the ventral tegmental area (VTA) cause arousal through innervation of the thalamus, BF and cortex. Arousal nuclei maintain BF cholinergic output to the cortex (g).

Sleep: The ventral preoptic nucleus (VLPO) is the main sleep-promoting centre. Its GABAergic output inhibits histamine release from the projections of the TMN and inhibits BF cholinergic neurons, helping to tip the balance of the system in favour of GABAergic projections from the BF to the cortex (j)

PPN-penuculopontine nucleus; LDT-lateral dorsal tegmental nucleus; ILN-midline and intralaminar thalamic nuclei; LC-locus coeruleus; BF-basal forebrain; DRN-dorsal raphe nucleus; TMN-tubomamillary nucleus; SN-substantia nigra; VTA-ventral tegmental area; VLPO-ventral preoptic nucleus; AH - anterior hypothalamus.

1.1.4 Disorders of Consciousness

We have yet to establish a satisfactory philosophical or neurophysiological definition of consciousness. As a result, we are dependent on pragmatic but unsatisfactory definitions of its impairment or absence. This has clinical and humanitarian implications when consciousness is actively manipulated or impaired by trauma or pathology. A brief consideration of actual and potential iatrogenic trauma argues strongly for continued research in this area.

Pharmacological manipulations of consciousness have no objective real-time endpoints. As unconsciousness can currently only be confirmed by retrospective interview, confirmation is neither timely nor independent of intact recall. This is a relatively theoretical concern during the majority of operations carried out under general anaesthesia, where higher drug levels may be maintained with relative safety. However, up to 20% of the patients requiring general anaesthesia for surgery are classified as American Society of Anesthesiologists (ASA) physical status III or worse and are therefore physiologically vulnerable to anaesthetic-induced vasodilation and negative inotropy [43]. Greater care and clinical judgment is required to ensure that these patients remain unconscious, in the practical sense, throughout the procedure. The medical literature and popular media contain many evocative reports of patients who were conscious during surgery. While such experiences are rare (the reported incidence of intraoperative awareness ranges from 0.01 to 0.1% [44-46]), fear of being awake and paralysed during surgery is common among patients and comparable in prevalence to the fear of postoperative pain [47]. The trauma associated with these experiences tends to be profound, particularly when surgical pain was experienced during neuromuscular blockade [46].

A large cohort of critical care patients may have comparable experiences related to inadequate pharmacological management of consciousness during painful or distressing interventions. Each year 4.4 million patients require intensive care in the United States and 130,000 in the United Kingdom [48]. Psychological distress is common during critical illness, associated with dyspnoea, pain, the threat to life, the alien environment and often delirium. Invasive and distressing critical care therapies, such as high frequency oscillatory ventilation, extra-corporeal life support, bedside surgical procedures (percutaneous tracheostomies, intercostal drain insertions) and radiologically guided interventions, while associated with increasing survival following critical illness, have not been accompanied by parallel improvements in the targets for analgesia and sedation. More invasive therapies may more frequently be associated with the use of neuromuscular blockade which, as with anaesthesia, increases the risk and implications of inadequate hypnosis [49]. Most intensive care units (ICUs) continue to rely on

behavioural measures of sedation despite their well documented limitations in this context, having been validated against one another but not against follow up interview, and even these tools are generally found to be underused [50,51]. Perhaps because of a different expectation framework (surgical patients are formally offered general anaesthesia and expect to experience nothing, critical care patients may not), the experiences of this group of patients do not make their way into the public domain as frequently. The incidence of distress and post-traumatic stress disorder (PTSD) following critical illness is however increasingly recognised. The point prevalence of substantial PTSD was 19-22% in a meta-analysis of UK patients. This is comparable to the recognised rates of PTSD in survivors of adult respiratory distress syndrome, myocardial infarction and cardiac surgery [52]. Post-ICU recall of frightening or psychotic in-ICU experiences is consistently predictive of PTSD among ICU survivors. Endotracheal suctioning is often reported by patients as causing pain and distress. This is a particular concern for patients who undergo prolonged weaning from mechanical ventilation, where sedation is recognised to potentially retard progress. Among these patients PTSD has been diagnosed in 12% at 3 months [53]. Critical illness neuropathy and myopathy occur in 50-70% of patients with the systemic inflammatory response syndrome (SIRS), confounding behavioural assessment of sedation adequacy, in a peripheral analogue of the locked-in syndrome [54].

While the impact of inadequate amelioration of noxious sensations and perceptions during surgery or critical illness may be severe, the experiences themselves are finite and with growing recognition of PTSD and its association with critical illness, the consequences are identifiable and treatable. Patients in whom the primary pathology is itself a disorder of consciousness pose a more profound and frightening problem.

The term "disorders of consciousness" (DOC) is used to describe the functional consequences of a spectrum of CNS pathologies following trauma, vascular accident, anoxia or other insult. Patients are by definition not brain dead as central respiratory drive is preserved, but meaningful communication is either severely limited or absent. Understanding of the spectrum of DOC remains incomplete and the detection of awareness in these patients, differentiating failure to communicate from having no conscious awareness *to* communicate, is fraught with difficulty.

Monsieur Noirtier de Villefort, a character in Alexandre Dumas' novel, The Count of Monte Cristo (1844), was depicted as "a corpse with living eyes", for six years only able to communicate by blinking his eyes. In 1966

Plum and Posner formally described the locked-in-syndrome (LIS) of quadriplegia and anarthria, arising usually due to a selective bilateral lesion of the ventral pons preserving rostral structures, in which consciousness is intact but no voluntary motor function (total LIS) or only eye movements (incomplete LIS) can be generated [55].

In 1972, Plum and Jennett described the vegetative state, defined by the Multi-Society Task Force on PVS (permanent vegetative state) and the Royal College of Physicians as a clinical condition characterised by a preserved sleep-wake pattern but no meaningful response to the environment and only reflex responses to stimulation [56,57]. This is utterly different to a locked-in state as by definition, consciousness is absent, yet differentiation from DOC with preserved awareness may be difficult.

Many cases of disorders of consciousness have attained a high media profile, igniting fierce if not always informed medical, philosophical, ethical and legal debates. In 1985, the death occurred of Karen Ann Quinlan, a young woman who 10 years earlier had suffered a prolonged cardiorespiratory arrest. Almost a year after the initial injury, she sustained spontaneous respirations upon discontinuation of mechanical ventilation and remained in a permanent vegetative state (PVS), characterised by stereotypical, non-purposeful movements and preserved sleep-wake cycles from then until her death from sepsis 9 years later. At autopsy, there was extensive thalamic and cerebellar damage but remarkable preservation of the cerebral cortex, with only parasaggital regions of the parieto-occipital and the occipital cortex showing significant neuronal loss. Brainstem nuclei were histologically intact, accounting for the preserved facial grimacing, protective airway reflexes, ventilatory drive, autonomic function and sleep/arousal cycles but at no point was meaningful communication or purposeful movement observed. This case illustrates the capacity for limited lesions to be associated with profound impairment or absence of consciousness. Careful assessment of the thalamus in this case revealed that injury was not global, but had selectively affected a number of small crucial nuclei, including intralaminar nuclei and those with connections to cortical attention areas [58]. This and other cases discussed later in this dissertation highlight the central role of thalamic nuclei as part of distributed networks subserving consciousness.

While the brain damage in this case was focal and the electroencephalogram showed disordered slow waves, in the case of Terry Schaivo brain damage was global and her EEG was reported as isoelectric [59]. Radiological investigations were very different in these two patients with the same diagnosis and ultimately the same outcome. The diagnosis of disorders of consciousness remains a clinical and extremely difficult one, particularly difficult

in patients with motor impairment precluding communication of awareness. Any ambiguity has profound implications for families, clinicians and policymakers. Almost half of the deaths in intensive care follow a decision to withdraw or withhold therapy [60]. While this is a somewhat emotive statistic, given that withdrawal of therapy usually occurs in recognition of its futility or an advance directive, it also occurs due to the absence of any prospect of a meaningful neurological recovery.

An audit of patients admitted for rehabilitation more than six months after severe acute brain damage, with a diagnosis of PVS, revealed misdiagnosis in 43% of cases. All of the misdiagnosed patients were anarthric and 65% had impaired vision. One patient had severe contractures precluding movement and awareness was only apparent when following surgical soft tissue release and intensive physical therapy, a slight shoulder shrug could be generated to allow communication [61]. Childs reported the misdiagnosis of PVS in 37% of patients admitted to a rehabilitation centre over a 5 year period [62]. More recently 41% of Belgian patients with a diagnosis of vegetative state were found to be misdiagnosed [63]. Misdiagnosed patients were found to be in a "minimally conscious state" (MCS), a condition differentiated from vegetative state (VS) by the presence of reproducible goal-directed behaviours.

Vegetative states (VS) are defined by arousal in the absence of awareness. MCS was defined and diagnostic criteria established in 2002 by the Aspen Neurobehavioural Conference Work Group. In this severe disorder of consciousness, definite voluntary behaviour rather than simple reflexes are demonstrable[64]. Careful repeated clinical assessment of these patients repeatedly if inconsistently reveals behavioural evidence of awareness of self or the environment through the capacity to localise sound or noxious stimuli, show visual tracking or manifest contingent facial expressions or vocalisation. In the UK, there has been controversy about the classification of visual fixation as a purposeful movement however in the US, this *is* a finding that excludes the diagnosis of VS. MCS patients may have a more favourable prognosis than VS patients with the potential for recovery of functional communication. It is likely that "miracle" recoveries from VS are the result of emergence from misdiagnosed MCS [65].

The potential role of functional neuroimaging in this context is clear. The capacity to circumvent barriers to communication such as aphasia, motor deficits and musculoskeletal pathology and detect any retained cognitive function or awareness may help prevent misdiagnoses in disorders of consciousness and provide reassurance to

families and carers. The first use of functional neuroimaging in the detection of brain activity related to cognition in a patient with a VS diagnosis was reported in 2006 [66]. The investigators detected activation in the middle and superior temporal gyri in response to sentences that did not occur in response to acoustically matched noise. While these findings parallel those of studies of auditory processing under anaestheisa [67], the investigators also reported activity in the inferior frontal gyrus when sentences contained ambiguous words. When asked to perform two different mental imagery tasks, the differences in activation (supplementary motor area activation when imagining playing tennis and premotor, parahippocampal and posterior parietal lobe activation when mentally navigating the rooms in her house) matched those of healthy controls. Following the publication of this case report, 54 patients (23 in VS and 31 in MCS) underwent functional MRI scans. While investigators consistently report the misdiagnosis of MCS as VS, when new clinical scoring systems such as the Coma Recovery Scale-Revised (CRS-R)[68] are compared to clinical consensus, the false-positive rate of MCS diagnosis is as yet unknown. In four patients with a diagnosis of VS, imaging suggested a residual capacity for cognition. In two of these cases, careful clinical assessment revealed misdiagnosis of VS that should have been classified as MCS. Nevertheless, in two patients with no detectable behavioural evidence of awareness, functional MRI scanning revealed an internal attempt at communication [69]. Disappointingly, in only one of the patients with a diagnosis of MCS, in whom residual cognitive function was expected was a task-related signal change detected. This may reflect the low sensitivity of current techniques (in which case more of the MCS patients may have been shown to be aware) or have occurred because clinical assessment scores remain unreliable. Both possibilities are strong arguments for the clinical importance of continued research into functional neuroimaging of disorders of consciousness.

1.2 Anaesthetic mechanisms of action

Relative to the modest amount that is actually known about how anaesthetic drugs exert their effects, the volume of work published on the topic is enormous. This is at least in part attributable to the confound inherent in experiments on an organ comprised of interdependent neuronal networks. While drug effects can be measured, determining which of these effects cause loss of consciousness and which are in fact the result of loss of consciousness has proven difficult.

The term "mechanism of action" is itself ambiguous, and is used to describe activity at a molecular level, any resultant modulation of neuronal activity, any consequent increase or decrease in the output of a specific nucleus, or a network or global effect.

1.2.1 Molecular effects

Like many medical advances of the era, the effect of anaesthetics was discovered first, and only subsequently did science begin to explore how. Research into the molecular mechanisms of action of anaesthetics was held back for decades because causality was attributed to a non-anaesthetic effect. Meyer and Overton noted a correlation between the potency of an anaesthetic gas and its lipid solubility or oil:gas partition coefficient [70,71]. This and the observation of reversal of anaesthetic effects under hyperbaric conditions drove hypotheses based on disruption of the lipid phase of nerve cell membrane as the mechanism by which neuronal excitability was reduced, possibly through the distortion of transmembrane proteins [72]. There were many inconsistencies in these hypotheses, including the fact that the effects of anaesthetics on the lipid bilayer were tiny and could be reproduced by a temperature change of 1^0C.

The depression by anaesthetics of light emitted by bioluminescent bacteria was known to be directly proportional to their potency in humans and when this relationship was demonstrated in a cell free preparation, Ueda and Kamaya showed that volatile anaesthetics directly inhibited the activity of the enzyme firefly luciferase. They proposed that this occurred through unfolding of the molecule, a specific protein interaction [73]. In their seminal work, Franks and Lieb demonstrated anaesthetic-protein interaction at clinical anaesthetic concentrations and showed that a wide range of anaesthetic compounds competed with luciferin, the natural ligand, for the luciferase binding site. They suggested that all anaesthetics act by competing with endogenous ligands for protein binding sites [74]. This proposal was considered "an interesting departure from the mainstream" [75] at the time and the influence of anaesthetics on the fluidity of the phospholipid membrane

continued to be studied [76]. However, the binding site and the interaction of anaesthetics with this site were later demonstrated by x-ray crystallography. This interaction was shown to be simply competitive inhibition and did not produce any significant conformational change in the protein itself [77].

The attraction of the Meyer Overton hypothesis was that it presented a simple unifying model of the effects of a highly diverse array of compounds. With time, a number of targets for anaesthetic-protein interactions have been identified which have the potential to provide the same unification with time. Two-pore-domain K^+ channels can be directly activated by volatile anaesthetics causing membrane hyperpolarisation [78], but their role in anaesthesia has not been established. Most volatile anaesthetics antagonise the N-methyl-D-aspartate (NMDA) glutamate receptor to a variable degree but selective NMDA antagonists like ketamine produce anaesthesia-like catatonic stupor but only at higher doses with lower doses causing behavioural abnormalities [79].

The $GABA_A$ receptor is a ligand-gated ion-channel that conducts chloride ions through its pore once opened by binding of GABA, the major inhibitory neurotransmitter of the central nervous system. This causes inhibition of synaptic transmission through membrane hyperpolarisation. Inhalational anaesthetics [80], barbiturates [81] and propofol [82] all potentiate the duration of activity of GABA at its receptor, enhancing chloride conductance by prolonging time that the ion channel is open. $GABA_A$ sensitivity to general anaesthetics is dependent on the subunit composition of the particular receptor, the distribution of which can vary widely throughout the CNS and insensitivity to anaesthetics can be induced by point mutations in the receptor structure [79]. Full characterisation of anaesthetic activity at this site may contribute to a comprehensive theory of anaesthesia to replace Meyer-Overton. The anaesthetic potencies of propofol and its analogues have been shown to depend on their potency for GABA potentiation and not lipid solubility [83].

1.2.2 Local effects

While much progress has been made towards elucidating the actions of anaesthetics at a molecular level once the red herring of Meyer Overton was overcome, we know less about how these molecular actions translate to effects on the activity of groups of neurons. As higher cognitive functions are dependent on activity in distributed networks, it might be assumed that anaesthetics must act widely across the brain. On the other hand, the states of sleep and wakefulness are governed by specific systems, activity in which has secondary effects across the entire brain. It is not known whether the specifically causal action of anaesthetics is global or local. Just as localised pathology can cause profound DOC, several investigators have shown that anaesthetic drugs administered hyperfocally can produce marked behavioural changes in animals, including impairment of the righting reflexes associated with EEG slowing.

The brainstem is an obvious potential target, specifically the nuclei of the ARAS. In 1959, Magni and colleagues showed that selective perfusion of the brainstem with barbiturates resulted in a state electrophysiologically similar to anaesthesia. However, it was not until 2001 that an anaesthetic-like state was produced by microinjection of pentobarbital into a specific zone within the brainstem, the mesopontine tegmental area (MPTA) [84]. While this study did demonstrate atonia and EEG slowing on MPTA injection, other sites tested often produced a degree of sedation and the absence of consciousness cannot be confirmed in animals. Later work by this group showed that the MPTA projects caudally to pontine, medullary and spinal cord areas involved in motor control and atonia as well as to rostral motor control areas including the substantia nigra, the subthalamic nucleus and the striatum [85]. This suggests that at least some of the behaviour seen in the earlier experiments were the result of anaesthetic-induced immobility rather than loss of consciousness. Anaesthetic-induced immobility has been shown to be mediated by spinal rather than central mechanisms, confounding behavioural assessments of consciousness [86,87]. Projections from the MPTA to the intralaminar thalamic nuclei have also been demonstrated [88] so it remains possible that specific foci within this region may play a role in arousal. Interactions between brainstem nuclei are complex however. Isoflurane *decreases* GABA levels in the pontine reticular formation, and local administration of muscimol (a $GABA_A$ agonist) promotes wakefulness while bicuculline (a $GABA_A$ antagonist) promotes REM sleep [89]. It may not be possible to administer drugs with adequate selectivity or to discriminate between the effects of microinjection on local interactions and distant projections. Nevertheless, sleep/wake systems is likely to be modulated by anaesthetics. GABA-ergic anaesthetics are associated with increased c-Fos expression (a marker of neuronal activity) in the sleep

promoting VLPO and decreased c-Fos expression in cholinergic basal forebrain, LDT and PPN neurons, monoaminergic and orexinergic arousal systems as well as in the cerebral cortex [34].

1.2.3 Network effects

How anaesthetics effect loss of the highest level of brain function, with the final common outcome of loss of consciousness is perhaps the most poorly understood aspect of their pharmacobiology. Many investigators now support the theory of information integration as a model of consciousness. This depends on synchronous activity in distributed networks and it is attractive to consider breakdown of communication between nodes of these small world networks with respect to loss of consciousness. Possible mechanisms of this would include central and peripheral interruption of network communication.

Central interruption of communication within a network would involve suppression of activity at the main hub, the thalamus, and activity here does appear to be pivotal [90]. Positron Emission Tomography (PET) studies have shown that metabolic activity and local blood flow are specifically reduced in the thalamus by both volatile anaesthetics [91] and propofol [92]. Connectivity between the thalamus and the cortex has been shown to be reduced during anaesthesia [93] and in disorders of consciousness [94]. However these effects may not necessarily be evidence for a so-called "thalamo-cortical switch", if this is defined as failure of thalamic transmission. Decreased thalamic activity may be secondary to deafferentation or a reduction in cortico-thalamic input.

Peripheral interruption of information integration would occur with a breakdown of cortico-cortical communication, leading to a failure of the synchronous network activity, necessary according to current models for conscious perception. Anaesthetics have been shown to impair gamma frequency information transfer between brain regions in rats [95]. Using propagation of cortical potentials evoked by transcranial magnetic stimulation as a model of cortico-cortical connectivity, Massmini and colleagues have shown that this is impaired during both sleep [96] and benzodiazepine administration [97] compared to wakefulness and REM sleep [98]. Analysis of the effects of propofol on the spontaneous low-frequency fluctuations in cerebral blood flow using fMRI has shown breakdown of connectivity within and between networks [99].

There remains therefore much to be understood about the interactions between neurons locally and across networks within the brain before a unifying theory of consciousness can be achieved. Likewise, there remains much to be understood about the actions of anaesthetic drugs at molecular, neuronal and network levels before a unifying theory of anaesthesia can be achieved. Anaesthesia and consciousness are inextricably linked fields of

research despite the diversity of scientific and medical disciplines involved in their study. The aim of this thesis is to contribute to the understanding and monitoring of clinical sedation and anaesthesia and explore possibilities for the improvement of patient care.

1.3 Overview of Chapters

Chapter 2: General materials and methods

The experiments described involve four modalities of study: behavioural measures, physiological measures, electroencephalography (EEG) and functional magnetic resonance imaging (fMRI). The technical details of the techniques and data analyses that are common to multiple experiments are described in this chapter. Techniques or analyses specific to an individual experiment are described in the relevant chapter.

Chapter 3: Exploring neural correlates of sedation using propofol

This chapter describes the first experiments investigating consciousness using sedative anaesthetics at our institution. After developing protocols for the safe conduct of these studies, a series of experiments were carried out at steady state levels of sedation. The cerebral responses to auditory and noxious stimulation were recorded in healthy volunteers in three behaviourally rather than pharmacologically defined states - awake, sedated and unresponsive. The results of two different approaches to fMRI analysis, evoked BOLD response analysis and connectivity analysis, are reported.

Chapter 4: The electroencephalography of ultraslow transitions in states of consciousness

An important observation during the previous series of experiments was the lack of reproducibility, even within-subjects, of the dose-response. A new technique of continuous data collection using ultraslow induction of anaesthesia was developed to maximise the temporal resolution and to identify as precisely as possible transitions in states of consciousness and their electrophysiological characteristics. The state of unconsciousness that has been most extensively studied in humans and across species is sleep. This chapter reports EEG data the analysis of which was focused on the behaviour of oscillations that have been carefully characterised in the context of physiological sleep. The similarities and differences between sleep, sedation and anaesthesia are explored.

Chapter 5: Combined EEG/fMRI of ultraslow transitions in states of consciousness

Having established a safe and useful experimental paradigm in the first experiment and then modified the technique to identify striking transitions in EEG activity under anaesthesia, the functional significance of these transitions was investigated using fMRI. This chapter reports the responses to auditory and noxious stimulation that are specific to defined neurophysiological states. These results are discussed with respect to data in sleep and in patients with disorders of consciousness.

Chapter 6: Resting state networks during anaesthesia

An alternative, data-driven approach to the analysis of spatially distributed activity within the ostensibly resting brain is explored in this chapter. Resting state networks have received increasing attention in recent years, particularly in the field of consciousness research, and the investigations presented here are represent a preliminary step towards future studies. Identification of resting state networks (RSN) is confirmed in two states of consciousness and the some features of RSN in both states are compared.

Chapter 7: Concluding remarks

The results of the presented experiments are considered in the context of current literature and clinical practices with a particular focus on the potential for insights gleaned to improve clinical management of sedation, anaesthesia and disorders of consciousness.

Chapter 2: General materials & methods

2.1 Experiment Design

Each experiment reported in this work involved the administration of controlled infusions of the anaesthetic propofol, a $GABA_A$ receptor agonist, to healthy volunteers. The investigations were based on both unimodal and multimodal measurements of neurophysiological parameters. As many of the techniques used were common to multiple experiments, this chapter describes the detail of these methodologies. The rationale behind the choice and development of particular techniques, why some were employed and others were not is discussed, and a technical report of the procedures given. Experiment-specific methods reporting particular paradigm designs, signal processing techniques or analyses are given in the relevant chapters.

2.1.1 Subjects

Molecular studies have provided crucial insights into the biochemical basis of pharmacological manipulations of consciousness. Animal studies have not only linked molecular biology to behaviour, but provided the opportunity to demonstrate or out-rule causality through lesion studies [79]. The vast majority of organisms naturally cycle through a state recognisable as sleep [100,101]. While consciousness is possibly the phenomenon of greatest complexity to emerge in nature, some functional susceptibility to the effects of anaesthetics is seen in remarkably simple organisms [102]. However, despite the ethical and practical constraints inherent to the human neuroscientific investigation in general, and to manipulations of human consciousness in particular, human studies are essential to link molecular biology and animal studies to the subjective experience that is consciousness.

Each of the studies was approved by the Local Research Ethics Committee (Central Oxfordshire Research Ethics Committee, Oxford, Oxfordshire, U.K.) and complied with the guidelines of the Declaration of Helsinki (1996).

2.1.2 Recruitment and participation

Any ethical framework for human studies of consciousness requires that subjects take part without coercion and have the opportunity to give informed consent, be fully educated with respect to potential risks and the adequacy of measures taken to minimise risk in the study group. In addition, investigators must take responsibility for the identification and exclusion of any volunteer on the basis of clinical assessment of individual risk. To facilitate this, recruitment and participation were specifically separated. Local advertising invited volunteers to make contact and an initial screening visit was arranged. Initial visits provided an opportunity for medical assessment of the subjects' suitability for participation (Volunteer Health Questionnaire, Appendix A) and for subject education in all operational aspects of the proposed experiment. Inclusion and exclusion criteria are given in Table 2.1. Volunteer engagement with risk education was keen, in particular as recruitment occurred shortly after the death of the pop singer Michael Jackson, whose cardiologist, Conrad Murray, was later found guilty of manslaughter for inappropriate propofol administration. The danger of death or addiction was frequently raised by potential volunteers at the screening visits. If, after completion of a screening visit to the satisfaction of both the potential volunteer and the investigators occurred, then a "cooling off" period of at least 48 hours was scheduled to give volunteers an opportunity to reconsider the information provided and change their mind before their first experimental session.

Table 2.1 Study inclusion and exclusion criteria

Inclusion Criteria	Exclusion Criteria
• Age between 18 and 50 • American Society of Anesthesiologists (ASA) physical status grade I or II • English speaking • Informed consent	• Tobacco or illicit drug use • Alcohol use > 14 units/week • History of psychiatric, neurological or psychological pathology • History of claustrophobia • Any contraindication to MRI (as outlined in the attached FMRIB Volunteers Safety Checklist) • Allergy to anaesthetic drugs • History or clinical signs of potential susceptibility to airway obstruction • Difficult venous access

Financial Compensation for Time

While it is not the policy of FMRIB to pay volunteers for participation in experiments, it is deemed appropriate and desirable to compensate them for their time. Onerous experiments involving propofol infusions were remunerated. Each person received £75 for each experimental session in which they participated, regardless of whether or not the session was successfully completed. While it had initially been proposed not to financially compensate volunteers for attendance at an initial screening visit it was pointed out by the research ethics committee that having given up some time for this visit, volunteers may feel inappropriately motivated to proceed to a session which did bring financial compensation for time and therefore £25 was given to each screening visit attendee, regardless of whether or not they subsequently enrolled.

Care of participants

A degree of personal responsibility was expected of the subjects and they were informed of the importance of full disclosure of any medical history and of adherence to instructions. Safe participation in the experiments involving propofol infusions required that volunteers followed the guidelines of the AAGBI for day case anaesthesia. Volunteers were provided with a written set of instructions describing the fasting, travel and supervision required to ensure their safe participation (Volunteer Instruction Checklist, Appendix A). Experiments were scheduled for the mornings to minimise the discomfort of fasting. Volunteers were given a light meal after full recovery and then provided with a taxi home. Participants were instructed in advance and asked to confirm on the day of the experiment that they would be accompanied at home until the following morning. They were instructed not to take alcohol, drive or participate in sport for the remainder of the day after the experiment. A phone call was made the following morning to each participant to ensure that they were well. No adverse incidents were reported.

2.2 Administration of propofol

In this section, the background to the selection of propofol as a tool for investigation of consciousness is presented. The precautions taken to ensure participant safety are described. The administration regimes implemented during the experiments are reported in the relevant chapters.

2.2.1 Pharmacokinetic and Pharmacodynamics

Propofol 2,6, diisopropylphenol, a derivative of phenol has been in clinical use since 1986. It enhances GABAergic inhibition at the postsynaptic membrane through its modulation of the $GABA_A$ receptor complex [103]. Propofol's pharmacokinetics have been described in detail and its pharmacodynamics have been extensively studied. It is ideally suited to investigative manipulations of consciousness. It has a short duration of action, as it is highly lipophilic, rapidly crossing cell membranes and being extensively distributed. It is metabolised to inactive compounds through oxidisation followed by glucuronide and sulphate conjugation in the liver. Its clearance exceeds hepatic blood flow as extrahepatic metabolism also occurs, with tissue perfusion the rate-limiting step. Following a bolus dose or a continuous infusion, plasma concentration follows a triexponential decay function [104]. The relationship between the plasma concentration of propofol at steady state during a constant infusion and the level of that infusion is linear [105], and therefore the resultant propofol plasma concentrations are predictable. Since 1997, target controlled infusion pumps have been available which incorporate pharmacokinetic parameters into a mathematical model, allowing users to set a target plasma concentration. The temporal relationship between plasma concentration and central nervous system effect site concentration (ESC) is not straightforward as there is a lag between plasma concentration and clinical effect. Incorporation of k_{eo}, the constant governing equilibration between plasma and effect site is necessary. This has been estimated using pharmacodynamics derived from behavioural and electroencephalographic parameters [106,107].

In our studies, 1% propofol (Diprivan™ 1%, AstraZeneca UK Limited, Luton, Bedfordshire, UK) was administered through a 20g intravenous cannula in the right forearm using an Alaris Asena PK™ (Cardinal Health, Alaris Products, Basingstoke, UK) pump with the Diprifusor™ (AstraZeneca UK Limited, Luton, Bedfordshire, UK) target controlled infusion (TCI) module that manipulates the plasma concentration to rapidly achieve a targeted effect site concentration (ESC). The "modified Marsh" model, which combines the Marsh pharmacokinetic model and pharmacodynamic estimation of k_{eo}, was used to manipulate propofol levels in our studies.

A key consideration in the selection of propofol for the investigation of consciousness is its extra-neuronal activity, which has implications for both subject safety and the interpretation of biological signals. All anaesthetics affect the cardiovascular and respiratory systems, upper airway tone and protective airway reflexes and cerebral blood flow. In addition to having a pharmacokinetic profile conducive to the manipulations needed, propofol's effects on other systems are better suited to the experimental setting than those of volatile or other intravenous anaesthetics. The effects of propofol on cerebral blood flow and autoregulation are addressed in chapter 2

2.2.2 **Cardiovascular and respiratory effects**

Propofol decreases arterial blood pressure, primarily through peripheral vasodilation although even in young healthy patients there is a small negative inotropic effect. Because the delay in transfer of drug from plasma to the effect site is greater than other agents such as thiopentone, the prevalence of relative overdosing with propofol on induction is relatively high when traditional clinical endpoints such as loss of eyelash reflex are relied upon. Hypotension following an induction dose of propofol is significantly attenuated by slow administration and cognisance of k_{eo}. In our experiments, we administered propofol by continuous infusion, with a very low initial target ESC. While this was a methodological decision, it was expected that this would also support maintenance of cardiovascular stability.

Apnoea occurs after a bolus dose of propofol on induction of anaesthesia. During a continuous infusion, respiration is sustained. Tidal volumes are lower and respiratory rate higher than baseline respiration and the ventilatory response to carbon dioxide is diminished. As with cardiovascular considerations, the mode of administration of propofol in these experiments, i.e. continuous infusion starting at low initial targets, substantially reduced the risk of clinically significant respiratory depression.

2.2.3 Airway Management

While cardiovascular and respiratory depression were anticipated, the degree of impairment in the selected young healthy participants was expected to be mild. Maintenance of airway patency was considered more likely to be a cause for concern. Propofol, more than other anaesthetic agents, produces profound relaxation of laryngeal and pharyngeal muscle tone and substantially depresses airway reflexes, hence its rapid and widespread adoption as the drug of choice when a laryngeal mask airway is to be used. Unlike cardiovascular and respiratory depression, airway obstruction is not substantially attenuated by the use of a continuous infusion. The main

factors affecting airway patency are the individual's anatomy and muscle tone, the latter having a dose dependent effect [108]. Each of these factors was considered during study design.

The target ESC during surgery depends on the co-administration of analgesics such as opioids. In the opioid free subject, the ESC of propofol required to prevent movement on insertion of a laryngeal mask airway (LMA) in 50% (EC_{50}) is 3.25 mcg ml^{-1} [109]. The EC_{50} for movement prevention in female surgical patients was reported as 6 mcg ml^{-1} [110]. In another study, the ESC required to prevent movement in response to a tetanic stimulus ranged from 2.8-7.5 mcg ml^{-1} [111] An upper limit of 4.0 mcg ml^{-1} was set for propofol ESC based on these published data and clinical experience of target controlled infusions. It was expected that increases in ESC beyond this would be associated with an unacceptable probability of airway obstruction.

In order to minimise the risk of airway obstruction a formal airway assessment was part of the initial clinical screening. While a variety of scoring systems based on clinical observation and measurement have been published, the positive predictive value of both individual measurements and scoring systems is relatively poor. Independent risk factors for airway compromise during sedation and anaesthesia include male sex, a history of sleep apnoea and Mallampati grades III and IV on oropharygeal assessment [112]. While it would be neither practical nor appropriate to exclude males, a history of sleep apnoea or snoring was sought and Mallampati assessment carried out at screening visits.

As an additional safety measure, the study design incorporated bench experiments in the physiology laboratory prior to functional MRI (fMRI) experiments. This ensured that only after subjects completed a (medically) successful protocol outside the fMRI scanner could they be given propofol in the more clinically challenging setting of an fMRI scanner. Subjects were carefully and directly observed for signs of obstructive respiratory movements throughout both bench and scanner protocols. One bench experiment was aborted prematurely due to the development of an obstructive respiratory pattern and that subject did not take part in a subsequent fMRI experiment. One other subject developed an obstructive respiratory pattern in the scanner despite successfully completing a bench protocol and this scan was aborted. Failure to predict this complication was most likely due to the semi-recumbent position of subjects during bench experiments (to allow computer screen observation), which was not as much of a challenge to airway patency as the fully supine position within the scanner.

2.2.4 Physiology monitoring

Both the physiology laboratory and fMRI scanner were equipped for the administration of sedative medication in compliance with the minimum monitoring guidelines of the Association of Anaesthetists of Great Britain and Ireland (AAGBI).

A senior anaesthetist was responsible for the administration of propofol and subject monitoring during each experiment. This person did not have any other study responsibilities during that session and stopped the experiment if they had any concerns over the safety of the volunteer.

Physiological monitoring including oxygen saturation, ECG and non-invasive blood pressure were recorded electronically throughout the experimental sessions and synchronised with and integrated into data collection (MP150, BIOPAC, Santa Barbara, CA). Additionally, subjects wore nasal cannulae that allowed both oxygen delivery at 2 litres/min and capnography of the expired CO_2 (GasAnalyser module, BIOPAC, Santa Barbara, CA). Depth and frequency of respiration was monitored using a pneumatic bellows applied around the upper abdomen.

2.3 Functional magnetic resonance imaging

Introduction

This section introduces the biology and physics of the Blood Oxygenation Level Dependent (BOLD) signal during magnetic resonance imaging, which is the basis of functional neuroimaging. Anaesthetic agents also directly affect cerebrovascular physiology. The expected effects of propofol infusions on cerebral blood flow and the BOLD signal are considered.

2.3.1 Magnetic resonance imaging of deoxyhaemoglobin

Due to the presence of iron, haemoglobin molecules have magnetic properties. Deoxygenated haemoglobin is paramagnetic, i.e. it has a significant magnetic effect on surrounding tissues and changes the relaxation time of water in blood. Haemoglobin oxygenation is therefore a sensitive marker of the level of blood oxygenation and thus of neuronal activity. Magnetic resonance imaging can detect haemoglobin oxygenation.

When placed in a strong magnetic field, the magnetic moment of protons (hydrogen nuclei in human tissues) tend to align to this field, B_0. Transfer of energy to these protons through the application of a radiofrequency pulse at the appropriate resonant frequency causes their magnetic moment to rotate away from B_0 and nuclei precess about their magnetic moment in phase. This energy is then released as the protons dephase and their magnetic moments return in alignment with B_0. A number of processes govern the time course of this energy release. T1 recovery/relaxation and T2 decay are tissue characteristics. T1 recovery occurs as the nuclei give up their energy to the surrounding tissues, which occurs rapidly in fat and slowly in water, and they recover alignment with B_0. T2 decay occurs as nuclei exchange energy with neighbouring nuclei due to magnetic field interactions and their spins dephase. This occurs rapidly in fat and slowly in water.

T2* decay has a similar origin but is the product of both the T2 decay process and the additional dephasing influence of local magnetic field inhomogeneities. Phase coherence produces a stronger signal than incoherence. Magnetic field inhomogeneities are introduced by the presence of paramagnetic substances such as deoxyhaemoglobin.

The rate of T2* decay therefore depends on local magnetic field inhomogeneities. This is affected by cerebral blood volume (CBV), cerebral blood flow (CBF) and local deoxyhaemoglobin concentration changes produced

by the haemodynamic response to neuronal activity. For short periods of activation the first two of these can be considered constant, with deoxyhaemoglobin levels varying with the haemodynamic response function (HRF).

Contrast is defined by the difference in the signal between tissues. The repetition time, TR, and the echo time, TE, are adjusted to optimise the desired contrast. The TR of the brain tissue is of the order of 1 second. In order to obtain an image in which the contrast between tissues occurs due to local magnetic field inhomogeneities rather than tissue characteristics of water or fat, T2* weighted images are obtained [113,114] using a long TR relative to the tissue T1 so that there is little signal difference due to tissue T1 differences. TE is relatively short so that the differences in signal between tissues are due to T2* decay. Technical details of the scan sequences used in these studies are given in chapter 2.

BOLD signal

The metabolic demands of neurons are the highest of any tissue. Neuronal activation produces an increase in metabolic demand, which is met by an increase in regional cerebral blood flow (rCBF). The HRF describes the temporal dynamics of local cerebral blood flow increases in response to neuronal activity. While rCBF rises in parallel with the elevated glucose consumption that accompanies increased neuronal activity, supply exceeds demand leading quickly to an increase in the oxygen content of venous blood from the active brain region. This focal elevation in venous blood oxygenation is the biological phenomenon underlying the BOLD signal [115,116], first described in rat brains at high magnetic fields [117].

As approximately 2 seconds is needed for blood to transit from arteries through capillaries to draining veins, BOLD signal increases (more diamagnetic oxyhaemoglobin, less paramagnetic deoxyhaemoglobin and therefore slower spin dephasing so more signal detected) are seen at this time lag following an increase in neuronal activity [118]. The signal reaches a plateau after 6-12 seconds and then falls at the same rate at which it rose [119]. A sharp undershoot is often, but not always, observed which has been attributed to passive dilatation of compliant venules [120]. BOLD based functional neuroimaging models the expected BOLD signal changes based on expected local haemodynamic response to neuronal activity increases. Areas in which the BOLD signal correlates with the model can be sought and thus local neuronal activation inferred. It is essential therefore that factors which may affect the underlying assumptions of the model are considered.

Hypercapnia

Hypercapnia produces significant cerebral vasodilation. Each 1 mm Hg elevation in $PaCO_2$ results in a 3-4% increase in cerebral blood flow [121]. The elevated baseline reduces the BOLD signal change [122]. This is a potentially disastrous effect given the expected rise in $PaCO_2$ with increasing propofol ESC. However, multiple intrinsic and extrinsic processes modulate cerebral blood flow and therefore assessment of the suitability of propofol infusions for BOLD signal based studies must consider the overall effect.

Autoregulation

Survival is dependent on the brain being able to maintain an adequate supply of blood and glucose to sustain neuronal activity in the face of fluctuations in perfusion pressure. The capacity of the cerebral vasculature to maintain cerebral blood flow across a range of perfusion pressures from approximately 50-150 mm Hg in this way was first described in humans in 1959 [123]. Various mechanisms have been proposed but the phenomenon is likely to be the result of multiple processes and remains incompletely understood. Hypertension, head trauma and drugs all affect the limits and response curves of cerebral autoregulation. While desflurane and isoflurane impair static and dynamic autoregulation in humans, relative cerebral vasoconstriction results in these processes being preserved under both low (100 mcg kg^{-1} min^{-1}) and high (200 mcg kg^{-1} min^{-1}) doses of propofol in health [124].

The relationship between arterial carbon dioxide and cerebral autoregulation is complex. Hypercapnia increases cerebral blood flow chapter 2 and slows the rate of autoregulation [125]. However this effect is modulated by the addition of propofol. A $PaCO_2$ above 55 mm Hg abolishes cerebral autoregulation in isolation or in the presence of sevoflurane anaesthesia. During propofol anaesthesia however, cerebral autoregulation is preserved [126]. Both animal and human data show that flow compensation within the cerebral vasculature for changes in cerebral blood perfusion pressure is preserved during propofol anaesthesia [127-129].

Regional and global cerebral blood flow

As functional neuroimaging has over the past 20 years been increasingly used to infer functional changes based on metabolic or blood flow fluctuations, there has been much interest in how these are affected by anaesthetics. Positron Emission Tomography (PET) studies in animals and humans have provided useful results.

PET is a quantitative imaging technique that has been used to measure and compare distribution patterns of cerebral glucose metabolism and cerebral blood flow under a variety of conditions, including anaesthesia and sedation. The procedure involves injection of a positron-labelled tracer such as flurodeoxyglucose (FDG) or water ($H_2{}^{15}O$), depending on what is to be measured. In the case of FDG the tracer is taken up into active neurons as glucose, but as it cannot be used as glucose it becomes sequestered intracellularly. Thus the amount of PET signal from a region is a measure of glucose uptake in that region, from which neuronal metabolic activity can be inferred. It takes between 30 and 60 minutes for FDG uptake to complete [91]. The accumulated tracer uptake can then be measured by detecting the annihilation gamma photons emitted when positrons hit nearby electrons. The source of the emitted photons is then localised with stereotactic registration to high resolution MRI or computed tomography (CT). Thus the temporal resolution of FDG PET is poor, describing regional cerebral glucose metabolism once steady state conditions have been maintained for at least 30 minutes. Radiolabelled water, $H_2{}^{15}O$, can be used to estimate changes in neuronal activity with greater temporal resolution. The molecule is small and inert and diffuses freely across the blood brain barrier, transported to tissues in proportion to regional blood flow. The emitted photons reflect tissue perfusion at a capillary level. After 20-30 seconds, clearance of water exceeds tissue delivery so tracer density decreases faster in areas with greater blood flow. The optimum time for imaging is 60-120 seconds after a bolus injection of tracer and multiple images may be taken to reduce noise. Thus O-15 PET has a much greater temporal resolution than FDG-PET and can be used to study relatively rapid changes in neuronal activity. However, at 1-2 minutes it is still significantly inferior to the BOLD signal based measurements. Nevertheless, since PET describes steady state metabolic activity and blood flow it has provided essential insights into the effects of anaesthetic drugs on regional cerebral blood flow and metabolism.

Propofol reduces cerebral metabolic rate [130] and as a result, cerebral blood flow in a dose dependent manner [131]. Kaisti et al. showed using O-15 PET that EC_{50} propofol produced global and regional reductions in absolute CBF (range 62-70%) and these reductions were significantly greater than the reduction produced by 1 minimum

alveolar concentration (MAC) sevoflurane (range 36-53%).[1] Further increases beyond EC_{50} or 1 MAC produced smaller, non-significant changes in blood flow [92].

A subsequent study [132] by the same group using inhaled labelled oxygen and carbon monoxide ($^{15}O2$ and $C^{15}O$) as PET tracer molecules to measure regional cerebral metabolic rate of oxygen consumption ($rCMRO_2$) and regional cerebral blood volume rCBV, in addition to the $H_2{}^{15}O$ tracer for estimation of rCBF, found that sevoflurane reduced rCBF less than propofol, as before, but that sevoflurane and propofol reduced $rCMRO_2$ to a similar degree (56-70% and 50-68% respectively). Sevoflurane but not propofol reduced regional oxygen extraction fraction in their study suggesting a direct effect of sevoflurane on neurovascular coupling.

Neurovascular coupling

Although the brain accounts for 2% of body mass, it consumes 20% of the body's glucose and oxygen and receives 20% of cardiac output. Blood flow and glucose metabolism within the brain are tightly coupled to local neuronal activity. The precise mechanisms linking demand to supply are not completely understood although several important contributing processes have been identified.

While it was initially thought that a consequence of metabolically active neurons (such as a decrease in oxygen or glucose or a local increase in CO_2) triggered local vasodilation, experimental manipulations of these factors revealed that blood flow is not regulated in this way [133-135]. This concept has been superceded by the discovery of neurotransmitter-mediated-signalling. Glutamate release by active excitatory neurons appears to stimulate neurochemical pathways, releasing vasoactive compounds including nitric oxide (NO, a potent smooth muscle relaxant and arteriolar vasodilator) [136] and arachidonic acid metabolites[137]. Strictly speaking therefore, the functional hyperaemia underlying the BOLD signal reflects synaptic activity rather than action potentials [138]. In addition to affecting baseline cerebral blood flow, both globally and regionally as described, the effects of drugs on neurovascular coupling must be considered.

---

[1] Importantly in their study they identified a methodological flaw that may explain why previous studies had reported that halothane and sevoflurane *increase* CBF. Their study incorporated measurement of drug and tracer levels through arterial sampling and then implemented a correction using these concentrations. Without accounting for the increase in drug and tracer concentrations their data would also have suggested that sevoflurane increased CBF. They hypothesise that this increased tracer may be due to a centralisation of the circulation induced by the anaesthetic, which results in a higher percentage of cardiac output being delivered to the brain. Nevertheless, there is evidence that volatile anaesthetics, unlike intravenous anaesthetics, may change reactivity within the cerebral vasculature.

Franceschini et al [139] investigated the effects of different anaesthetics on neurovascular coupling using diffuse optical imaging and EEG. They measured the induced changes in baseline cerebral blood flow and the response to electrical forepaw stimulation and a hypercapnia challenge (which has been shown to be equivalent to that characterising neuronal activation [140] in rats under six different anaesthetics. They confirmed the findings of Eng et al [128] that CO_2 reactivity was lowest with propofol and highest with volatile anaesthetics, particularly isoflurane. The greatest haemodynamic responses to stimulation occurred under isoflurane and alpha chloralose and the smallest under propofol. Interestingly, by examining the relationships between N1, P1, N2 and P2 components of the somatosensory evoked potentials, this group was able to confirm that the haemodynamic response is driven by cortico-cortical synaptic activity rather than thalamic inputs. The BOLD signal is therefore most sensitive to the influence of anaesthetics on cortico-cortical transmission.

Propofol in fMRI

Both volatile and intravenous anaesthetics have extra-neuronal effects that contribute to the fMRI signal. The choice of drug is a matter of balancing practical considerations and unwanted effects. Practical considerations such as subject comfort and safety, capacity for controlled dose manipulation and the need for airway support potentially interrupting data collection across a key transition in the level of consciousness, certainly support the use of an intravenous rather than a volatile agent and favour propofol over other intravenous agents. With respect to unwanted effects the key concerns were the effects of inevitable mild to moderate hypercapnia and any pharmacological modulation of cerebral autoregulation. As outlined in this section, of the available agents, propofol provides the best preservation of baseline cerebral blood flow in these circumstances due to vasoconstriction and the preserved integrity of cerebral autoregulation in the context of hypercapnia.

2.3.2 Funcitonal MRI acquisition and analysis

Technical details of fMRI acquisition common to all experiments

Volunteers were scanned using a 3 Tesla human Magnetic Resonance Imaging system, with a 1 meter bore magnet (Oxford Magnet Technology Ltd, Oxford, U.K.), using a birdcage radio frequency coil and a reduced bore head gradient coil (Magnex SGRAD MKIII. Magnex Scientific Ltd, Oxford, U.K.). The system was controlled by a Varian Unity Inova console (Varian Medical Systems, Palo Alto, California, USA) using Siemens' gradients (Siemens Medical Ltd, Bracknell, Berkshire, U.K.).

Subjects were positioned carefully using small custom-made foam cushions to support the head and neck. During pilot scans, it was found that the weight of the mandible led to obstructive respiratory movements under deep sedation with resultant increases in $EtCO_2$ and head motion artifacts; additional support cushions were therefore positioned to maintain what was essentially a hands-free jaw-thrust maneuver from the outset. This maintained airway patency throughout the propofol infusions in all but one subject.

For functional scans the acquisition consisted of a whole brain gradient-echo echo-planar imaging sequence with 41 contiguous coronal oblique slices of 3.5mm thickness inclined at 10 degrees to the axial plane (repetition time = 3000ms, echo time = 30ms, flip angle =90^o, 224 x 224 mm field of view, 64 x 64 matrix).For the registration of functional data to stereotactic standard space, a 3D Turbo Flash T1-weighted (axial) high resolution anatomical scan was obtained at a separate visit. The imaging parameters were TR = 20 milliseconds, TE = 4.6 milliseconds, flip angle = 120^o, Field of View 256 by 256 mm with a matrix of 256 by 256 and 64 contiguous slices of 3mm thickness.

Preprocessing steps

Each fMRI scan consisted of a series of volumes, measuring the BOLD signal from the entire brain in voxels of size 3mm x 3mm x 5mm (spatial resolution), taken every three seconds (temporal resolution). Before statistical analysis, a number of preprocessing steps were carried out to remove artifact and improve the signal to noise ratio. Four dummy volumes were acquired at the beginning of each scan and the experimental paradigm began with the fifth volume. This is to allow for steady state imaging fields to be established and these four volumes were discarded as the first pre-processing step.

All fMRI scans were analysed using software written by the FMRIB analysis group implemented in FSL (FMRIB's Software Library, www.fmrib.ox.ac.uk/fsl). Standard published algorithms were used for pre-processing of data, statistical analyses and registration of functional scans and statistical maps to a stereotactic standard space template (MNI152 T1 1mm).

Motion Correction

There is always some head motion during an MRI scan, often less than 1mm but this can be enough to produce signal distortion. There are two main effects of head motion during a scan. Areas of the brain can be in different positions at subsequent timepoints. This can be corrected through application of a realignment process using a linear transformation. A velocity-dependent phase shift also occurs when the protons move within the field. Spin that has moved from one slice to another is now excited at a different time and it takes a few TRs for the steady state to recover. This results in an artifact known as spin-excitation history that manifests as a signal intensity change. Correction for the change in signal intensity this produces is based on the displacement vectors calculated during spatial realignment. A motion correction algorithm (MCFLIRT - Motion Correction using FMRIB's LInear Registration Tool) was applied to all scans prior to further processing [141]. All volumes were realigned to a common reference image, the middle timepoint. Motion correction regressors were included as regressors of no interest in the general linear model when performing statistical analyses.

Fieldmap unwarping

As brain, air and bone have different magnetic susceptibilities, the presence of a head in the scanner bore produces magnetic field inhomogeneities, distorting B_0. This is a particular problem at the frontal and mastoid sinuses where air/bone interfaces result in signal loss and secondary registration errors in the frontal and temporal lobes, respectively.

A phase-difference image of B_0, a fieldmap, was obtained for unwarping of functional scans. Although this cannot recover lost signal, it corrects geometric distortion. Fieldmap based correction of images was carried out using FUGUE (FMRIB's Utility for Geometrically Unwarping Echo Planar Images (EPIs)) [142].

Spatial smoothing

Spatial filtering serves to increase the signal to noise ratio through local averaging. Adjacent voxels are likely to display similar signal changes but random variations will tend to cancel each other out. There are also statistical reasons for applying spatial filtering. Random field theory, applied in later statistical analyses, requires the data to be spatially smooth for its underlying assumptions to be valid. Spatial smoothing was carried out using a Gaussian kernel of full width half maximum (FWHM) of 5mm. The signal intensity of the entire 4D dataset was then normalised by a single scaling factor (grand mean intensity normalisation) rather than forcing individual volumes to have the same mean intensity, which would undermine group level analyses. Finally, a highpass temporal filter of 50 seconds was applied to remove the low frequency artifact effect of scanner drift.

Removal of non-brain signal

Scalp, skull, eye and neck tissues are of no interest and were removed prior to statistical analysis using an automated method (BET-Brain Extraction Tool, [143]). While this is a rapid and generally reliable technique, it is dependent on the contrast between brain and non-brain tissues. Each functional scan was visually inspected for the accuracy of brain extraction before any further analysis. Satisfactory results were obtained for fMRI scans without EEG. The presence of EEG gel on the scalp of the subjects in the combined EEG/fMRI experiments changed the signal contrast between the scalp and underlying tissues and automated extraction proved on visual inspection to have been inadequate. These scans were therefore re-processed and non-brain structures removed by manually masking and then subtracting them using a graphical software tool (FSL View, part of FSL).

Cardiorespiratory artifact removal - ICA

The pulsation of major head vessels and the cerebrospinal fluid produces its own BOLD signal change. Respiratory excursion of the lung apices with ventilation also impacts upon the functional signal as oxygenated lung tissue moving within a magnetic field produces distortion. Both pulse and respiratory excursion were recorded during each scan so that their effects could be regressed out of the dataset. While this could be expected to be constant during the steady state scans, dynamic scans where the cardiorespiratory physiology was not constant required the removal of these trends, which were likely to be correlated to drug level and therefore confound analyses. These scans were therefore subjected to a further de-noising step during preprocessing to remove this non-neural signal.

Independent component analysis (ICA) has been used for the removal of spurious physiological noise where the effects of cardiorespiratory physiology cannot be adequately modelled [99]. Each of the combined EEG/fMRI datasets was decomposed into spatially independent linearly mixed components MELODIC (Multivariate Exploratory Linear Optimized Decomposition into Independent Components, part of FSL [144,145]). These components consisted of spatial maps with associated signal timecourses. For each scan, components were inspected visually for spatial distributions or signal timecourses that could be attributed to pulsations (CSF, circumferential rings) or respiration (slices artifacts and/or timecourses matching the recorded respiratory excursion). Such components were identified and then the datasets reconstructed, regressing out the physiological noise. Examples of each type of noise component are given in figures 6.1 and 6.2 and in Appendix B.

Statistics

fMRI data analysis was carried out using FEAT (FMRI Expert Analysis Tool, part of FSL). Timeseries statistical analysis was carried out using FILM (FMRIB's Improved Linear Model) with autocorrelation correction using a prewhitening algorithm [146].

For each scan involving stimuli, a linear model was created derived from the expected BOLD signal responses to stimulation. Separate regressors were included for each auditory stimulus, each noxious stimulus, each button press and motion. Subject level (first level) analysis sought brain areas where the BOLD signal changes could be explained by one of the regressors in the model. Areas of statistically significant correlation with the model were identified after multiple comparisons correction using cluster based thresholding [114].

Within-subject, between state contrasts (second-level) were estimated again using FEAT performing a fixed effects t-test. This revealed areas that in an individual subject displayed significantly different activation patterns between neurophysiological states. These contrast results were then passed to a group level mixed effects group mean analysis. For scans without stimulation, resting state scans, investigation of signal correlations across brain networks used independent component analysis.

Further discussion of the specific statistical tests applied to each experiment is given in the relevant chapters.

Registration

The spatial resolution of fMRI scans (3mm x 3mm x 5mm) is high compared to other neuroimaging modalities such as EEG or PET but is still poor relative to structural scanning. In order to compare spatial locations across subjects, functional images are mapped to a high-resolution structural space template in a two step registration process. Registration aligns images so that a voxel co-ordinate contains the same anatomical location in both images.

All registrations in these studies were carried out using FLIRT (FMRIB's linear registration tool) [141]. Functional images were first registered to the individual's high resolution T1 weighted structural scan. A rigid body transformation was used for within subject registrations with 7 degrees of freedom (x, y, z translations, side-side, front-back, up-down rotations and a single global scaling) and sinc interpolation. After registration to subject space, an affine transformation with 12 degrees of freedom (six for rigid body transformation and an additional three scalings and three skews) registered the data to a standard space template (MNI 152 T1 1mm brain, Montreal Neurological Institute, Quebec, Canada), generated by averaging 152 brains.

2.4 EEG acquisition and analysis

Introduction

EEG data was acquired during two types of experiments: pure EEG studies carried out in the physiology laboratory (bench data) and combined EEG/fMRI studies carried out in the 3T MRI scanner. Simultaneous EEG/fMRI experiments are a relatively novel technique. While commercially available algorithms for the removal of fMRI artifact in EEG data are available and provide satisfactory data, matching artifact free data was collected for these experiments so that corresponding artifact-free data would be available. The effect of simultaneous EEG recording on MRI data quality was also a concern. The presence of conducting wires and electrodes of the EEG system can potentially degrade the quality of MRI data due to the magnetic susceptibility of the electrode assemblies, generation of inhomogeneities in the static and dynamic magnetic fields and electromagnetic noise emitted by the recording equipment. Sebald et al studied the image noise originating from the EEG recording equipment and found it to be coherent noise eliminated by appropriate shielding of the EEG equipment [147]. It was concluded that concurrent EEG and fMRI could be performed without compromising the image quality significantly if suitable equipment is used. The electrodes and conductive gel in

the EEG cap causes some perturbation in the B_1 field resulting in small regions of signal loss in the periphery [148]. Non-brain tissue removal algorithms failed to identify the brain/scalp interface in this dataset, necessitating manual removal. This is attributable to the presence of the conductive gel on the scalp in these studies.

2.4.1 Acquisition

MR compatible 32 channel EEG caps (BrainCap MR, Easycap GmbH, Herrsching, Germany) were used for EEG acquisition. Inbuilt electrodes were sintered Ag/AgCl sensors with 5 kOhm resistors directly after the sensor except the ECG electrode which had a 15 kOhm resistor. A schematic of the montage used, based on the standard international 10-20 arrangement of electrodes, with electrode co-ordinates, is shown in figure 2.1. After careful positioning of the cap, the skin under the electrodes was first cleaned with isopropyl alcohol before injecting a high chloride abrasive electrolyte gel (Abralyte 2000, Easycap GmbH, Herrsching, Germany) through a hole in the electrode to reduce impedance. Impedances were kept below 5 kilohms throughout all experiments.

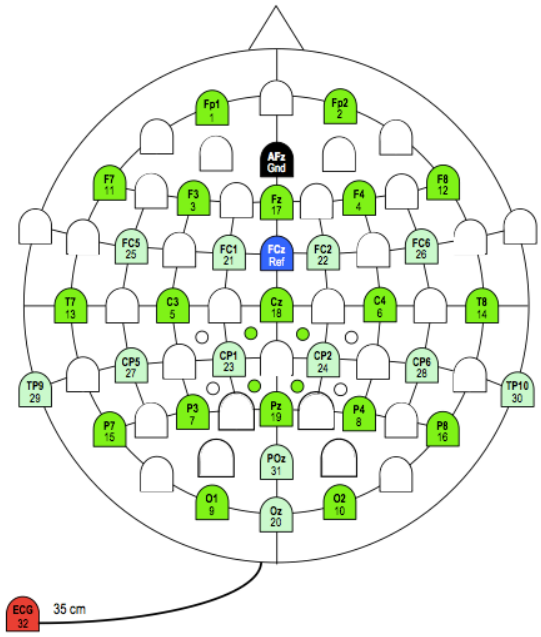

Coordinates

Channel-Number	Name	Theta	Phi
1	Fp1	-90	-72
2	Fp2	90	72
3	F3	-60	-51
4	F4	60	51
5	C3	-45	0
6	C4	45	0
7	P3	-60	51
8	P4	60	-51
9	O1	-90	72
10	O2	90	-72
11	F7	-90	-36
12	F8	90	36
13	T7	-90	0
14	T8	90	0
15	P7	-90	36
16	P8	90	-36
17	Fz	45	90
18	Cz	0	0
19	Pz	45	-90
20	Oz	90	-90
21	FC1	-31	-46
22	FC2	31	46
23	CP1	-31	46
24	CP2	31	-46
25	FC5	-69	-21
26	FC6	69	21
27	CP5	-69	21
28	CP6	69	-21
29	TP9	-113	18
30	TP10	113	-18
31	POz	67	-90
32	ECG		

Figure 2.1 A) Schematic of the 10-20 EEG electrode montage used and B) the associated spherical polar coordinates of the electrode positions. Green/light green labels highlight the 32 channels used. The reference electrode was FCz (blue) and the ground electrode was in the AFz position (black). Electrocardiographic signals were recorded from one channel for offline cardioballistographic artifact removal.

Cables from the EEG electrodes were twisted into branches of 8 cables that were brought together to unite into a single 50 cm twisted cable tree behind CPz. This cable tree was connected to two 16 channel MR compatible biopotential amplifiers (BrainAmp MR plus, Brain Products GmbH, Munich, Germany). Additional channels were connected through an auxiliary device (BrainAmp ExG MR, Brain Products GmbH, Munich, Germany)

and recorded ECG, vertical eye movements (VEOG) and horizontal eye movements (HEOG). When being used in the fMRI scanner any loops in the cabling were eliminated.

The amplifiers were connected using MR-safe fibre optic cables to a universal serial bus (USB) adaptor and then to a laptop computer dedicated to EEG recording, running a commercial EEG acquisition software package (BrainVision Recorder, BrainProducts GmbH, Munich, Germany). This simultaneously recorded the timings of fMRI volumes (gradient onset markers), stimuli and button presses. Signals were acquired at 5000Hz and initially referenced to channel CPz. The amplification hardware imposed a highpass filter of 0.1Hz and a lowpass filter of 250 Hz on acquisition. The acquisition software applied a highpass filter of 0.5 Hz and a lowpass filter of 70 Hz as well as a notch filter of 50Hz.

2.4.2 fMRI gradient artifact removal

MR artifacts are generated by the switching of gradient fields and by the radiofrequency pulse generation in the scanner bore. The artifact induced in the EEG channels by MR gradient switching is a very high amplitude signal (as much as 10,000 μV) relative to the microvolt signal of interest. These voltages develop rapidly with slopes up to 25,000 μV/ms) and hence have gradients more than 500 times faster than spontaneous EEG. A sample of the raw EEG obtained in the scanner is shown in figure 2.2. However, since this artifact is temporally stable, exactly the same currents are induced during each volume, so provided the scanner timing is carefully recorded at a high sampling rate, MRI gradient artifact removal based on artifact template subtraction is relatively straightforward if computationally demanding.

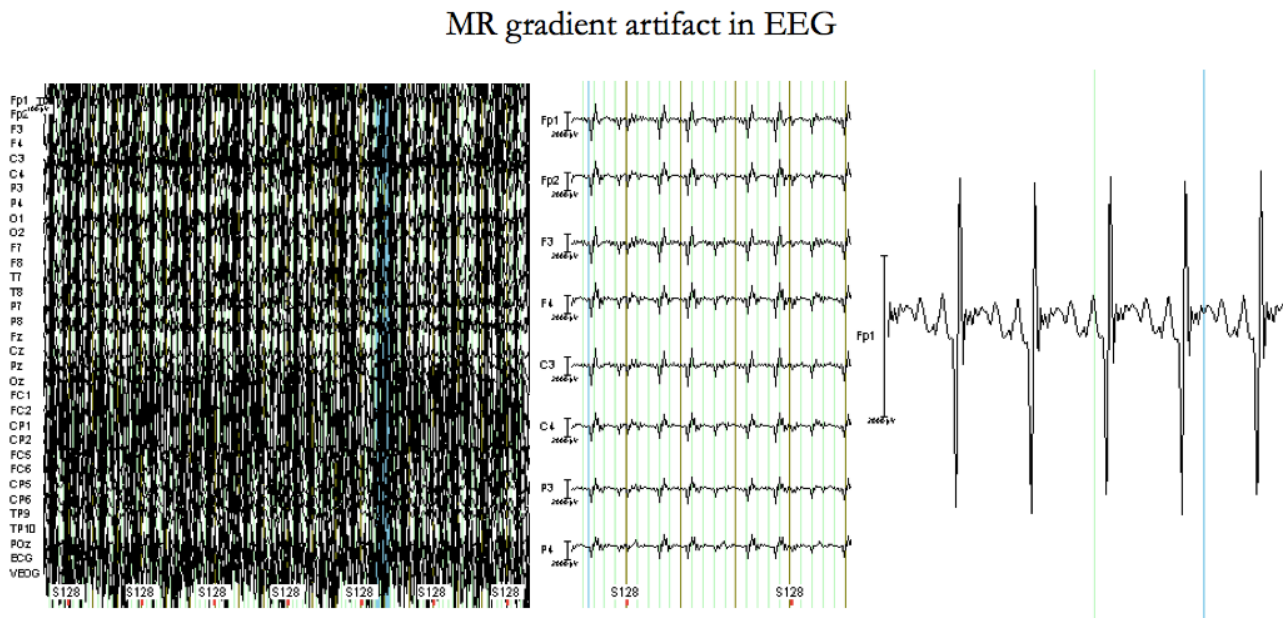

Figure 2.2 The panel on the left shows the gradient artifact in the full set of EEG channels. The high voltage artifact obscures all electrophysiological data. Increasing the vertical scale on which the signal is displayed and the temporal resolution (middle panel) shows the artifact to be systematic and repeated. The artifact in a single channel, Fp1 (right panel) can be seen to be stereotypical, with the same series of deflections during each readout (TE). This allows a template to be generated and then subtracted. S128 labels are volume markers and appear one per TR or every 3000 milliseconds.

FMRI gradient artifact removal was performed using BrainVision Analyser (Version 1.0). Data were upsampled to 50,000 Hz (sampling interval 20 μs) using spline interpolation. Gradient artifact averaging was performed based on the gradient onset markers recorded during acquisition. A sliding average of 16 volumes was applied to optimise the gradient artifact removal for a slight drift in TR (~1 millisecond) over the course of the 48-minute scans, which causes a slow change in artifact structure. Following gradient artifact removal data were downsampled to 500 Hz and a lowpass filter of 30 Hz (Butterworth zero phase filter, 48 dB/octave) applied.

Cardioballistographic artifact removal

The origin of cardioballistographic artifact (CBA) is pulse-synchronous micromovements of the scalp and therefore the electrodes within the magnetic field. As these movements are time-locked to the ECG, simultaneously recorded ECG serves as a guide for CBA template generation. Pulse artifact removal was performed using a correction algorithm implemented in BrainVision Analyzer (Verson 2.0) software. R wave markers were identified in the dataset from the ECG channel. The delay time between the R wave and the ballistocardiographic artifact was estimated by calculating the smoothed global field power (GFP) distribution

for all EEG channels that contribute significantly to the GFP distribution. Within this distribution the local minima to the left and right of the GFP maximum were determined and the temporal midpoint between these two minima was defined as the exact middle of the GFP power distribution. This delay time was then used to define a template artifact for removal based on the first 101 R waves that was then removed at all R waves in the dataset.

Blink artifact removal

For both bench and fMRI data, the frontal effects of blink electromygraphic signals were removed. Blinks were identified using an automated algorithm in BrainVision Analyzer (Version 2.0) that parsed the VEOG channel. Blink identification was confirmed by visual inspection of the data. Infomax restricted independent component analysis was used to remove blink artifact in the remaining EEG channels by constraining the data domain available to the procedure to the interval around the blinks. Data was inspected visually for the adequacy of artifact removal.

2.5 Stimuli

The stimuli studied were selected because of their importance for the understanding of consciousness in general and sedation/anaesthesia in particular. In this section the choice of stimuli is discussed and the technical details describing their generation and presentation provided.

2.5.1 Auditory Stimuli

Much work has been done on the impact of sedative anaesthetic medications on the processing of auditory stimuli. Several studies have shown the persistence of evoked activity in Heschl's gyrus but not auditory association areas during anaesthesia [67,149], although such findings have not been consistent [150,151]. Due to the robust activation seen in response to word tasks in several published fMRI studies of anaesthesia, it was envisaged that in addition to investigating this inconsistency, the inclusion of auditory tasks in the experimental paradigms presented in this work would provide a form of data quality control. This was of particular importance for the combined EEG/FMRI studies where, as described in chapter 2, the presence of EEG equipment in the scanner has the potential to degrade fMRI images.

Auditory stimuli were presented binaurally using MR compatible electrostatic headphones (MRC Institute of Hearing Research). Auditory volume adequacy was checked before each experiment by playing sample stimuli, in the case of the fMRI experiment, while the scanner was running.

Tones

Computer-generated tones of 1KHz for 60ms were presented, with a view to measuring auditory evoked potentials during bench EEG experiments. These were included in fMRI paradigms to investigate the differences between processing of complex and simple auditory stimuli.

Word Tasks

In the first series of experiments, a list of 12 words was repeated three times at each propofol dose. Different wordlists were presented at each state of consciousness. Playing this wordlist backwards generated meaningless sounds, acoustically similar (regarding volume, frequency distribution and duration) to the wordlist. The word lists were also used as the basis of a memory test [152]. At the end of each paradigm presentation, the subjects were presented with a list of 24 words, the original 12 words and 12 new words, in a random order and asked to identify which of the words they had previously heard. The false-positive count was subtracted from the true-

positive count to yield a "discrimination index" ranging from −12 to +12 with an expected score of 0 on guessing.

For the second series of experiments memory formation was not being studied and a different paradigm was developed. A list of 200 single syllable words was complied from the MRC Psycholinguistics Database (Machine Usable Dictionary v2.0) and recorded using Audacity (http://audacity.sourceforge.net/). The words were spoken by a male actor and matched for concreteness and imagery, and presented at a rate of one per second. The stimulus presentation program selected words from the list at random and presented them in pairs, one pair per minute at jittered inter-stimulus intervals. Subjects were asked to identify, using a two option button box, whether the two words were the same or different. Once a word had been presented it was discarded and was not used again. This task involved processing of a complex auditory task, decision making and generation of a motor response and was a simplification of the task presented in [153].

2.5.2 Noxious Stimulation

The key behavioural feature of anaesthesia is the loss of protective withdrawal to pain. While it is not possible to genuinely reproduce the level of pain that would constitute a threat or a surgical stimulus in an experimental setting, it was nevertheless important to study the way propofol affects cerebral processing of noxious stimulation.

Noxious thermal stimuli

Noxious stimuli were delivered for the first series of experiments (Chapter 3) by a purpose built, in-house designed thermode, applied to the dorsum of the left hand. This device rapidly heats to a specified temperature, maintains that temperature for 3 seconds, and because of the large surface area of the thermode energy is then rapidly dissipated. A thresholding procedure was performed before each experiment using thermal stimuli, to establish the temperature that reliably produced a pain rating of 7/10 on an 11-point numerical rating scale (0 = no pain, 10 = worst pain imaginable) was established. This temperature was then used for all experimental stimuli. Subjects were not aware that the stimulus would be of constant intensity.

Noxious laser stimulation

While thermal stimuli produce robust activation of the "pain matrix" during fMRI, it is more challenging to generate thermal stimuli of adequate precision and intensity to elicit cortical evoked potentials on the EEG. The rate of increase in cutaneous temperature is slow, absorption of the energy depends on skin factors and the control of heat delivery and transfer can be unpredictable. Of additional concern in the second series of experiments, involving a long series of many stimuli, was the risk of thermal damage to skin with repeated heating while unconscious.

Monochromatic radiant heat sources such as infrared laser circumvents these difficulties and elicit reliable cerebral potentials [154]. In EEG and combined EEG/fMRI experiments (Chapters 4 and 5), noxious laser stimuli (5ms duration, 5mm $1/e^2$ diameter, 1.34micron wavelength) were applied over a 6 cm^2 area, 2 cm above the lateral malleolus, on the right leg. Stimuli were generated by an infrared neodymium yttrium aluminium perovskite (NdYAP) laser (DEKA STIMUL 1340, Electronic Engineering, Italy), providing a highly reproducible nociceptive stimulus. This produced a characteristic double sensation, an initial sharp pin-prick followed by a brief more diffuse unpleasant ache. These sensations have been shown to be due to the selective activation of A-delta and C fibres, respectively, and are temporally separated by the differences in conduction velocities of these two types of fibres [155].

A thresholding procedure was performed before each experiment using laser stimuli to establish the energy level that reliably produced an intensity rating of 5/10 on an 11-point numerical rating scale (0 = no sensation, 10 = most intense sensation imaginable). Laser stimuli rated subjectively at 4-5/10 have been shown to reliably elicit evoked potentials in the scalp EEG without causing tissue damage [156]. This energy level was then used for all experimental stimuli. Subjects were not aware that the stimulus would be of constant intensity. To avoid skin damage the heat spot was slightly shifted within the demarcated stimulus area after each stimulus.

Details of the experimental paradigms including the number and presentation of auditory and noxious stimuli are given in the relevant chapters.

Chapter 3: Exploring neural correlates of sedation using propofol

Introduction

Movement, in the form of speech or facial expressions for example, is the only way humans can provide evidence to others of their awareness. Functional neuroimaging could potentially overcome this limitation allowing direct visualisation of the mechanics of consciousness. Investigations of consciousness and its impairment by drugs or disease will help move functional neuroimaging and clinical neuroscience towards that point. The experiments reported in this chapter, the first human functional neuroimaging studies of consciousness in this institution, had three aims. These were:

i) Development of protocols and procedures for the safe conduct of experiments involving anaesthesia, and establishing the feasibility of such investigations in this laboratory.
ii) Development of relevant stimulus paradigms capable of producing robust responses in the form of modality-specific BOLD signal changes in fMRI scans, anaesthetic modulation of which could be analysed.
iii) Acquisition and analysis of fMRI data in healthy volunteers, awake and during sedation with propofol, to investigate the effects of this drug on the central processing of external stimuli.

3.1 Protocols and procedures

The therapeutic index of anaesthetics is narrow and propofol, while an extremely safe drug in trained hands with appropriate equipment, can be fatal if administered inappropriately. Careful administration overcomes dose-related adverse effects but immune-mediated adverse reactions do occur, rarely but unpredictably. Anaphylaxis and anaphylactoid reactions occur during 1 in 6,000-10,000 anaesthetics [157]. The vast majority of these reactions are due to neuromuscular blocking agents, antibiotics or latex. Volunteers were asked about previous drug reactions and also about food allergies, specifically allergies to egg or egg proteins. The incidence of propofol anaphylaxis is reported to be 1 in 60,000 [1572]. Nevertheless, preparation for rare events is fundamental to safe anaesthesia practice and the laboratory was therefore set up with the capacity to deal with both dose-related and immune-mediated adverse effects. This project was purely research, with no benefit to

[2] Propofol is formulated in a lipid emulsion containing 10% soybean oil, 2.25% glycerol and 1.2% egg lecithin (a purified egg yolk component), the protein component of eggs (ovalbumin) is in the egg white. Evidence now suggests that egg allergic patients are in fact not more likely to develop propofol anaphylaxis than the general population.

volunteers arising from their participation. The required safety standards were therefore adhered to and where possible exceeded.

Published standards for the safe provision of anaesthesia in magnetic resonance imaging facilities were referred to [158]. The guidelines mandate the nomination of a consultant anaesthetist for any procedures, with anaesthesia assistance on a par with that available in the operating theatre. For each experiment, one of two senior anaesthetists was nominated as the responsible consultant and one other medical practitioner with advanced life support training was available for the duration of the experiment. Chapter 2 details the steps taken in terms of Ethics Committee oversight, the attendance of appropriately trained and equipped medical personnel, and the physiological monitoring throughout the experiments, to ensure the safety of participants.

Stimulation

Chapter 2 discusses the choice of auditory and noxious stimuli for study and the technical details of their generation and presentation.

Auditory processing under anaesthesia has been extensively investigated in behavioural, electrophysiological and neuroimaging studies and was therefore considered an excellent standard stimulus for initial experiments. Unconscious learning during propofol anaesthesia has been reported, where words presented during anaesthesia were identified upon recovery in word-stem completion and word recognition tasks, showing significant implicit memory formation [159,160]. However other groups have found any implicit learning to be weak [161], only associated with awareness [162], or entirely absent [163,164]. Persistent mismatch negativity (MMN) as well as intact but attenuated P100 and P300 components of the auditory evoked potential (AEP) have been reported during propofol sedation in patients with a Ramsay Sedation Scale (RSS) score of six (i.e. unresponsive to auditory or tactile stimulation) in the postoperative period [165]. However, electrophysiological monitoring of the depth of sedation during assessment was poor in this study and use of the RSS does not permit discrimination between patients just at the sedative threshold for loss of behavioural response and for those far more deeply sedated.

An fMRI study using sevoflurane showed auditory-related activation in response to word stimuli at 0.5 MAC that were limited to the thalamus and primary auditory cortex, but no such activations at 1.0 MAC [150]. At a propofol dose of 2 mcg ml^{-1}, BOLD activations in response to musical stimuli were preserved in the primary auditory cortex but attenuated in secondary processing areas of the superior temporal gyrus [149]. The same

pattern of auditory activation was later demonstrated at higher propofol levels (> 4.0 mcg ml^{-1}), at which the differences between activations elicited by words and those elicited by non-speech human vocal sounds disappeared [67].

Abolishing any experience of noxious surgical stimuli is the primary purpose of anaesthesia. In spite of this, there remains relatively little information on the way the brain processes noxious stimuli under the influence of anaesthetic drugs. If pain is a multidimensional experience with cognitive and emotional components, whether unconscious processing of the noxious stimulation of surgical tissue damage constitute an experience of pain is a matter of philosophical debate. From a practical perspective, surgical stimulation produces predictable physiological responses including hypertension, tachycardia and stress hormone release in the absence of any conscious experience. During balanced anaesthesia, analgesia is provided not by the hypnotic agent but by co-administered analgesics such as nitrous oxide, opioid and non-opioid analgesics or local anaesthetic regional block.

In one study, both thiopentone and propofol increased the pain threshold and reduced the amplitude of cortical evoked potentials following noxious laser stimulation [166]. While this study suggested some analgesic effect, a contradictory study reported increased ratings of thermal pain stimuli at propofol doses which did not impair cognition [167]. Specific inhibition of activity in the dorsal root ganglion has not been shown with either volatile anaesthetics or propofol [168,169].

Pain is perhaps then the ideal stimulus to study when investigating modulations of consciousness. Painful stimuli must by definition involve co-activation of distributed brain regions subserving the many dimensions of the percept, somatosensory, cognitive, affective and emotional that are fused into the conscious experience. Impairment of consciousness may separate these components or eliminate one or more of them, rendering the response to noxious stimulation just that, an electrical response that is not pain.

The first studies therefore involved a series of behavioural and fMRI experiments investigating the effects of propofol on cerebral processing of auditory and noxious stimuli at different steady state levels of sedation.

3.2 Methods

An experimental paradigm was developed which assessed cognitive impairment during propofol administration in order to define three behavioural states: awake, sedated and unresponsive.

During pilot sessions a number of tests were assessed and modified in order to select a simple task, suitable for use within the confines of the fMRI scanner that reproducibly measured the cognitive impairment caused by propofol. To assess sedation, the volunteer was timed reciting the letters of the alphabet, the days of the week and then the months of the year in sequence. The individual's sedated state was defined as the propofol effect site concentration (ESC) at which the verbal task was prolonged by 30% above baseline (awake), with a 10% tolerance. The unresponsive propofol level was taken as the level at which the volunteer no longer responded to verbal prompting. Loss of verbal contact was deliberately chosen as an end point as this is easily defined, testable and reproducible and used in both clinical practice and research as a definition of the transition from sedation to anesthesia [170].

Recruitment and participation

The study was approved by the local Research Ethics Committee. Eight healthy volunteers, four males and four females, between the ages of 21 and 37 were recruited to participate in the study. All subjects completed the protocol. The procedures for volunteer recruitment and assessment were as described in Chapter 2. The documentation provided for volunteers and the consent form signed are provided in Appendix A. Volunteers in this study participated in two experimental sessions, at least one week apart, and informed consent was independently obtained before each session. Each subject therefore completed the experimental protocol twice, first in a physiology laboratory, then again in the fMRI scanner. The purpose of the pre-scanning laboratory session was twofold, to ensure that subjects would safely tolerate the administration of propofol and to determine the subject-specific propofol effect site concentrations expected to produce the designated clinical sedation endpoints during the subsequent fMRI session.

Experiment setup

Volunteers attended each session, having fasted for the previous six hours as instructed. They had been advised to wear comfortable, loose fitting clothing and a short-sleeved top. A 20g peripheral intravenous cannula (BD Adsyte Pro^{TM}, Beckton Dickinson UK Ltd.), was inserted in the right forearm and connected to the propofol infusion pump. Nasal cannulae with two channels, one for oxygen delivery and the other an expired gases sampling line for capnography, were worn. Non-invasive blood pressure, pulse oximetry and ECG monitoring were established. The subjects were monitored continuously during both the pre-scanning and scanning sessions, as outlined in Chapter 2. During each session subject physiology was recorded both manually and electronically.

At the pre-scanning session the propofol ESC was determined individually for each subject for each of the defined cognitive states. This was achieved slowly by increasing the target ESC, by 0.2-0.4 mcg ml^{-1}, waiting for the target ESC to be reached and then asking the subject to perform the sedation assessment task. This was repeated until the desired clinical state was achieved. As this was time consuming, part of the design rationale was to determine the level at which each subject reached the desired state. In the scanning session, the predetermined ESC was targeted straight away. This resulted in an interesting problem. Five of the eight subjects became unresponsive at the target sedated ESC. If a subject was no longer responsive to verbal command at the sedated ESC as determined at the bench session, the order of the experiment was reversed so that the unresponsive fMRI data was collected first and then the target ESC was reduced in a stepwise manner mirroring the procedure at the bench until the criteria for the sedated state were met. As the criteria for state definition were behavioural, this may be regarded in one sense as controlling for order effects, however as discussed in chapter 4, this may be complicated by anaesthetic hysteresis.

Stimuli

Noxious thermal stimuli of 3 seconds duration were delivered by a purpose built, in-house designed thermode, applied to the dorsum of the left hand (see chapter 2). Twelve of these noxious thermal stimuli were delivered in each state of consciousness during each of the experiments. Subjects were asked to verbally rate the average intensity of these 12 stimuli on the same scale at the end of the "awake" and sedated blocks. The 12 thermal pain stimuli were presented (inter-stimulus interval mean±SD = 55±7 seconds), interleaved with auditory stimuli.

Auditory stimuli (see chapter 2) were presented binaurally with magnetic resonance-compatible electrostatic headphones (MRC Institute of Hearing Research, Nottingham, United Kingdom). Volume adequacy was checked before the experiment began.

A list of 12 words was repeated three times at each propofol dose. Different wordlists were presented at each state of consciousness. Playing this wordlist backwards generated meaningless sounds, acoustically similar (in terms of volume, frequency distribution and duration) to the wordlist. Computer generated tones provided a second, non-complex auditory stimulus. The full auditory paradigm consisted therefore of words, reversed words and 12 computer generated pure tones.

At the end of each paradigm presentation, the subjects were presented with a list of 24 words, the original 12 words and 12 new words, in a random order and asked to identify which of the words they had previously heard. The false positive count was subtracted from the true positive count to yield a "discrimination index" ranging from +12 to -12 with an expected score of 0 on guessing. Discrimination index was assessed after each paradigm presentation, before the infusion rate was changed, except for the unresponsive state, where memory recall was tested at the end of the experiment when awake and in the recovery area.

A thresholding procedure was carried out before each experiment started. Thresholding was performed after all monitoring was in place, the subject was comfortably settled in the position in which they would remain for the duration of the experiment and lighting was dimmed. At the bench experiment dimmed lighting served to mimic the conditions in the scanner room. Consistency of ambient conditions across thresholding and data collection was maintained. The thermode temperature that reliably elicited a subjective pain rating of 7/10 on an 11-point numerical rating scale (NRS) (0 no pain, 10 intolerable pain) was established. Then a volume for auditory stimuli was identified by each subject, which they could hear clearly but was not so loud as to cause discomfort. In the scanner experiment volume thresholding was carried out while the scanner was running to provide appropriate background noise.

3.3 Data analysis

FMRI summary statistics, cardiorespiratory observations, discrimination index and propofol effect site concentration were analysed using Minitab® Statistical Software (Minitab Inc, PA, USA). A p-value of <0.05 was considered statistically significant. Paired t-tests and repeated measures analyses of variance (ANOVA) were used as appropriate.

Each fMRI acquisition consisted of 664 volumes. Four "dummy volumes" were deleted before further processing to ensure the signal had reached equilibrium. Preprocessing was carried out as described in Chapter 2. Timeseries analysis of raw 4D fMRI data was carried out for each session using FILM (FMRIB's Improved Linear Modeling).

3.3.1 GLM-based analyses

First level analysis of paradigm-related changes in BOLD signal identified areas within individual subjects' brains responding to specific stimuli. The general linear model for this analysis consisted of two explanatory variables: (1) timing of auditory stimuli and (2) timing of noxious stimuli, each convolved to the expected haemodynamic response function. Motion parameters were included as covariates of no interest. For each voxel, the higher the parameter estimate from the model fit, the better the data can be explained by the stimulus, implying activity in response to the stimulus.

Group level analyses were performed using FEAT in order to assess a) the efficacy of the stimuli in eliciting BOLD responses in the awake state at baseline and b) significant changes in those BOLD responses due to propofol-induced changes in observed neurophysiological state. Group mean responses to stimuli at each state were calculated and states were compared using an analysis of variance (ANOVA) and paired t-tests.

To determine the statistical significance of the observed activations while controlling for multiple comparisons in each analysis step, Z statistic images were thresholded using clusters determined by $Z>2.3$ and a (corrected) cluster significance threshold of $p = 0.05$.

3.3.2 Connectivity Analyses

Region-of-interest-based connectivity analysis

Functional connectivity is defined as the temporal correlations between spatially remote neurophysiological events. Effective connectivity is the influence that one neuronal system or part of a system exerts on another. [171]. For example, if a painful stimulus is received, different regions of the brain will deal with different components such as somatosensory signals, the fear or sense of threat, the unpleasantness or the memory formation and learning required for future avoidance. Analysis of the functional connectivity of the primary somatosensory cortex will identify the network of areas subserving all facets of the experience but an effective connectivity analysis may reveal that activity in the prefrontal cortex (attention) rather than the primary somatosensory cortex (sensation) drives activation of the anterior insula (unpleasantness) [172,173] .

Detection of significant correlations between the BOLD signal timeseries of different brain regions is relatively straightforward methodologically and computationally, relative to the causal models required for effective connectivity studies. While they identify components of a distributed neural network, inferences cannot be drawn about the direction of inter-regional influences. In addition, correlated changes may indicate independent drive from a separate common source. Nevertheless, this approach to fMRI analysis is particularly useful in the study of consciousness, when the participation of certain brain regions in a distributed network and their contribution to the synthesis of a complete percept, may be altered.

In order to investigate changes in functional connectivity between brain regions, the individual subjects' mean BOLD signal timeseries from thirteen regions of interest, significantly activated by the stimuli in the group level analyses of the volunteers' awake scans, were extracted from each of the functional scans. Anatomical masks were hand drawn, without reference to functional activation maps, over these regions of interest. These masks, drawn in standard space, were then registered to each subject's functional space. For each subject, mean timeseries consisting of the 660 BOLD signal intensities were than extracted for the following regions: hippocampus, Broca's area, amygdala, anterior cingulate cortex, posterior division of the superior temporal gyrus, primary somatosensory cortex, thalamus, putamen, pontine tegmentum, precuneus cortex, primary auditory cortex, substantia nigra and insular cortex. Qualitative estimation of functional connectivity changes was done by calculating and plotting Pearson's correlation coefficients for pairs of regions of interest.

Whole-brain connectivity analysis

Two specific regions of interest were selected for further interrogation. The thalamus was chosen based on the extensive literature on its role in the neurophysiology of consciousness [90,92,174]. The putamen was included due to the striking observation of changes in striatal responses to both types of stimulation (noxious and auditory) across states of consciousness in the previous analyses.

The functional connectivity of the thalamus and putamen was calculated for each subject, at each level of consciousness. This was done using a general linear model within FEAT, with regressors at the first level derived this time from the mean signal timeseries of two specific regions of interest – thalamus and putamen. Multiple comparisons constraints and significance thresholds were as for the stimulus based analyses. Repeated measures ANOVA across levels of sedation identified areas of the brain where the functional connectivity to the thalamus or the putamen was significantly altered by deepening sedation.

3.4 Results

3.4.1 Physiology and behavioural parameters

Repeated measures ANOVA confirmed statistically significant differences ($p<0.001$) in propofol levels between conditions, (Figure 3.1(a)) although the folly of basing either experiments or clinical practice on ESC without additional means of depth of anaesthesia assessment is clearly illustrated by the overlap in dose ranges between the sedated and unresponsive states. Haemodynamic changes of non-functional origin can be a concern when analysing the BOLD signal during drug manipulations; however, differences in blood pressure, heart rate, oxygen saturation and carbon dioxide level levels between conditions, were non-significant during both bench and scanner experiments (Figure 3.1(b,c,d)).

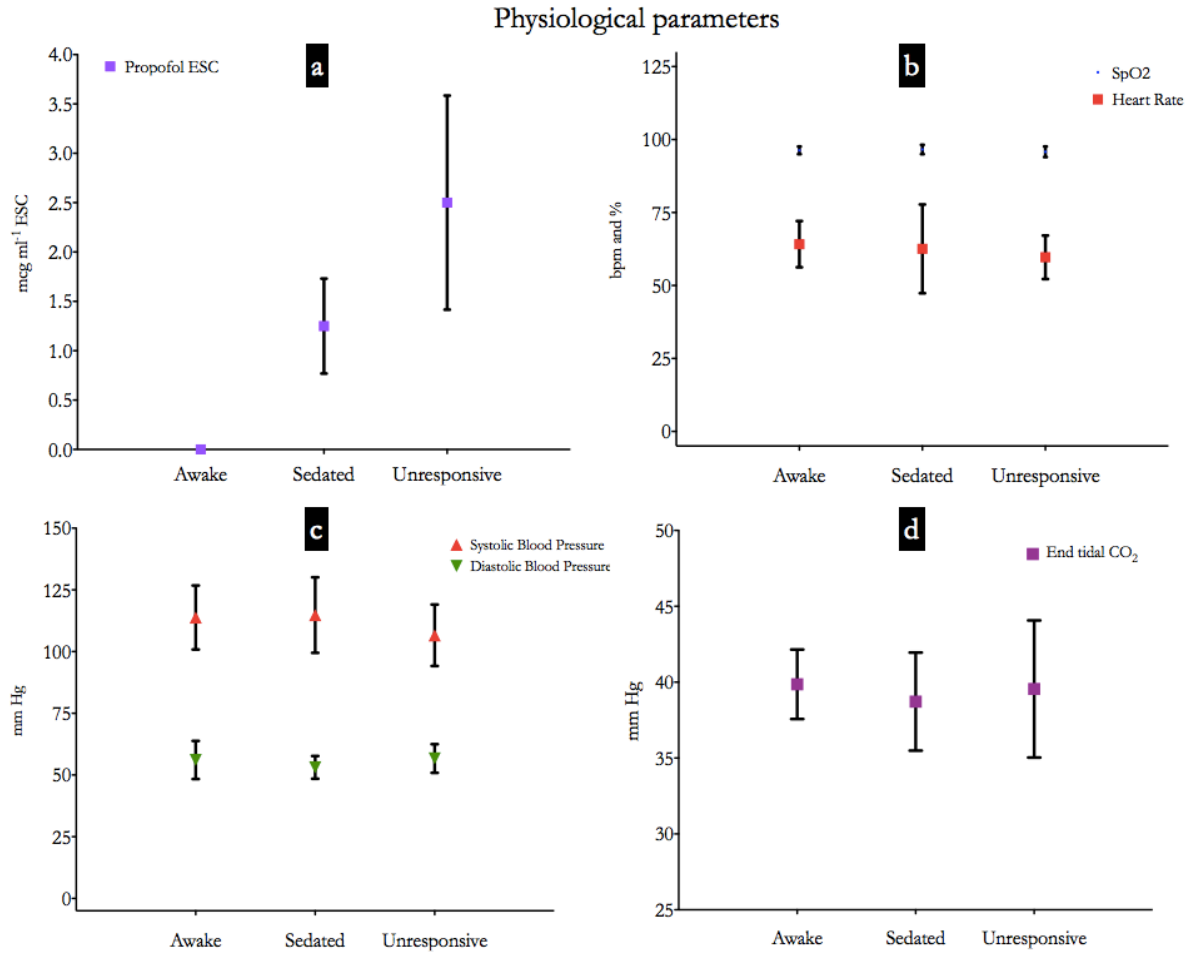

Figure 3.1 Physiological parameters during the scanner experiment. There was a significant difference in propofol levels between states (a). There were no significant changes in haemoglobin saturation or heart rate (b), blood pressure (c) or end tidal carbon dioxide levels (d) across the three states. ESC-effect site concentration; SpO2 haemoglobin saturation; CO2-carbon dioxide; data are mean ± SD.

To assess any global changes in BOLD signal with propofol that may have impacted statistical analyses, the mean of the BOLD signal during each scan was calculated for an array of regions of interest (ROIs). Anatomical ROI maps derived from the Harvard-Oxford cortical and subcortical atlases were registered into subjects' functional space and the mean BOLD signal timeseries under each translated map extracted. No significant systematic change was identified in the underlying BOLD signal across the levels of consciousness (ANOVA-GLM, $p = 0.791$), suggesting that changes in BOLD responses to stimulation at each level of sedation were more likely to be a result of changes in brain activity than changes in the baseline BOLD signal (Figure 3.2).

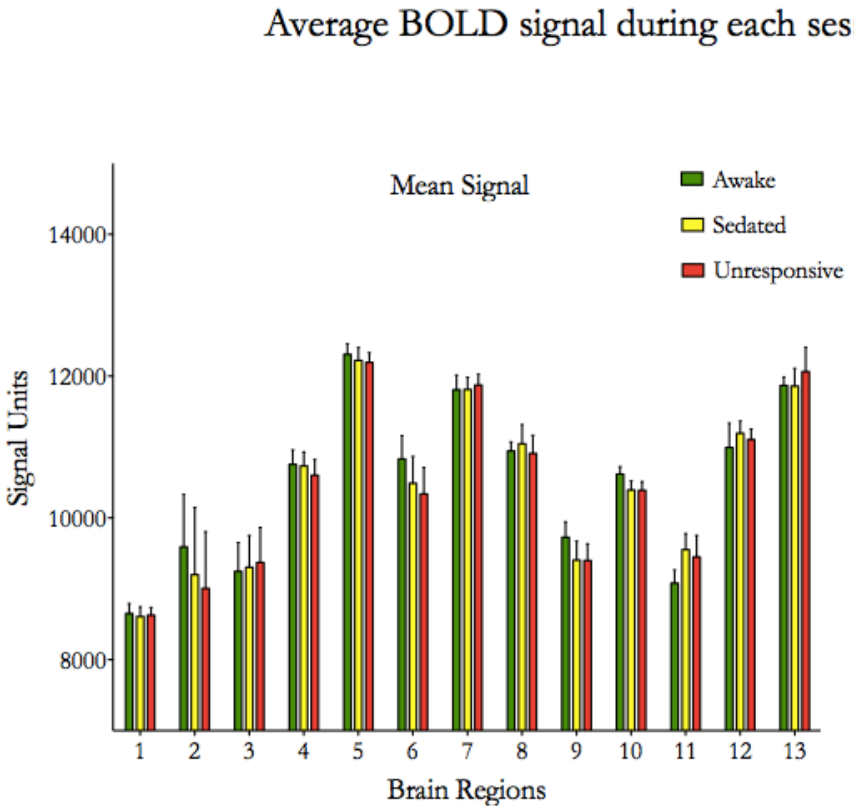

No.	Region
1	ACC
2	Amygdala
3	Broca's Area
4	Hippocampus
5	Insula
6	Midbrain
7	PAC
8	PCC
9	Pons
10	Striatum
11	S1
12	S2
13	Thalamus

Figure 3.2 Mean and standard deviation of the BOLD signal from the thirteen regions of interest (ROIs) at each levels of sedation i.e. awake, sedated and unresponsive. No significant difference in the mean BOLD signal was found between conditions (repeated measures ANOVA, $p > 0.791$).

The sedated condition was defined by a prolongation of the time taken for the performance of a verbal task at the non-scanning session. In the scanning session, the time required for completion of the verbal task *was* significantly longer (paired t-test: $p = 0.002$) when sedated compared to "awake" (figure 3.3(a)), confirming that this criterion was adhered to for all subjects including those who were scanned in reverse order. Discrimination

index decreased significantly with increasing depth of sedation (repeated measures ANOVA $p<0.001$) (figure 3.3(b)). There was no significant difference between pain ratings when the "awake" and sedated conditions were compared (paired t-test, $p = 0.291$). In this group of subjects, no psychophysical evidence was found for either an analgesic or a hyperalgesic effect of propofol.

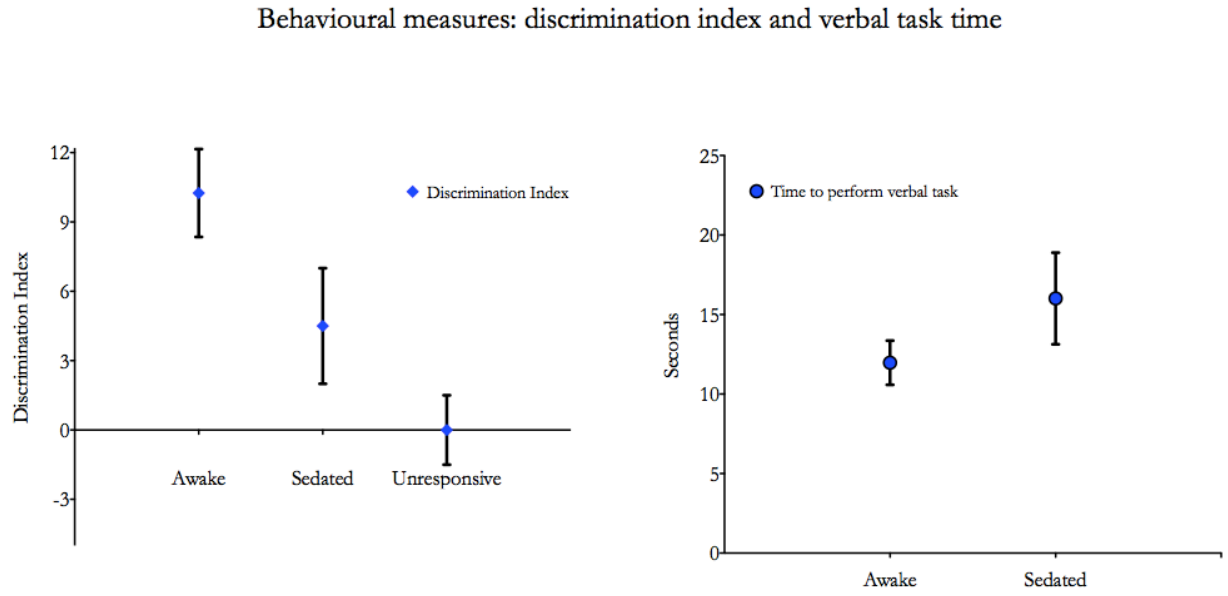

Figure 3.3 Discrimination index and time taken for verbal task completion. The plot on the right illustrates the methodology used to define the sedated state (i.e. a significant impairment in the time taken to perform a verbal task) and the plot on the left shows the associated deterioration in memory. The high score on the discrimination index at baseline (awake) was significantly reduced in the sedated state. When subjects were asked to identify words in a list that had been played while they were unresponsive, their discrimination index was no better than would be obtained by chance.

3.4.2 BOLD responses to stimulation - Group Mean Activations

Noxious thermal stimuli

Awake, noxious thermal stimuli produced significant BOLD signal changes across a network of regions. Activation occurred in the insula (anterior and posterior), thalamus, putamen, anterior cingulate cortex (ACC) and cerebellum bilaterally and in the primary somatosensory cortex, as shown in Figure 3.4. These are areas of the brain often described as belonging to the "pain matrix": an array of brain regions that represent the widespread sensory, cognitive, affective and behavioural responses to noxious stimulation to produce the multidimensional experience that is "pain" [175]. The thermode was therefore shown to provide a reliable noxious stimulus, eliciting both reported pain and BOLD signal changes in the absence of actual tissue damage.

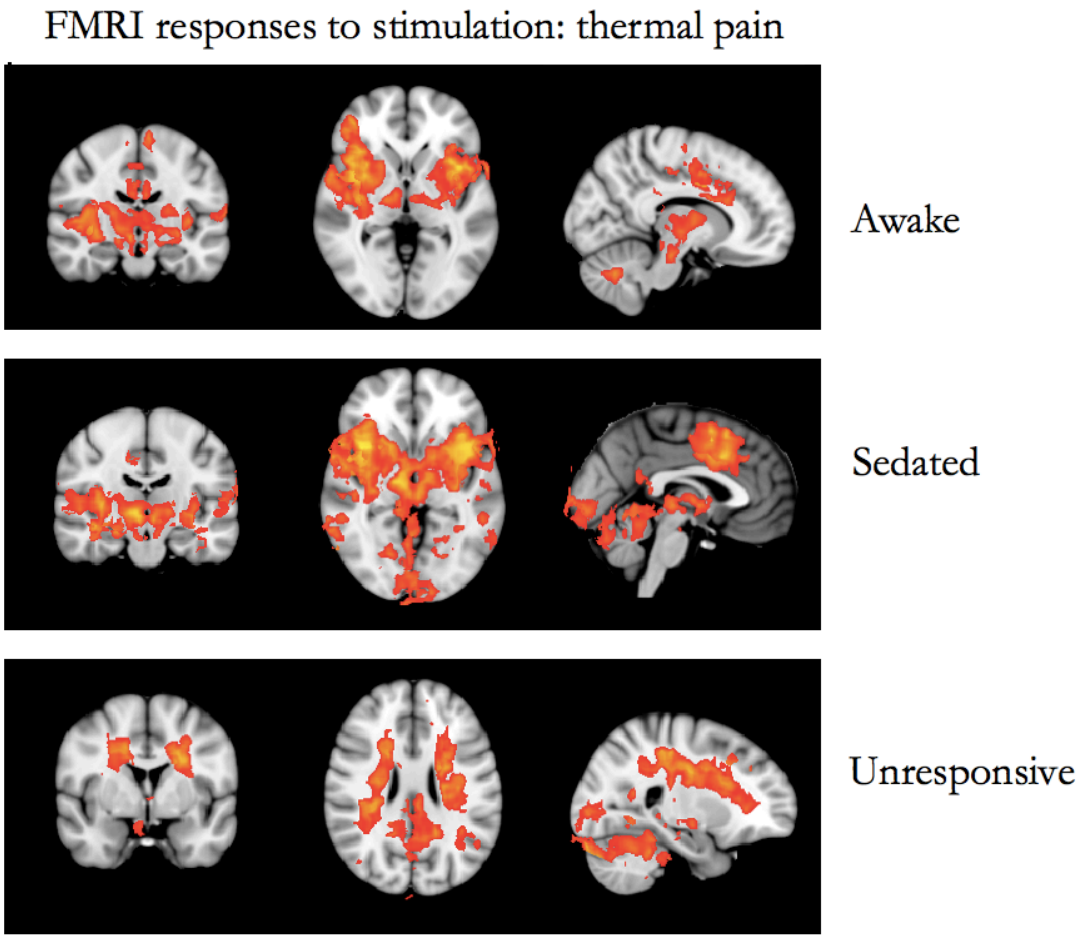

Figure 3.4 FMRI responses to noxious thermal stimulation in each of the three conditions. In the awake condition robust activation is seen in the primary somatosensory cortex, the insula, cingulate, thalamus and putamen bilaterally. This activation persists in the sedated condition but disappears when subjects are unresponsive, with only artifactual white matter patterns seen. In subsequent experiments, BOLD signal changes attributable to white matter are removed in the denoising process (technique described in chapter 2, used in chapters 5 and 6). However this technique was not being used at this time.

Robust activation in response to noxious stimulation persisted in sedated subjects. A paired t-test comparing thermal pain response parameter estimates in the awake and sedated conditions showed no significant difference in brain activation. It is interesting that areas normally showing attenuated BOLD responses with analgesia (thalamus, S1, ACC, prefrontal cortex, posterior insula) were not significantly attenuated by low dose propofol, consistent with the absence of any significant change in the pain ratings reported by the subjects. As discussed in the introduction to this chapter, propofol is an anaesthetic with weak if any analgesic action [176], which has even been associated with an increase in the subjective experience of noxious thermal stimulation [167]. It would be difficult to disambiguate the cognitive effects of sedative levels of propofol from any analgesic or hyperalgesic effect it may have. It has been suggested that purported hyperalgesia may be related, in some

instances, to an impairment in cognitive modulation of pain perception [177]. In the unresponsive condition, activation was not observed in any cortical or subcortical structures, (only white matter artifact was seen), indicating that loss of behavioural responsiveness was associated with loss of measurable cerebral responses to noxious stimulation.

Auditory stimuli

Words produced widespread activation within bilateral temporal lobes (superior and middle temporal gyri), parietal somatosensory areas, thalamus, putamen, anterior cingulate and frontal opercula in awake subjects (Figure 3.5).Beeps and words played backwards did not activate anterior cingulate or opercular cortices but did produce a response in the temporal lobes and the thalamus, as well as a small region within the right inferior frontal gyrus. The responses were specific to the complexity of the presented stimulus and the degree of broader cognitive/associative processing entrained (Figure 3.5).

Once sedated, the spatial extent of temporal lobe BOLD signal changes to both words and meaningless sounds was reduced. Words continued to produce activation within the frontal operculum but activation in response to meaningless sounds was confined to the primary auditory cortex. When subjects were unresponsive, meaningless sounds were not associated with any measurable change in BOLD signal. Words continued to elicit responses in the brainstem and thalamus, the primary auditory cortex and the primary somatosensory cortex but more rostral activations had ceased.

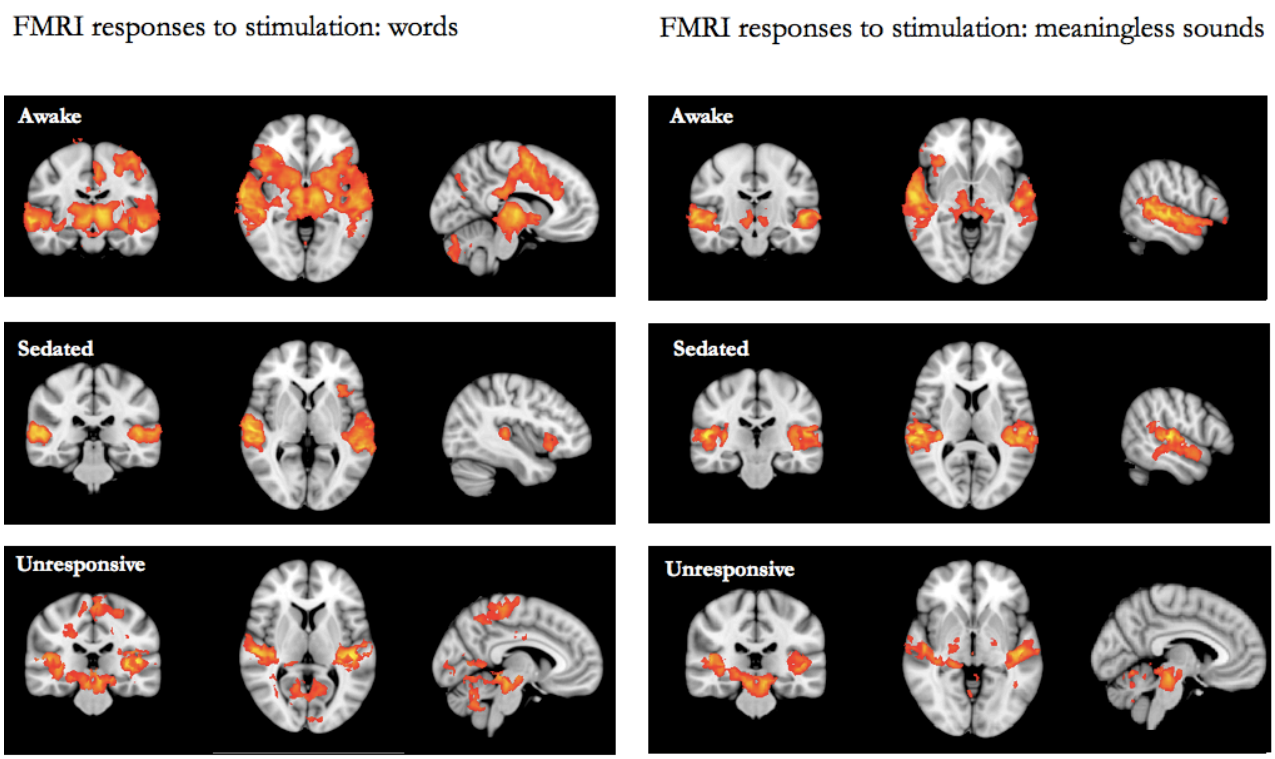

Figure 3.5 FMRI responses to words when awake (top left) involve widespread bilateral activation within the temporal lobes, frontal opercula, primary somatosensory cortex, thalamus and putamen while awake but this activation is limited to primary processing areas once sedated (middle left). The reduced activity persists however during the unresponsive state (bottom left).

FMRI responses to meaningless sounds (beeps and words played backwards) were less extensive when awake (top right), limited to the thalamus and primary auditory cortex. This activation was seen consistently however, in both the sedated (middle right) and unresponsive (bottom right) states.

3.4.3 BOLD responses to stimulation - ANOVA

The results of the analysis of variance revealed the areas where propofol caused significant changes in the BOLD signal responses to auditory and noxious thermal stimulation. Activations by noxious stimuli showed significant bilateral reductions in the anterior insula and reductions in the putamen and globus pallidus contralateral to the stimulus (Figure 3.6). BOLD signal changes in response to binaurally presented auditory stimuli showed significant bilateral reductions in both cortical and subcortical regions with deepening sedation (Figure 3.6). This was seen in the anterior insula, anterior cingulate cortex and superior temporal gyrus, bilaterally. The significantly modulated subcortical structures were the putamen, pallidum and amygdala, again

bilaterally. Paired t-tests comparing the states showed that responses to noxious thermal stimulation disappeared between the sedated and unresponsive states while the responses to auditory stimulation showed a reduction in activation between the awake and sedated states and a further reduction between sedated and unresponsive states, with persistent modality specific activation detectable even in unresponsive subjects. Post hoc paired t-tests showed that these differences represented a reduction in activation with increasing levels of propofol

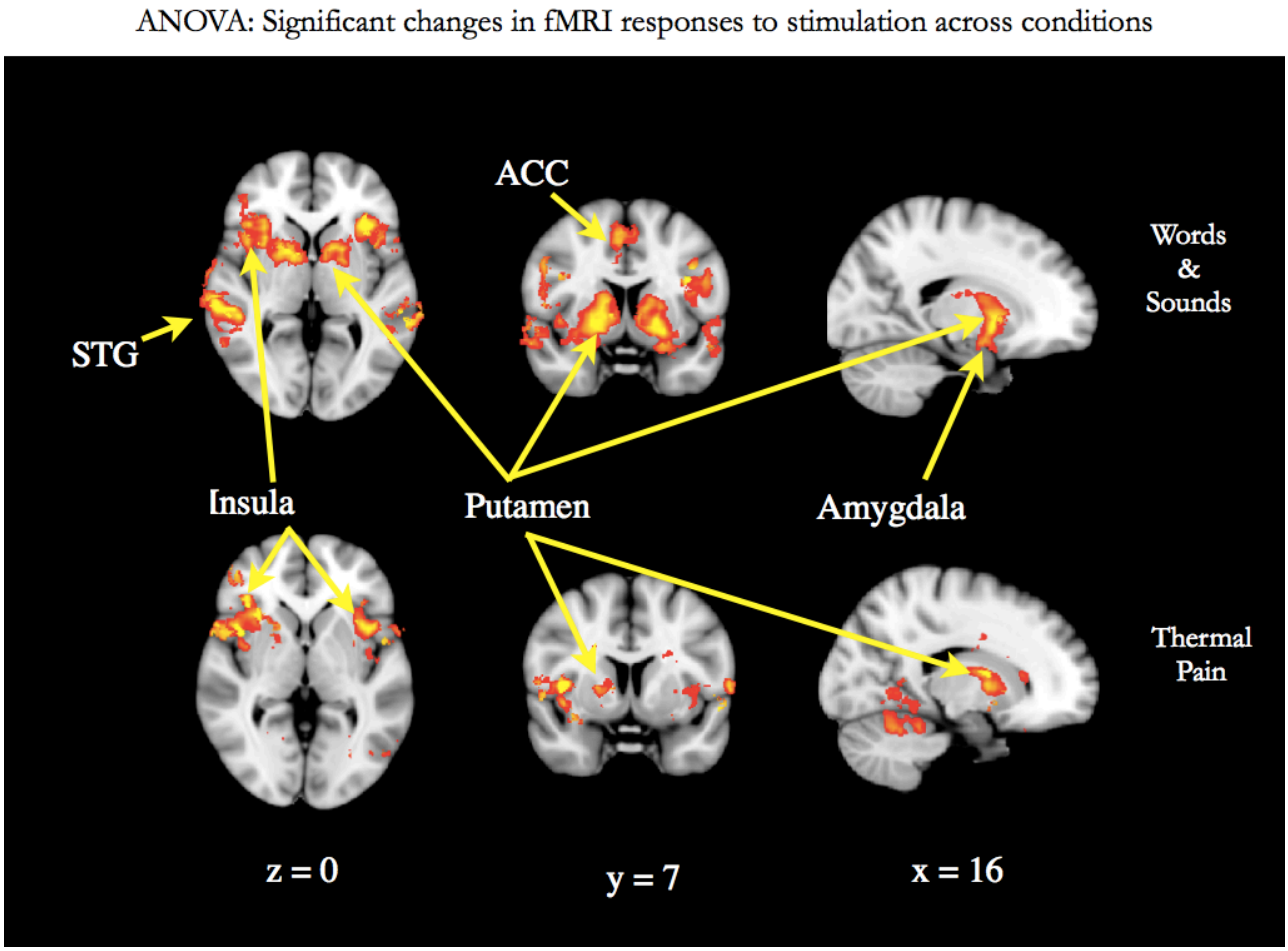

Figure 3.6 Changes in activation patterns between auditory and thermal pain conditions. The upper row of images shows the regions where there was a significant difference in the BOLD response to auditory stimulation (all stimuli, words, beeps and meaningless sounds included) when the state of consciousness changed. This occurred in the insula, anterior cingulate cortex, superior temporal gyrus, amygdala and putamen bilaterally.

The lower row of images shows that there was a significant decrease in activation in the anterior insula and the putamen in response to thermal pain with increasing doses of propofol.

3.4.4 Connectivity Analysis

The term functional connectivity refers to significant correlations in signal changes between regions of the brain. Co-activation of brain regions implies only that regions are simultaneously involved in a process. It does not imply that activity in one region produces activity in another. This experiment was not designed for an effective connectivity analysis; however, co-activations were investigated. For the 13 regions of interest interrogated, Figure 3.7 illustrates the strength of the timeseries correlation between regions and the modulation of this correlation that was found to occur with neurophysiological state change. We found that the correlation between the thalamus [red circle] and the regions of interest was minimally changed despite the clinical observations. The only exception was a reduction in connectivity between the thalamus and the putamen. While thalamic connectivity appeared to be thus preserved, we found a clear reduction in the strength of the correlation between the BOLD signal from the putamen (blue circle) and those same regions of interest.

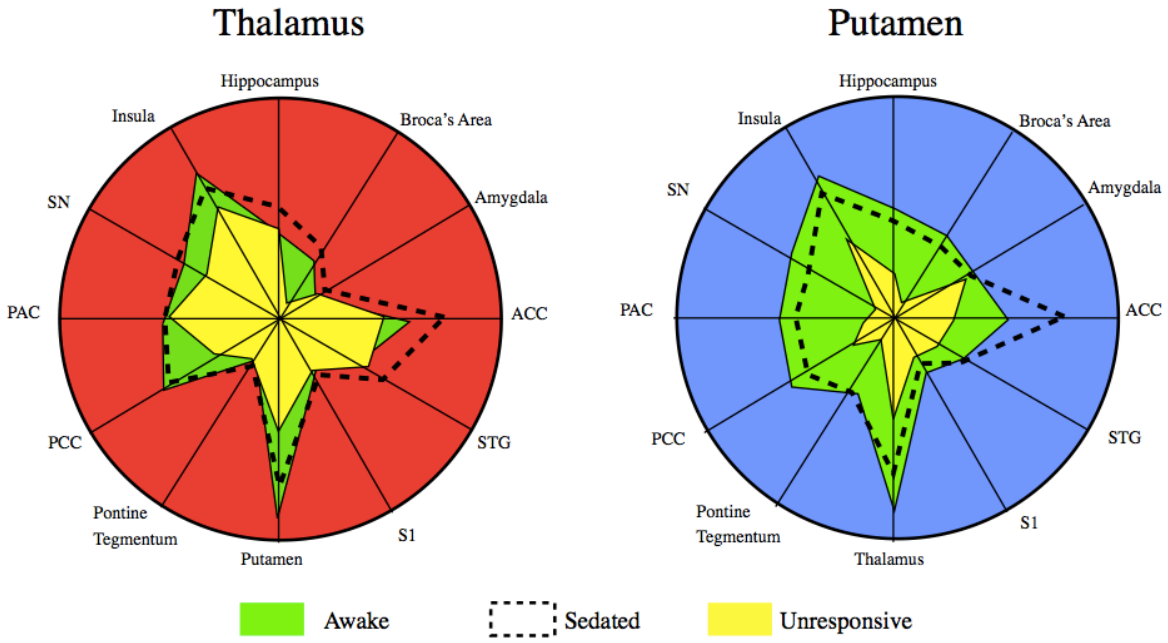

Figure 3.7 Correlation between the mean timeseries of 12 regions of interest and the thalamus (left) or putamen (right). This schematic illustrates changes in functional connectivity. Each region of interest whose connectivity was investigated occupies a point on the unit circle. For each condition (awake, sedated, unresponsive) the strength of timeseries correlation (from 0 to 1) between each region and the node of interest (thalamus or putamen) determines the length of that regions's 'arm' in the star. The green star shows the correlation when awake, the dotted line shows the correlation when sedated and the yellow star shows the correlation when unresponsive).

Correlation implies functional connectivity. The functional connectivity between the putamen and a number of regions can therefore be seen to be reduced in the unresponsive state, when the functional connectivity of the thalamus is not.

This investigation provided a qualitative exploration of the data, suggesting a decrease in striatal co-activation with other brain regions during sedation. Formal statistical evaluation of the suggested pattern of connectivity modulation was provided by the voxel-wise fMRI analysis based on regressors derived from seed regions in the thalamus and putamen. The results of the repeated measures ANOVA are shown in Figure 3.8. This gives a spatial map of those areas where connectivity was identified as being significantly altered across the defined states of consciousness. With respect to the thalamus, we found statistically significant decreases in the functional connectivity *only* with the putamen and a small region within the left posterior insula. However, statistically significant changes in functional connectivity with the putamen were widespread and confirmed the relative neurophysiological isolation of the putamen from other relevant structures, as suggested by our qualitative analysis of the signal correlation.

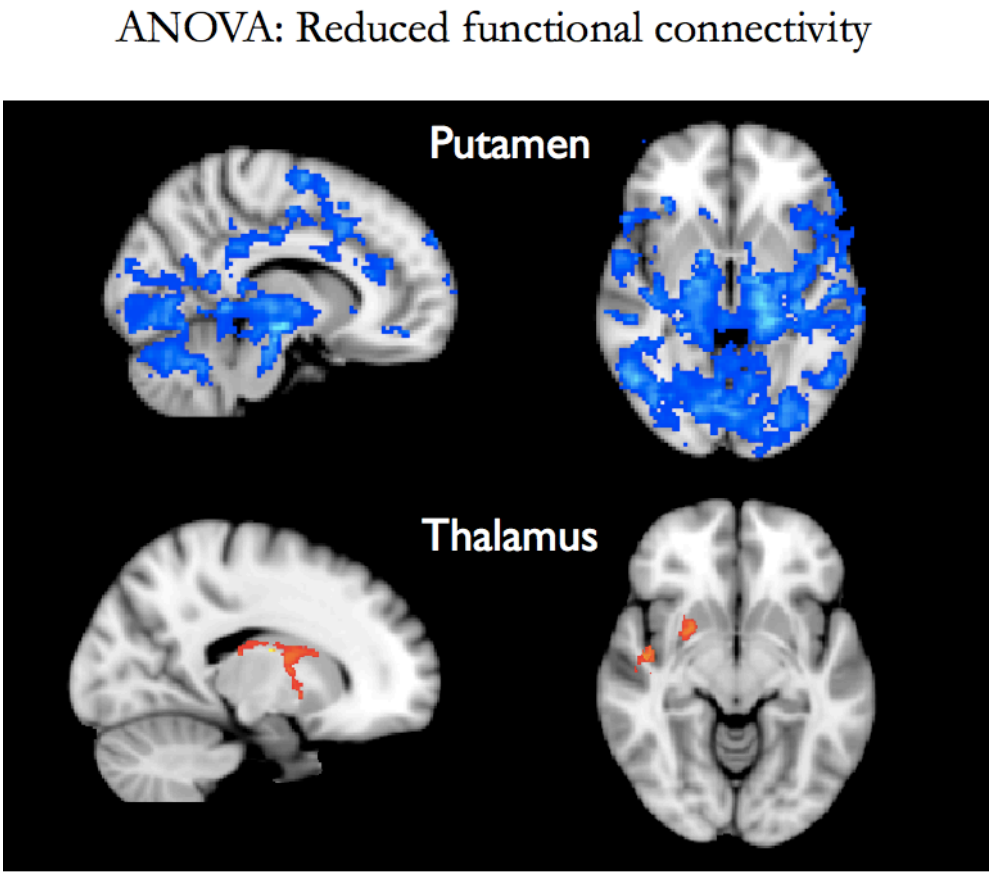

Figure 3.8 ANOVA of functional connectivity changes with (top, blue) the putamen and (bottom, red) the thalamus. This shows that, consistent with the changes in correlation between the local mean timeseries (figure 3.7), functional connectivity between the putamen and many brain regions (including thalamus, insula, anterior cingulate, temporal and lateral occipital cortices) decreased with impaired consciousness. The only region found to have a significant reduction in functional connectivity with the thalamus, was the putamen. Other regions maintained their connectivity with sedation, as suggested in figure 3.7.

3.5 Discussion

In this study, increasing levels of propofol produced the expected changes in behaviour: a reduction in verbal task performance, increasing memory impairment and failure to respond. Movement suppression during anaesthesia has been shown to occur at least in part at a spinal level [178,179]. Propofol has been shown to produce immobility through the suppression of activity in the ventral horn of the spinal cord [180]. The range of propofol levels at which responses to verbal stimulation is lost has been reported as 1.3-4.3 mcg ml^{-1} in healthy surgical patients under controlled conditions of single drug administration. The same study found that the range of propofol ESCs required to prevent a movement on incision was 2.8-7.5 mcg ml^{-1} [111]. As significantly higher levels of propofol are generally required to produce surgical immobility than were reached in this experiment, the behavioural state we defined as unresponsive is unlikely to be due to anaesthetic immobility but rather due to loss of consciousness with failure of perception.

ANOVA produced a somewhat unexpected result in terms of modulation of responses to stimulation at increasing levels of propofol. Stimulus-induced activity in the putamen, but not in the thalamus, significantly decreased as consciousness was reduced to the point of loss of response to verbal stimulation. This finding was further interrogated with an analysis of the functional connectivity of these structures. During the transition from awake to unresponsive, a clear reduction in functional connectivity between the putamen and a wide range of other cortical and subcortical regions occurred, while the connectivity of the thalamus with these regions was maintained. The thalamus and the putamen appear to be differentially influenced by anaesthetics.

Evidence for a thalamo-cortical switch

Studies of sleep and anaesthesia have suggested that recruitment of endogenous sleep promoting pathways may be a final common outcome of the diverse actions of anesthetic drugs [27,34,79,181]. The common denominator in studies of both sleep and anesthesia is often the observation of a proportionally greater reduction in the metabolic activity and/or blood flow within the thalamus compared to other brain regions.

Regional cerebral blood flow (rCBF) was measured with positron emission tomography over the course of a night's sleep in 37 male volunteers. Profound decreases in rCBF were seen during slow wave sleep (SWS) in the brainstem, thalamus and basal forebrain, each of which showed recovery of rCBF during REM sleep [32]. These results have been reproduced by other groups [182].

The reduction in thalamic glucose metabolism with lorazepam is closely correlated with the degree of sedation [183]. While early functional neuroimaging of isoflurane anaesthesia in healthy volunteers (n=5) showed only a uniform global reduction in glucose metabolism [184], later work by the same group identified a change in the pattern of glucose metabolism under halothane. Relative reductions were found in the thalamus, basal forebrain, cerebellum and occipital lobes [91]. A study in eleven subjects given isoflurane or halothane reproduced these findings with relative reductions in glucose metabolism in the thalamus, midbrain, basal forebrain and cerebellum [90]. This pattern has also been identified in the regional cerebral blood flow changes seen with Xenon anaesthesia [185]. The reduced thalamic activity reported during sleep and anesthesia may reflect a direct change in the activity of thalamic nuclei, which then inhibits thalamo-cortical transmission. Alternatively, reduced excitatory input to the thalamus from other sites may lead to the observation of reduced local blood flow and metabolism [93,186].

Overall these observations have contributed to the concept that a change in thalamic information transfer to the cortex is pivotal in producing sleep or an unconscious state and a thalamo-cortical "switch" has been proposed. This 'switch' idea is supported by the association between reduced thalamic activity and disorders of consciousness. Following traumatic brain injury (TBI), thalamic hypometabolism is more marked in patients with VS and MCS than in those with post-traumatic amnesia who in turn have lower thalamic metabolic rates than recovered patients or healthy controls [187,188].

Evidence against a thalamocortical switch

In contrast with the consistent picture of specific thalamic deactivation with volatile anaesthetics described above, propofol reduces relative metabolism in cortical regions, specifically frontal and parietal lobes [92,130,131]. Bonhomme and colleagues found cortical activation to be reduced at lower doses than those required to reduce activation within the thalamus during propofol administration[189]. Midazolam also reduces cortical and thalamic metabolism in parallel [190]. Inferences about connectivity between brain regions based on techniques with relatively poor temporal resolution, such as PET, may not be appropriate. Preservation of thalamocortical connectivity during anaesthesia has been observed in an investigation of local field potentials (LFPs) in animals under isoflurane, even during deep anaesthesia with burst suppression [191]. As the picture of selective thalamic deactivation and thalamo-cortical uncoupling is not consistent across anaesthetic agents, it is perhaps unlikely that a block in information transmission at the level of the thalamus is common site of action.

As a model of anaesthesia, physiological sleep is of course inadequate due to preservation of protective arousal. Failure of arousal upon intense sensory input during anaesthesia limits the parallels that can be drawn. Disordered or failed perception with failure of arousal in response to intense stimulation is however seen in a number of pathological conditions, consideration of which may form the basis of useful alternative analogues.

Tononi and Edelman propose that activation and deactivation of distributed neural populations in the thalamo-cortical system is probably not itself a sufficient basis for conscious experience unless activity of the relevant neuronal groups subserving that experience is rapidly and effectively integrated. Each moment of consciousness is composed of independent components, from which specific experience is synthesised. They propose that the fusion of differentiated processes into a single conscious experience may be achieved by re-entrant, synchronised oscillations in the groups of thalamo-cortical and cortico-thalamic neurons [186].

The phenomenon of blindsight illustrates the interdependence between the spatially distributed encoding of specific aspects of sensory experiences and the integration of these subprocesses into a conscious percept.

Visual field perimetry accurately reveals defects (scotomata) due to lesions in the corresponding striate or primary visual cortex (V1) on the medial aspect of the occipital lobe. Such lesions are associated with a lack of awareness of visual stimuli presented within the scotoma. In 1974, Weiskrantz et al reported the results of visual field testing in a patient with hemianopia following excision of an occipital lobe arteriovenous malformation.

They found that while the subject reported no awareness of stimuli presented within the scotoma, when pressed as to "guess" certain features such as colour, shape or orientation, the guess was correct significantly more frequently than would be expected by chance [192]. This "blindsight" has been well described in subjects in whom some or all of the striate cortex has been destroyed. The residual capacity to detect features of stimuli not consciously perceived has been associated with the development or strengthening of a pathway from the contralateral lateral geniculate nucleus to the ipsilateral motion area of the temporal lobe (MT/V5) and possibly with an interhemispheric connection between MT/V5s [193]. Extrastriate pathways, conveying information on aspects of visual stimuli that are not consciously perceived, can bypass V1. This illustrates that while primary sensory processing is not sufficient for conscious perception, it is necessary. It also shows that in the absence of integration of all the necessary components of an experience, conscious perception does not occur.

Basal Ganglia Circuits

How are these re-entrant loops recruited and sustained? A potential role for circuits through the basal ganglia is clear within this construct. The functional neuroanatomy is briefly reviewed here and figure 3.9 gives a schematic of the connections of the basal ganglia.

The basal ganglia comprise the striatum (caudate, putamen), the globus pallidus (internal and external GP), the subthalamic nucleus (STN) and the substantia nigra (SN). They exert control on motor, oculomotor, emotional, associative and cognitive function within the brain [194]. This is achieved through the modulation of inputs from cerebral cortex [195]. Di Martino reported a resting state fMRI study in humans demonstrating functional organisation consistent with the existence of parallel loops through the basal ganglia, potentially subserving the multiple integrative functions as required by for conscious perception [196].

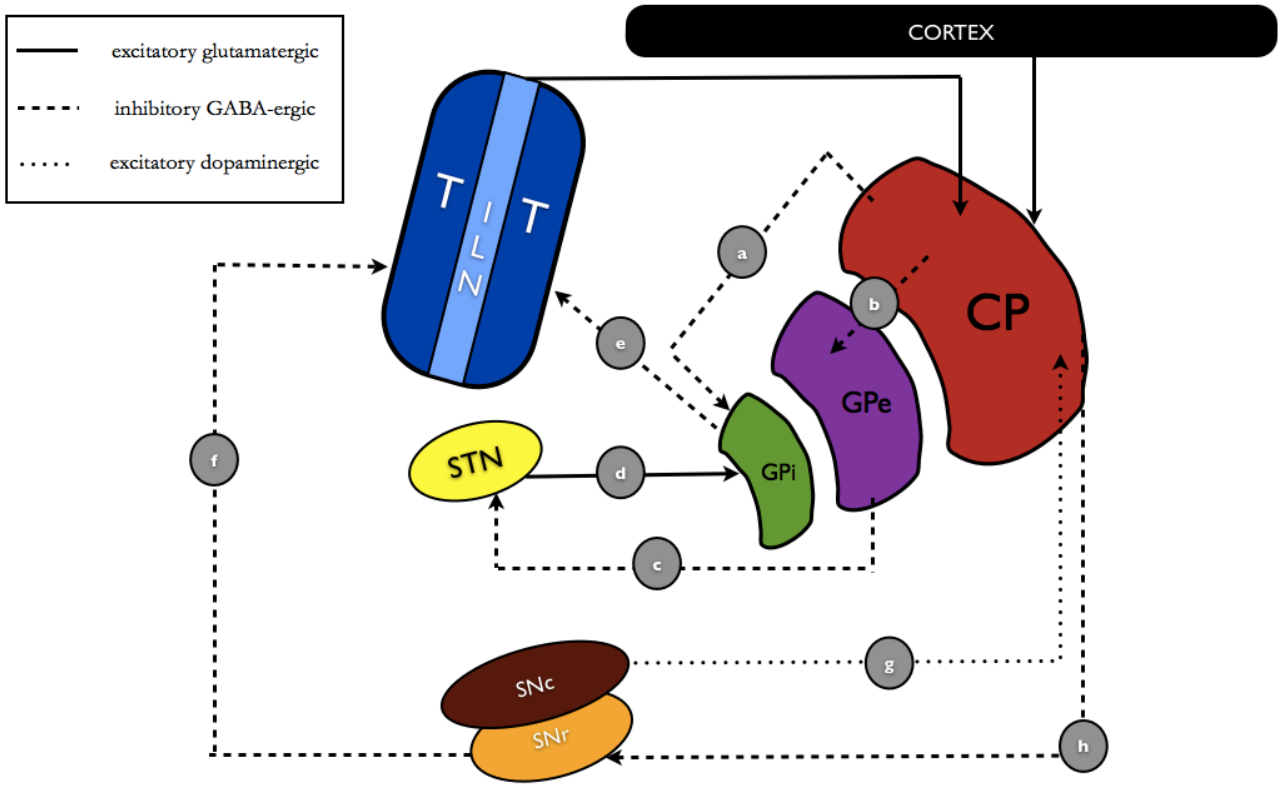

Figure 3.9 Schematic of circuits through the basal ganglia that modulate thalamocortical transmission. The circuitry serves to balance excitation and inhibition of thalamocortical neurons through a series of inhibitory and disinhibitory (inhibition of inhibition) activities.

The caudate/putamen (CP) is the principal site of signal entry to the circuit. The internal globus pallidus (GPi) and substantia nigra (SNr) are the output nuclei and they project to specific and non-specific thalamic nuclei. Transmission of an excitatory signal to the CP though the circuits to the GPi and SNr modulates the tonic inhibition they exert on thalamocortical neurons. The CP receives glutamatergic afferents from the cortex and the intralaminar nuclei of the thalamus, and dopaminergic afferents from the substantia nigra pars compacta (SNc) (g).

Striatal output neurons that are part of the direct pathway (a) inhibit the inhibitory output of the GPi (e), disinhibiting the thalamus and increasing thalamocortical transmission. Direct output neurons also project to the substantia nigra pars reticulata (SNr) (h) inhibiting its inhibition of thalamic nuclei. Striatal output neurons that are part of the indirect pathway (b) inhibit the output of the external globus pallidus (GPe) (c), thus reducing its inhibition of the subthalamic nucleus STN, promoting STN excitation of the GPi (d). Thus inhibition of thalamocortical transmission by the GPi is promoted.

CP - caudate/putamen; GPi - internal globus pallidus; SNr - substantia nigra pars reticulata; SNc - substantia nigra pars compacta; GPe - external globus pallidus; STN - subthalamic nucleus.

Neuronal circuits through the basal ganglia form parallel segregated closed loops, from a functionally specific region or group of regions of the cerebral cortex to the basal ganglia and back to the same cortical areas. They appear early in evolution and are well conserved in vertebrates [197]. The striatum and subthalamic nucleus constitute the input portals to these loops. The primary inputs are multiple overlapping glutmatergic corticostriate projections. Modulatory inputs include glutamatergic projections from the midline and intralaminar thalamic nuclei (ILN), dopaminergic projections from the substantia nigra pars compacta (SNc) and serotonergic projections from the DRN. The cholinergic peduncolupontine nucleus (PPN), part of the ARAS, forms reciprocal connections with each of the basal ganglia [198]. In fact projections from the striatum to the PPN have been implicated in control of the sleep-wake cycle [199]. The transition from slow wave sleep (SWS) to REM sleep is associated with a large increase in blood flow to the striatum [32].

Inhibitory GABA-ergic medium spiny neurons project from the striatum directly to the main output nuclei, the internal GP and substantia nigra pars reticulata (SNr). They also project indirectly to the output nuclei via the external GP (inhibiting its GABA-ergic inhibition of the subthalamic nucleus which is excitatory to internal GP and SNr) antagonising the effect of the direct pathway on output nuclei. The direct pathway therefore decreases the output of the basal ganglia while the indirect pathway increases it [194].

Basal ganglia output from the internal GP and STN comprises GABA-ergic projections to the thalamus, midbrain and medulla. Somatopy is maintained through the circuits and the output modulates the activity in the thalamocortical neurons in which the signals originated, filtering out uncorrelated inputs [200]. This produces reinforcement of some signals and suppression of others, contributing to error detection and suppression, attentional modulation, response selection and motor planning [194].

It is perhaps unsurprising to find that the striatum is specifically vulnerable to lower doses of anaesthetics, considering the frequency with which transient dystonic movements are observed during the induction of anesthesia [201]. Observations similar to those in this experiment have been noted in other contexts by researchers investigating somatotopy within the striatum of anesthetized animals [202]. This group noted that both spontaneous and stimulus-induced activity within the striatum was exquisitely sensitive to different anesthetic agents. These changes occurred prior to changes in S1 responses. The observations in this experiment suggest that the putamen is particularly sensitive to propofol and that prior to the failure of thalamocortical

transmission, at the point at which subjects fail to perceive and lose verbal contact, the thalamo-regulatory influence of cortico-striato-thalamo-cortical circuits may be disrupted. Our experiment cannot distinguish between direct propofol modulation of the striatum itself and striatal deafferentation secondary to drug activity at another site such as the cortex, brainstem or indeed the thalamus [203].

In this experiment, activation of the putamen to noxious stimulation was one of the responses affected by propofol. Basal ganglia structures are not commonly reported in the acute pain literature [204,205] but involvement in the processing of nociceptive information, including attention to noxious information, motor preparation and response selection are increasingly recognised [206-208], and dedicated nociceptive pathways to the striatum have been identified [209]. Iardola and colleagues have observed bilateral activation of the putamen with capsaicin induced pain and the basal ganglia have also been found to play a role in chronic pain conditions such as atypical facial pain [210] and burning mouth syndrome [211].

The thalamic intralaminar nuclei comprise the largest group of efferents from the thalamus to the striatum [212,213]. Described formerly as "non-specific" thalamic nuclei, the anterior and posterior intralaminar nuclei of the thalamus together with the paralaminar portions of the thalamic association nuclei are recognised as central to consciousness [37,214]. These nuclei project to both the cortex and striatum [194,215]. Gross central nervous system pathologies (e.g. hemispherectomy) can co-exist with the preservation of consciousness [216], while small lesions affecting specific regions can impair consciousness, perception and/or generation of organised motor responses [214]. Minimally conscious states may occur with thalamic strokes affecting the reticular (RT) or intralaminar (ILN) thalamic nuclei or lesions of the reticular formation [212]. While we failed to detect a change in thalamocortical connectivity with respect to an *averaged* BOLD signal from the thalamus, individual nuclei may be independently modulated. This is significant in the context of the expected association of thalamocortical disconnection with unresponsive states. Further imaging studies at higher field strength may unmask such changes in primary and association thalamic nuclei although the gross anatomy of the critical ILN and RN makes non-invasive interrogation challenging.

3.6 Conclusions

Cortical activity constitutes the contents of consciousness, but the state of consciousness and perception of those contents requires their dynamic integration into experience (cognitive binding) and the generation of

appropriate responses (motor, cognitive, affective, memory formation) [217]. Integration is dependent upon positive feedback loops facilitating the transmission of relevant signals through the thalamus. Cortical afferents to the thalamus travel via the striatopallidal fibres, and reversible thalamic suppression due to deafferentation has been described [36]. Basal ganglia circuits are involved in regulating signal transmission from thalamus to cortex. This experiment shows that levels of propofol producing sedation but not surgical anesthesia, impair the function of these circuits before thalamo-cortical connectivity is interrupted.

The aims of this experiment were to establish protocols for the safe administration of anaesthetics to volunteers in the laboratory and the fMRI scanner (both outside the hospital), to deliver stimuli in multiple sensory modalities capable of reliably producing cerebral activity so as to provide a model for the study of consciousness and its impairment, and to explore the effect of steady state propofol sedation on the cerebral response to sensory stimulation. Both the methodological and the scientific objectives of the experiment were achieved. The discovery of the sensitivity of the striatum to propofol leads to the possibility that sedation is at least in part a result of impairment of its integrative role, co-ordinating the re-entrant feedback loops through the thalamus which appear to be a fundamental activity in the generation of conscious perception. It casts doubt on the proposal that unconsciousness is the result of a simple transmission *block* at the level of thalamus and favours instead a more complex *modulation* of thalamic and neocortical function during sleep and anaesthesia.

Chapter 4: EEG of ultraslow transitions in states of consciousness

Introduction

An important methodological issue was highlighted during the conduct of the first set of experiments, namely the within-subject, between context variability in the effect site concentration of propofol at which behavioural transitions occurred. As described in the previous chapter, this was used to advantage, eliminating order effects in the scans. However, this may not have been ideal.

Anaesthetic hysteresis, the existence of distinct forward and backwards paths between states, is well described. While induction of anaesthesia has been described as a binary phase transition [218], the dose-response curve is much steeper than that seen during emergence from anaesthesia. As this has been shown to be unrelated to any change in pharmacokinetics, it has been attributed to a pharmacodynamic change [219]. The process of recovery from anaesthesia is likely to be mechanistically different from the process of induction. Several experimental lesions have been shown to affect (widen or collapse) anaesthetic hysteresis without directly affecting drug uptake, distribution or metabolism [220]. Kelz and colleagues demonstrated that isoflurane and sevoflurane reduce c-Fos expression (a marker of neuronal activity) in orexinergic neurons, a key part of the wake-promoting system. Transgenic mice deficient in these neurons and mice treated with orexin-1 receptor antagonsists do not exhibit any change in the characteristics of anesthetic induction. They do however show markedly delayed emergence from anaesthesia [221].

It was clear following this first series of experiments that a reproducible pharmacological discriminant does not exist and the direction of transitions being observed is relevant and difficult to control. In order to investigate state of consciousness changes it would be necessary to obtain continuous data across these transitions, with retrospective transition identification.

It was not obvious how best to identify state transitions. While behavioural changes are easily observed, and failure to respond to verbal stimulation is a widely used definition of loss of consciousness, the definition of surgical anaesthesia identifies at least one additional transition: failure to move in response to a surgical stimulus. It has been shown with both volatile and intravenous anaesthetics that elimination of the motor response to surgical stimulation and surgical awareness are anatomically dissociable but functionally

interdependent [86]. Nevertheless a further state change beyond the loss of behavioural responsiveness (LOBR) is of key clinical and scientific interest. As absence of movement to stimulation of surgical intensity cannot be sought in a volunteer study, a second neurophysiological measure, electroencephalography (EEG) was introduced. The hypothesis was that by using a continuous ultraslow induction, covert state changes beyond LOBR would be identified. By continuing to collect data during the recovery from this infusion it would be possible to investigate the nature of anaesthetic hysteresis.

4.1 Methods

An experimental paradigm was designed which delivered a constant intensity of auditory and noxious stimulation during ultraslow induction of and recovery from deep propofol sedation. This experiment was carried out in a physiology laboratory equipped for the safe delivery of sedative medication, consistent with AAGBI guidelines. A senior anaesthetist was responsible for administration of the propofol infusion and attended to subject monitoring and safety as described in Chapter 2. A second investigator was responsible for stimulus presentation and data collection.

This experiment served two important purposes. Firstly, EEG data free from fMRI artifact was collected. Secondly, the capacity of individuals to tolerate the sedation regime was assessed with respect to cardiorespiratory physiology and maintenance of airway patency. Only subjects who tolerated this experiment comfortably were permitted to participate in a later experiment (chapter 5) where the paradigm executed here was repeated in the more clinically challenging environment of the MRI scanner.

Recruitment and participation

The procedures for volunteer recruitment and assessment were as described in Chapter 2. Seventeen recruited subjects were given a detailed explanation and demonstration of the study procedures at an initial visit at which their medical suitability for participation was also assessed. A "cooling off" period of at least 48 hours was then allowed to elapse before the experiment was scheduled. On attendance for the experiment volunteers provided written informed consent to participation.

Two subjects failed to complete the protocol. One developed hypotension (80/40 mm Hg) quite early in the induction phase of the propofol infusion. This was therefore discontinued and 500ml Compound Sodium

Lactate (Hartmann's Solution) administered while the subject was allowed to wake up. There were no adverse effects. A second subject developed an obstructive respiratory pattern shortly after loss of responsiveness, which while not affecting physiological parameters, produced a visible artifact in the EEG during online visual inspection from head movement. This would also have resulted in excessive movement artifact in the scanner. The responsible anaesthetist deemed it inappropriate to increase the propofol level further and the experiment was aborted.

Experiment setup

Volunteers arrived fasting having been advised to wear comfortable, loose fitting clothing and a short-sleeved top. 32 channel EEG recording was established as described in Chapter 2. Subjects were then positioned on a surgical trolley with side-wings within which pillows were placed for comfort and safety. A U-shaped travel pillow was placed around the subject's neck to maintain a comfortable and stable head position throughout the experiment. Protective laser goggles were donned. Subjects reclined at 45^{o} so that they could comfortably observe a computer screen in front of them. Figure 4.1 shows the subject in position. A 20g peripheral intravenous cannula was inserted in the right forearm and connected to a propofol infusion pump. Nasal cannulae with two channels, one for oxygen delivery and the other for capnography were worn. Non-invasive blood pressure, pulse oximetry and ECG monitoring were established. Thresholding procedures were then carried out. Firstly, a volume for the auditory stimuli that subjects could hear clearly but was not so loud as to cause discomfort was identified. Then with the room lights dimmed and the experiment conditions established the laser energy that reliably produced an intensity rating of 5/10 on a numerical rating scale was identified. This energy level was then used for that subject for the remainder of the experiment.

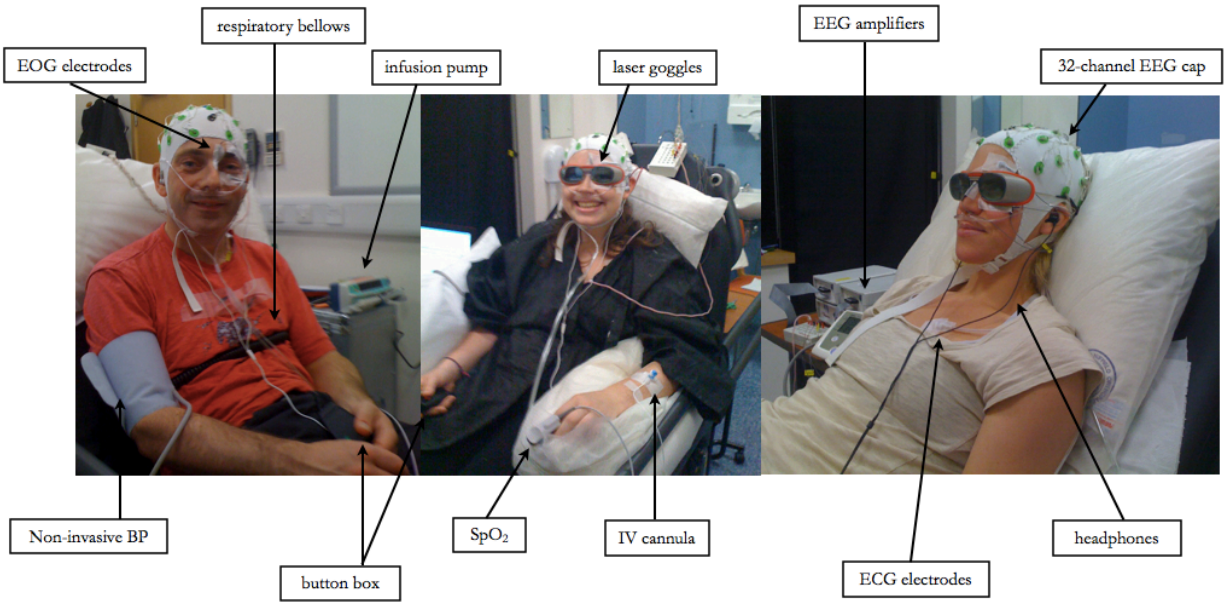

Figure 4.1 Illustration of experiment setup with subjects reclining on a surgical trolley. EOG: electo-oculogram, ECG: electrocardiogram, EEG: electroencephalogram, SpO2: pulse oximetry, IV: intravenous, BP: blood pressure.

Propofol infusion

Subjects had been carefully instructed as to what to expect during the experiment. They were advised that data would be gathered continuously over two hours. For the first 10 minutes subjects lay still with eyes closed for the acquisition of resting state data without drug. After 10 minutes the sequence of stimuli began and the propofol infusion was started with the target effect site concentration being set to 0.2 mcg ml^{-1}. The target ESC was increased by 0.2 mcg ml^{-1} every two minutes for 38 minutes while stimulation continued. After 38 minutes the target ESC reached 4.0 mcg ml^{-1} but the estimated ESC did not reach 4.0 mcg ml^{-1} for a further 10 minutes. Stimulation continued throughout this time giving a total induction phase duration of 48 minutes. Subjects stopped responding to stimuli at a variable point in this phase. After 48 minutes stimulation stopped and 10 minutes of resting state data were collected at this ESC. Finally, at 58 minutes, the target propofol ESC was set to 0.0 mcg ml^{-1} and the 48 minute stimulation paradigm was repeated, with subjects becoming responsive to stimulation at a variable point in this phase. The plot of the propofol level over the course of the experiment is given in figure 4.2.

Stimuli

Three types of stimuli were delivered, words, auditory beeps and laser, the choice and details of which were described in Chapter 2. A 16 minute pseudorandomised sequence of three types of stimuli was designed and

repeated six times: three times during induction, and then after a 10 minute pause during which resting state data was again collected, three further times during recovery. Word task stimuli consisting of pairs of words were presented at a rate of one per minute and subjects indicated using left and right buttons on a button box whether the words were the same or different. Simple auditory beeps (60 ms, 1000 Hz) were presented at a rate of one per minute. Subjects were asked to listen passively to these beeps, and no response was sought. Finally, noxious laser stimuli to the lateral aspect of the right lower leg were presented at a rate of two per minute. After a three second interval, a visual analogue rating scale (VAS) was displayed on a computer screen in front of the subjects and while responsive, they moved the slider on this scale to the right or left in order to rate the intensity of the laser stimulation.

Data collected

The laser, word and beep stimulus timings as well as the timings of any button presses were input into the EEG recording software (BrainVision Recorder, Brain Products GmbH, Munich, Germany) for offline analysis of evoked potentials. Laser intensity ratings, word task responses and the reaction times for button presses were recorded into stimulus presentation software (Presentation®, www.neurobs.com) for offline analysis of error rates, reactions times and propofol induced analgesia or hyperalgesia. A schematic of the experiment design is given in figure 4.2.

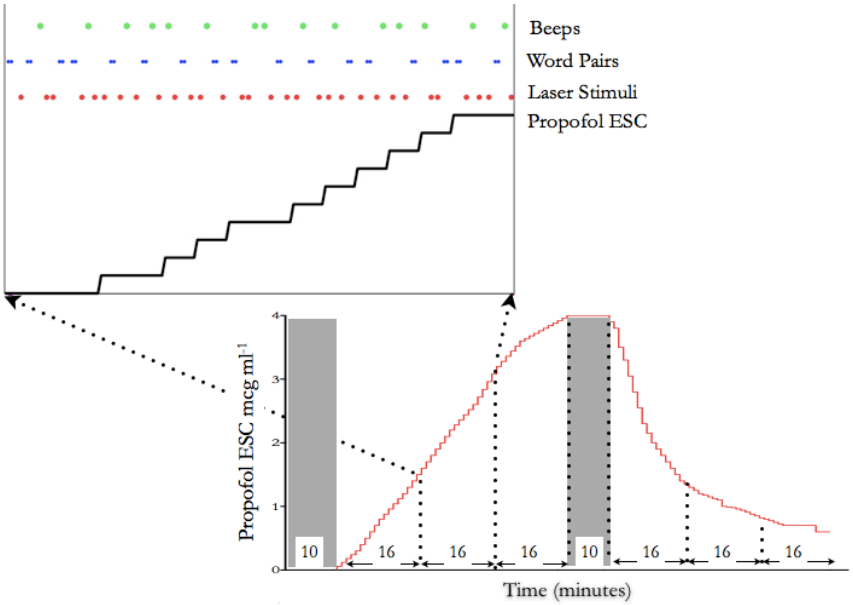

Figure 4.2 Schematic of the experimental design and propofol ESC levels delivered. Propofol ESC (red line) was increased following 10 minutes in resting state (grey box). The sixteen minute stimulation paradigm (expanded in box at top left of diagram) was repeated three times during induction and, following 10 minutes resting state at 4.0 mcg ml^{-1} propofol, repeated three further times during recovery.

4.2 Analysis

Behavioural data, specifically the ESC at loss of behavioural response (LOBR) and recovery of behavioural response), laser intensity ratings and word task reaction times were analysed using Prism 5.0 (GraphPad Software).

4.2.1 EEG preprocessing and time-frequency analysis

Preprocessing of EEG data was carried out in BrainVision Analyzer2. After blink artifact removal datasets were downsampled to 500 Hz, re-referenced to a common average and bandpass (0.5-30Hz) filtered (Butterworth zero phase filter, 48 dB/oct). Preprocessed EEG data were then analysed in Matlab (The Mathworks, Inc.) using custom written code and the EEGLab v7.2.9 analysis toolbox [222]. Time frequency analyses were carried out as described in Chapter 2, using Chonux (www.chronux.org).

Permutation entropy

Permutation entropy quantifies the complexity in a timeseries. A relatively straightforward pattern matching algorithm can be applied to the data to measure its complexity, which approximates 1 when the number of independent signal generators is maximal and falls towards zero with increasing simplicity [223]. Several investigators have proposed permutation entropy as a potentially reliable measure of GABAergic anaesthetic effects [224-226]. As EEG becomes dominated by activity in lower frequencies, it becomes less complex. They also hypothsised that an ordinal approach based on the number of patterns rather than the amplitude of waves should be more robust to non-neural artifact than Fourier transform based analyses. Permutation entropy calculated in this way was in one study found to be more robust to blink artifacts than spectral or approximate entropy, even in the absence of complex pre-processing [224]. Their published algorithm (Appendix C) was applied to 3 second epochs of EEG data in an exploratory analysis seeking an EEG transition beyond LOBR.

Spindle oscillations

Spindles consist of a series of waxing and waning oscillations in the alpha frequency band (8-14 Hz). They occur during sleep and sedation, waxing when increasing numbers of hyperpolarised thalamocortical neurons oscillate in phase and then waning again as the oscillations dephase. During sleep and sedation, spindle oscillations appear as activity in the alpha band of the EEG. The frequency of spindle oscillations has been suggested to drop with increasing depth of anaesthesia. Some investigators have also found that

spindle oscillations in centroparietal thalamocortical neurons have a faster frequency than those in neurons projecting from the thalamus to the frontal cortex [227-229].

The prevalence of spindles at frequencies within the alpha band (9-14 Hz) was investigated by modifying a published pattern detection algorithm ([230]Appendix D) and applying this to EEG data from each channel in each subject. The overall prevalence of spindles of each frequency during each 3 second epoch was calculated by averaging the spindle count across channels. The topographic distribution of spindle activity was investigated by plotting the spindle prevalence at each co-ordinate on the scalp montage.

Slow wave activity

Time-frequency or spectral analysis of activity within the 0.5-30Hz band was carried out using Chronux (www.chronux.org) [231,232]. A multi-taper spectral estimation algorithm applied an optimal set of orthogonal tapers (Slepian functions) with automatically optimised variance and bias properties before applying the fast Fourier transfer algorithm. Data were epoched into three second non-overlapping windows for spectral estimation yielding a frequency resolution of 0.3 Hz.

Frequency power progression was plotted for each subject and each channel. Activity within specific bands of interest, such as alpha (9-14 Hz) and the slow wave (0.5-1.5 Hz) frequencies, was extracted by summing the spectral estimation across the bandwidth at each time-point. A median filter of order 20 (1 minute smoothing) was applied. Topographic distribution of slow wave power was investigated by averaging EEG power within the 0.5-1.5 Hz band across each experimental phase of interest and plotting the power at each electrode co-ordinate on the scalp montage.

Peri-stimulus analysis

For each subject, peri-stimulus epochs of EEG data at Cz were extracted for both laser stimuli and auditory tones. Epochs spanned the period from 500 ms pre-stimulus to 2500 ms post-stimulus. As K-complexes, which contain frequency components in the delta range, may be evoked by auditory and laser stimuli during sleep [233], no further filtering was applied. Signal-to-noise was increased by averaging these epochs within each experimental phase and across subjects. Experimental phases were defined behaviourally and by slow wave activity (SWA) as described in chapter 2.

4.3 Results & Discussion

4.3.1 Cardiorespiratory parameters

Cardiorespiratory parameters over the course of the 116 minute experiment are presented in figure 4.3. There was no clinically significant change in any physiological parameter over the course of the experiment. Systolic blood pressure was higher (mean (SD): 121.8(9.4) and 106.5 (11.3)) and heart rate lower (71(1.5) and 57.8(0.8)) at baseline than at 4.0 mcg ml^{-1} propofol. Respiratory rate remained a little above baseline throughout and expired carbon dioxide levels rose with decreased depth of respiration as expected, although the increase was not clinically significant.

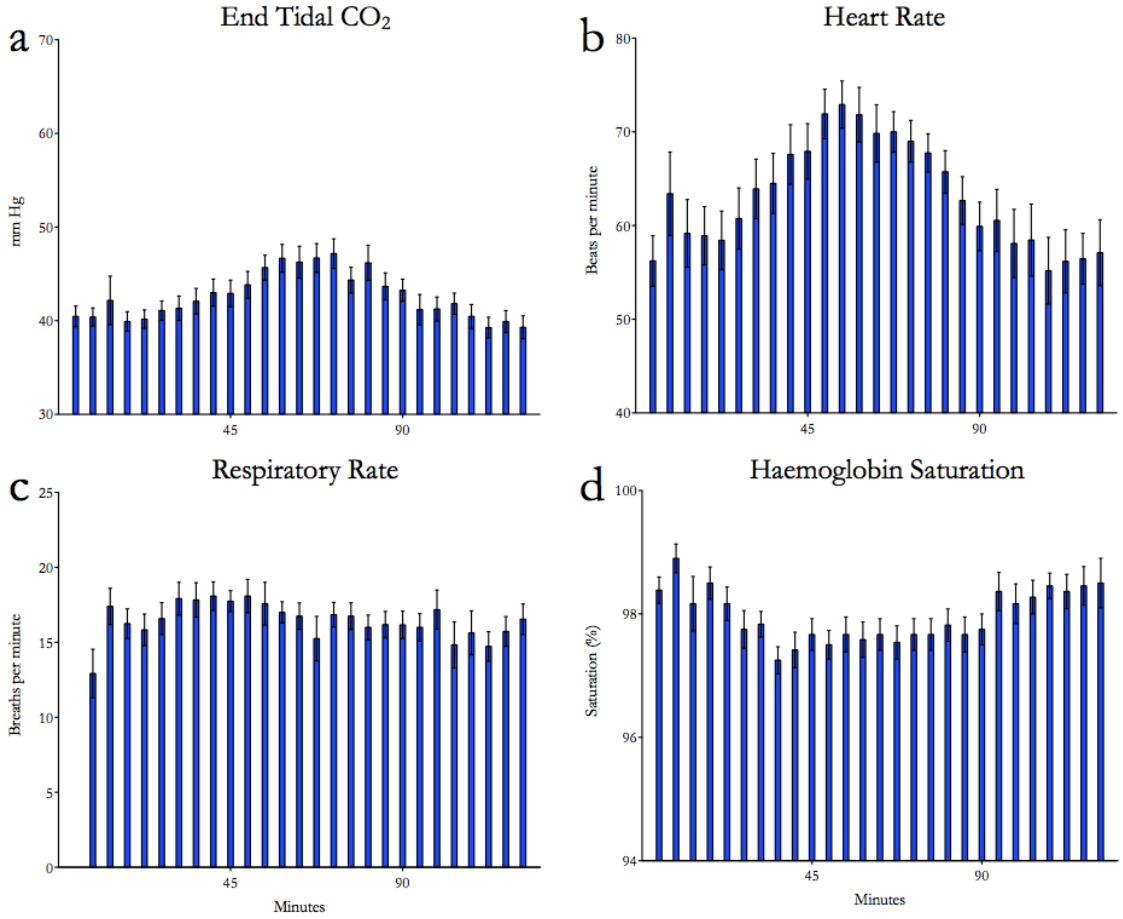

Figure 4.3 Physiological monitoring over the course of the experiment. The expected rise in heart rate (b) with lower blood pressure at higher propofol levels is seen as is the rise in expired carbon dioxide (a), which was due primarily to reduced depth rather than rate of respiration (c). Oxygenation did not change significantly (d).

4.3.2 Inter-individual dose-response variability

There was substantial inter-individual variability in the ESC at which the last response to stimulation occurred (mean[SD], 1.57 [0.6] mcg ml^{-1}) as shown in figure 4.4. Likewise, there was substantial inter-individual variability in the ESC at which the first response to stimulation occurred during recovery (1.23[0.45] mcg ml^{-1}). This highlights the importance of pharmacodynamic rather than pharmacokinetic parameters being used to classify neurophysiological states for analysis.

Anaesthetic hysteresis

Part of the motivation for recording continuous rather than steady state data was the body of literature supporting the theory of anaesthetic hysteresis. Examining the behaviour of the sixteen subjects in this study this phenomenon was indeed observed. The ESC at which LOBR occurred was significantly higher

than the ESC at which recovery of behavioural response (ROBR) occurred (paired t-test, p=0.006, figure 4.4). This is not expected to be a shortcoming of the pharmacokinetic model. Friedman and colleagues [220], described the property of resistance to state change in neural circuits as neural inertia and showed that it is not due to any error in the pharmacokinetic models used. They demonstrated anaesthetic hysteresis in two different species (mice and Drosophila) and showed that the resistance to state change could be modulated by genetic and pharmacologic manipulations of sleep physiology. They proposed that neural inertia serves to protect the conscious or unconscious state from inappropriate transitions arising from random fluctuations. While delayed emergence from anaesthesia has been described in patients with narcolepsy where there is loss of orexinergic neurons [234], pharmacological treatment of narcolepsy appears to be associated with normal emergence times [235].

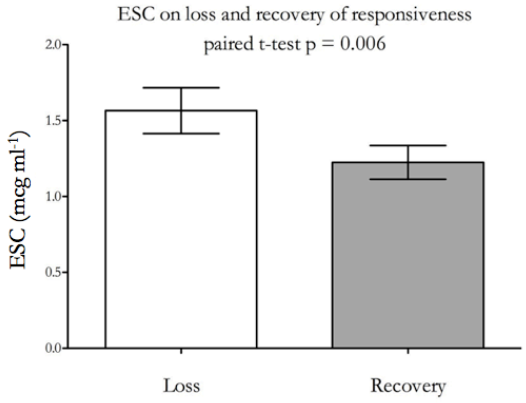

Figure 4.4 Average propofol effect site concentration (ESC) level associated with the last response during induction and first response during recovery to stimulation (n=16). There was, as expected, a significant difference between the propofol level at which behavioural responses to stimulation were lost and those at which they recovered (p = 0.006).

4.3.3 Psychomotor impairment

As propofol ESC rose, psychomotor impairment developed and the mean time to response for the word task lengthened. Significant prolongation of reaction times occurred in subjects regardless of the ESC at which LOBR occurred. Splitting the responses during induction into the first and second halves of each subject's responsive period showed that responses during the second half of a subject's responsive period were significantly slower than those during the first half (p=0.015, figure 4.5(a)). Similarly, responses during the first half of subjects' recovery were significantly slower than those during the second half (p=0.001, figure 4.5(b)). Despite the difference in ESC during the recovery phase, there were no significant differences in reaction times between the matched halves of these periods (early induction/late recovery (figure 4.5(c) and late induction/early recovery (figure 4.5(d))).

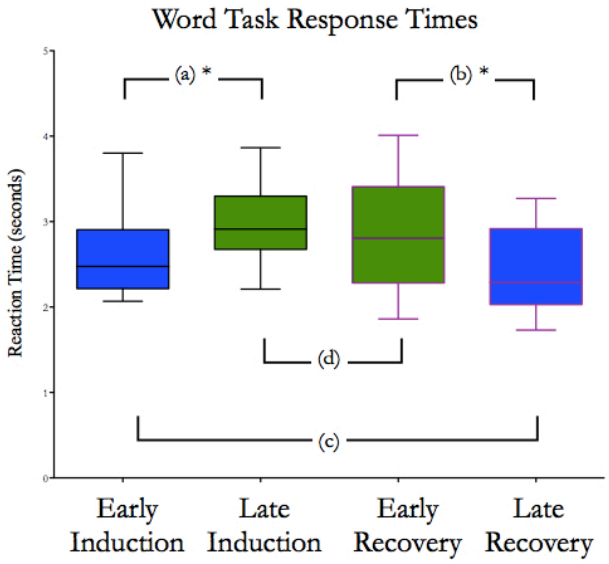

Figure 4.5 Word task reaction times during the early and late induction and recovery periods. Significant prolongation in reaction times to the word task when the first half of the responsive period during induction was compared do the second (a). A significant recovery of reaction times was also seen when the two halves of the responsive period were compared (b). Response times at low levels of propofol (early induction and late recovery) were not significantly different to one another(c), nor were those at higher levels of propofol (d). * - $p < 0.05$

As the word task was simple, designed to be only just complex enough to recruit higher cognitive centres, it was perhaps unsurprising that very few errors were made and that behavioural impairment was only manifest in a delayed reaction time (figure 4.6).

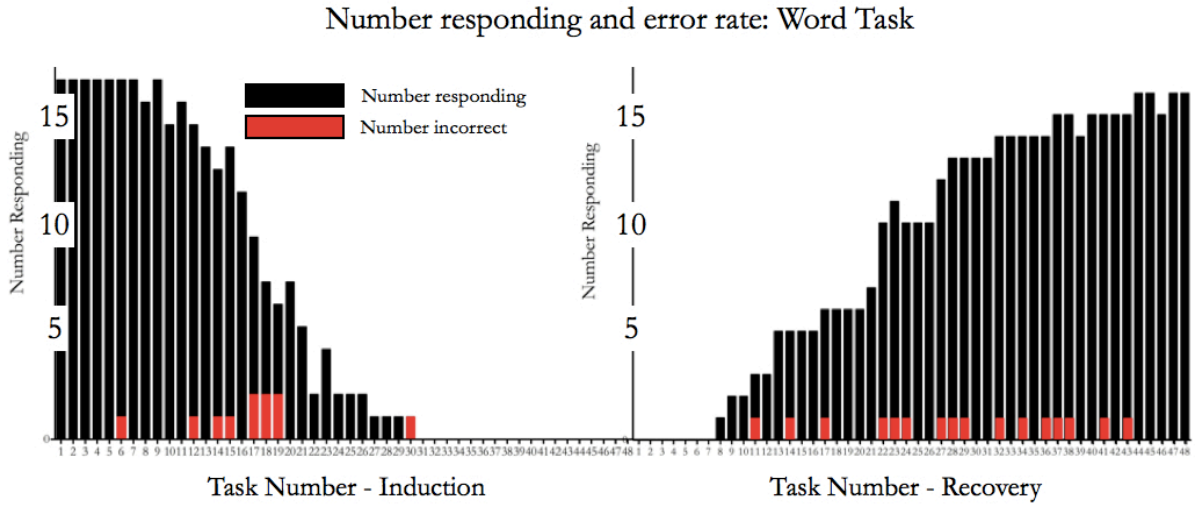

Figure 4.6 Number of participants responding and the corresponding word task error rate over the course if the induction and recovery phases. Very few errors occurred and the primary manifestation of sedation until the LOBR was the increase in reaction times (figure 4.5).

4.3.4 Propofol induced hyperalgesia

Increased sensitivity to pain following general anaesthesia has been described, albeit inconsistently, with both volatile and intravenous anaesthetics [166,167,236,237]. Clinical assessment in surgical patients is confounded by sensitisation related to surgical trauma and polypharmacy. At the same time, other studies have attributed an analgesic effect to propofol [238]. This study afforded the opportunity to investigate this phenomenon in a controlled experiment. It was also important to identify or rule out any systematic propofol related analgesia or hyperalgesia as the study was designed on the premise of a constant level of stimulation throughout. For this reason a visual analogue scale (VAS) rating of each laser stimulus was included in this experiment. There was a significant increase in the subject's mean intensity rating when the induction phase was compared to the recovery phase (figure 4.7).

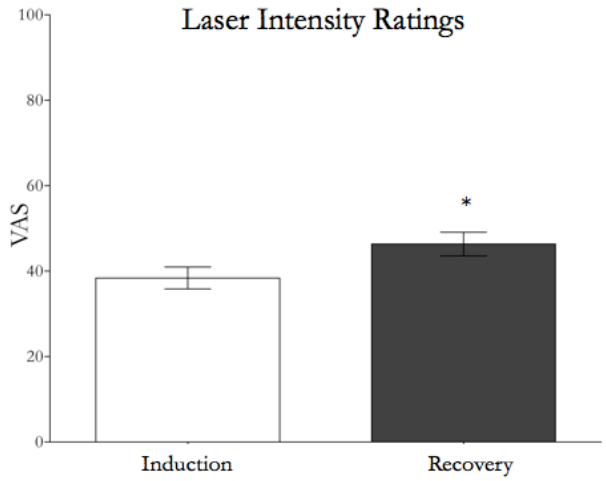

Figure 4.7 Subjects' mean laser intensity ratings during induction and recovery were compared. Ratings were found to be significantly higher during recovery than during induction suggesting the development of hyperalgesia. (paired t-test, $p < 0.05$).

Stimuli delivered early in the experiment, while propofol ESC rose from 0.0 to 0.6 mcg ml^{-1} had no dose matched stimuli during the recovery phase, because this was completed at 0.6 mcg ml^{-1}. This early period was therefore regarded as an initial or baseline phase. Ratings obtained between a propofol ESC of 0.6 and 1.5 mcg ml^{-1} were used to compare the subjective intensity of noxious laser stimuli of the same energy level, administered at the same ESC of propofol, before (induction phase) and after (recovery phase) sedation. Multiple regression analysis with a general linear model was carried out with subject, stimulus number (1-96), ESC of propofol and phase (induction and recovery) as regressors of interest. The position of the stimulus in the sequence from 1 to 96 did not significantly affect the stimulus rating ($p = 0.785$). A significant effect

for subject ($p < 0.001$), ESC ($p = 0.05$) and phase ($p < 0.001$) was found. Mean pain ratings at each ESC were significantly higher during the recovery phase than the induction phase ($p<0.05$, corrected, figure 4.8).

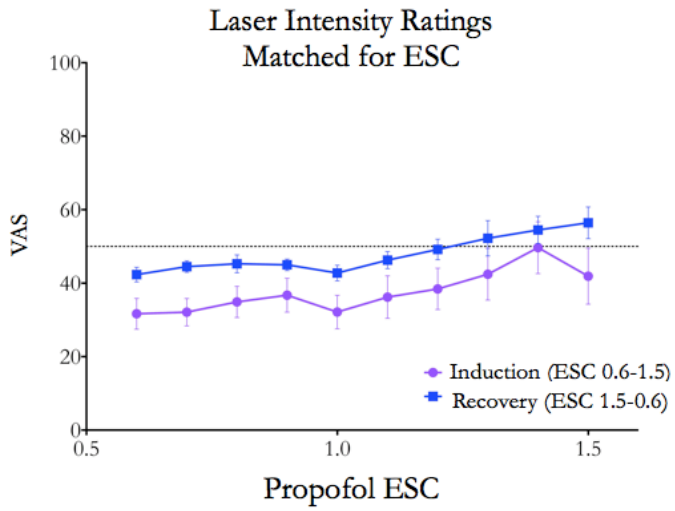

Figure 4.8 Laser intensity ratings for matched propofol ESC across subjects showed significantly higher laser intensity ratings during recovery compared to induction ($p < 0.05$ corrected).

It appeared at first that there was an increase in the subjective experience of noxious stimuli following the administration of propofol. However, closer inspection of individual subject data revealed why this may not in fact be the case. As a significant effect for subject was noted in the multiple regression analysis, median ratings for induction and recovery phases were compared for each subject. Eight of the subjects had a significant higher median intensity rating during the recovery phase compared to the induction phase (Mann Whitney U test, $p < 0.05$), but the other half showed no significant difference (figure 4.9)

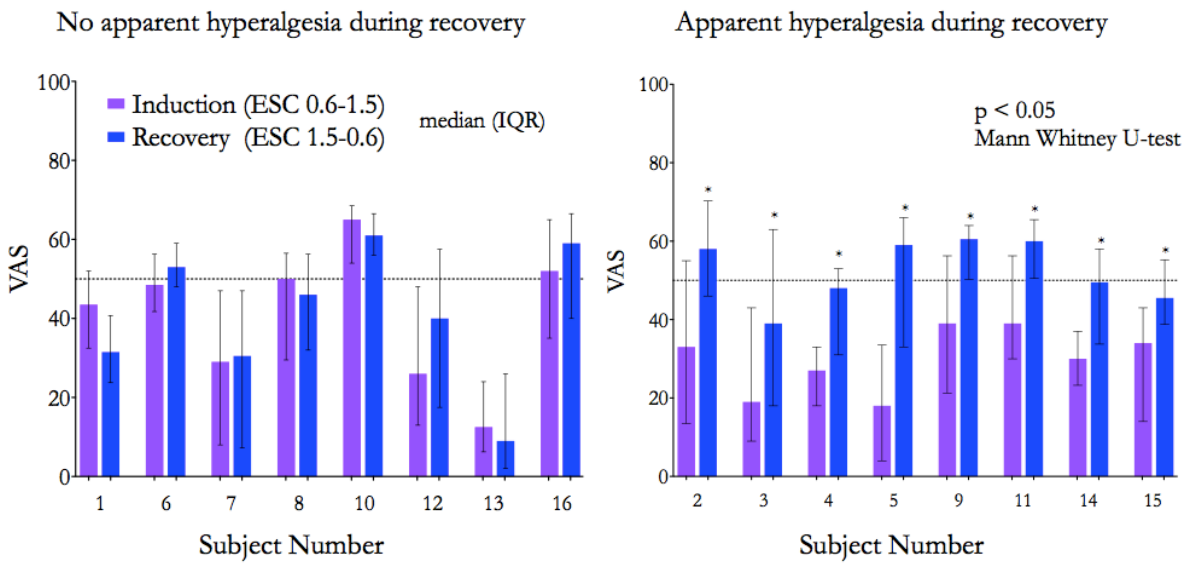

Figure 4.9 Median and interquartile range of the laser intensity ratings for the induction and recovery phases of the subjects demonstrating no hyperalgesia (left) and apparent hyperalgesia (right) during recovery . Half of the subjects (8/16) rated laser stimuli significantly higher ($p < 0.05$, Mann-Whitney U test) during recovery from the propofol infusion than during induction of anaesthesia.

On further interrogation of the data, it transpired that the group who appeared to develop hyperalgesia in fact showed an early drop in the subjective intensity of the laser stimuli (figure 4.10). During the recovery phase, these subjects demonstrated a return to the initial intensity level to which the stimuli were thresholded, giving the mathematical impression of hyperalgesia.

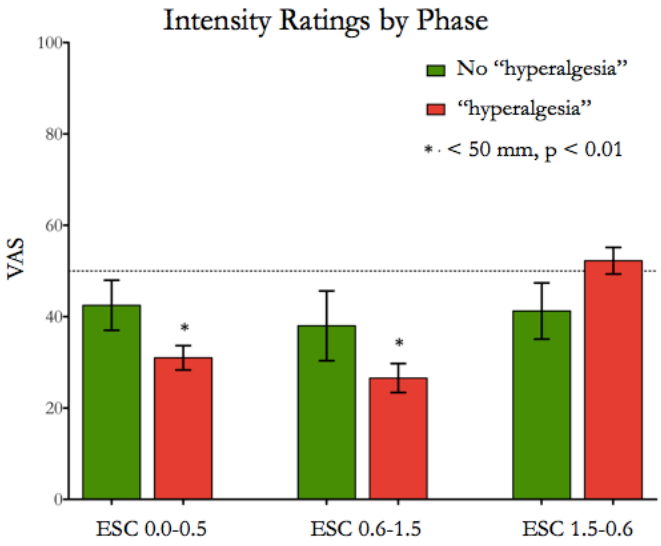

Figure 4.10 Subjects who appeared to display hyperalgesia during recovery in fact habituated rapidly to the stimulus following thresholding. During the initial period they rated stimuli significantly lower than the intensity (5) to which thresholding had been targeted. During recovery, none of the subjects rated stimuli significantly different to 5.

In order to fully understand this phenomenon, it will be necessary to better understand the interactions of propofol at a cellular level with tissues involved in nociceptive signaling. Habituation to repeated noxious stimuli is well described [239] and lack of such habituation has been associated with chronic pain syndromes [240]. One interpretation of the pattern found in this experiment is that eight of the subjects demonstrated habituation to the laser stimuli during the initial phase, which normalised while they were unresponsive. While the "recovery phase" was also preceded by a series of stimuli, a sort of unresponsive initial phase, one could hypothesise that cognitive processing of the stimuli was disrupted at this time and therefore this possibly centrally-driven habituation didn't occur and pain ratings returned to those determined at threshold. Overall, the study group showed a small decline in the subjective rating of laser stimuli, so that the mean[SD] subjective intensity of the stimuli delivered over the course of the experiment was (41.3[6.1]).

4.3.5 EEG Time-Frequency Analysis

Following preprocessing, the first analysis of EEG data carried out was an investigation into the progression of activity in each frequency over the course of the experiment as described in chapter 2. Power across the 0.3-30Hz over the course of the experiment is shown in Figure 4.11. This figure contains data averaged across channels and across subjects but the progression of activity in each frequency band was highly similar in each channel and each subject. Figure 4.12 shows the spectrogram from a representative single channel in a single subject. The same pattern is clear. Spectrographic analysis of the ultraslow sedation and recovery showed the shift towards larger amplitudes [241] and slower frequencies [242]which are known to occur during administration of GABAergic agonists in detail.

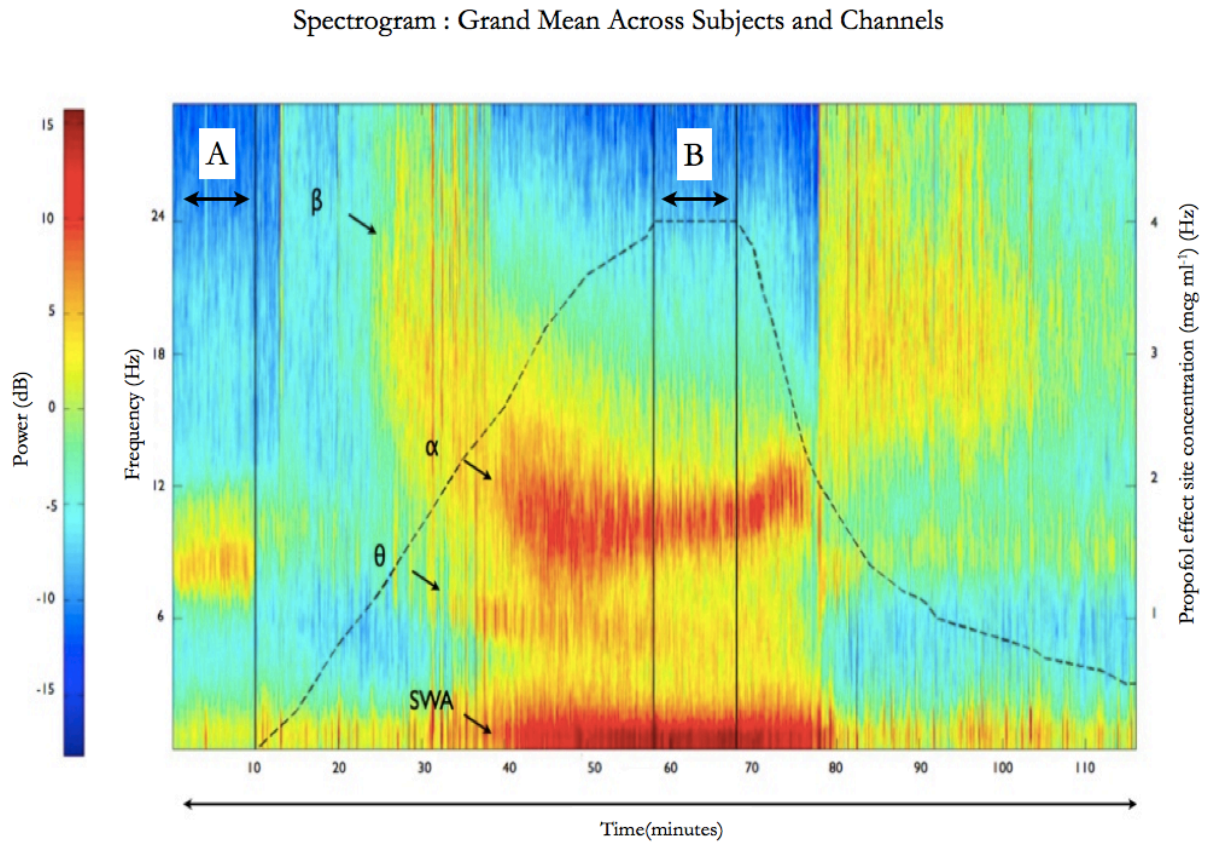

Figure 4.11 Grand mean power in each frequency within the 0.5-30 Hz band over the course of the experiment. A: resting state awake, B: resting state at peak propofol level. During the first 10 minutes, the dominant activity is alpha, which disappears when the eyes open and stimulation begins. As propofol levels increase (dotted line), there is an initial increase in beta activity (15-30Hz) which subsequently wanes to be replaced by alpha and theta. Within the alpha band the frequency slows from above to below 12 Hz with increasing propofol and this is reversed during recovery. Slow wave activity (SWA) is the dominant feature during high propofol levels.

The Beta Band

Approximately halfway between the start of the propofol infusion and LOBR, a marked increase in activity was seen in the 15-30 Hz (Beta) band. This persisted across LOBR (single subject spectrogram Figure 4.12), and then waned over the first 5-10 minutes of unresponsiveness. Persistence of the beta activity after LOBR and its subsequent abolition illustrates this important feature of low dose sedation in a subject without neuromuscular blockade. Beta activity is a prominent feature of sedation with low levels of propofol [243] and occurs when a sedative infusion of the benzodiazepine midazolam achieves amnesic levels [244,245].

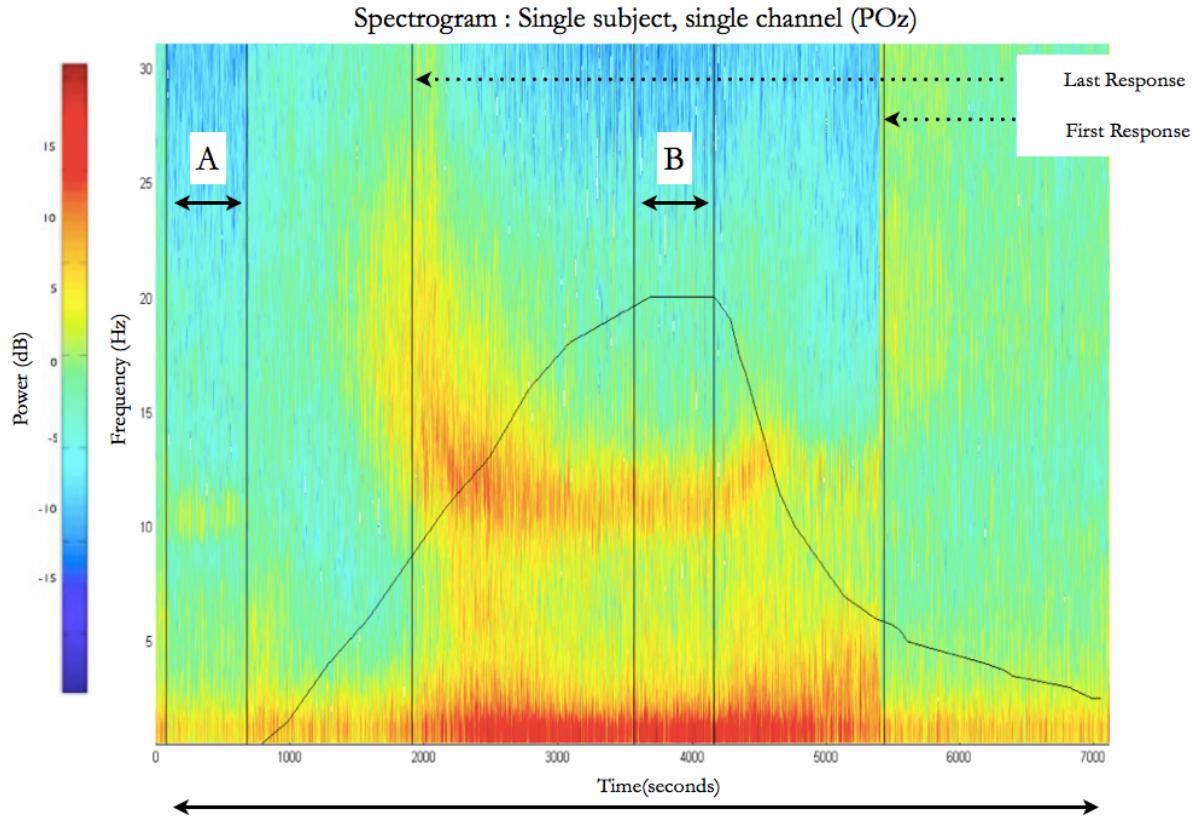

Figure 4.12 Representative single subject, single channel spectrogram over the course of the experiment. Beta activity rises from half-way through the responsive period of induction and wanes following the last response to stimulation. The patterns of alpha, theta and slow wave activity seen in the grand mean data are still seen clearly at single channel level.

An equivalent phase of unresponsive Beta activity was not a prominent feature of the unresponsive part of recovery, the appearance of pronounced beta activity coinciding instead with ROBR, which then persisted throughout the remainder of the recovery period. Interestingly, relatively prolonged increases (< 30 minutes) in beta activity have been reported following clinical recovery from sedation [245]. As frontal

electromyographic (EMG) activity is predominantly 20Hz and above [246,247], some of this activity during recovery may be attributed to eye opening. Additionally, the pharmacokinetics of propofol mean that the lowest ESC during recovery was 0.6 mcg ml^{-1}, similar to the ESC at which the beta increase first appeared during induction. Nevertheless, this difference between induction and recovery is potentially of clinical relevance. Beta Ratio is an important contributory component in the calculation of the Bispectral Index (BIS)™ [248], and this asymmetry may reduce the sensitivity of processed EEG (pEEG) parameters, part-dependent on Beta activity, to the detection of emergence during or after anaesthesia.

Increased beta activity at low levels of sedation has been associated with paradoxical excitation (increased motor activity and/or affective disinhibition) [249]. Paradoxical excitation and disinhibition have been well described both during induction of [250] and after recovery from [251] the administration of anaesthetic drugs in general and propofol in particular.

McCarthy and colleagues [252] used computational modeling of network dynamics to show that increased beta activity could theoretically be attributed to an effect of low dose propofol on the interaction between $GABA_A$ potentiation reduction of an intrinsic potassium current, the M current. At higher levels of propofol, post-synaptic $GABA_A$ potentiation would predominate and beta activity wane.

The increase in beta activity may be linked to the findings of Chapter 3, namely that cortico-thalamo-cortical loops through the basal ganglia are particularly sensitive to modulation by low dose propofol. Beta oscillations are prominent in somatosensory and motor cortical areas, the cerebellum and the basal ganglia. Activity in waking is task-dependent, increasing during tonic activity and decreasing during a motor task. Abnormally synchronised beta activity in the basal ganglia is associated with bradykinesia [253]. Increased numbers of neurons oscillating in synchrony results in an increase in the amplitude of beta activity measured at the scalp. Gilbertson and colleagues showed that cued movements are slowed during periods of elevated beta band synchrony and suggested that increased beta synchrony is associated with promotion of existing posture, impairment of new movements and prolonged reaction times to motor tasks [254]. The increase in beta activity in this experiment was temporally coincident with a significant delay in the word task reaction times during the induction phase. It is difficult to reconcile the return of normal reaction times and persistence of beta activity throughout the recovery phase with the basal ganglia/bradykinesia hypothesis

given the potential for EMG contamination of the signal. The relationship between the behavioural manifestations of low dose GABAergic sedation and beta oscillations is likely to be complex and possibly, like anaesthesia itself, an endpoint common to a number of processes. As discussed in chapter 3, the basal ganglia perform a complex role balancing competing afferent signals and cortical feedback to promote amplification of "genuine" signals and spurious "noise" reduction. It seems likely that further investigation of the neural underpinnings of the beta oscillation (or beta oscillations, as there is substantial evidence that activity within this frequency band is not unique to a single process [255]), often overlooked in studies of anaesthesia, may illuminate subtle disorders of movement and cognition.

The Theta Band

Oscillations in the 4-8 Hz band are classically referred to as "Theta" activity. Theta is a neurophysiologically ambiguous term as it describes two oscillations of different origins, hippocampal theta and cortical theta.

The hippocampal theta oscillation has been extensively studied in animals and is associated with memory, spatial encoding, locomotion, modulation of synaptic plasticity through long term potentiation and depression, and sensorimotor integration [256].Cortical theta on the other hand is less robust and has been less extensively studied, particularly in humans. Hippocampal and cortical theta rhythms are not coherent in either sleep or waking, suggesting independent generators[257]. Cortical theta oscillations are described during spatial learning and working memory tasks [258]. They are also seen during quiet wakefulness and early sleep but are not a feature of slow wave sleep. Hippocampal rather cortical theta is seen during REM sleep [257].

During this experiment, distinct theta activity ~ 6 Hz appeared soon after LOBR and waned as sedation deepened (figures 4.11 and 4.12). Any interpretation of the pattern of cortical theta oscillations is difficult given the relative paucity of literature on this activity in humans but it does represent a specific similarity between the process of deepening sleep stage and the induction of anaesthesia.

While theta activity is interesting as it is associated with Stage 2 NREM sleep, the time-frequency analysis showed that two dominant rhythms of human sleep, spindles and slow waves, were also the dominant activities through the unresponsive period of the experiment. These were investigated in detail.

The Alpha Band

Over the course of the experiment a distinct pattern of activity was observed in the alpha (8-14Hz) band. Activity at ~10Hz appeared as soon as the eyes closed for the first 10 minute resting phase of the experiment. This attenuated almost immediately on eye opening at the onset of stimulus presentation.With LOBR there was a marked increase in alpha activity across a broader range of frequencies, initially at the higher end of the band (~13-14 Hz), then slowing (~10-12 Hz) with deepening sedation. This slowing was reversed just before ROBR. During the responsive part of the recovery phase, a relatively modest amount of alpha activity at the lower frequency (~8-10Hz), which was seen in the initial resting phase, persisted.

Occipital neurons oscillate at ~10Hz during quiet wakefulness with eyes closed. These alpha waves were one of the first rhythms to be observed by Hans Berger in some of the earliest EEG studies, published in 1929, although he acknowledged the contribution of Caton, who first observed that electrical potentials on the brain surface and scalp of cats increased in amplitude during sleep [259].

4.3.6 Spindles

Spindles, waxing and waning oscillations in the alpha frequency band, are characteristic of NREM sleep. They are prominent in stage 2 NREM sleep and present but less prevalent in SWS [260]. They are also seen during sedation and anaesthesia across several drug classes and indeed much of the early work investigating the underlying physiology was done in anaesthetised cats [261-263].

The thalamus functions in two modes. In tonic mode, the cells' individual action potentials relay signals to the cortex with high fidelity. In burst mode, synchronous electrical activity (spindles) blocks sensory input to the cortex [264].

Spindles are resonant oscillations within thalamo-cortico-thalamic loops generated by the reticular nucleus (RE) of the thalamus. They appear with progressive thalamic hyperpolarisation, such as occurs when the balance of sleep-wake inputs from brainstem monoaminergic nuclei and basal forebrain cells to the thalamus shifts towards sleep, or with the administration of hyperpolarising drugs [265]. Isolation of the cortex from the RE nucleus by surgical resection extinguishes spindles [266].

Sustained membrane hyperpolarisation below −60 mV de-inactivates Ca^{++} conductance leading to a low threshold spike (LTS) [267]. RE cells generate rhythmic spike bursts of inhibitory post-synaptic potentials (IPSPs), which are imposed on thalamocortical (TC) cells. TC spike bursts are transferred to the cortex and induce rhythmic EPSPs [268]. The ratio of corticothalamic (CT) to TC neurons is 3:1 so TC bursts elicit amplifying CT feedback volleys to the RE network which, by virtue of its extensive connections, entrains further thalamocortical neurons into the oscillation, hence waxing amplitudes. The waning of spindles is due to bisynaptic (cortical and RE) inhibition of TC cells overcoming direct TC excitation [269,270]. This waxing and waning pattern is often noted to depend on the mechanism of spindle generation. Spontaneously generated spindles during sleep and barbiturate anaesthesia wax and wane as they originate at the thalamus. Spindles elicited by direct cortical stimulation or during ketamine anaesthesia appear maximal from the onset and only wane, which has been suggested to be a result of the high background cortical activity, eliciting maximum neuronal entrainment by CT neurons from the outset [265,268].

Therefore, spindles are a localised oscillation organised by the RE nucleus. There is no cross talk between TC neurons, and TC-RE-CT networks show a systematic organisation of projections: distinct networks through primary somatosensory systems, coarser networks through the projections of thalamic association nuclei, and diffuse projections from the RE to anterior and posterior intralaminar nuclei [268]

Spindles and anaesthesia

One of the many similarities between sleep and anaesthesia is the occurrence of spindle oscillations. Lydic and colleagues showed that the mechanisms modulating spindle activity during halothane anaesthesia were similar to those seen in sleep. Halothane reduces acetylcholine (ACh) release from the medial pontine reticular formation (mPRF). This is coincident with the appearance of spindles, which disappear as ACh levels recover [271]. Spindles are seen during deepening propofol anaesthesia [272] even during burst suppression [273]. The mean frequency of spindles is reportedly higher in propofol anaesthesia than in sleep [274]. This has special relevance for the interpretation of spindle activity under propofol since as mentioned, the resonant oscillatory frequency may vary between different areas of the cortex.

Resting neurons oscillate at a specific resonant frequency which reflects local properties of corticothalamic circuits[275]. Feshcenko and colleagues noted the different spatiotemporal dynamics of the propofol induced

alpha rhythm compared to baseline, and attributed this to resting behaviour extending beyond the occipital cortex. They hypothesised that an oscillation arising out of the resonant properties of local networks such as TC columns would be maintained when oscillations arising out of distant cortico-cortical connections are disrupted by anaesthetics [276]. While these authors noted the continuous nature of alpha activity under propofol, in contrast to the episodic waveforms of the same frequency described as sleep spindles, it is likely that the neurophysiological principles behind the emergence of these idling oscillations are the same, therefore in this discussion alpha and spindle activity are discussed together although alpha most correctly describes activity in the awake subject and spindle describes activity at alpha frequencies in the sedated subject.

Spindles vary in frequency over the course of a night's sleep, with an increase in high frequency spindles (~13 Hz) and a decrease in low frequency spindles (~11 Hz) over successive sleep cycles [277]. Zygierewicz and colleagues described differential topographic distributions for slow (frontal) and fast (parietal) spindles [229]. Frequency differences in spindles may therefore reflect differential activity levels in different corticothalamic networks.

The algorithm published by Sleigh and colleagues [230] was modified to detect spindles at different frequencies within the alpha band (chapter 2 section X, appendix D). This algorithm parses the data from the first datapoint and identifies sequences of peaks and troughs forming three cycles of the frequency of interest. If a series of three cycles is found to start at this point the algorithm adds the datapoints involved to the "spindle" bin and skips to the end of the three cycles before continuing. If not, the algorithm moves along to the next datapoint and checks again. For each 3 second epoch, the proportion of datapoints that have been classified as "spindle", spindle prevalence, is returned. It is important to note that this measure is amplitude independent, as long as the activity exceeded the set threshold of 5 μV.

High frequency (14 Hz) spindle (HFS) activity appeared before LOBR. After LOBR the prevalence of HFS began to decline and there was an increase in the prevalence of lower frequency spindles (LFS, 10-12 Hz). This may represent either a gradual slowing of the inherent frequency at which all corticothalamic neurons were oscillating, or a change in the subgroups of neurons generating the spindles. The algorithm used can

not distinguish between these two processes. The timecourse of spindle activity of each frequency is shown in figures 4.13 and 4.14 which show spindle prevalence at each frequency over the course of the experiment.

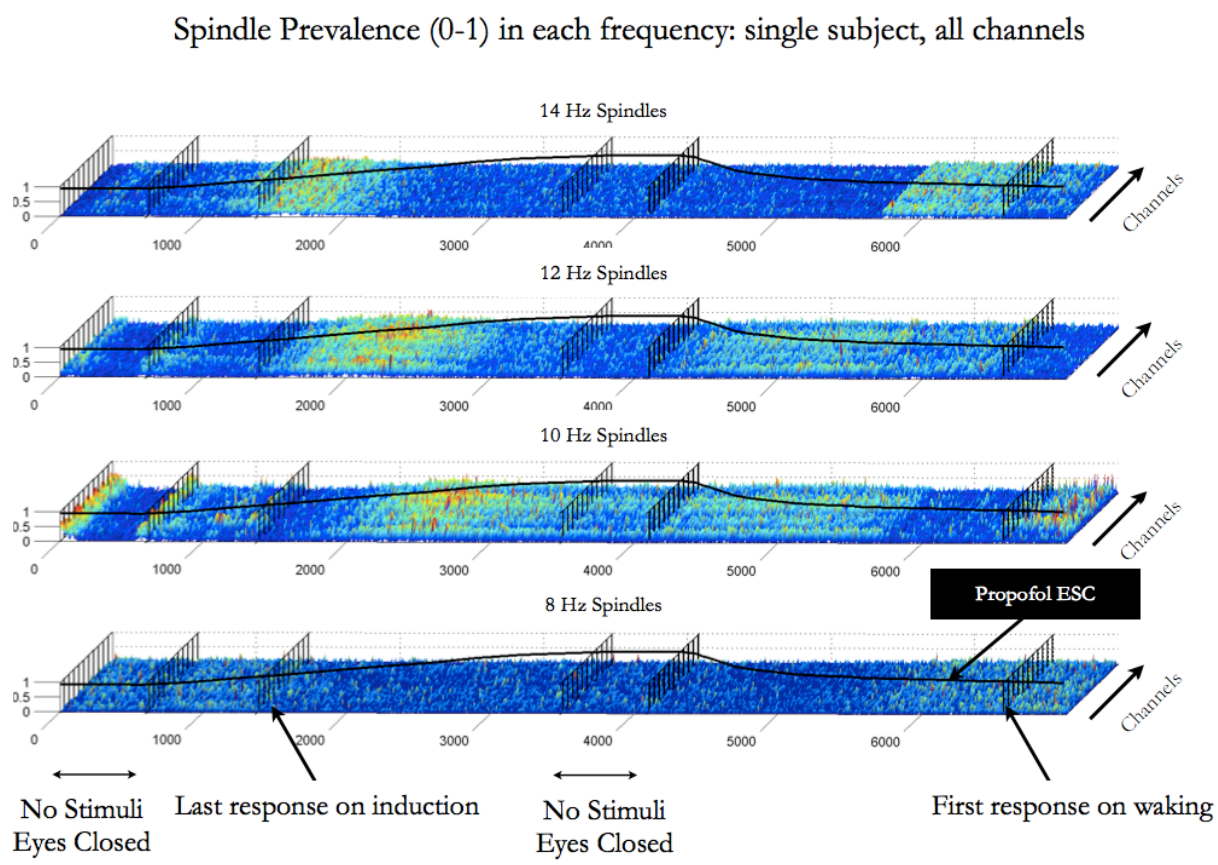

Figure 4.13 Representative single subject data showing spindle prevalence (as estimated using the algorithm of Sleigh and colleagues[230] from 0 = none (blue) to 1 = continuous (red). Early high freqeuncy spindles are replaced by lower frequencies as depth of sedation increases. This reverses during recovery.

During quiet wakefulness with eyes closed, there was early alpha activity at 8 and 10 Hz that waned towards the end of the rest period. There was a prompt drop in alpha activity with the onset of stimulation and eye opening. Contemporaneous with the increase in beta activity and impairment of motor task performance described in the preceding section, the prevalence of HFS (12 and 14 Hz) rose. HFS continued to increase in prevalence after LOBR but at this point LFS also started to appear. As sedation deepened, HFS activity peaked and waned. LFS activity peaked a little later and all spindle activity in each frequency had declined almost to resting awake levels by peak ESC. The difference between spindle activity at peak ESC and that during the initial resting state was the distribution activity across frequencies within the alpha band. At peak ESC, 10 and 12 Hz activity was more prominent than 8 or 14 Hz waves. The process reversed during

recovery with the same patterns of frequency dominance, although the prevalence of spindle activity was never as high as during the slow induction, perhaps a function of the relatively rapid drug washout curve.

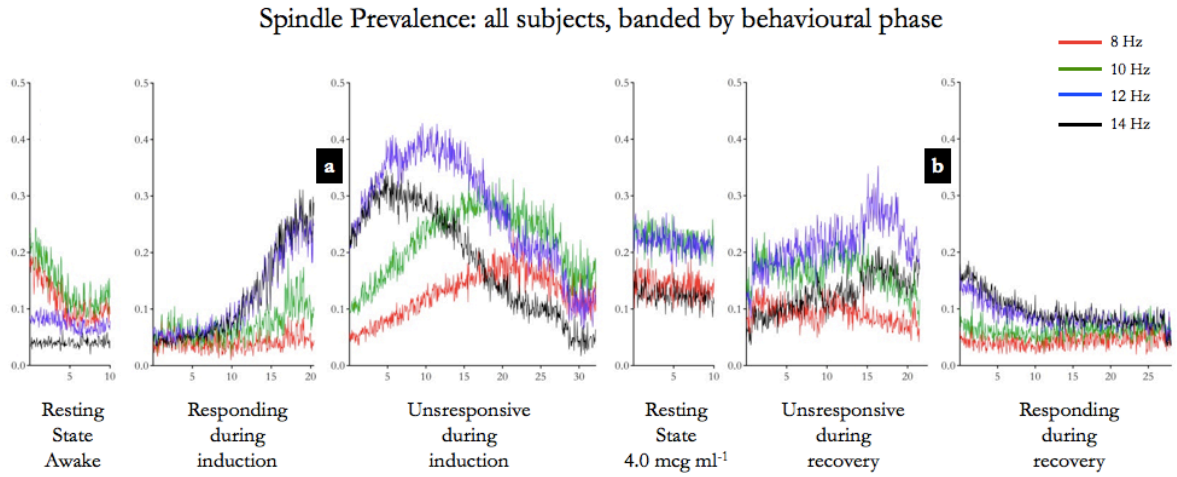

Figure 4.14 Individual subject spindle prevalence (averaged across channels) was then averaged across subjects, banded according to LOBR (a) and ROBR (b). The first segment shows activity during the first 10 minutes, during which the initial alpha rhythm faded.

The second segment contains data from the beginning of the experiment to the subject's last response. The rightmost part of this segment contains data from only four subjects - the others having become unresponsive one by one (see figure 4.6). Point 'a' is the starting point of the third segment and is the first datapoint after each subject's last response to stimulation. Each subject's contribution to this segment therefore ends when they reach 4.0 mcg ml^{-1} propofol.

The fourth segment shows that activity within the alpha band is distributed differently under anaesthesia compared to early sedation and the resting state awake, with 10 and 12 Hz spindles twice as prevalent as the 14Hz spindles seen in early sedation and the 8Hz activity prominent in the resting state awake.

Point 'b' is each subject's first response to stimulation during recovery. The fifth segment shows the reversal during recovery of the pattern seen on induction. The last segment shows the persistence of higher frequency spindles while recovery remains incomplete (ESC 0.6 mcg ml^{-1} at the end of the experiment).

To investigate this more fully, spindle prevalence at each channel in each phase described was averaged across subjects and plotted topgraphically (figure 4.14). Awake alpha activity during 'eyes closed' was, as expected a fronto/occipital oscillation. The HFS seen in early sedation were both fronto/occipital and centroparietal. As sedation deepened and LFS were increasingly prominent, they were shown to have a frontal or frontocentral topography.

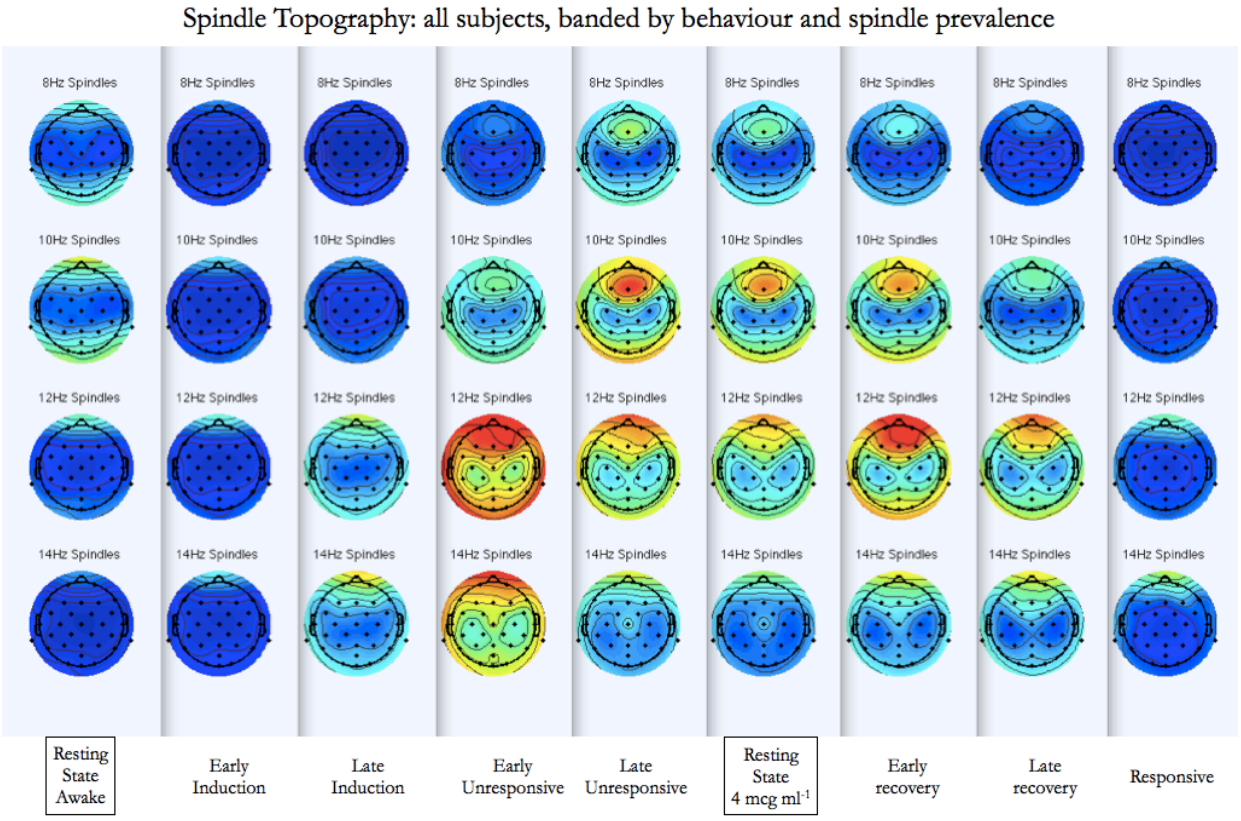

Figure 4.15 Topographic representation of spindle prevalence over the scalp (0 = none, blue; 1 = continuous, red). From top to bottom: 8Hz, 10Hz, 12Hz, 14Hz.

Resting state awake (1st column) shows the distribution associated with typical fronto-occipital alpha, which disappears on eye opening (2nd column). During the second half of the responsive period (3rd column) some HFS appear.

HFS are more prominent than LFS early during the unresponsive period (4th column). As sedation deepens, LFS become more prominent than LFS and the topography changes from fronto-parietal to frontal (5th and 6th columns).

HFS recovery their prominence as propofol levels fall (7th and 8th columns) and spindles disappear on recovery (9th column).

These data illustrate that spindles, alpha frequency oscillations of hyperpolarised thalamocortical neurons seen in physiological sleep, are a prominent feature of sedation and anaesthesia with propofol. Further evidence is provided of the topographic distinction between HFS and LFS and a relationship between spindle frequency and depth of sedation is suggested. While a decrease in spindle frequency with increasing propofol concentrations could be attributed to the effects of increasing hyperpolarisation [264], the topographic changes cannot. Changing spindle distribution suggests that thalamocortical units in different

cortical areas may be differentially sensitive to the effects of anaesthetics. One explanation may be that if spindle activity is viewed as an idling rhythm in neurons refractory to sensory input, the observed topographic progression is consistent with the expectation of early isolation of sensorimotor and parietal association areas, at first manifest in performance impairment, then in association areas and finally in frontocentral cortical regions.

In order to better understand the decline in spindle prevalence with deepening sedation, the next step was to analyse the slow oscillation, the ~ 1Hz signature wave of SWS which interact with thalamocortical spindles during physiological sleep.

4.3.7 EEG Slow Waves

Background

A landmark series of publications in 1993 identified and established the underlying neurophysiology of a sub-band of what had until then been described as sleep delta waves (0.1-4 Hz). Steriade and colleagues discovered that activity within this delta band represented at least two processes, delta activity (1-4 Hz) and a novel slow oscillation (~1 Hz). This slow oscillation was described in pyramidal cortical neurons in anaesthetised cats (pentobarbital, ketamine/N_2O or ketamine/xylazine). Neurons exhibited this behaviour at a resting membrane potential more negative than −60 mV. At this level of hyperpolarisation they displayed a functional bistability, oscillating between long lasting periods of depolarisation (superimposed with action potentials) and periods of electrical silence. These two states have been variously described as UP/DOWN and ON/OFF. Because of the potential ambiguity between descriptions of surface positive/depth negative deflections and the functional state of the cortical neurons in each phase, the UP/DOWN nomenclature is not used in this dissertation, which adheres rather to the more functionally descriptive ON/OFF terms.

This ON/OFF flip flop occurred in functionally and anatomically diverse cortical areas and was described as an emergent property of neocortical networks when hyperpolarised [278]. It survived extensive thalamic lesioning and callosotomy and was present even in isolated cortical slices[279]. In fact the slow rhythm found in thalamic RE cells was found to be synaptically driven by the cortex [280]. Slow oscillations could be blocked

by stimulation of the pedunculopontine cholinergic neurons or the noradrenergic locus coeruleus, which shift the balance of modulatory inputs in favour of depolarisation or waking [281].

Further studies into the phase relationship between neuronal slow oscillations and the surface EEG showed that sleep slow waves are the result of extensive synchrony within these underlying oscillations [282]. Later, Massmini and colleagues described the entrainment of cortical neurons into the slow oscillation as a travelling wave, sweeping across the cortex with a defined site of origin and pattern of propagation [283]. On the basis of this large series of experiments the authors contrasted oscillatory behaviours during states of vigilance. In the waking brain, large numbers of diverse neural networks are constantly engaged in network-specific changes in firing rates and phase relations. In the sleeping brain large numbers of heterogenous neurons are engaged in low frequency phase synchronised oscillations. Importantly, slow wave sleep is an active brain state, with firing rates during the depolarisation phase of ON/OFF oscillations as high as during waking and REM sleep. They proposed that a brain engaged in such synchronised low frequency oscillations is functionally deafferented [284]. In this state, the individual operations involved in integrative processes, which are a prerequisite for the conscious state, are overwhelmed by cortical and thalamic neurons' participation in these spreading waves [282]. This hypothesis suggests that the slow oscillation may be the hallmark of the brain that is isolated from external inputs and involved only in an internal dialogue. EEG slow wave activity is therefore a key target of investigations into unconsciousness and anaesthesia. Several authors whose research involves administering anaesthetics to animals while recording cortical electrophysiology have reported titrating anaesthesia to the presence of continuous slow waves. However, this has not been advocated as an endpoint for titrating clinical anaesthesia in humans. The feasibility of such an approach was therefore investigated using this dataset.

Un-preprocessed slow wave activity

In the first instance, absolute and relative power in the SWA band was plotted for each individual. These individual plots are shown in (figure 4.16). As these data illustrate clearly, there are both remarkable similarities and interesting differences between subjects' SWA. Activity is negligible at baseline but rises sharply in association with LOBR. Activity then rises quickly to a peak. In most subjects activity plateaued at this level then declined sharply just prior to ROBR[3].

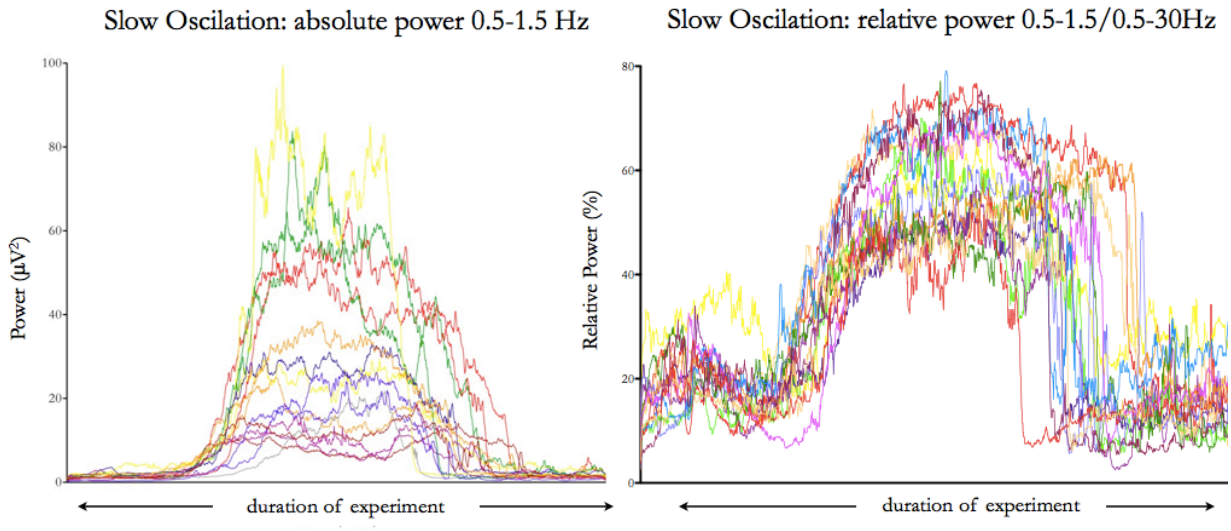

Figure 4.16 Absolute and relative power in the 0.5-1.5 Hz frequency band. Data from all 16 subjects plotted for the full 116 minute experiment. Propofol ESC is omitted for clarity. Left: absolute power of SWA shows the same pattern for each subject although there is marked variability between subjects in the peak power. Right: SWA power as a percentage of the total power in the 0.5-30Hz band. This shows a consistent pattern, with a rapid rise in SWA which reaches a plateau at which it remains until dropping off sharply during recovery.

The level at which SWA peaked varied significantly from subject to subject (range 10.84-83.78 μV^2). The amplitude of activity at the scalp in a given wave is a function of the number of cortical neurons oscillating synchronously at that frequency. In this experiment, the peak power of SWA was negatively correlated with subject age **(**figure 4.17). Voxel based morphometry (VBM) was used to estimate the grey matter volume in the frontal, temporal, insular, parietal and occipital lobes, the hypothesis being that the number of neurons available to participate in SWA would influence the amplitude of activity that could be generated. Peak power in SWA was positively correlated with frontal grey matter volume only (p=0.02 corrected), which

[3] The EEG of some subjects at higher levels of propofol contained brief epochs of isoelectricity. While these epochs rarely reached the criterion of 0.5 seconds, which defines burst suppression (BS), their presence still impacts upon SWA. Subjects who attained particularly deep levels of sedation unsurprisingly showed a decrease in SWA peak amplitude, which recovered with drug offset and the end of BS.

declines with age. This is not unexpected in the light of work published by Massimini and Murphy showing the origin of most SWA to be frontal [285]. The effect of age on peak SWA may therefore be a function of age related changes in frontal grey matter volume. In this study however, only an association is shown between SWA peak power and age, and unfortunately the age range is narrow. SWA peak power may equally be a function of the strength of synaptic connections facilitating SWA synchrony, which may also vary with age.

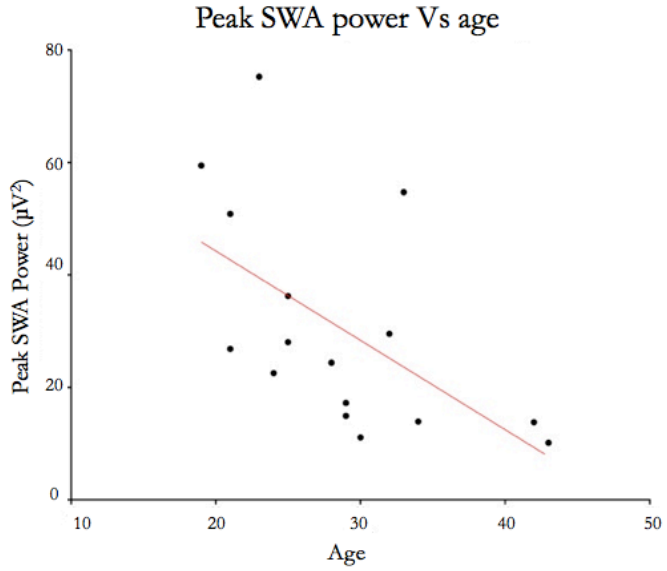

Figure 4.17 The peak SWA power was inversely correlated with subjects' age ($R^2 = 0.33$, $p = 0.02$).

SWA and behavioural responses

The exact relationship between LOBR and the onset of SWA is difficult to appreciate in the initial representation of raw data. Banding the data by behavioural transitions (LOBR, ROBR), as was done for investigation of spindle prevalence progression, showed the nature of the switch from minimal to plateau SWA, with a clear transition from the rising SWA phase to its plateau phase. This progression reversed on drug offset and in fact the downslope in the SWA power consistently predicted imminent ROBF (figure 4.18). The topographic distribution of SWA during each phase of the experiment is also shown in this figure, showing that the highest amplitude in SWA is frontal. This is consistent with what is known about SWA in sleep but it also has practical implications for clinical measurement, in that access to and measurement of frontal EEG using commercial monitors is established widespread practice.

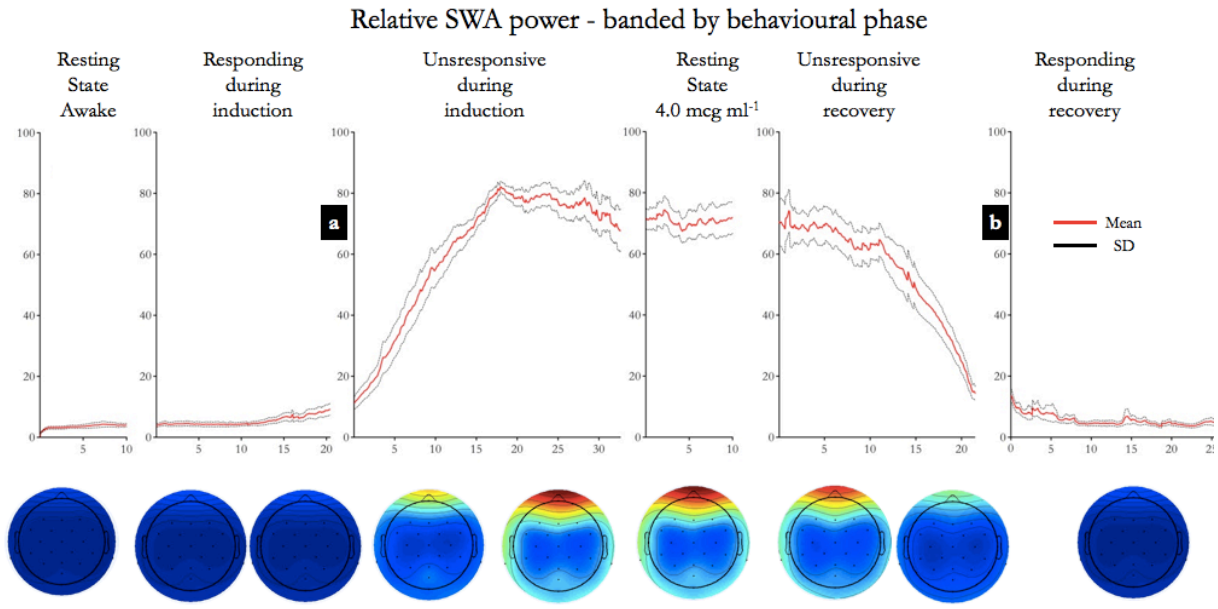

Figure 4.18 Each individual's SWA data was divided according to behaviour, as in figure 4.14. The top plot shows the mean (red) and standard deviation (black) relative SWA power during each behavioural phase with a: last response and b:first response. Following LOBR, SWA continues to rise until activity reaches saturation, after which point it remains at a plateau (with a slight decrease due to burst suppression) until after the drug is discontinued. Relative SWA power decreases sharply prior to ROBR.

Topographic representations of relative slow wave power (blue 0% - red 100%) below this show that the highest SWA power is frontal, consistent with the finding that SWA peak power is correlated with grey matter volume in the frontal lobe but not in other cortical regions.

4.3.8 Evoked Potentials

An evoked potential is a transient change in ongoing EEG evoked by the presentation of a stimulus. Uncued brief stimuli, including auditory and noxious laser stimuli, can be detected as event related potentials (ERPs) in the scalp EEG. The specific signal changes following stimulation relate to different aspects of the evoked cerebral activity.

Evoked potentials are complex waveforms. Fifteen distinct components can be measured within an auditory evoked potential (AEP). Early components appear between 0 and 8 ms after the stimulus and are associated with activation of the cochlea and auditory brainstem nuclei. Between 8 and 50 ms "mid-latency" AEPs are produced by activation of the auditory thalamus. Long latency AEP components occur between 50 and 300 ms and represent widespread cortical activation [286]. The components that have been studied with respect to their behaviour under anaesthesia are the early negative deflection, N1 (at ~ 100 ms) and P3 (at 250-600 ms). N1 is an exogenous potential, determined by the physical nature of the stimulus and frequently described under anaesthesia. P3 is an exogenous potential determined by attention and cognition associated with the stimulus [287].

Laser evoked potentials (LEPs) appear at longer latencies due to the impulse conduction distance from the lower limb. LEPs typically comprise three main components, negative deflections N1 and N2 (at 140-170 and 180-280 ms respectively) which are often not distinguishable from one another, and the positive P2 deflection (after 310-410 ms) [156]. The early negative component is associated with primary somatosensory cortex activation whereas the later positive component is modulated by attention or distraction [288]. During stage 2 NREM and slow wave sleep, N2 and P2 latencies do not change but amplitude decreases [233]. LEPs have been elicited during alphalaxone anaesthesia in monkeys [289], but in another study utilising pentobarbital in rats, LEPs disappeared [290].

K-complexes are large potential changes first described in the early 1930s as occurring both spontaneously and in response to tone stimulation during NREM sleep [22]. They have been regarded as variants of evoked potentials [291] and frontal negative waves consistent with K-complex morphology have been reported in response to auditory and laser stimulation during physiological sleep [233]. However the functional significance of K-complexes and whether or not they are in fact evoked or spontaneous has been debated. The work of Amzica and Steriade investigating the electrophysiology of the slow oscillation established that EEG slow waves are in fact rhythmic series of (usually spontaneous but potentially evoked) K-complexes, with the same underlying neurophysiology, their genesis dependent on the cortical hyperpolarisation of sleep [292,293].

Results

Peri-stimulus epochs were extracted as described in chapter 2 Epochs were averaged within phases defined by both behavioural and EEG spectral measures, as in figures 4.14 and 4.18. The phases were therefore:

- Early responsive
- Late responsive (with increased beta activity and psychomotor retardation)
- Unresponsive, rising SWA
- Unresponsive, plateau SWA
- Unresponsive falling SWA
- Early recovery, responding
- Late recovery, responding

During the baseline early responsive phase, robust potentials were elicited by both tones and laser stimuli confirming the efficacy of the stimulation (figure 4.19) although the magnitude of the LEPs was small relative to that of the AEPs. Baseline AEP components were N1 (140ms, −6.5) and P3 (230ms, 8.45 μV). Baseline LEP components were N1/2 (250ms, −2.5μV) and P2 (460ms, 2.1μV).

LEP Progression

With the onset of early EEG changes (beta activity), the nadir of LEP negativity, N1/2, was found to have a significantly increased latency (490 ms compared to 230 ms at baseline) and a P2 potential was observed at 550 ms. The amplitude of N1/2 was significantly reduced but P2 reduction did not quite reach statistical significance (p=0.06). Laser stimuli also produced slow wave phase resetting during the "plateau SWA" phase. The pronounced negative deflection with subsequent large slow wave, identified as a K-complex following tonal stimulation during the "falling SWA" recovery phase, was also seen here in response to laser stimulation. During the early responsive phase of the recovery, LEP morphology recovered and amplitudes matched those of the late responsive phase during induction. LEP amplitudes returned to baseline in the later part of recovery (figures 4.19 and 4.20).

AEP progression

The amplitudes of both N1 and P3 components of the AEP were significantly reduced during the late responsive phase, during which activity in the beta region of the spectrum had increased and significant psychomotor retardation was noted. Latencies were unchanged. When subjects were unresponsive, tonal

stimulation was followed by a series of slow waves. These data are averaged across trials and subjects, and the results show that stimulation resulted in a phase-resetting of the slow waves. This was seen both during the "rising SWA" and "plateau SWA" phases but synchronisation was more robust and persisted for longer during the plateau phase. During the recovery or "falling SWA" phase, a pronounced negative potential preceded high amplitude synchronised slow waves, morphologically a K-complex. Once subjects became responsive again the K-complexes disappeared and AEP morphology returned to the pre LOBR parameters, with significantly lower amplitudes than baseline. Amplitudes returned to baseline during the later part of the recovery (figure 4.19 and 4.20).

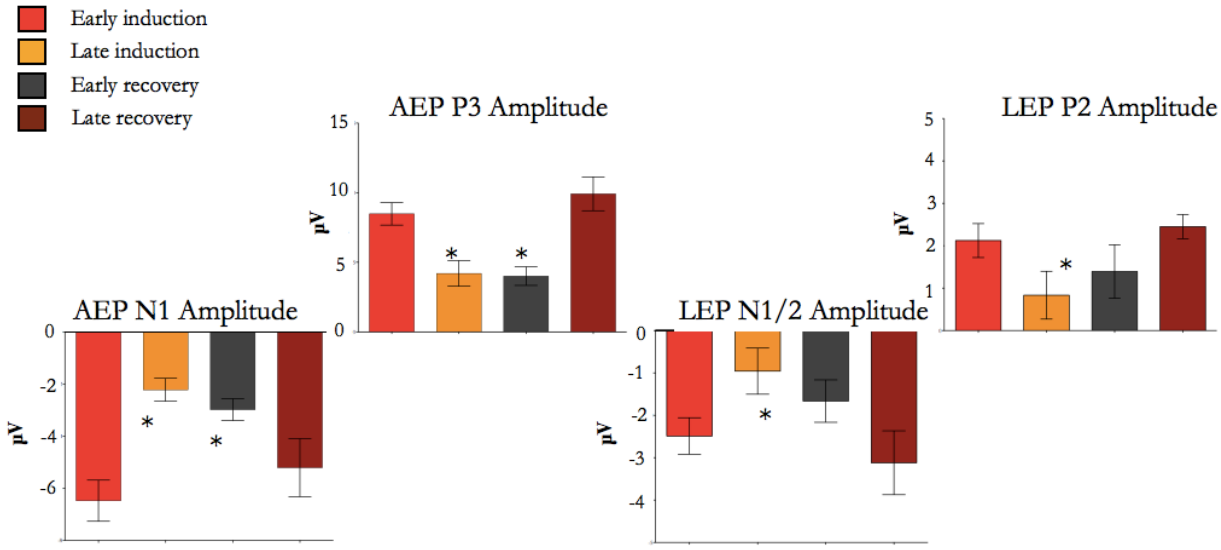

Figure 4.19 Changes in AEP and LEP component amplitudes by phase. AEP amplitudes were large, significantly reduced by propofol and only returned to baseline late in recovery. LEP amplitudes were smaller and showed an earlier recovery to baseline (* $p < 0.05$, corrected).

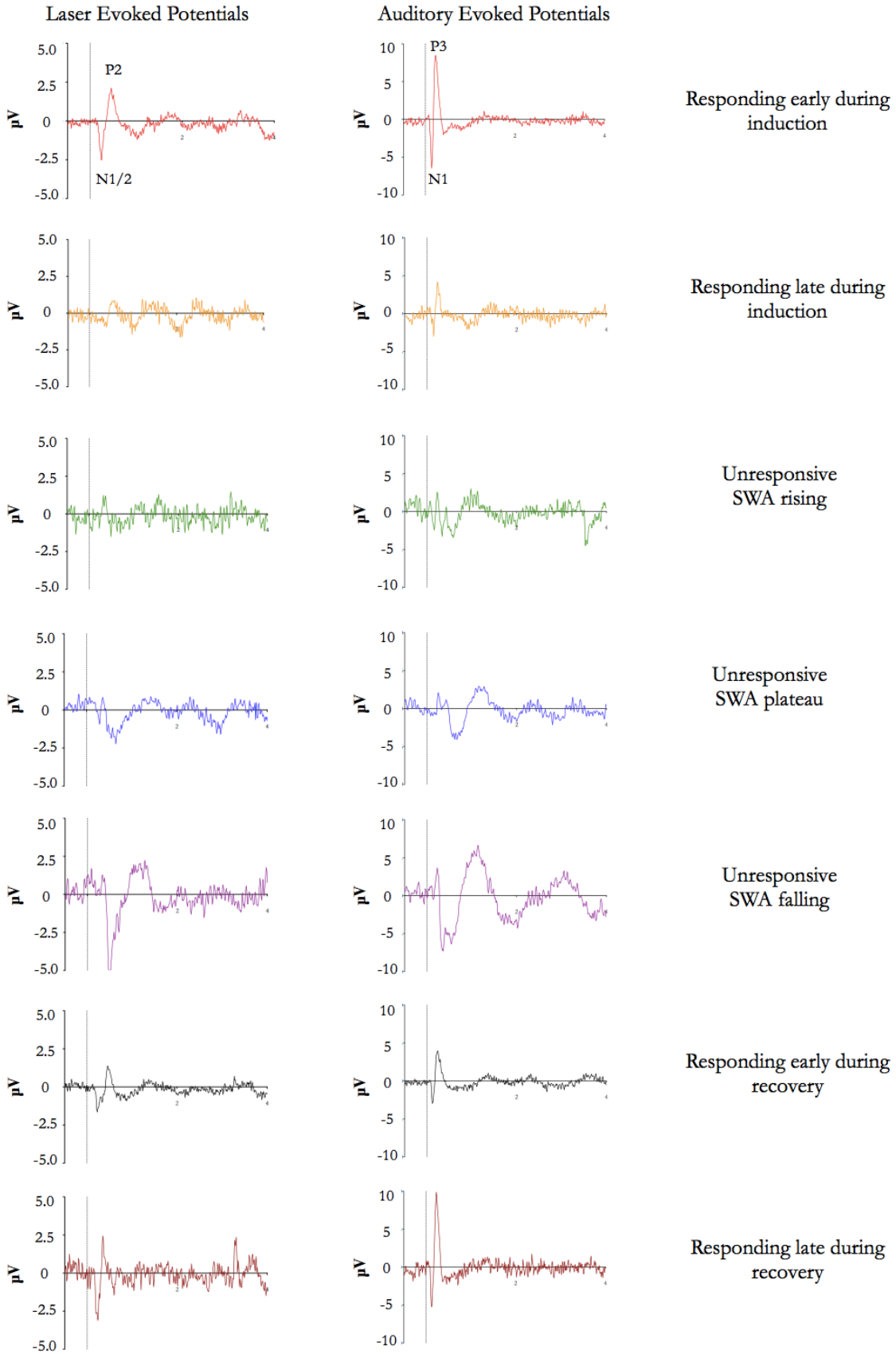

Figure 4.20 Laser evoked potentials (LEP - left) and auditory evoked potentials (AEP - right) during each phase of the experiment as now defined by slow wave activity. A reduction in the amplitude of both LEPs and AEPs is noted early in the induction phase. K-complexes are noted during recovery.

K-complexes

The changes in ERP amplitude and latency observed during responsive phases with significant psychomotor impairment is expected. Reciprocal changes during recovery phases show a symmetry specific to the responsive periods of the experiment. The unresponsive phases however reveal a marked asymmetry. Stimulation during the wakeup phase, when SWA was falling, elicited large K-complex potentials. As reported in chapter 4, the ESC at which LOBR occurred was significantly higher than the ESC at which ROBR occurred (paired t-test, p=0.006, figure 4.4). These ERPs may shed light on the nature of the anaesthetic hysteresis observed. During induction, a direct transition from evoked cortical potentials to event related synchronisation of spindles and slow waves occurred. During recovery however, at an ESC that in the same individual was associated with intact behaviour, stimuli instead elicited K-complexes, suggesting that before ROBR, subjects transited through a state more akin to physiological sleep than anaesthesia.

During sleep, K-complexes can occur spontaneously or be elicited by sensory stimuli including auditory and noxious events [294]. As shown by Amzica and Steriade, the neuronal flip-flop from hyperpolarised silence (OFF) to spiking (ON) of the slow oscillation is the same process which produces K-complexes and this becomes more organised with deepening anaesthesia[292,293]. Thus a K-complex is a single, often externally triggered slow wave. Massimini and colleagues reported that transcranical magnetic stimulation (TMS) reliably elicits cortical responses in awake and sleeping humans. Awake, triggered oscillations are high frequency and entrain a wide network of cortical regions. Asleep however, responses are stereotypical high amplitude and low frequency and do not produce activation in distant cortical areas. They suggested that this failure represented a breakdown in effective cortico-cortical connectivity. They also noted that TMS stimulation during sleep could trigger the ON/OFF transition, which would result in a phase resetting in the slow oscillation [96].

The hypothesis of neural inertia would predict that relatively higher levels of sedatives are required to change the state of consciousness from awake to unresponsive and that relatively lower levels must be obtained to drive the brain to transition back to waking. This would explain the differences in ESC at LOBR and ROBR. However the presence of a distinct electrophysiological state during recovery suggests that this is not just a function of pharmacology or inertia.

While the individual nuclei of the reticular activating system have diverse and extensive efferent connections modulating the state of arousal, they also receive afferents from the cerebral cortex itself [295,296]. This experiment has shown that during anaesthesia, the cerebral cortex is primarily engaged in slow waves and spindles, oscillations underlying an internal dialogue rather than the high frequency oscillations of intact conscious processing. Reduced cortical input changes the activity of sleep and wake-promoting nuclei, resulting in a different balance of sleep/wake driver output during the recovery phase. Hence, when ESC had dropped to a level consistent with intact behavioural responses, physiological sleep persisted instead. In contrast, during induction, the balance of sleep-wake centre activity favoured wakefulness and there was no reason for physiological sleep to emerge, so wakefulness persisted until the propofol overcame it. While the observations to not mitigate against the concept of neural inertia, it is clear from these data that despite ultraslow induction of anaesthesia, the transition to wakefulness was associated with a period of EEG activity consistent with physiological sleep which was not seen during induction.

4.3.9 Permutation Entropy

The main aim of processed EEG is to reduce the complex superposition of signals seen at the scalp into a single parameter describing the underlying activity. Time-frequency analyses in their many manifestations (median frequency, spectral edge frequency and band power progression analyses presented in this chapter) measure linear signal properties. The complexity of neuronal interactions in the cerebral cortex is such that non-linear parameters may provide additional information about the processes underlying the signal.

Entropy refers to the amount of disorder in a system. In the awake brain, the number of independent signal generators is huge and the timeseries of scalp potentials is disordered. During sedation and anaesthesia, cortical oscillatory systems become more organised and the number of independent signal generators decreases. Neurons of the corticothalamic systems are corralled into spindles by inhibitory potentials from the thalamic reticular nucleus and driven into bistable slow oscillations by the overwhelming hyperpolarising influences. This reduces the disorder in the system, the signal becomes simpler and entropy falls.

While conceptually intuitive, the realisation of entropy as a robust metric is complicated by the non-stationarity of the system. Approximate entropy (AE) is dependent on long stationary noise-free signals and is therefore impractical for use in clinical anaesthesia. Bandt and Pompe proposed permutation entropy (PE) as an alternative quantification of signal regularity better suited to this application [223]. PE estimation is based

on the comparison of neighbouring values. This approach would be particularly well suited to the analysis of EEG during anaesthesia as it is fast, not dependent on complex pre-processing and reportedly relatively unchanged by the introduction of additional noise to the system. Permutation entropy examines consecutive subvectors within the signal and compares neighbouring patterns. It is therefore independent of amplitude.

As described in chapter 2 and appendix C, permutation entropy can be relatively simple estimated using an open source algorithm [224]. To calculate PE a series of measurements are first converted into a series of ordinal patterns (such as slopes, peaks, troughs and ties). This removes the amplitude component of the timeseries that had made it non-stationary. The number of occurrences of each pattern in the data series whose PE is being estimated is then counted (figure 4.21) and the normalised probability distribution of these patterns calculated.

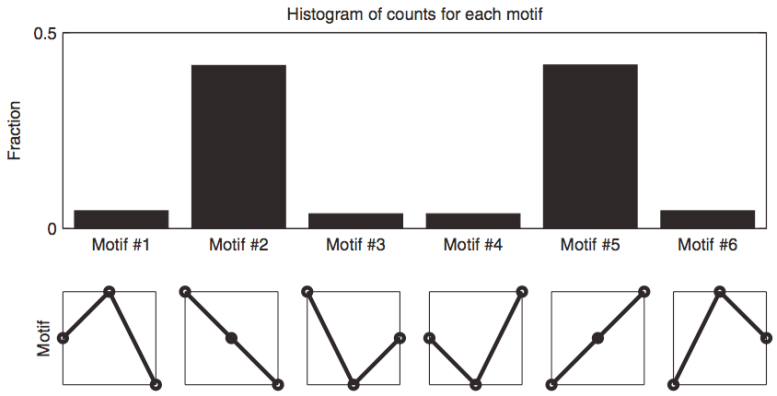

Figure 4.21 From Olofsen, British Journal of Anaesthesia 2008. This figure demonstrates the patterns sought by the PE algorithm. The prevalence of each pattern is counted. As the EEG becomes simpler, there are fewer peaks and troughs and more straight lines.

When the EEG is dominated by high frequencies each pattern is equally prevalent. As EEG slows there are fewer peaks and troughs so the probability of observing one falls, and more slopes so the probability of observing this pattern rises. Estimations of permutation entropy have been applied to data recorded during clinical anaesthesia and found to be capable of separating consciousness from unconsciousness [226]. PE was found to be less sensitive to extraneous signals while awake and to have a greater predictive value for differentiating consciousness from unconsciousness than AE [225]. Olofsen and colleagues applied PE to the EEG of 21 patients receiving sevoflurane and 9 patients receiving propofol. They found that PE reliably

tracked anaesthesia induced changes in EEG frequency and could be used to generate pharmacokinetic/ pharmacodynamic models of comparable accuracy to those based on BIS.

The algorithm published by Olofsen was used to calculate a composite PE index (CPEI) for sequential 3 second epochs across the duration of the experiment in each channel, for each subject. Figure 4.22 shows the change in CPEI over the course of the experiment, indicating the points at which LOBR and ROBR occurred. CPEI did reliably track the major changes in frequency distribution found in time-frequency analysis. CPEI increased at the same time as beta activity did and decreased after LOBR. CPEI also showed an increase just prior to ROBR in some subjects. CPEI, while sensitive to the effects of propofol, did not provide a quality or quantity of information comparable to spectral analysis and this route of analysis was not pursued further in this experiment.

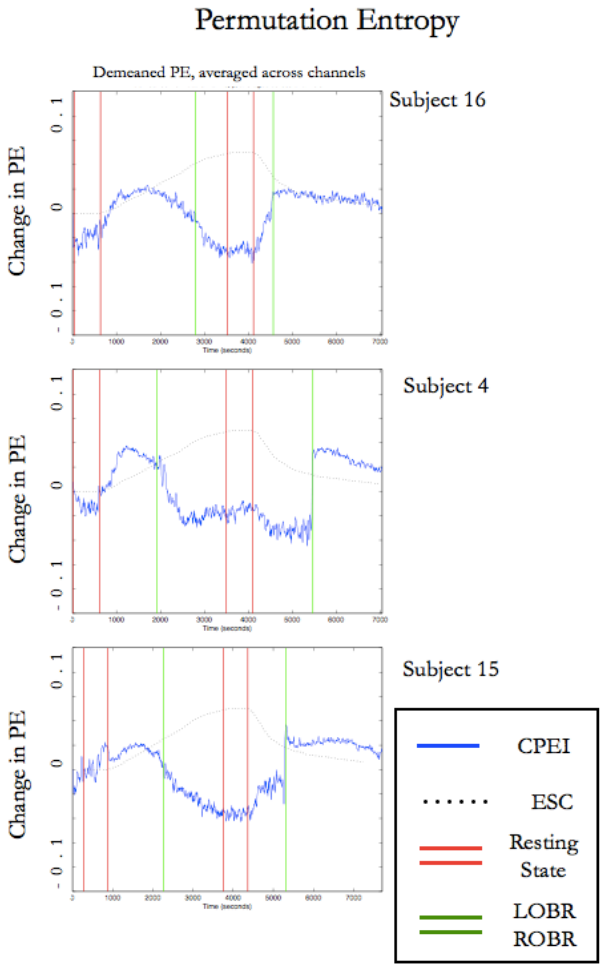

Figure 4.22 Shows the pattern of change in the composite permutation entropy index in three representative subjects. Red lines demarcate the resting states and green lines show the last and first responses during the experiment. While the changes measured do track those observed with other techniques (spectral power estimation, spindle prevalence), they are very small and did not reliably change prior to ROBR. This technique was not used beyond this exploratory analysis.

Conclusion

Using EEG, we can define and detect a second transition in neurophysiological state, subsequent to behavioural unresponsiveness, to SWA saturation, where the number of neurons entrained into the traveling slow oscillation is maximal for the individual. This finding raises the possibility of using SWA as a measure of depth of sedation or anaesthesia. The prospect of quantifying a recognised physiological activity to guide appropriate drug administration in an individual would represent an important advance in anaesthesia.

As introduced in chapter 2, current processed EEG monitors rely on algorithms designed to quantify and scale the available range of signals and generate a dimensionless number statistically associated with adequate anaesthesia. While these algorithms do have a sound basis in neurophysiology, based as they are on activity in the various frequency bands described as well as signal coherence between different frequencies [248], they are designed for a *population*. Therefore they are subject to the same statistical limitations when implemented in individuals as pharmacokinetic/pharmacodynamic models. In fact, unlike PK/PD models, age is not incorporated into the calculations, despite well described age related changes in EEG activity. In many senses the capacity of clinicians to interpret the output of such "black box" devices has been hindered by their opacity in terms of both the inputs and the output. It is likely that this has significantly retarded widespread adoption of EEG monitoring in anaesthesia.

To be relied upon as a significant clinical assay, it would be useful to understand the implications of these two transitions in SWA (from minimal to rising then to plateau) for cognition and perception. To further investigate this, a more advanced version of this experiment was carried out whithin a functional MRI scanner, with a subset of the subjects who completed this first EEG experiment. This is detailed in the next chapter.

Chapter 5: EEG/fMRI of transitions in states of consciousness

Introduction

The experiment reported in Chapter 4 revealed a transition in neurophysiological state subsequent to the loss of behavioural responses (LOBR) but before the onset of burst suppression, where the slow wave activity (SWA) power reached its maximum and thereafter remained at a plateau. The transition to "SWA saturation" may be a clinically useful phenomenon, indicating the complete isolation of activity within the cerebral cortex from external perturbation. However, this change in EEG activity reflects the summation of millions of dispersed signals into a global or at best a regional measurement. The underlying neurophysiology can only be understood by examining the local activity of neurons and the networks in which they participate. As described in chapter 4, EEG analysis remains the subject of some distrust in clinical anaesthesia. The difficulty to date in relating the stereotypical changes in EEG signals at the scalp to underlying and localised brain function has contributed to this skepticism [4]. Combined EEG-fMRI exploits the temporal resolution of EEG and the spatial resolution of fMRI simultaneously and therefore affords an opportunity to investigate that precise relationship.

Spatial resolution of EEG

Scalp EEG signals are the result of the summation of underlying potentials and are thus limited by the anatomy, physiology and physics of these potentials as described in section X. While EEG has successfully yielded functional and diagnostic insights, there are significant limitations to the inferences about activity that can be drawn. Scalp potentials are dependent upon synchronous activity in large numbers of cortical pyramidal neurons with their dipole vectors oriented perpendicular to the scalp. Activity involving fewer neurons, that which is less coherent or which is electrically invisible (such as tangential dipoles originating in the cortical sulci) may not result in measurable potentials.

Volume conduction of deep electrical signals to the scalp results in poor spatial resolution. The capacity for source localisation therefore, even with large numbers of channels (high density EEG, <128 channels), is limited. There is no unique solution to the ill-posed problem of computationally identifying the true 3-dimensional origin of electrical activity detected in 2-dimensional sensor data. A 32-channel EEG montage was used in these experiments. While the activity in a single channel can inform analysis of global activity, few

---

4 1 "As long as the raw EEG remains a mysterious wavy line to anaesthetists, the EEG monitors will remain in a time warp of under-utilization and distrust."[219].

inferences can be drawn about regional or local activity from such data. Acquisition of data in a greater number of channels requires additional expensive equipment and adds to the time required for experimentation, already onerous on subjects, without escaping the inverse problem. Multimodal data acquisition strategies, including simultaneous EEG-fMRI, exploit the advantages of each of these complementary techniques.

Temporal resolution of fMRI

The temporal resolution of fMRI is on the order of several seconds whereas EEG has a temporal resolution limited only by the Nyquist limit for the sampling rate used (5000 Hz here) and is therefore on the order of milliseconds. fMRI does not have the capacity of EEG to tease out temporally distinct individual components of evoked activity.

FMRI is also critically dependent on the sensitivity and specificity of the criteria defining experimental sessions. Pharmacological manipulations are themselves vulnerable to within-subject, between-session variability, and the range of propofol doses at which motor responses to verbal and noxious stimulation are abolished is wide [111]. Reliance upon population based models for the definition or prediction of neurophysiological state, even using subject-specific targets as was attempted in chapter 3, introduces additional uncertainty and reduces the power of the study to detect state-specific responses. In the previous experiments, pharmacodynamic variability was managed by developing a working behavioural definition to quantify sedation. This was not an ideal solution however. Another concern that arose during earlier experiments was that the relative sensory deprivation of a dark environment with the additional soporific effect of the repetitive background scanner noise, dampened by earplugs, could cause subjects to fall into physiological sleep. This would result in a behavioural transition independent of (or differentially dependent upon) the pharmacology. Neurophysiological state would therefore differ across subjects at this behavioural transition, driven in some subjects mainly by physiology and others mainly by pharmacology.

Studies investigating issues of consciousness are particularly suited to, and essentially dependent upon, multimodal observations for the definition of state. The addition of EEG to the a continuous fMRI acquisition would allow retrospective definition of state-consistent "windows" or temporal regions of interest (tROIs) for analysis. Simultaneous EEG can also inform the interpretation and analysis of fMRI where there are no

behavioural criteria defining tROIs. It would be logical, for example, to explore the change in fMRI activity in response to external stimuli before and during SWA saturation.

5.1 Methods

Technical details of simultaneous combined EEG-fMRI acquisition and analysis are presented in chapter 2. Here the practical considerations are addressed, and a detailed description of the conduct of the experiment is presented.

Subjects

Fifteen of the subjects who completed the EEG experiment described in chapter 4 proceeded to take part in the combined EEG-fMRI experiment reported in this chapter. Subject preparation was the same as for the EEG experiment in terms of fasting and post-infusion supervision (Appendix A). Two subjects completed the series but when the scans were visually inspected offline for quality control, it was immediately clear that excessive head motion during portions of the scan rendered significant portions of their data unusable. This was confirmed by the failure of motion correction algorithms to remedy the issue. A third subject developed a respiratory pattern consistent with upper airway obstruction at higher levels of propofol and the scan was aborted before completion. Twelve of the subjects therefore completed the full scan series described below uneventfully.

Paradigm Modification

The experimental paradigm used in the bench experiment was used in the scanner with a number of small modifications due to technical limitations. The original paradigm called for an initial 10 minute period of rest with the eyes closed, a 48 minute period of stimulation during ultraslow induction of anaesthesia, a further 10 minute period of rest at the peak propofol level of 4.0 mcg ml-1 and finally a 48 minute stimulation period during propofol elimination. In the bench experiment the entire sequence was acquired without interruption. At the spatial and temporal resolution required of the fMRI data however, a 116 minute scan generated 6 gigabytes (GB) of data. The system used had a 4GB limit above which further scanning overwrote previously acquired data. This was not a problem that could be resolved at the time as the scanner was about to be replaced after this final experiment. The functional acquisition was therefore divided into a sequence of four scans of 10, 48, 10 and 48 minutes with a pause of three to five minutes between scans during which the scan was written to disk.

The haemodynamic response to neuronal activity that produces the BOLD signal is associated with a time delay, beginning 3-6 seconds following stimulation, peaking at 6-10 seconds and then declining over the subsequent 3 seconds [114]. During the bench experiment, subjects were asked to rate the intensity of each laser stimulus in order to assess the analgesic effects if any of propofol. The inclusion of a rating scale during functional scanning would introduce both cognitive and motor tasks that are associated with BOLD signal changes of their own. The task of rating aspects of a stimulus has been shown to influence the rating given and also changes the pattern of activation seen in response to both painful and non-painful stimuli [297]. Rating noxious stimuli during the scan would provide little information that was not already obtained during the bench experiment and *not* rating them would allow any change in cerebral activation occurring at LOBR to remain uncomplicated by any change in the associated motor activity. It was therefore decided that the passive experience of noxious stimulation would be studied in the scanner and no ratings would be sought. A computer screen was visible to subjects via a mirror directly overhead. Instead of projecting rating scales to the computer screen as was done at the bench, a black screen with a central white fixation cross was displayed.

Auditory tones were listened to passively, as at the bench experiment, but the motor response to the word task was retained to maintain the complexity of the cerebral processing involved (audition, discrimination, decision making and selection of a motor response) and to provide a means of detecting the crucial behavioural transition of LOBR.

Safety considerations

To date there have been very few combined EEG-fMRI studies of anaesthesia. Published studies of anaesthesia, both isolated fMRI [298,299] and combined EEG-fMRI [300], have all used a stepwise approach whereby the target level, be it behavioural or pharmacological, was established and allowed to reach equilibrium before a block of steady state functional data was acquired. This is an ethically and methodologically sound technique that optimises subject safety in a potentially hazardous environment by allowing airway and cardiorespiratory stability to be established before allowing the relative loss of contact that occurs during scanning. One of the first studies using combined EEG-fMRI enrolled patients with tracheostomies to ensure the maintenance of a patent airway [300]. No group has thus far conducted a continuous acquisition during drug level changes in spite of the fact that such an acquisition has the potential for greater statistical sensitivity, using bespoke, subject-specific scan periods

(temporal regions of interest) rather than pre-defined blocks. A number of practical steps were taken to reduce any risk of harm to the participants.

1. Pre-scanning experiment. Only subjects who tolerated the infusion regime outside the scanner proceeded to the same infusion regime within the scanner. This approach eliminated two unsuitable subjects but failed to detect a potential problem in one subject, who developed upper airway obstruction in the scanner. This is most likely because the semi-recumbent position adopted during the bench experiment was replaced with the fully supine position in the scanner.
2. Monitoring. As with the bench experiment, full anaesthesia monitoring in accordance with the AAGBI guidelines [301] was used throughout the scan. MRI compatible equipment including pneumatic respiratory bellows, carbon-fibre ECG leads and fibre-optic SpO2 cabling was used to protect subjects from burns which would be caused by currents induced in wires by the switching magnetic gradients. The anaesthetist responsible for drug administration was in the console room adjacent to the scanner with the infusion pump and the monitors. A second investigator was in the scan room with the subject throughout the experiment. This second investigator was responsible for the safe administration of the laser stimuli. Because a laser was being used in the scan room, a protective shield over the console room window prevented visual contact with the subject or second investigator. A protocol for communication between the two investigators was therefore devised. After the subject became unresponsive, input to the projector screen was switched from the fixation cross to show the physiological observations to the operator inside the scan room. This screen was also used to type messages to the scan room investigator if any concerns arose. The scan room investigator held an emergency button that could be used to abort the scan at any time.
3. Pressure point protection. During piloting it was clear that subject comfort for the duration of this long experiment would have a significant impact on their experience and also on the quality of data obtained, dependent as it is on movement being kept to an absolute minimum. During natural sleep, pressure ischaemia is prevented by periodic position changes during the night. During anaesthesia however, this protective adjustment is lost and pressure areas are at risk due to immobility if left unsupported for relatively short periods of time [302]. EEG electrodes were a particular source of discomfort so foam padding was placed under the head, within the coil.
4. Airway support. In order to minimise obstruction to the airway that may develop as a result of decreased muscle tone under anaesthesia. the foam padding used to protect from pressure discomfort at the EEG

electrodes was also placed behind the angle of the mandible bilaterally. This was trialled in pilot experiments and successfully provided airway support in all but one subject.

5. Eye protection. Wavelength specific protective lenses were sewn into a fabric mask as commercial protective goggles were too large to fit in the head coil once the head was surrounded by padding and an EEG cap.

After the subject was positioned comfortably in the scanner and initial setup and shimming completed, a fieldmap was obtained. Following this 10 minute scan, a thresholding procedure was carried out as in the previous experiment, to establish the laser energy that was reliably verbally rated by the subject as 5/10 on an 11 point numerical rating scale. This was the energy level of all the stimuli delivered during the subsequent experiment for that subject.

Data Collected

Twelve subjects completed the full experiment protocol. Resting state scans were obtained in both conditions (awake and anaesthetised) for fourteen subjects. Induction scans from 0.0 to 4.0 mcg ml-1 ESC propofol were obtained for twelve subjects. Recovery scans were obtained for thirteen subjects. Once subjects woke in the scanner excessive head movement rendered adequate motion correction impossible. Motion artifact-free scan data was however obtained up to ROBR. In this chapter the results of the induction and recovery scan are presented and discussed. Chapter 6 presents the results of the resting state scans.

5.2 Results

5.2.1 Physiology and behavioural data

Cardiorespiratory parameters

There was no clinically significant change in heart rate (figure 4.1 (b)), haemoglobin saturation (range 95-99%), or blood pressure (mean (SD): baseline 123.1(8.3) vs peak propofol 100.5(11.9)), over the course of the scan . Expired carbon dioxide levels increased over the course of the scan to a greater extent than during the previous experiment, illustrating the importance of the choice of propofol as the investigation drug (chapter 2). This was probably due to hypoventilation in the supine position, in which a greater reduction would occur relative to the semi-recumbent position used in the previous experiment. The rate and depth of respiration measured by pneumatic bellows decreased during the induction scan (figure 4.1 (c, d)).

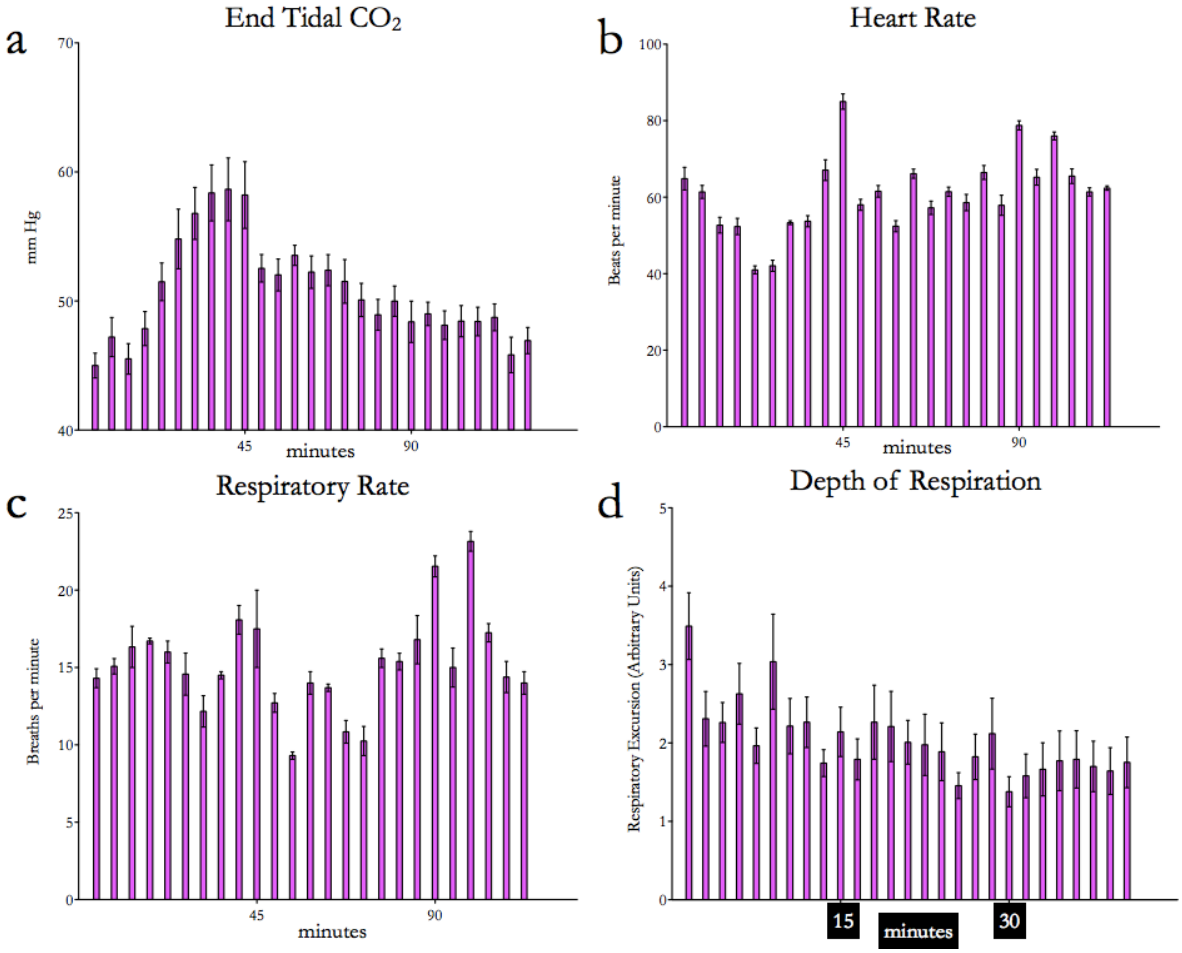

Figure 5.1 Physiological monitoring over the course of the experiment. The expected rise in carbon dioxide (a) was more marked during this experiment than during the previous experiment. This was associated with a decrease in the rate and depth of respiration (c,d, data on depth of respiration only available for 48 minute induction scan). There was no clinically significant change in heart rate.

Correction of functional MRI signal for physiological noise

The change in BOLD signal associated with neuronal activity is of the order of only a few percent. Signal to noise ratio is very sensitive therefore to the introduction of "noise", signal changes arising from non-neuronal influences. Head motion is a major source of non-neuronal signal change. The steps taken to deal with this noise are given in chapter 2. In addition to detecting and correcting head movement, motion parameters are included as regressors of no interest in the generalized linear model (GLM) so that the resultant signal change is accounted for, reducing the unexplained variance and improving the statistical significance of activation signals.

Correction of physiological noise is more difficult. At the sampling rate of fMRI (3 seconds), the frequency of the cardiac and respiratory cycles is above the Nyquist frequency so signal aliasing occurs and notch filtering is ineffective. One method of physiological noise correction (RETROICOR, [303]) involves measuring the cardiac and respiratory cycles with accurate timing, alongside synchronisation of scans and physiological processes. The

physiological noise is modelled as a linear combination of a set of sinusoid functions representing the effects of the respiratory and cardiac processes and their harmonics. This method depends on the stability of cardiorespiratory processes. In practice, the variability of cardiac and respiratory period length has limited the clinical application of this method [304]. This is of particular concern in this dataset, where not only does period length vary over the course of the experiment, but pharmacological manipulation would confound any attempt to model the relationship between physiological oscillations and BOLD signal change.

This rise in arterial carbon dioxide in the awake subject would result in an approximately 15-20% increase in baseline CBF [121]. However, as discussed in chapter 2, the relationship between arterial carbon dioxide levels is altered by propofol, which lowers resting CBF while maintaining autoregulation and neurovascular coupling. The parameters describing the relationship between CO_2 and BOLD signal in this context have not been quantified. In addition, the effects of CO_2 can be expected to be global rather than regional and affect the amplitude of BOLD signal changes rather than the pattern of cerebral activation. Highpass filtering (maximum cycle 50s) and ICA-based denoising were therefore relied upon to substantially reduce any signal changes attributable to a rise in arterial carbon dioxide.

Behavioural Data

State and trait anxiety index scores were consistent within subjects across sessions. (figure 5.2).

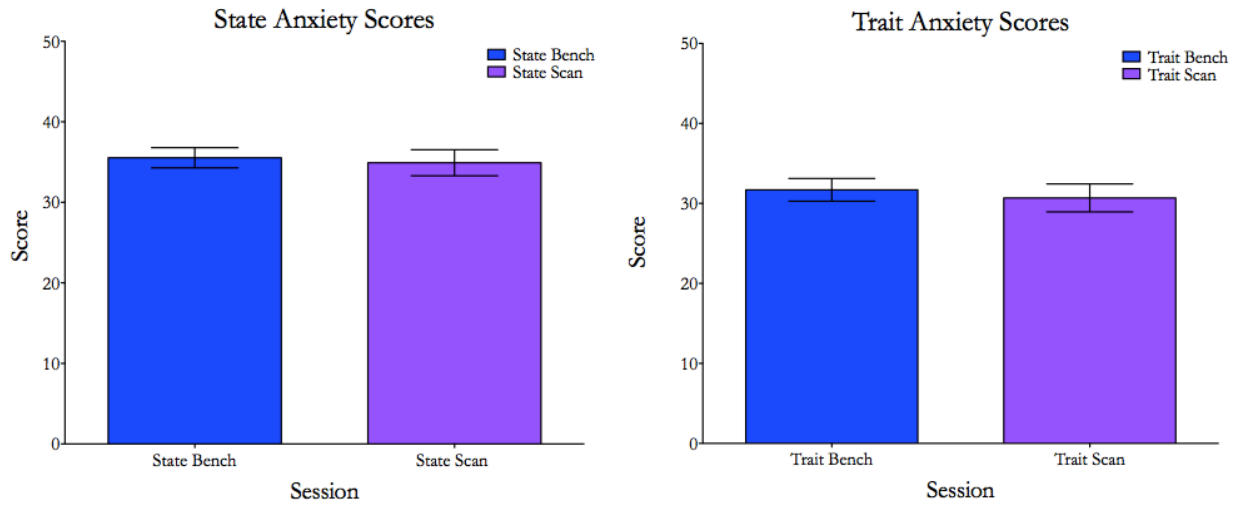

Figure 5.2 There was no change in state or trait anxiety scores when subjects attended to take part in this experiment compared to those when they took part in the previous experiment (paired t-tests).

Laser Energy

The laser energy required to elicit an intensity rating of 5/10 in the scanner (mean ± SD, 4.828 ± 0.79) was significantly higher than the energy required in the bench session (4.375 ± 0.78, paired t-test, $p < 0.01$, figure 5.3). The reason for this is unknown but may be attributable to the novelty of the stimulus at the first experiment or the change in environment from the lab to the scanner. As trait anxiety scores were unchanged this cannot be directly attributed to heightened anxiety at one session relative to another.

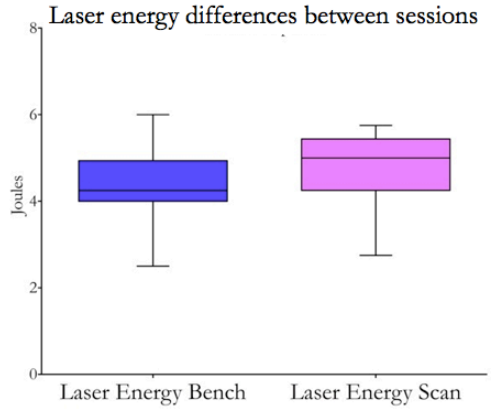

Figure 5.3 The laser energy required to elicit the threshold intensity of 5/10 was significantly higher in the scanner session than at the previous experiment (paired t-test, $p < 0.01$).

Effect Site Concentration

There was an unexpected difference not only between the ESC at which LOBR and ROBR occurred in the scanner relative to the bench (replicating the findings in chapter 3), but in the way that the experimental setting influenced the *direction* of this difference (figure 5.4). While the ESC at LOBR was lower in the scan than at the bench, the ESC at ROBR was not higher, as one might expect, but in fact lower.

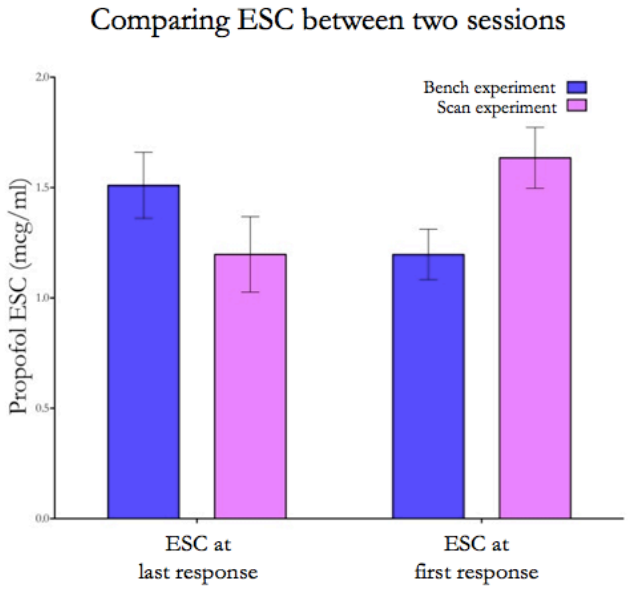

Figure 5.4 At the bench session, the mean (SD) ESC at LOBR was at 1.57(0.6) mcg ml^{-1} and that at ROBR was significantly lower at 1.23(0.45) mcg ml^{-1}, (paired t-test, $p = 0.006$). In the scanner however, the mean (SD) ESC at LOBR was 1.25(0.68) mcg ml^{-1}, significantly lower than ESC at LOBR in the bench experiment (paired t-test, $p = 0.005$). ESC at ROBR in the scanner was 1.64(0.54), significantly *higher* than that at LOBR in the same experiment (paired t-test, $p = 0.022$).

This clear, within subject, between session variability in the ESC at which behavioural transitions occurred highlights the risks associated with reliance upon pharmacodynamic models, however carefully the pharmacokinetic parameters have been calculated.

The effects of sedative anaesthetics are dependent on the level of ongoing stimulation. In the bench experiment, the room was relatively brighter (although the lights were dimmed) and the investigators were within the subject's field of view. The higher level of overall stimulation may have caused subjects to remain awake until drug effects overwhelmed arousal, with the onset of slow wave activity immediately after LOBR. The anticipated soporific effect of the scanner environment with low ambient light, lack of visual contact with the investigators and rhythmic background noise, may have caused subjects to stop responding to stimulation at a neurophysiological state closer to stage 1 or 2 NREM sleep.

In the bench experiment, recovery from propofol sedation involved transition through a neurophysiological state similar to NREM sleep stage 2, with few slow waves and evoked K-complexes. One explanation for the earlier (at higher ESC) occurrence of ROBR in the scanner compared to the bench may be the relatively high level of auditory stimulation in the form of background scanner noise compared to the silence of the physiology laboratory, rousing subjects from this level of sleep.

This hypothesis is one possible explanation of the observed variability in ESC associated with each behavioural transition. The key point arising from this observation is that neurophysiological state cannot be inferred from ESC. Just as the behavioural transitions occurred at unpredictable doses, so would the invisible transition to SWA saturation. FMRI scanning of anaesthesia can only be fully informed by simultaneous EEG assessment of the neurophysiological state.

Word Task Reaction Times

By splitting the responses into the first and second halves of each subject's responsive period, as was done for responses during the bench experiment, significant psychomotor impairment was again noted. The mean (SD) time to response for the word task lengthened from 2.4(0.37) seconds to 2.83(0.62) seconds across this division (paired t-test, $p = 0.001$). The improvement in reaction times during recovery across the same division did not reach statistical significance ($p = 0.1$) but this is perhaps unsurprising given the early return to responsiveness in this session and therefore the relatively prolonged recovery period.

5.2.2 EEG parameters

The procedures for recovery of EEG data acquired during fMRI scanning, removing gradient switching and cardiobalistographic artifacts, were outlined in chapter 2 Despite extensive processing and artifact removal, the quality of EEG data obtained during fMRI scans was significantly worse than data recorded in the bench session and considerable residual artifact remained. Residual artifact was however constant throughout the experiment so any changes in the power within specific frequencies were due to propofol. Time frequency analyses are therefore expressed as relative power, the proportion of total EEG power accounted for by activity in the frequency band of interest. Head movement during recovery was too severe to allow removal of artifact and therefore no EEG data from the wakeup scan could be analysed. EEG results from the 48 minute induction scan are reported here.

Spindles

Spindle detection was carried out using the algorithm of Sleigh and colleagues [230], as in previous experiments. As this is based on pattern matching rather than the Fourier transform, it was expected that it would remain robust to the substantial residual artifact in the alpha band. The overall estimated prevalence of spindles in the relatively noisy scan data was lower than in the earlier artifact-free dataset, most likely because noise interfered with spindle pattern detection. However, the same patterns of frequency progression seen in the bench experiment were again observed (figure 5.5). Following LOBR the same fast spindle dominance as before was seen. 14 and 12 Hz spindles appeared and almost doubled in prevalence before waning as sedation deepened further. 10 and 8 Hz spindles increased in prevalence as faster spindles waned and as in the bench experiment, spindles in all the measured frequencies fell to a steady level before peak propofol levels.

Low frequency spindles (8-10Hz) were also prominent for the first eight to ten minutes of the experiment and then waned towards the midpoint of the responsive phase, which corresponded to the emergence of significant psychomotor impairment. These are the frequencies that dominated the alpha band during the resting state phase of the bench experiment. It is likely that this low alpha activity represents the effects of having the eyes open in a dark scanner, with minimal visual stimulation.

Slow wave activity

The key transition identified in the bench experiment was the saturation of SWA. High amplitude, low frequency slow wave activity was in fact easily detectable in the processed EEG data, as the majority of the residual artifact was low amplitude high frequency signal. Some signal in the frequency band (0.5-1.5 Hz) was present from the outset of the experiment, due to incomplete removal of CBG artifact, which occurs with the heartbeat and therefore in the slow wave frequency band. In spite of this, a marked increase in SWA was clearly seen starting shortly after LOBR. Crucially, the second transition, beyond LOBR, to SWA saturation was again observed (figure 5.5). SWA saturation in EEG data obtained during fMRI scanning demonstrates the reproducibility and resistance to noise of this parameter. It also defined a transition that could be used to divide the 4-dimensional dataset of 960 whole-brain volumes taken over 48 minutes into state-consistent temporal regions of interest (tROIs) for analysis.

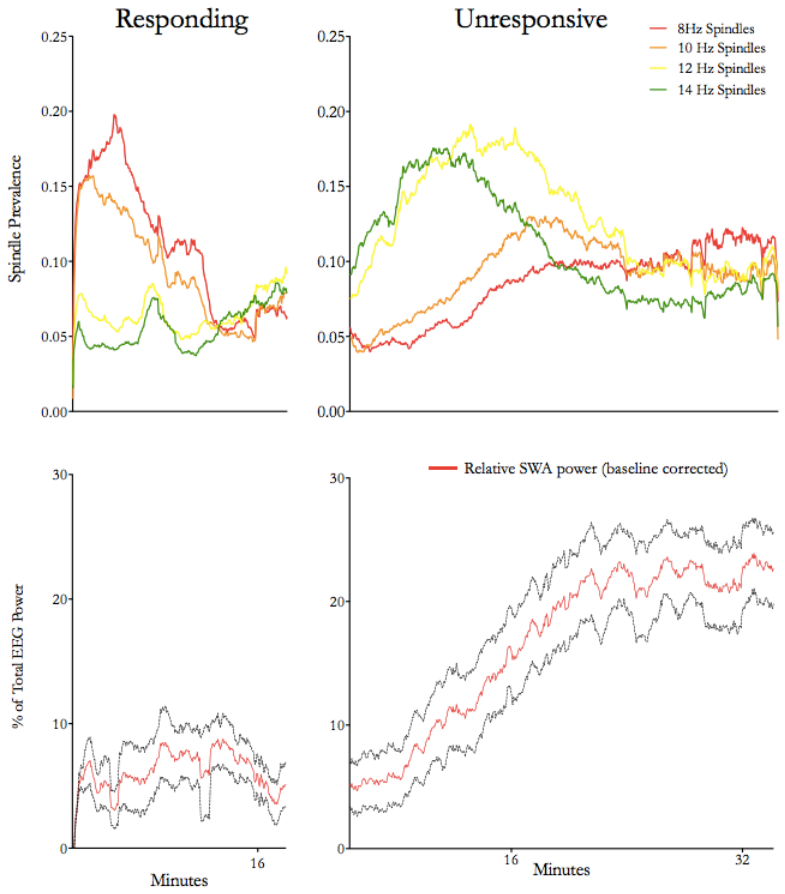

Figure 5.5 Spindle and slow wave activity during the induction scan: group data. The measured prevalence of spindles was high at the beginning of the scan, potentially due to the dark room, but these waned before subjects became unresponsive. The same changes in spindle prevalence and frequency were seen in these data as were seen in the previous experiment. Crucially, by banding the data by LOBR again, the transition to SWA saturation can clearly be seen during the unresponsive part of the experiment.

5.2.3 fMRI results

Temporal Regions of Interest

Despite the limitations of EEG data after artifact removal, two of the key waveforms of sleep and anaesthesia were successfully detected and their progression through the experiment measured. This allowed the detection of a number of transitions that informed analysis of the functional MRI data. The 4D functional MRI datasets were divided into epochs based on the associated EEG changes.

The first fMRI epoch was defined as the first half of each subject's responsive phase, and was associated with baseline alpha activity ("baseline"). The second fMRI epoch was defined as the second half of the responsive period, where early alpha was waning. This epoch ("impaired") was associated with a significant deterioration in psychomotor performance as measured by the reaction time taken for the word task. The third EEG epoch should have begun at LOBR in each subject. In three subjects however, there was a lag of several minutes between LOBR and the onset of SW activity. This is consistent with the low ESC at which LOBR occurred in the scanner compared to the bench, and suggests that subjects did become unresponsive at a neurophysiological state analogous to stage 1 NREM sleep. The third fMRI epoch ("LOBR") began therefore only when slow wave activity began to rise rather than strictly at LOBR, and ended at the transition to SWA saturation. In practice this involved discarding 1-2 minutes of fMRI data in each case to maintain consistency of neurophysiology within analysis epochs. The fourth fMRI epoch was SWA saturation ("SWS"), during which SWA plateaued. The EEG of two of the subjects developed isoelectric periods meeting the criteria for burst suppression (< 5 mA for >0.5 seconds). FMRI data during burst suppression was not included in the tROI for SWA saturation. Epochs thus defined were first subjected to a GLM based analysis to estimate the average response to each type of stimulation in each neurophysiological state and then contrasted in subsequent analyses.

State-specific stimulus responses

Here, responses to stimuli presented during each of the four different neurophysiological states defined in chapter 3, and the significant changes in activation across those states, are reported and discussed. This is the result of a GLM based analysis of temporal regions of interest (baseline, impaired, LOBR, SWS) derived from the same continuous fMRI acquisition. Throughout the following sections, activation associated with laser stimulation is represented on spatial maps in red/yellow and that associated with auditory stimuli in blue. In setting up the analysis model, the timecourse of each of the stimuli (laser, beeps, words) for the individual's

tROI was input and convolved to a canonical haemodynamic response function. Motion correction parameters were included in the model as regressors of no interest. First level analysis within FSL using FEAT yielded spatial maps showing significant areas of activation for each stimulus type (contrast of parameter estimate or COPE maps). An example of an individual's first level fixed effects analysis is given in figure 5.6.

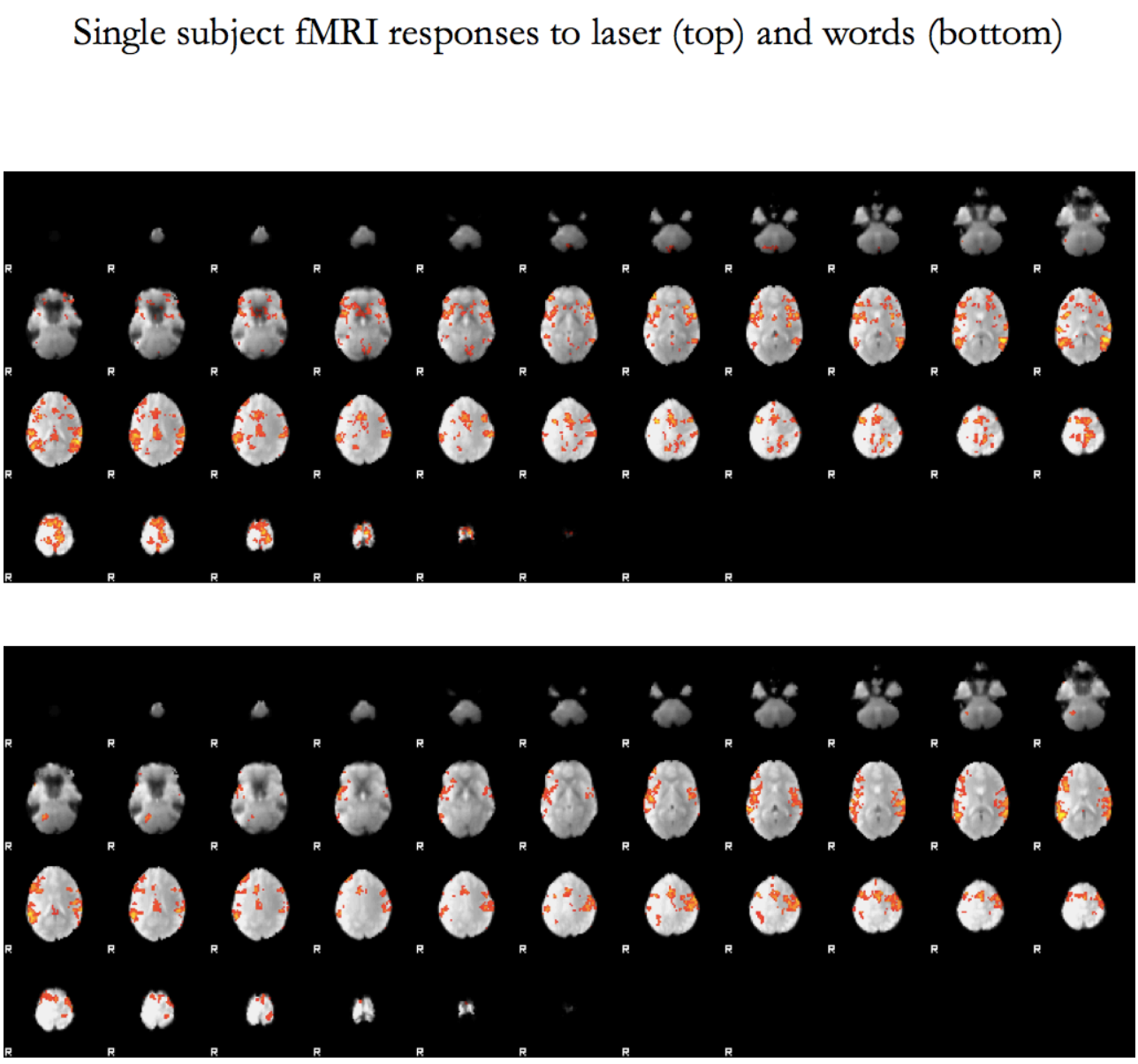

Figure 5.6 Representative single subject fMRI responses to laser (top) and words (bottom). Without co-registration to standard space and averaging across subjects, identification of the areas activated can be difficult. However, activations to laser stimuli can be seen in the insula, cingulate and somatomotor cortices while the auditory and somatomotor areas can be see to be active in response to the word task.

COPE maps and their associated variances (VARCOPEs) were then included in higher level mixed effects analyses to estimate the group mean activation. Multiple comparisons correction using cluster based

thresholding [114] at a cluster threshold of $Z > 2.3$, and a significance level of $p < 0.05$, was applied. Paired t-tests were constructed using a between-states, within-subject fixed effects contrast the COPEs and VARCOPEs of which was then passed up to a group level mixed effects analysis to estimate the group mean change in activation pattern associated with the change in neurophysiological state.

Baseline stimulus responses

Analysis of responses to stimulation during the baseline period reveals the efficacy of the stimuli in eliciting BOLD signal changes. This is an important result as it illustrates the feasibility of the study and the validity of the experimental setup, given the expected deterioration in fMRI signal quality in the presence of EEG equipment. Beep stimuli did not produce robust activations in the scanner despite eliciting excellent auditory evoked potentials in the bench experiment. This was most likely a failure of the volume thresholding procedure, which played sample words to the subject with simultaneous background scanner noise, adjusting the volume until the words could be clearly heard. The beeps were subsequently played at the same volume, which may have been inadequate for a stimulus requiring only passive listening rather than attention and discrimination. Words and noxious laser stimuli did however produce a robust and plausible pattern of activation suitable for statistical analysis.

Baseline responses to noxious laser stimulation

A network of brain areas showed significant activation in response to noxious laser stimulation. This consisted of the primary and secondary somatosensory cortex, the primary motor cortex, the anterior and posterior cingulate cortex, precuneus cortex, insular cortex, the putamen, thalamus and the temporoparietal junction (TPJ) bilaterally (figure 5.7). The peak voxels were in the primary somatosensory cortex and the temporoparietal junction contralateral to the stimulus.

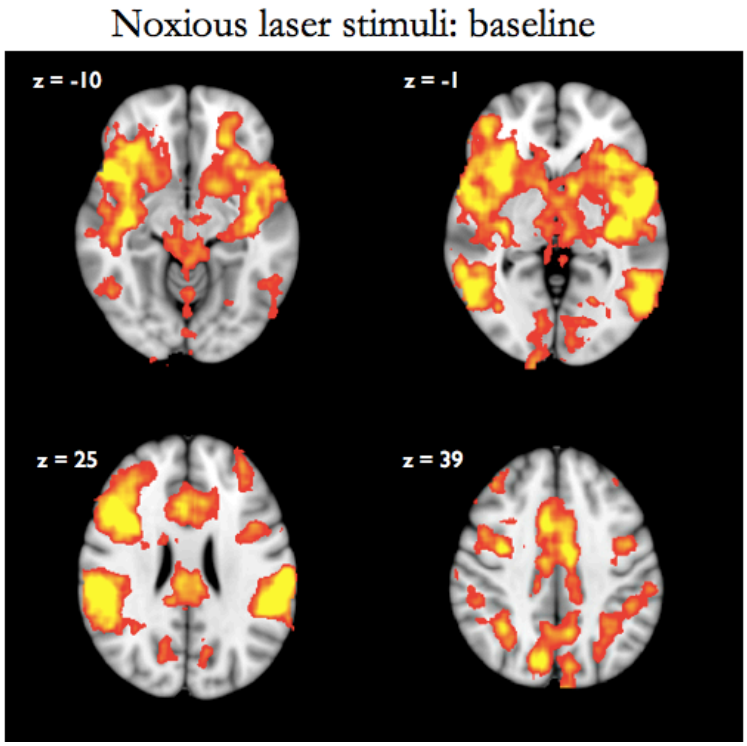

Figure 5.7 Group mean responses to noxious laser stimulation during the early responsive phase, or 'baseline'. Activation is seen in the primary and secondary somatosensory cortex, the primary motor cortex, the anterior and posterior cingulate cortex, precuneus cortex, insular cortex, the putamen, thalamus and the temporoparietal junction (TPJ) bilaterally.

This network includes many of the areas traditionally described as components of a pain matrix. This term has been widely used to describe the brain areas involved in the sensory, cognitive and emotional components of the subjective experience of pain through parallel processing in somatosensory, thalamocortical and limbic networks [305]. In fact the initial proposal of a neuromatrix encompassed more than central nervous system pathways. Melzack proposed a full body-self framework incorporating the sensory experience as well as the cognitive, emotional/stress, endocrine, autonomic and even immune response to the homeostatic threat associated with pain and its actual or perceived origin. With the advances of functional neuroimaging, the term "pain matrix" became perhaps *too* centralised, associated with a rigid pattern of cerebral, cerebellar and brainstem activation to acute noxious stimulation. The concept in this manifestation has been widely criticised, due to the inconsistency of the regions included and the failure of this concept to adequately reflect the many types of pain experiences[175]. In effect, there is no such thing as a unitary pain experience with a matching "on-pain/off-no pain" node or network. Rather, pain is a highly malleable, emergent experience dependent upon mood, cognition, context and nociceptive input. It therefore must involve the co-ordination of activity, across various brain regions, reflecting an array of contributing processes (cognitive, affective, sensory) in order to manifest as an unpleasant experience. Indeed the generation of the subjective experience of pain with distributed but integrated processing of activity in multiple dimensions across a pain matrix is an excellent illustration of the broader concept of consciousness, dependent on the integration of multiple facets of perception to construct

an experience of the internal or external environment. As in this dataset, activation is often seen in some, but not all, of the areas that have over the years been included in the purported pain matrix. Therefore the diagnostic strength of functional neuroimaging with respect to pain lies in interpretation of the *pattern* of activation rather than just the *presence* of activation. Ideally, the specific dimensions of the pain experience which are modulated by an endogenous or exogenous intervention could be inferred from changes in this pattern of activation.

Baseline responses to the word task

The word task elicited extensive cerebral activation as expected (figure 5.8). Widespread bilateral activation of the superior temporal gyrus (including Heschl's gyrus and planum temporale) and middle temporal gyrus was seen along with the left primary motor and somatosensory cortex (the auditory stimulus was associated with a motor task carried out with the right hand). There was also extensive activation in the thalamus, putamen, amygdala and hippocampus bilaterally.

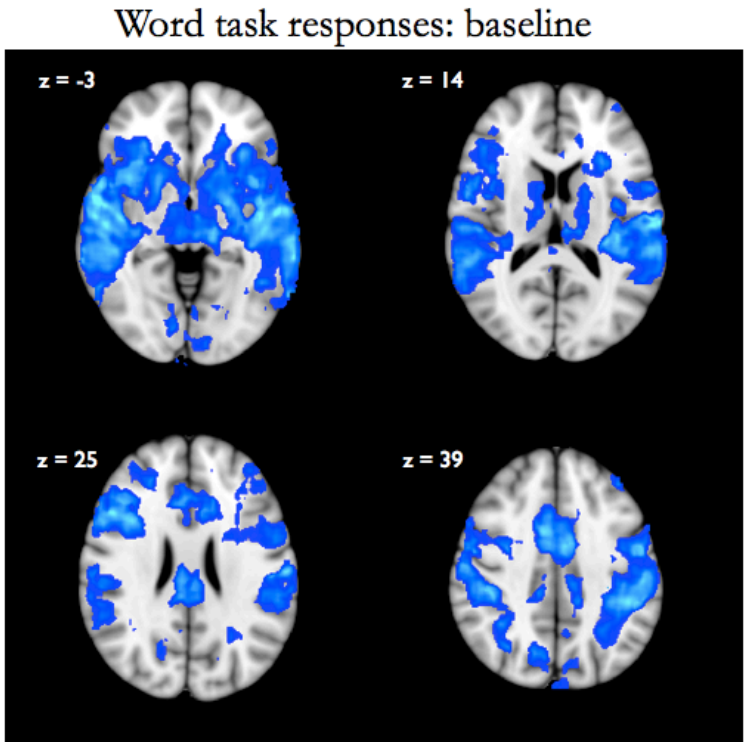

Figure 5.8 Group mean responses to the word task during the early responsive phase, or 'baseline'. Activation is seen throughout the temporal lobe, in the thalamus, putamen, amygdala and hippocampus as well as in the left primary motor and somatosensory cortex.

Auditory processing occurs largely within the temporal lobe. Afferent neurons from cochlear hair cells in the organ of Corti travel in the vestibulocochlear nerve (Cranial nerve VIII) to the cochlear nucleus of the pons. Projections from the cochlear nucleus decussate in the trapezoid body and ascend through the superior olivary complex to the inferior colliculi and from there to the medial geniculate nucleus of thalamus and then the

cortex. The primary auditory cortex (Broadmann areas 41 and 42, Heschl's gyrus) is tonotopically organised and receives signals encoding pitch and volume from the medial geniculate nucleus [306]. Adjacent areas in the temporal lobe are responsible for higher-level sensory processing. Wernicke's area in the posterior division of the superior temporal gyrus of the dominant hemisphere (Broadmann area 22) has traditionally been associated with lexical processing. It is now acknowledged that speech and language processing involves the broader temporal lobe including superior, middle and inferior temporal gyri and hippocampi bilaterally as well as Broca's area in the frontal lobe. Indeed, auditory processing within the temporal lobe is also an excellent example of the principle of information integration.

Stimulus responses in the impaired state

The impaired state was associated with sustained subject responsiveness despite a significantly prolonged reaction time. Responses to each type of stimulation in this state showed a persistent but more constrained pattern of activation. Paired t-tests revealed the areas where there was a statistically significant decrease in activation from baseline. No areas were found to show increased activation to either task in the impaired state compared to baseline.

Responses to noxious laser stimuli in the impaired state

Noxious stimuli were associated with more restricted activation patterns during this phase. Activation was seen in the insula and anterior cingulate gyrus bilaterally, the left thalamus, and the left somatosensory and primary motor cortex, all contralateral to the stimulus (figure 5.9).

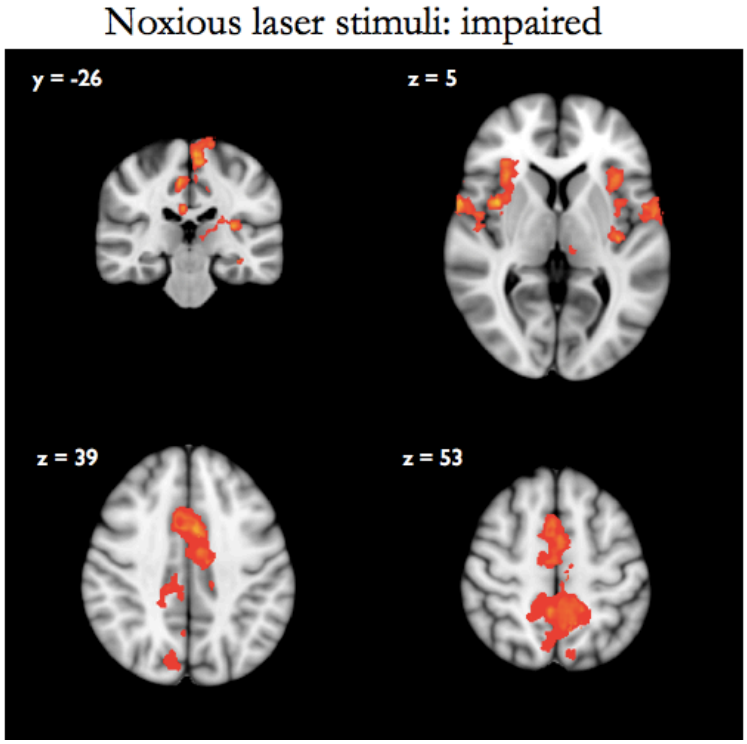

Figure 5.9 Group mean responses to noxious laser stimuli during the late responsive phase, during which reaction times were 'impaired'. Statistically significant activation in response to noxious stimulation was limited to the insula, anterior cingulate, thalamus and primary somatosensory cortex.

Contrasting this to the baseline state in a paired t-test revealed that the areas where BOLD signal changes were significantly reduced were the secondary somatosensory cortex (SII) on the left, contralateral to the stimulus, and the temporo-parietal junction (TPJ) bilaterally (figure 5.10). No significant change in activation was found in the insula.

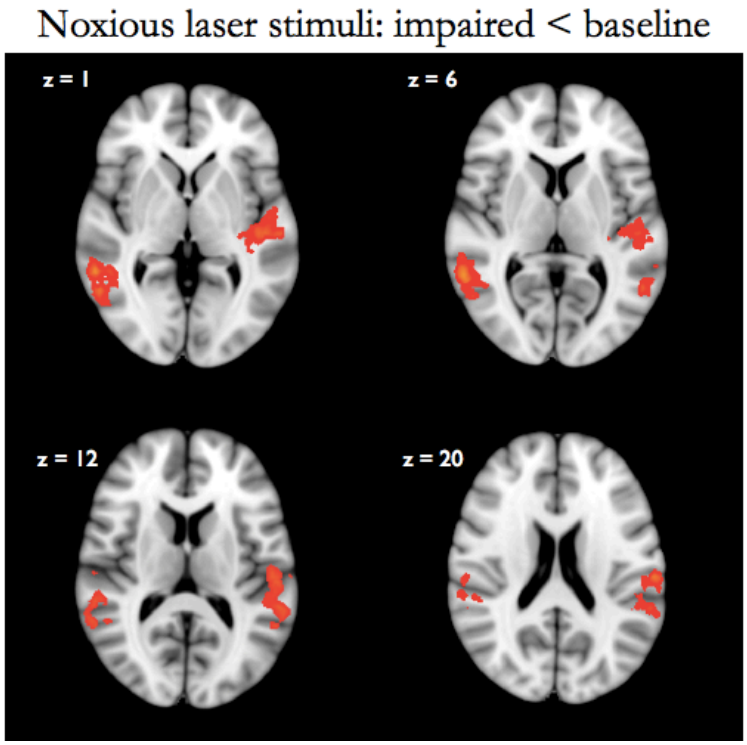

Figure 5.10 Areas showing significantly reduced activation in response to laser stimulation in the impaired state compared to baseline (paired t-test, $p < 0.05$). Reduced responses are seen in the secondary somatosensory cortex contralateral to the stimuli and the temporoparietal junction bilaterally.

SII and the posterior insula

Pain and temperature specific neurons in Lamina I of the spinal cord project to the ventromedial nucleus of the thalamus and from there to the posterior insula [307]. Both the posterior insula and the secondary somatosensory cortex (SII) respond to noxious thermal stimulation [308]. However, SII, located in the parietal operculum, is also activated by non-noxious stimulation, showing a graded response to increasing stimulus intensity below and through the pain threshold, while the posterior insula only responded to stimulus intensities above the pain threshold [309]. Intact insular processing may in fact be a prerequisite for the construct of the pain experience. Greenspan and colleagues studied six patients with unilateral insular lesions. Three of these patients demonstrated significant laterality in pain sensitivity. The common feature in their lesions was involvement of the parietal operculum and posterior insula [310]. As no systematic analgesic effect of propofol was identified in the previous experiment, a reduction in insular activation to noxious stimulation would not be expected. Impairment of SII function, the higher-order processing of sensory stimulation including attentional modulation, learning and memory [311], is more consistent with the behavioural impairment observed.

Temporo-parietal junction

The finding that activation of the temporo-parietal junction in response to noxious laser stimulation is significantly reduced during pharmacological impairment of consciousness with psychomotor dysfunction is consistent with the hypothesis that the impairment arises as a result of the failure of information integration.

The TPJ, at the posterior extreme of the sylvian fissure, is involved in conscious perception and temporal order processing. Gestalt perception, grouping individual processes into a global scene, was an early incarnation of the information integration hypothesis [312]. In an fMRI study, manipulating the individual objects within an image without changing the global scene, found that the brain areas showing activation when the scene was perceived rather than when it was not, were the TPJ and the precuneus [313].

Visual or auditory extinction, simultanagnosia, where individual objects can be perceived one at a time when presented individually but only one is perceived when more than one is simultaneously presented, may occur in patients following lesions to the peri-sylvian structures. Injury to the TPJ has been shown to be the most reliable predictor of visual extinction [314]. Healthy volunteers demonstrate extinction in a detection task following transcranial magnetic stimulation (TMS) to the right TPJ [315].

The TPJ has also been shown be activated when perception involves temporal order discrimination [316]. Temporal discrimination of sensory events is essential in higher order processing has been shown to be impaired in psychiatric and neurological conditions associated with disordered perception, including dyslexia, schizophrenia, autism and attention deficit disorder [317].

Timing is central to comprehensive percept formation. Bats rely in intra-aural differences in sound arrival times to form an accurate topographic map of their surroundings. Perception may therefore be disordered in the when the brain's internal temporal framework is disrupted. Interval timing, on the order of seconds, depends on an intact striatum, and motor and perceptual timing deficits are characteristic of Parkinson's disease [318]. Thalamo-cortico-striatal circuits are activated in tasks which require the integration of a perception over time [319]. The result of this analysis coupled with those of the experiment reported in chapter 3 [320] suggest that an accurate temporal framework is essential for the integration of neuronal events across a network of brain regions into an experience. It is plausible that disruption of this temporal binding may be responsible for the early behavioural changes of sedation and the associated impairment of higher order processing. Anaesthetic disruption of the brain's temporal framework may underlie an interesting and potentially significant difference between sleep and anaesthesia - following a nights sleep there is an awareness that a period of time has passed, whereas under anaesthesia any perception of the passage time is lost [321].

Responses to the word task in the impaired state

Activation during the word task was again seen across a wide network of regions corresponding to those activated at baseline, with the peak voxel again in Heschl's gyrus (figure 5.11).

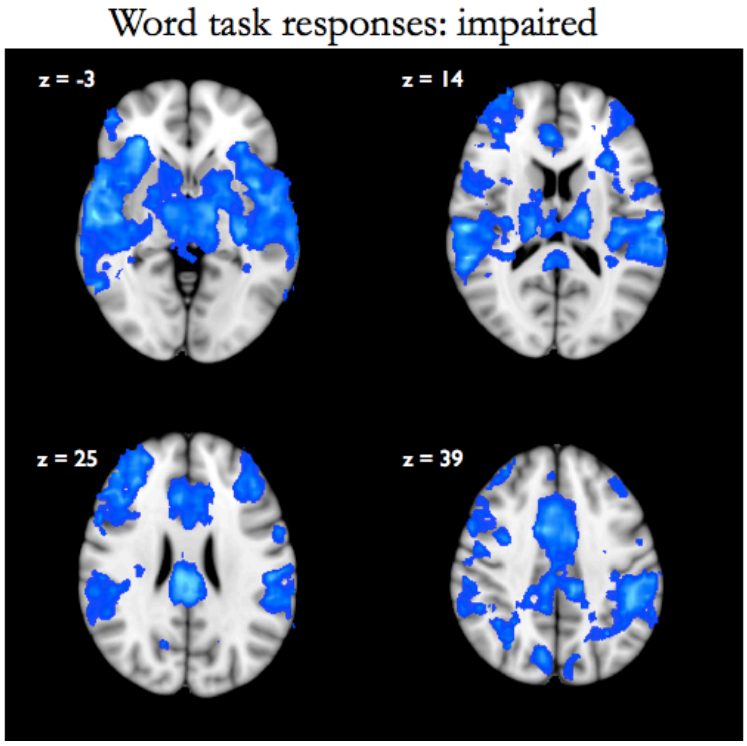

Figure 5.11 Group mean responses to the word task during the late responsive phase, during which responses to the word task were 'impaired' (reaction time significantly slower). Activation is again seen throughout the temporal lobe, in the thalamus, putamen, amygdala and hippocampus as well as in the left primary motor and somatosensory cortex, as it was at baseline.

Formal statistical comparison of these responses to baseline revealed significantly decreased BOLD signal changes across the temporal lobe in both the primary auditory cortex, the auditory association cortex, the TPJ, and also in the left somatosensory and motor cortices, contralateral to the hand in which the button box was held (figure 5.12).

Activation in both states is extensive and the spatial resolution of these scans is not high enough to disentangle subtle aspects of auditory processing within the temporal lobe that were affected by the propofol. At the bench experiment, this neurophysiological state was associated with a decrease in the amplitude of the evoked potential (AEP) relative to baseline, which also indicates a decrease in the number of neurons firing coherently in response to stimulation. The scan results show that this reflects a decrease in activity in both primary and secondary auditory areas but cannot reveal the specific processes affected.

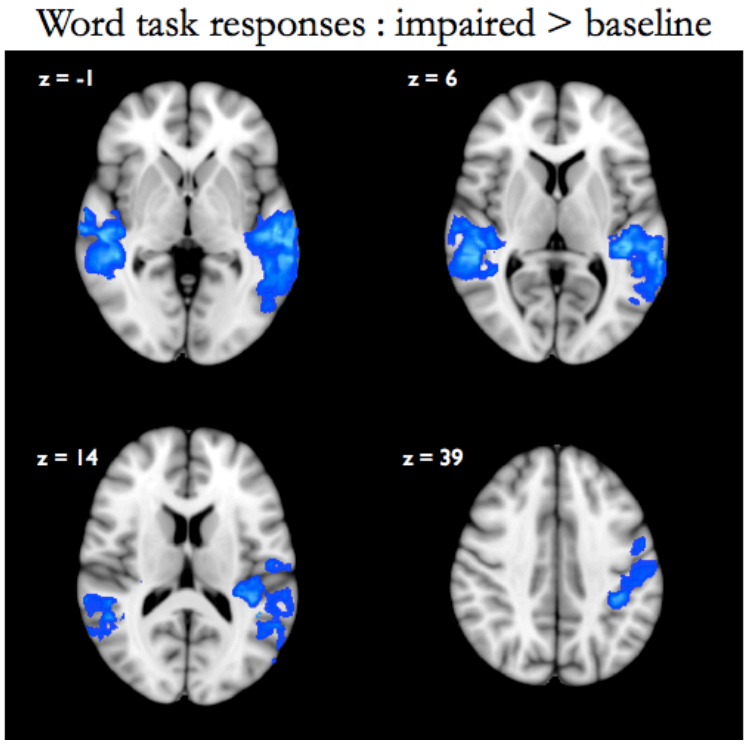

Figure 5.12 Areas showing significantly reduced activation following the word task in the impaired state compared to baseline (paired t-test, $p < 0.05$). Reduced responses are seen in the temporal cortex and the temporoparietal junction bilaterally and in the left primary somatosensory and motor cortical areas, contralateral to the hand in which the button box was held for the responses.

Propofol and auditory processing

While the extent of temporal lobe activation decreased at this level of propofol, the pattern did not change. It is perhaps surprising that no decrease in activation was noted in the frontal lobe areas involved in complex language processing. This is most likely due to the relative simplicity of the task coupled with the low level of propofol during the impaired state. Failure of frontal lobe language processing has been shown to occur with propofol sedation in other studies [149,151]. Stimuli in the studies that identified a decrease in frontal activation were sentences and music. Another study which presented words and matched non-word sounds during propofol sedation failed to show any change in frontal lobe activation [67]. A region of interest analysis of activity in the left inferior frontal lobe during low dose propofol sedation showed persistent activation in this region [322]. While behavioural impairment was noted in the significant prolongation of reaction times at this state, our earlier results showing the anaesthetic sensitivity of the basal ganglia, responsible for motor timing and co-ordination, show that the reaction time delay is more likely to be a motor than a cognitive deficit.

Loss of behavioural response and SWA onset

The definition of the second transition was behavioural rather than neurophysiological, although it was followed quickly by a change in neurophysiology with the onset of rising slow wave activity (SWA). The behavioural transition was the point at which the subject failed to respond to the word task, rather than any behaviour

associated with the noxious laser stimulation. It is notable but not surprising then that there was no further significant change in the cerebral activation pattern in response to pain across this transition. Group mean analysis showed that responses persisted in those areas in which activation had remained following the initial loss of S2 and the TPJ, including the thalamus, the anterior cingulate, posterior cingulate, precuneus, primary somatosensory cortex and motor cortex (figure 5.13). The paired t-test comparing responses to laser stimulation before and after LOBR showed that no brain areas demonstrated a statistically significant decrease in activation across this transition.

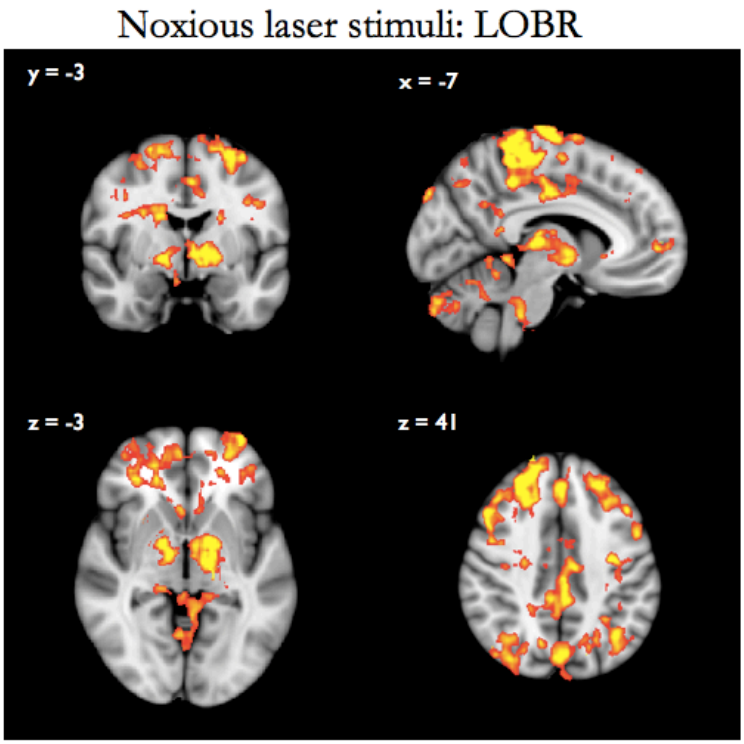

Figure 5.13 Group mean responses to noxious laser stimuli during the unresponsive phase between the loss of behavioural responses (LOBR) and the saturation of slow wave activity (SWA). Activation persists in the thalamus, anterior cingulate, posterior cingulate, precuneus and the primary somatosensory and motor areas.

Activation in response to the word task did however change with this transition, as would be expected since the transition point was defined as the point at which a word failed to produce a behavioural response (LOBR). During the tROI between LOBR and SWA saturation, significant task related BOLD signal changes were confined to primary processing areas, identified only in a small region in each thalamus and primary auditory cortex bilaterally (figure 5.14).

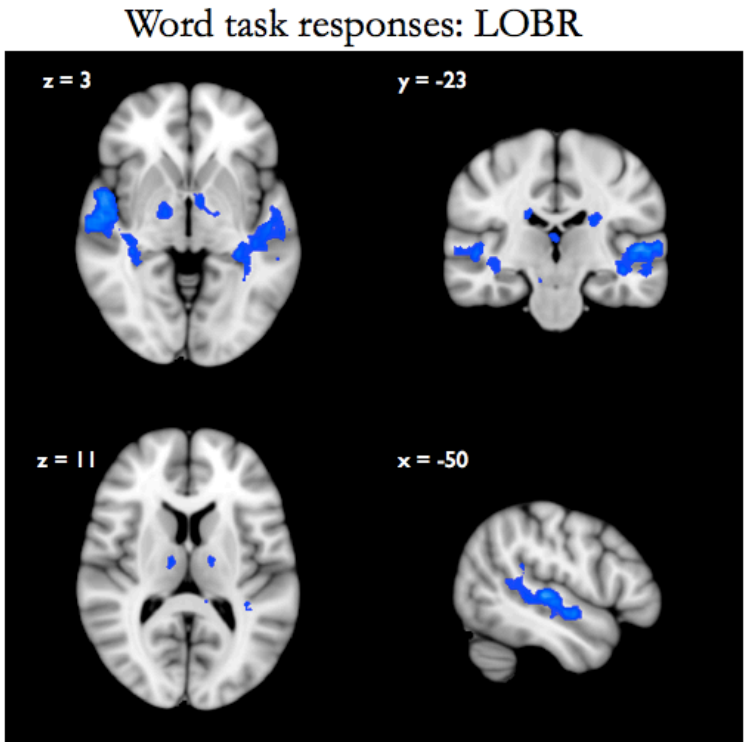

Figure 5.14 Group mean responses to the word task during the unresponsive phase between the loss of behavioural responses (LOBR) and the saturation of slow wave activity (SWA). Activation persists in the thalamus, and primary auditory cortex bilaterally.

A two-tailed paired t-test was used to identify regions where activation in this state was significantly increased or reduced compared to the previous impaired state. Again no areas showed an increase in activation across this transition. Significant reductions in activation were identified in areas associated with higher order processing of auditory stimuli, the thalamus, auditory association cortex, anterior and posterior cingulate cortex and at this stage, the frontal lobes (figure 5.15)

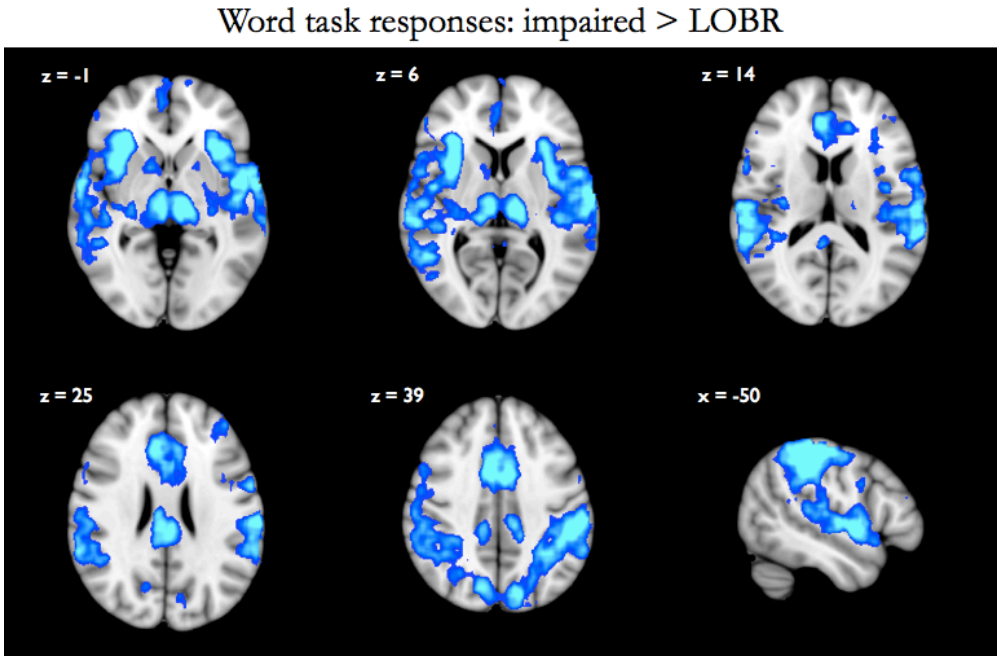

Figure 5.15 Areas that showed significantly less activation in response to the word task following LOBR. The loss of activation is extensive, involving the thalamus, auditory association cortex, anterior and posterior cingulate cortex and the frontal operculum.

This contrast confirms that thalamic and modality-specific primary cortical processing persists during the period of the experiment after LOBR but before SWA saturation. During this phase auditory and noxious stimuli fail to engage the broad network of areas where higher level processing integrates these signals to construct a perception.

Low level propofol associated with impaired motor performance (the first transition) was associated with the loss of secondary processing of noxious stimuli, although in the absence of an associated motor task, failure of perception cannot be objectively confirmed for these stimuli. Higher cortical processing of auditory stimuli persisted longer, until LOBR, at which point responses to these stimuli were also reduced to primary processing.

Slow wave saturation

Having identified a neurophysiological transition beyond LOBR, where slow wave activity reached a plateau, cerebral activity at this state was analysed. During the first three tROIs, modality specific networks were identified and as sedation deepened, activity within specific regions of functional significance was reduced or ceased to show any activation. During the tROI defined by SWA saturation however, both auditory and noxious stimuli were associated with markedly different patterns of activation (figure 5.16). During SWA saturation, both laser and auditory stimuli were associated with activation in the precuneus and the lateral occipital cortex, and laser stimuli were also associated with activity in the frontal cortex.

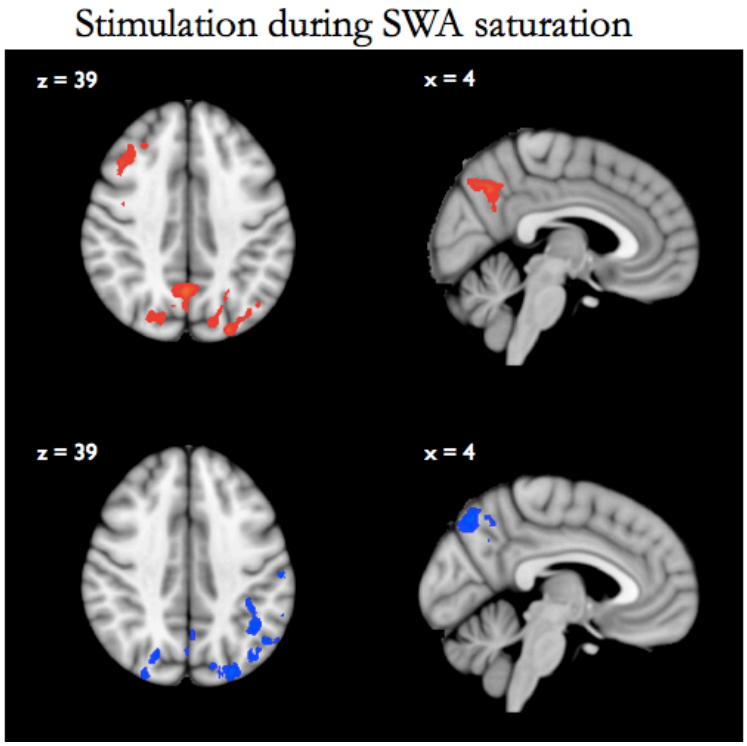

Figure 5.16 Group mean activation maps for responses to laser (red) and word tasks (blue), show that while these stimuli no longer elicited activity in their modality-specific networks, activation persisted in the precuneus and lateral occipital cortex in response to both stimulus types, and in the frontal lobe in response to laser stimulation.

The paired t-test comparing activation during the tROI between LOBR and SWA saturation to that during SWA saturation, showed this transition to be the point at which the primary somatosensory and auditory processing systems ceased to be activated by external stimulation. Figure 5.17 shows that the two primary networks (thalamus and S1 with respect to noxious stimulation, thalamus and Heschl's gyrus with respect to auditory stimuli) are no longer activated following SWA saturation. This identifies a fundamental change in cerebral activity which is associated with a concomitant change in the electrical activity measured at the scalp.

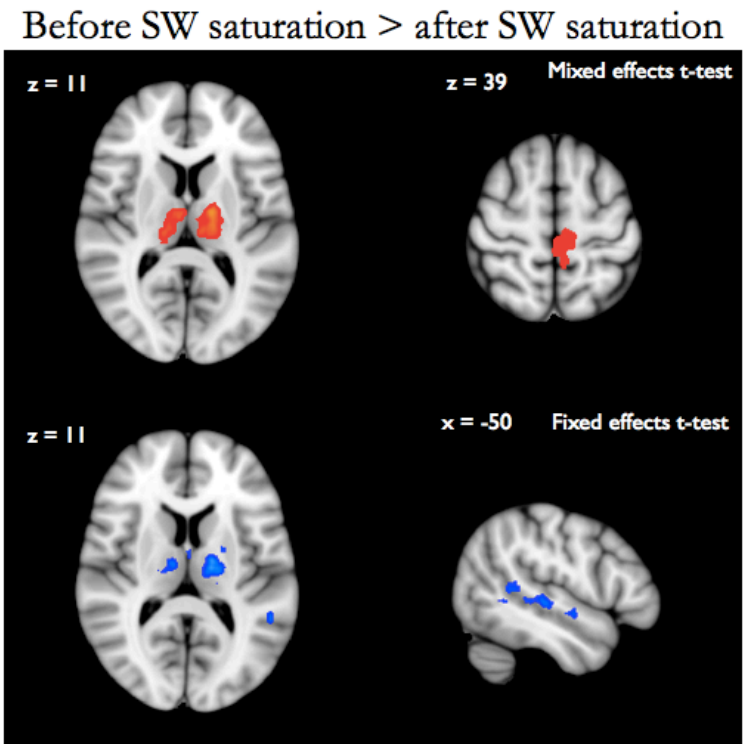

Figure 5.17 Results of a paired t-test comparing responses to laser (red) and word tasks (blue), before and after the saturation of slow wave activity (SWA). Contrasting activity during these two states reveals that the areas where responses to laser stimulation are significantly reduced in association with SWA saturation are the thalamus and the primary somatosensory area (in the leg area of the sensory homunculus). This was the result of a mixed effects analysis. No areas were identified in a mixed effects analysis of responses to the word task across this transition However, the results of the fixed effects analysis are given here to show that the reduction in primary processing had occurred but the magnitude of signal change did not reach statistical significance after multiple comparisons correction.

While one would not argue that the level of propofol at which this electrophysiology was identified would allow surgery, it must be remembered that arousal is a balance between sleep and wake systems and that the intensity of stimulation during this experiment was very low compared to surgery. Arousal occurs in response to stimulation, both during sleep and during anaesthesia [323,324]. The spino-reticulo-thalamic tract conveys nociceptive signals to the reticular activating system and from there to the intralaminar nuclei of the thalamus [325]. During anaesthesia, reducing the afferent input arising from surgical stimulation or neuraxial or regional nerve block decreases the level of anaesthetic agent required to maintain the same degree of hypnosis [326]. Therefore one could postulate that since the level of propofol at which SWA saturated in this study was sufficient to block modality specific thalamic and cortical responses to stimuli of this intensity, then titrating propofol ESC upwards to maintain this electrophysiological state during surgical stimulation would represent genuinely target controlled anaesthesia.

Slow Wave saturation and the thalamo-cortical switch

As shown in the previous EEG experiment, thalamocortical oscillations, in the form of spindle activity, *do* continue following SWA saturation. While the prevalence of spindles drops with SWA saturation, this is inevitable. The neocortical neurons driving cortico-thalamic feedback and spindle propagation remain in silent hyperpolarisation for half of the cycle of the slow oscillation. Spindles indicate a continuing thalamo-cortical dialogue. These results show that this dialogue occurs in isolation from, and unperturbed by, the environment. This is consistent with the hypothesis of a thalamo-cortical switch but suggests that the mechanism involves thalamocortical *isolation* rather than a breakdown in connectivity between the thalamus and the cortex.

In chapter 4 it was proposed that SWA saturation reflected the entrainment of the maximal number of neurons into the cortical slow oscillation. The sequence of events described in this chapter suggests that, perhaps, through a direct hyperpolarising action on neocortical cells, or modulation of the balance of sleep wake drivers to favour hyperpolarisation, or possibly both, propofol imposes a state of refractory sleep on neocortical cells which is not the result of thalamo-cortical disconnection.

Activation during SWA saturation

It may be reasonably expected that following the abolition of activation in modality-specific primary thalamo-cortical networks, no activations would be found in the group mean analysis of responses during SWA saturation. In fact this was not the case and this analysis revealed an intriguing change in brain activity. Residual responses during SWS were found in the precuneus cortex and lateral occipital cortex and, in the case of noxious stimuli, the middle frontal gyrus (figure 5.16). These are parts of the default mode network (DMN) [327] (see chapter 6). This pattern of activation suggests that stimulation, while no longer impacting upon those cortical areas necessary for the content of consciousness (although not in isolation sufficient for the state of consciousness), continues to elicit changes in local cerebral blood flow and therefore by inference, neuronal activity. The precuneus and parieto-occipital associative areas have been extensively studied in recent years because recovery of function in these regions has been associated with recovery from disorders of consciousness including coma and vegetative states.

The precuneus cortex and consciousness

The term "precuneus" refers to the posterior region of the medial parietal cortex (mesial aspect of Broadmann area 7) [328]. During quiet wakefulness, the precuneus has the highest metabolic rate of any area in the human brain [329]. As part of the DMN it is tonically active during the resting state and is deactivated during attention-demanding tasks (thus anti-correlated with task networks), which has been interpreted as representing tonic awareness [330]. Metabolic activity in the precuneus is markedly and selectively reduced in states of altered consciousness including sleep [32,331], sedation [332] and post-anoxic or hypoperfusion insults associated with DOC [333,334]. The anti-correlation between precuneus activity and stimulation has been reported to be absent or reversed when consciousness is impaired [335].

Over the past decade, it has been repeatedly shown that an increase in the metabolic activity of the precuneus cortex is associated with recovery from DOC. In a patient who was in, but recovered from a vegetative state (VS) following carbon monoxide poisoning, and who underwent FDG PET before and after recovery, Laureys and colleagues reported that the main decrease in metabolism seen in the VS that was not seen after recovery was that in the precuneus [336]. Activity in the precuneus and adjacent posterior association areas has been suggested for the differentiation of VS and MCS [337].

The connections of the precuneus facilitate higher associative processing. It shares reciprocal connections with the prefrontal cortex, the supplementary motor area and the anterior cingulate cortex. It also has reciprocal connections to the TPJ, the association cortex which is involved in the integration of auditory, somatosensory and visual information. Projections to the dorsal thalamus link to association nuclei but there are no connections with specific primary sensory thalamic nuclei and or their associated primary sensory cortical regions. Cholinergic projections from the mesencephalic reticular formation to the precuneus could mediate arousal directly, without the thalamocortical system [328]. Administration of physostigmine to healthy volunteers anaesthetised with propofol resulted in behavioural arousal and restoration of consciousness in 8 of 11 subjects and this was associated with the restoration of normal blood flow levels in the precuneus and thalamus [338]. Interestingly, decreases in precuneus metabolism in VS and MCS are often associated with increased metabolism in the ARAS [335].

The findings reported here suggest that sensory stimulation during a plane of anaesthesia characterised by maximal slow wave activity, when the thalamocortical system is refractory to external perturbation, causes increased regional blood flow in the precuneus and posterior parietal association cortices. This may be the result of cholinergic signals from the ARAS attempting to rouse the brain to the most basic level of introspective or environmental vigilance.

Emergence from Anaesthesia

Following the acquisition of 10 minutes of resting state fMRI data at an ESC of 4.0 mcg ml^{-1} propofol, the propofol was discontinued and allowed to wash out. The timecourse of effect site elimination is shown in figure 4.2. A final 48 minute scan was acquired, repeating the stimulation paradigm of the previous 48 minute induction scan, beginning from the moment the propofol was discontinued.

The motion correction parameters for some of these subjects are shown in Appendix E, which illustrates the methodological difficulties (which were anticipated and indeed materialised) with dynamic imaging of emergence from anaesthesia. All subjects moved their heads substantially at the point of recovery of behavioural responsiveness (ROBR) leading to a large epoch of meaningless data. Nevertheless, it can be clearly seen in these plots of motion correction parameters that the scan data *prior* to ROBR was not contaminated with excessive movement artifact, in fact subjects were almost completely still. Therefore analysis of the wakeup portion of the dataset was limited to the BOLD signal fluctuations during the brief period from propofol discontinuation until the few seconds before the return of responsiveness. Scans were truncated at the volume immediately before ROBR and then subjected to the standard preprocessing steps (see chapter 2).

The marked head movement during the wakeup scan introduced additional, high amplitude, non-template artifact to the EEG rendering artifact removal algorithms ineffective and this data was not recoverable.

In order to dissect the neurophysiology underlying recovery from anaesthesia with the same resolution as was applied to the induction, drug infusion would have to continue so that the rate of ESC decline was slowed to mirror the rate of increase during induction. This was not feasible within the experiment design but will considered in future studies. Because of the rapid ESC decay, the unresponsive period for analysis was,

depending on the individual subject's recovery rate, 3-12 minutes. This resulted in only 3-12 word tasks and 6-25 laser stimulus observations for averaging.

A mixed effects analysis estimating group mean activations to laser stimuli during this period showed the recovery of activation within the thalamus and frontal cortex (figure 5.18). The same analysis for fixed effects revealed that activation in the medial postcentral gyrus *was* present but did not survive the significance threshold of the mixed effects analysis, probably due to the relatively low number of stimuli averaged.

Group mean maps of the activations occurring after word presentation during this period showed significant activity in the thalamus and putamen bilaterally (figure 5.18). No activation was seen in the auditory cortex but this may again be due to the small number of observations available for analysis. No further activations were seen in the fixed effects analysis.

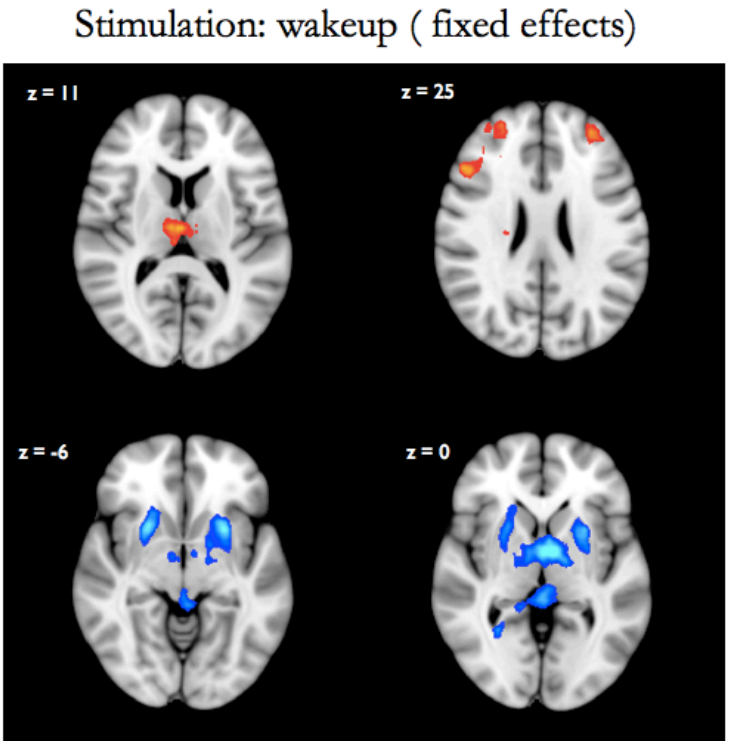

Figure 5.18 Group mean activation maps - fixed effects - for responses to laser (red) and word tasks (blue) during the unresponsive phase of the wakeup scan. This analysis, though statistically weak due to the low number of stimuli, shows recovery of thalamic activation in response to each stimulus type

It is certainly disappointing that more could not be gleaned from these scans. Recovery of thalamic activation in response to somatosensory stimulation prior to ROBR was noted and is likely to be related to the resurgence of spindle activity seen during this phase in the bench experiment (chapter 4).

As the experiment consisted of almost three hours in the scanner, it would not have been feasible to gather data on a more gradual emergence. Building on this experience, another experiment, designed specifically to look at

emergence from slow wave saturation through to recovery of consciousness, could go directly to an ESC such as 4.0 mcg ml^{-1} first, then set the target ESC to a lower level and once this target was achieved and maintained, perform a short scan to gather an adequate number of stimulus responses at that level before repeating the stepwise target decrease, and so on. If functional neuroimaging is to have a convincing role in the assessments of coma, VS and MCS, such an experiment should seek to establish whether the precuneus activation persisted at higher drug levels producing burst suppression and if not, whether the return of precuneus activation as drug levels are slowly reduced *is* indeed the first response during recovery as it appears to be during recovery from disorders of consciousness.

Conclusion

This functional MRI experiment aimed to related the electrophysiological changes described in chapter 4 to specific changes in brain activity. The experiment was designed to allow temporal regions of interest to be defined retrospectively by both behaviour and electrophysiology, removing the effects of pharmacokinetic and pharmacodynamic variability between subjects and conditions. The combined EEG/fMRI approach also allowed the detection and interrogation of an otherwise invisible electrophysiological transition. The first achievement of this experiment was the safety and success with which it was carried out. From a methodological standpoint it established a firm basis for future work on anaesthesia and consciousness in the unit, in terms of both subject safety and stimulus efficacy. Robust BOLD responses to the word tasks and laser stimuli were seen during the baseline phase and significant changes were detected as the intervention proceeded.

Low levels of sedation were associated with reduced activity in associative areas including S2 and extensive regions of the temporal lobe. Impairment of TPJ activation by low levels of propofol corroborates the findings of the earlier experiment with respect to the basal ganglia (chapter 3) supporting the hypothesis that the maintenance of a synchronising temporal framework co-ordinating local stimulus processing is central to conscious experience. Saturation of slow wave activity was identified as the point beyond which the thalamocortical system is isolated from the external environment. This may be useful in guiding the care of sedated or anaesthetised patients. Finally, activation of the precuneus cortex, possibly by ascending cholinergic projections from the mesopontine reticular nuclei, may reflect attempted and failed arousal during this refractory sleep-like state.

Chapter 6: Resting state networks during anaesthesia

6.1 Background

Functional MRI data presented so far in this thesis have been analysed by examining the time course of signal intensity variations in each voxel for correlation with either a model or the signal from another region, the latter a measure of functional connectivity. Functional connectivity between the regions of the brain is not exclusive to the relatively high frequency variations associated with task performance. Low frequency (<0.1 Hz) fluctuations in signal intensity in distributed regions of the brain involved in motor function have been found to be highly temporally correlated, even in the absence of a motor task, suggesting a functional origin [339]. Similar resting correlations were subsequently reported between right and left visual cortices, right and left amygdalae [340] and within sensorimotor and language processing networks [341]. Networks of regions showing these coherent low frequency fluctuations have been termed "resting state networks" (RSN) yet the precise origin of the signal is not known. They are still seen after cardiorespiratory and other physiological fluctuations are accounted for and separated from functional data by sampling at higher frequencies to avoid aliasing [340]. This and the changes in RSN that have been identified with cognitive state changes and neurological diseases suggest that the covarying fluctuations may reflect signaling between the nodes of functional networks. For example, functional connectivity increases between language processing areas following a language task [342] and between areas active during motor tasks following motor learning [343]. Furthermore, functional connectivity is reduced in disease states, for example within the "default mode network" (DMN) in early Alzheimer's disease [344]. RSN remain detectable following callosotomy for intractable epilepsy [345,346]. This suggests that subcortical mechanisms contribute to synchronisation, which may be of relevance to anaesthesia research.

The default mode network

From early days of functional neuroimaging, a pattern of task-associated decreases in blood flow in the posterior cingulate, precuneus and medial prefrontal cortices was frequently noted. This pattern appeared consistently and was task-invariant, i.e., independent of the nature of the task or any task-specific goal-directed behaviour. It was proposed that this finding in fact showed rest to be just a different task, reflecting the active nature of human consciousness, introspection, planning and reflection, and that this "task" was interrupted by the demand to perform another. Interruption of this activity would explain the associated task-induced decrease in blood flow [347]. This was supported by a large meta-analysis of 370 PET scans contrasting a variety of cognitive tasks (visual, motor, mental imagery, language) with rest periods, showing that this network was more

active during conscious rest than during the tasks [348]. Breakthrough work by Raichle and colleagues in 2001 interrogated the origins of the decreases in blood flow in these regions by measuring the associated change in oxygen extraction fraction (OEF), which was found to increase with rest. They proposed that these regions were in fact tonically active during the "baseline" state and that their activity was suspended during tasks. The term "Default Mode Network" reflects the concept of tonic activity in these areas between tasks rather than specific *activation* above a baseline by the processes of consciousness [329,330].

Generally, RSN are identified in one of two ways. Where a locus is known or expected to be part of a specific network, this can serve as a seed region of interest, thus identifying the network as those areas that have correlating BOLD signal fluctuations (as in the functional connectivity analysis in Chapter 3). In the absence of an *a priori* hypothesis, independent component analysis (ICA) has been shown to be capable of identifying independent networks of temporally coherent activity across the brain and to effectively differentiate between these networks and signal changes due to cardiorespiratory variation [349] (for implementation, see chapter 2).

Fox and colleagues [327] investigated the temporal relationship between fMRI signals from two groups of brain areas during three resting conditions: fixation, eyes closed and eyes open. The two groups consisted of brain regions known to show task-related activations (frontal eye fields, dorsolateral prefrontal cortex, supplementary motor area) and regions known to show task-related deactivations (lateral parietal cortex, posterior cingulate/ precuneus cortex, medial prefrontal cortex). Close temporal correlations were found between areas within each network type. Signals from areas in different networks were found to be anti-correlated. These and corroborative results [350] led to the hypothesis that the brain may function by switching between default mode and task-directed activity.

RSN through normal human development

RSN have been identified from the earliest stages of human development. Several studies have shown that RSN are present in both preterm and term infants [351-354]. RSN have even been tentatively identified in the foetal brain *in utero* [355], and are reliably detected in children and adolescents [356]. The repertoire of RSN and the complexity of thalamocortical networks in particular, has been shown to be low in preterm infants, but is similar to that of adults by early infancy, coinciding with the maturation of thalamocortical projections that occurs after 33 weeks [353].

RSN in disease

As RSN activity appears to be fundamental to the normal function of the human brain, it has been extensively investigated as a diagnostic and prognostic tool in disease. Task-related deactivations are reduced in patients with Alzheimer's disease (AD) relative to patients with mild cognitive impairment (MCI), who in turn show reduced deactivations compared to healthy controls [357]. This may be secondary to neuronal loss in AD. Patients with AD and MCI often show atrophy of the structures of the medial temporal lobe, particularly the hippocampus. Studies of RSN have shown the connectivity between the hippocampus and the posterior cingulate cortex to be reduced in patients with MCI [358] and AD. The strength of the correlation between the posterior cingulate cortex, the lateral parietal cortex and the medial prefrontal cortex, (all part of the DMN) is reduced in patients with schizophrenia [359].

Functional connectivity within RSN is decreased after traumatic brain injury [360] and increases with recovery [361]. A single-subject report of functional connectivity in the vegetative state (VS) shows the diagnostic potential of RSN analysis in DOC. The VS patient showed a persistent DMN-like pattern of signal correlation between a seed region of interest in the posterior cingulate/precuneus cortex (PCC/PrCC) and the medial prefrontal, temporoparietal and parahippocampal cortices. Unlike healthy controls however, connectivity between the PCC and the medial thalamus was absent. While the pattern was similar to that in healthy controls, the strength of the functional connectivity within the network was reduced. The VS patient also showed a typical pattern of anti-correlation between the PCC and areas of the task-active network, however the anti-correlations were significantly reduced compared to the healthy control subjects [3625].

[5] Strangely, as cerebral blood flow is absent following brain death, this group used data from a brain dead patient as a comparator to show that the same pattern was not observed.

RSN in animals

With RSN increasingly being investigated in health and disease, and many neurological diseases relying on animal models for the investigation of new therapies, RSN have been sought and identified in several species. Spatiotemporal networks including visual and somatosensory RSN have been identified in rats [363,364] and macaque monkeys[365].

RSN and anaesthesia

Vincent and colleagues[366] were the first to demonstrate the persistence of RSN during anaesthesia in a study of macaques under 0.8-1.5% isoflurane. Simultaneous EEG confirmed the presence of continuous slow wave activity (SWA) with occasional burst suppression. They demonstrated correlated low frequency activity within the oculomotor network and between left and right somatosensory ROIs. They also investigated the functional connectivity of the precuneus cortex under anaesthesia and discovered a network of correlated activity, analogous to the DMN in humans, that included the dorsal medial prefrontal cortex, the lateral temporoparietal area and the posterior parahippocampal cortex. This discovery was in direct contradiction with the hypothesis that the role of the DMN was in some way associated with the ongoing internal dialogue of the stream of consciousness [330,367]. The results suggest instead that these networks reflect a more fundamental functional activity of the brain. Anti-correlations between networks, similar to those seen between the DMN and task-active networks in humans, have recently been described in rats [368]. However, the anti-correlation between these networks disappeared with anaesthesia, suggesting that *between*-network interactions rather than the simple presence of the networks themselves may be associated with conscious functions.

The evidence in humans is not so clear. An fMRI study scanned healthy volunteers resting awake, and then anaesthetised at 1% and 2% end tidal concentrations of sevoflurane (EtSevo). The investigators looked for temporal correlations with the signal from a seed region in the primary motor cortex and identified a motor network in the awake condition that encompassed the premotor cortex and the supplementary motor area (SMA). This network was found to be present at 1% EtSevo, although its extent and associated transhemispheric connectivity were reduced. This network was not detected at 2% EtSevo [369]. Martuzzi and colleagues [370] reported preservation of RSN under anaesthesia while noting a reduction in the functional connectivity of the

hippocampus. However this study only used 1% sevoflurane (0.5 MAC)[6] and so the results show the reduced functional connectivity of higher processing areas under sedation rather than the preservation of RSN under anaesthesia. At 1.0 MAC sevoflurane, functional connectivity within the DMN has since been shown to be significantly reduced [371]. In that study, 1% sevoflurane was associated with a specific functional disconnection between posterior and anterior structures within the DMN. This has also been shown to occur in deep [372], but not light sleep [373].

A similar experiment using propofol at two levels of clinically quantified sedation (mean ± SD mcg ml^{-1} ESC: mild sedation 1.55± 0.51, deep sedation 2.8± 0.85), reported decreased connectivity within cortico-cortical and thalamocortical networks and also noted a decrease in the negative correlation between the DMN and task-active networks [99].

As part of the experiment reported in chapter 5, ten minutes of fMRI data were acquired while the subject was awake, resting with eyes closed. A further 10 minutes of resting state data was acquired at 4.0 mcg ml-1 ESC propofol prior to the wake up scan. These data were analysed using independent component analysis (ICA) to explore the effects of deep levels of anaesthesia on spatiotemporal correlations across the brain. A second analysis examined changes in these spatiotemporal correlations over the course of the anaesthesia induction scan. The ICA approach used here does not allow comparison of the strength of any correlations identified under different conditions, therefore this was primarily an exploratory analysis and future work with novel analysis techniques, as they develop and become available, are planned to further interrogate this dataset.

[6] The sigmoid shape of sevoflurane's response curve means that the probability of not being anaesthetised at 0.5 MAC in air is >0.9

6.2 Methods

Pre-processing steps

Paired resting state datasets, 10 minutes awake and 10 minutes at 4.0 mcg ml-1 ESC propofol, were acquired for 14 of the subjects. Each of these groups of 14 scans were separately analysed with group-ICA. In addition, the 48 minute induction scan was divided into six 8-minute epochs, each of which contained identical, time locked stimuli and were matched for propofol ESC (figure 4.2). The six groups of 8-minute scans (n=12 each) were also separately analysed using ICA.

The preprocessing steps described in Chapter 2 were applied to these data: removal of non-brain tissue, motion correction, fieldmap-based unwarping, spatial smoothing, grand mean intensity normalisation and highpass temporal filtering at 0.02 Hz. The frequency at which the correlations of interest have been reported is generally < 0.1 Hz. The highpass filter threshold was selected to remove the effects of any scanner drift over the course of the scan but this may not have been low enough for all signals of interest to survive the filtering algorithm. The scans were co-registered to MNI152 standard space (chapter 2) prior to group analysis.

Analysis was carried out using probabalistic independent component analysis [144], implemented in MELODIC version 3.0 of FSL (see chapter 2) following voxel-wise de-meaning of the data and variance normalisation.

Voxel-wise temporal concatenation of each of the two groups of 4D datasets was performed and then each concatenated dataset was decomposed into maps with maximal spatial independence. This identified networks of voxels showing significant temporal covariance. The dimensionality of the decomposition was arbitrarily limited to 30, although there is no ideal number of components into which the data can be decomposed [374].

Resting States

Spatial maps of components were visually inspected to identify functional networks and signals of cardiorespiratory origin. Because of the low sampling rate of fMRI (TR 3 seconds; $^1/_3$ Hz), aliasing occurs causing overlap of signals of cardiorespiratory and functional origin. Scanning at a high sampling rate may help overcome these problems but ICA decomposition may still be more effective [374].

A spatial map of the cerebral ventricles and draining cerebral veins, signal in which accounted for 7.51% of the variance explained by ICA (4.39% of total variance) is shown in figure 6.1. The physiological origin of this signal is supported by the single peak in the spectrogram of signal frequencies and its presence to some extent in almost all subjects.

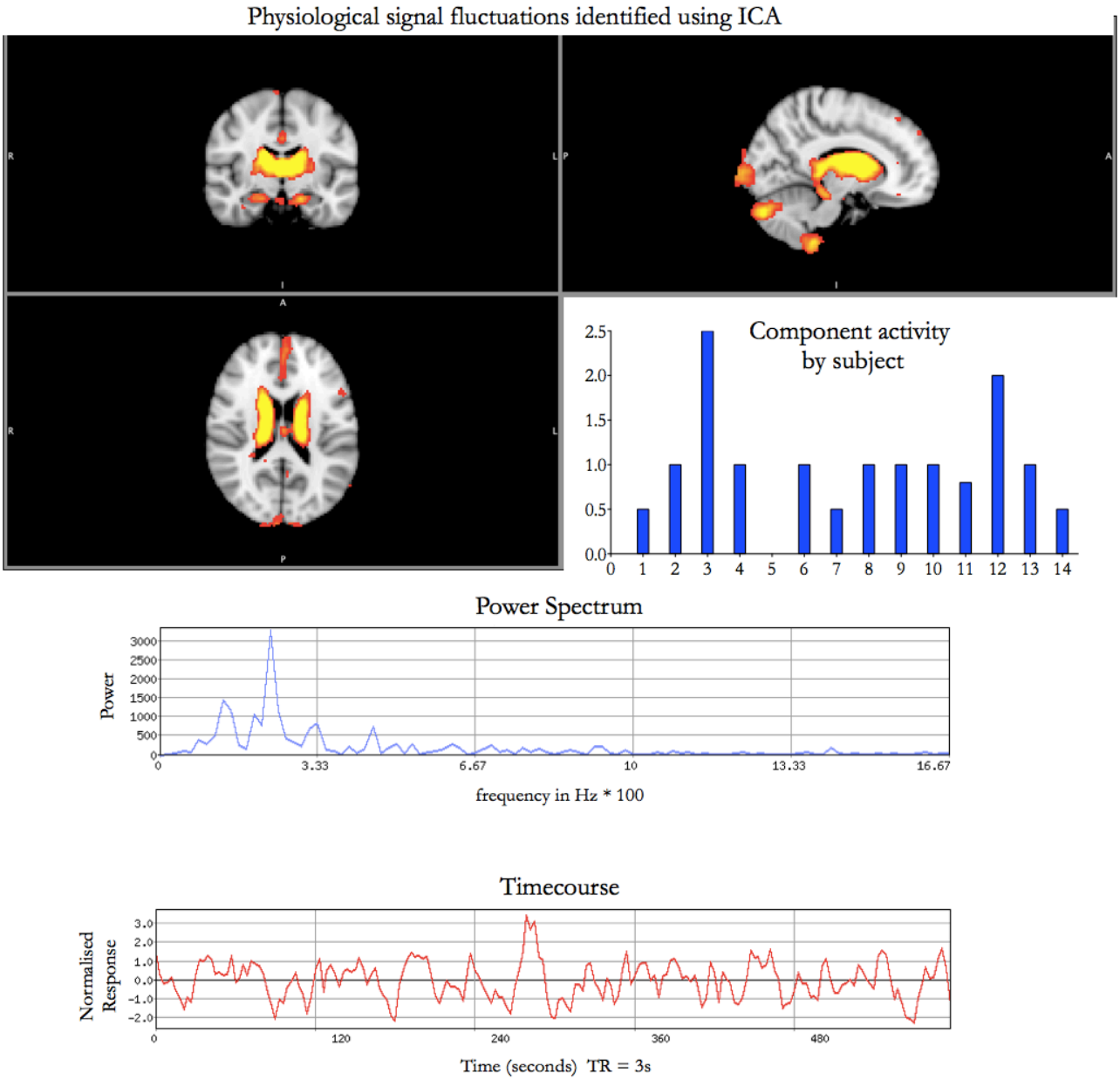

Figure 6.1 Example of physiological noise identified as a spatiotemporal component extracted from the group dataset (n=14) using ICA decomposition. The spatial map localises the coherent activity to a set of voxels containing cerebrospinal fluid and the CSF-brain border.

In contrast, non-physiological signal localised to cerebral white matter (figure 6.2) was characterised by several frequency peaks inconsistent with physiological or functional signal changes..

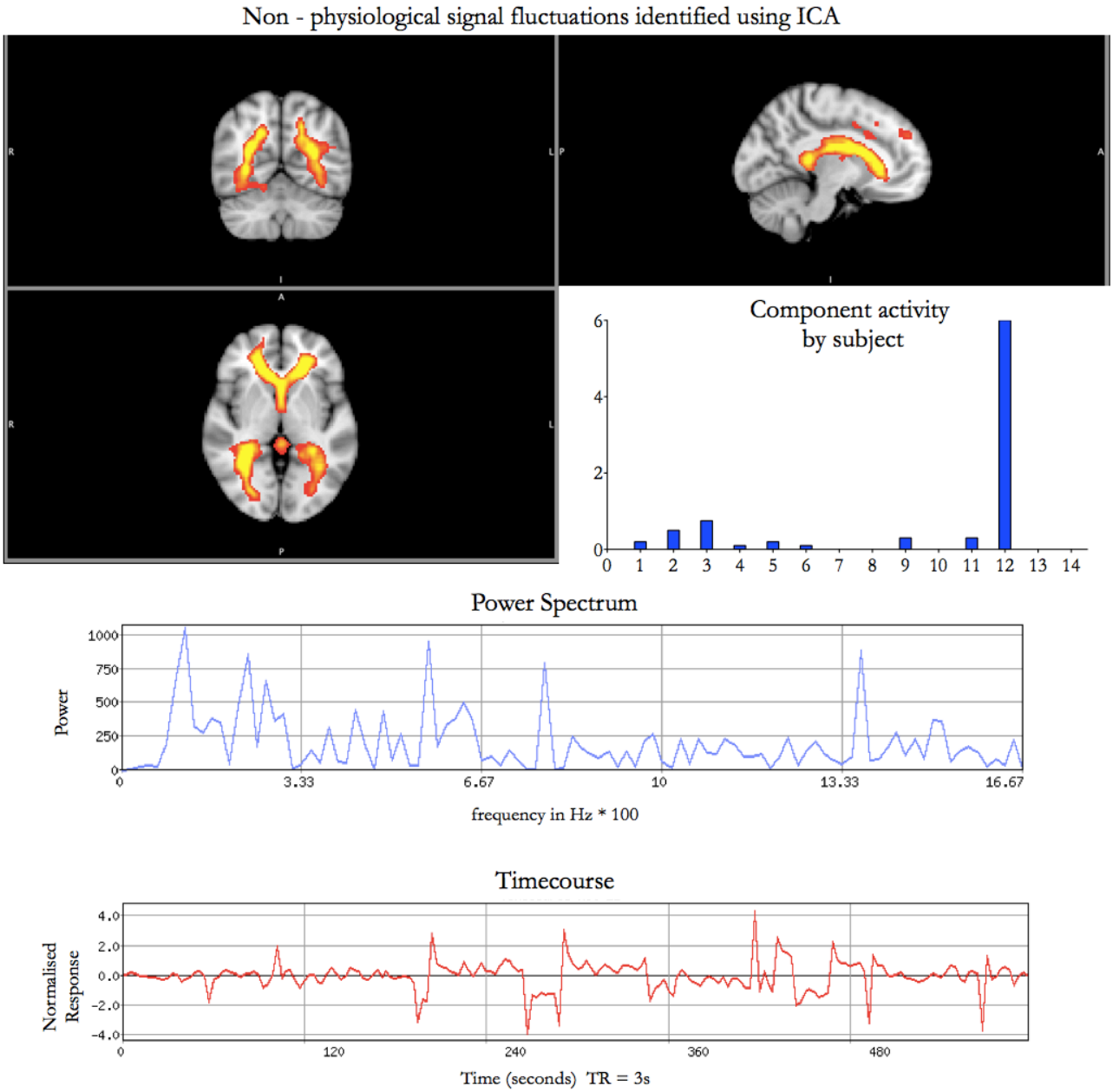

Figure 6.2 Example of non-physiological noise identified as a spatiotemporal component extracted from the group dataset (n=14) using ICA decomposition. The spatial map localises the coherent activity to a set of voxels along white matter tracts. Coherent activity across these voxels is present in only one subject. The power spectrum shows several frequency peaks and the first principal component of the set of timecourses of this coherent activity features low amplitude fluctuations and random spikes.

A number of recognisable functional networks were identified in the resting awake scan (eyes closed) dataset including the default mode network, the executive-control network bilateral primary auditory areas, bilateral somatsensory areas, associative areas and the visual cortex (figure 6.3).

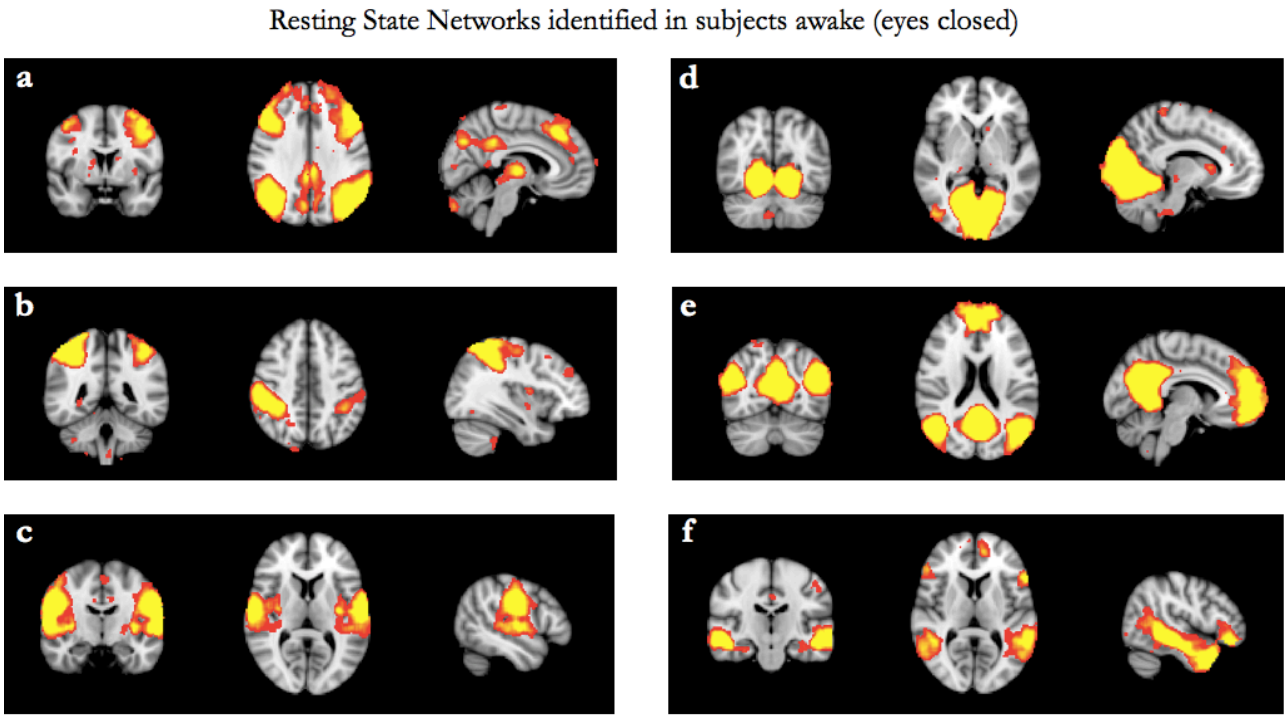

Figure 6.3 Six networks of temporally coherent BOLD signal fluctuations identified during the resting state awake scans using group level ICA decomposition. a) frontoparietal executive control network; b) bilateral somatosensory cortex; c) bilateral primary auditory cortex; d) bilateral visual cortex; d) default mode network; e) association network

ICA decomposition of the resting state scans at 4.0 mcg $ml^{-1,}$ revealed two recognisable networks, the other 28 components being clearly physiological or non-functional signals (examples provided in Appendix C). The two networks identified are shown in figure 6.4.

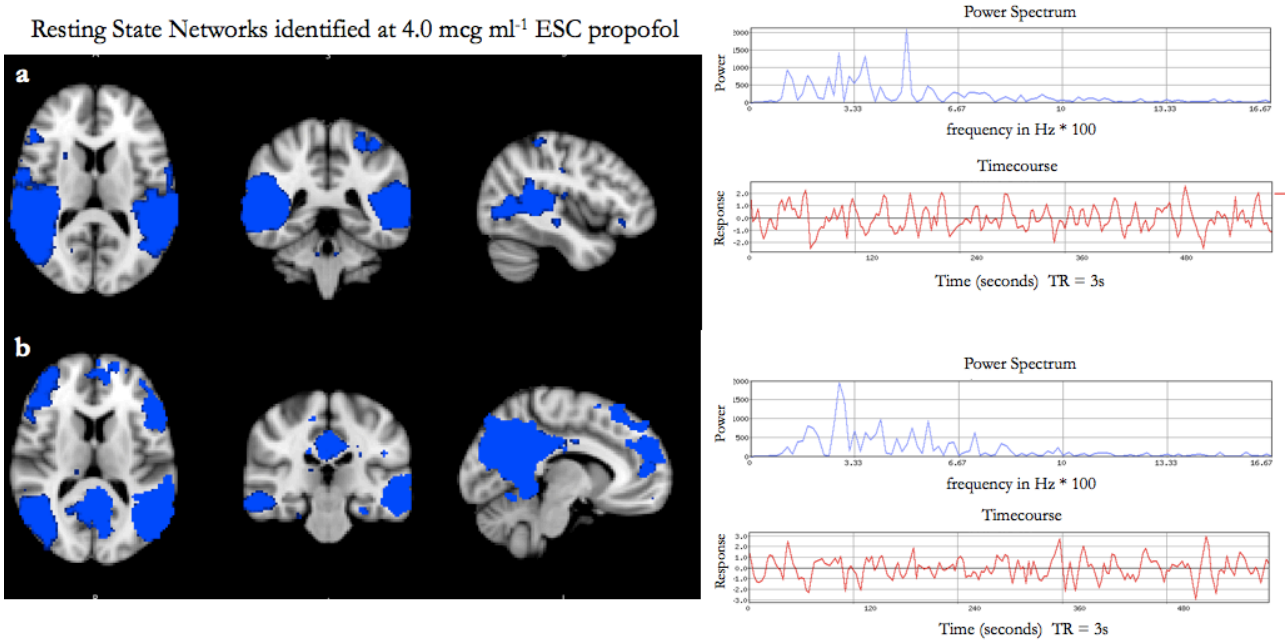

Figure 6.4 Two networks of temporally coherent BOLD signal fluctuations identified during the resting state scans at 4.0 mcg ml-1 ESC propofol using group level ICA decomposition. a) executive -control network; b) default mode network. Additional frequency peaks are seen in the power spectrum and the timeseries include high as well as low frequency fluctuations. A reduced signal to noise ratio may account for the failure to find more network at this level of propofol and may also account for the reduced within and between network correlations during anaesthesia reported in the literature.

This is an important demonstration of the persistence of preserved functional connectivity within RSN, even at this level of propofol. It shows that fluctuations in neuronal activity in these areas remain synchronised in the absence of conscious awareness or even unconscious stimulus processing, as verified by the experiment reported in chapter 5. It supports the hypothesis that RSN reflect anatomical connections between distant brain regions that continue to engage in some common activity in all living brains studied to date.

Spatial and spectral features of one of the networks that was identified in both conditions, awake and at peak propofol, are shown in figure 6.5. The first and most obvious difference is the diminution of the extent of connectivity between the bilateral temporal and prefrontal regions under anaesthesia. The clear change is in the characteristics of the associated signal fluctuations. The timecourse plotted in figure 6.5 is the first principal component of the matrix of timecourses of all voxels within the component's spatial map. A distinct difference is seen between the spectral power distribution of the awake RSN and that at peak propofol. In the awake RSN the timecourse consists of low frequency, high amplitude fluctuations with a single frequency peak at approximately 0.01 Hz. At peak propofol there are several higher frequency peaks in the power spectrum. If this

represents increased random variation in BOLD signal under anaesthesia relative to any remaining RSN driven fluctuations, this may explain why the strength of temporal correlation within RSN has often been reported to be reduced under anaesthesia [369-371].

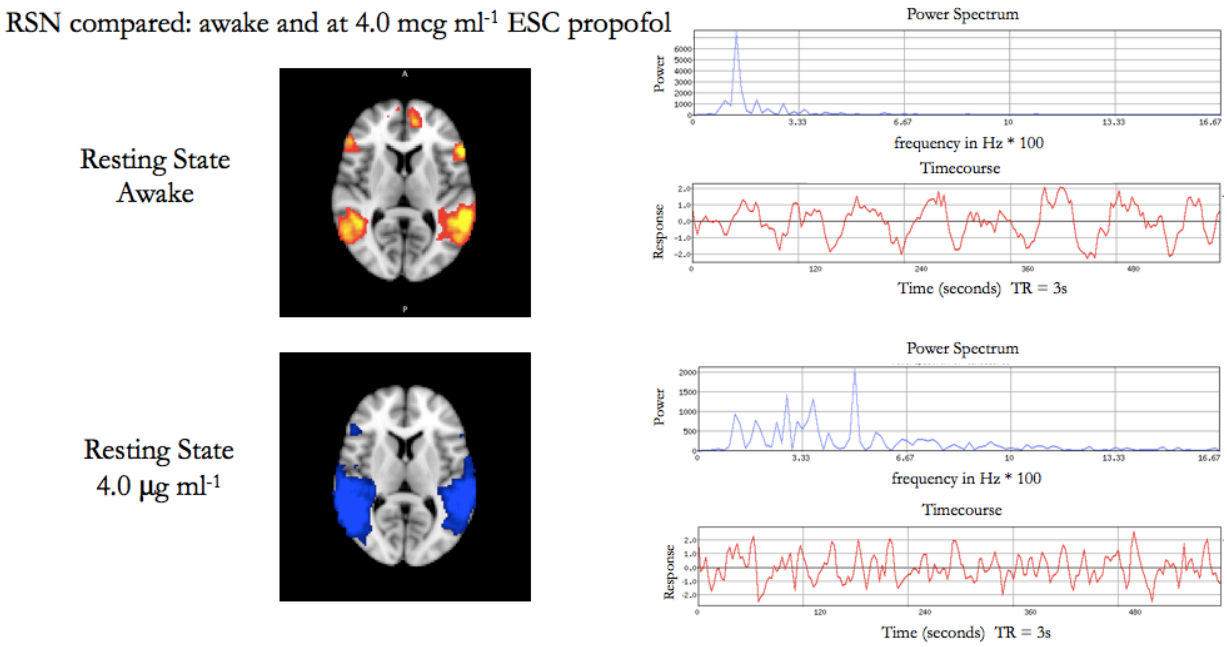

Figure 6.5 Comparing the executive-control network identified during the resting state scans awake (top, red/yellow) and at 4.0 mcg ml-1 ESC propofol (bottom, blue) using group level ICA decomposition. Despite involving the same temporoparietal and dorsal frontal areas, the spatial extent of the network and the spectral distribution of power in the signal fluctuations have both changed. Fewer brain regions are identified as part of this network during anaesthesia and the timecourse contains more activity at relatively higher frequencies.

Future analysis of these data will quantify the strength of the connectivity in these networks in the two conditions and compare the awake and anaesthetised states in terms of correlations or anticorrelations between networks in order to confirm or contradict the hypothesis that within or between - network functional connectivity may be disrupted by anaesthesia [99].

6.3.2 Spatiotemporal network behaviour during induction

One of the networks present in the awake and the peak propofol ICA decomposition comprised much of the secondary somatosensory and auditory cortex bilaterally (figure 6.4). The analysis reported here explores the hypothesis that if anaesthesia involves isolation of the thalamocortical system from the external environment, as proposed in chapters 4 and 5, then activity in such a network may mimic the awake resting state, as if these brain regions were resting, unperturbed by stimuli. This network of brain regions with associative functions is of

particular interest as its involvement in stimulus processing was shown in chapter 5 to be impaired relatively early.

The 48 minute scans of each of the 48 subjects were divided into six 8-minute temporal regions of interest (tROIs). The same temporal concatenation and subsequent ICA decomposition that was applied to the resting state data was then applied to each group of twelve 8-minute scans.

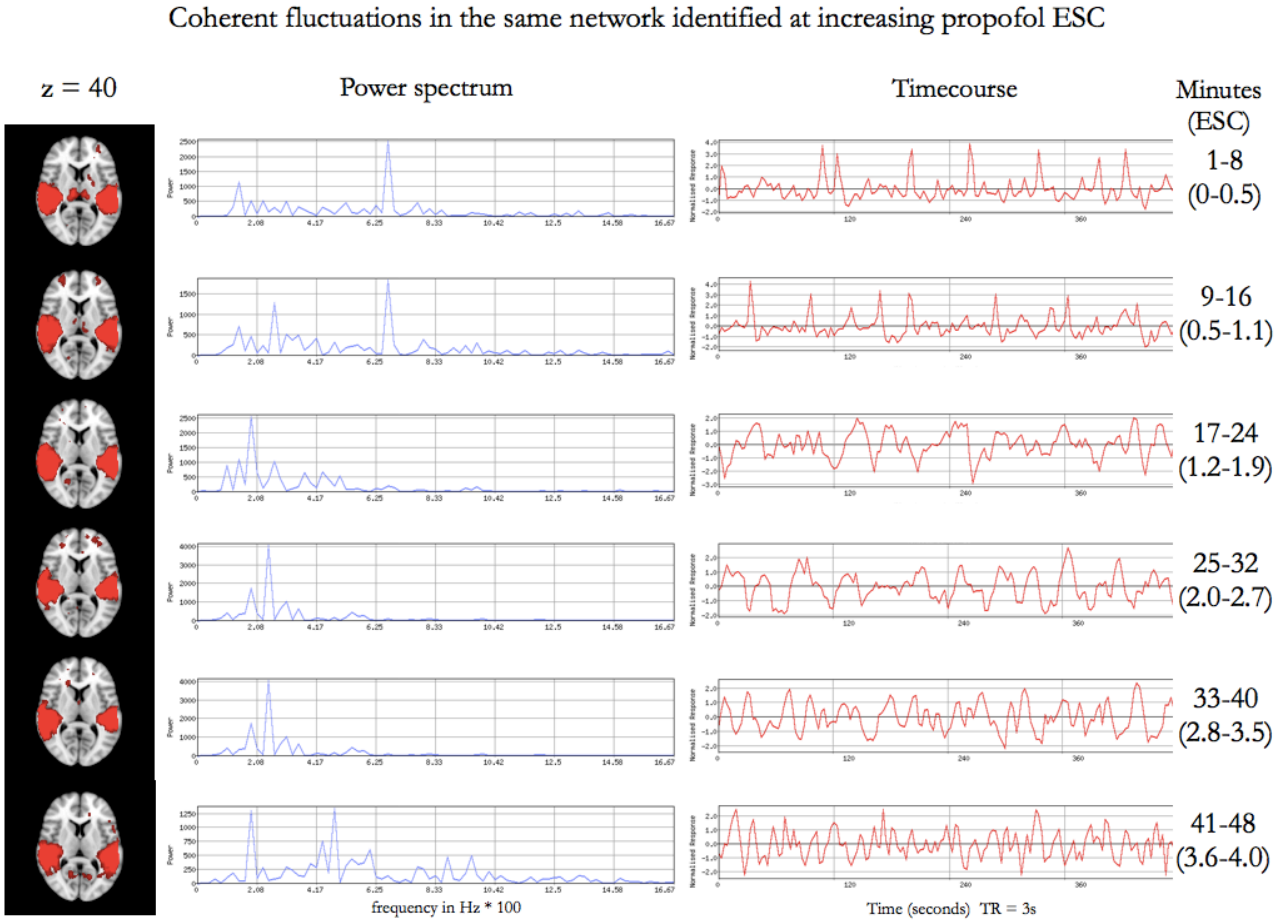

Figure 6.6 Group ICA decomposition of epochs during the induction of anaesthesia. Spatial maps identifying the network of interest are shown on the left. The power spectrum of activity (blue) shows a shift from higher to lower frequency activity as anaesthesia deepens. This can be seen in the associated timecourse (red), where activity changes from stimulus-dependent to stimulus-independent. The time within the experiment and the associated propofol levels are given on the right hand side.

The bilateral associative network was seen in all six of the tROIs (figure 6.6). During the first eight minutes activity in this network was clearly stimulus driven. The segments of data for each tROI contained identical time-locked stimuli. Word-task-evoked BOLD signal changes dominate the timeseries (see Appendix F for the relationship between word task timing and BOLD timeseries spikes). The frequency spectrum shows a large spike in power at a higher frequency than was seen in the resting state awake (figure 6.5). This is only marginally different to the second tROI, in which BOLD responses to stimulation can still be seen, although a second smaller, lower frequency peak is seen in the spectrogram. By the beginning of the third tROI, over half of the subjects had become unresponsive and only two remained responsive at the end of this period. A clear change in the frequency characteristics of the timeseries is seen at this point, with slower fluctuations appearing. The higher frequency activity is gone and the spectrum shows a peak at the same low frequency that was seen in the resting state awake. In fact, the timeseries and spectrogram look remarkably similar to the resting state awake in figure 6.5. This low frequency activity continues to dominate until the final tROI, during which it is accompanied by activity at a higher frequency of unknown origin and similar to that seen in the resting state at peak propofol (figure 6.5). One interpretation of this finding is that once a subject becomes unresponsive, cortical areas no longer engaging with the exterior enter their default mode, as if they were resting. The associated signal fluctuations may be either reduced under higher doses of propofol or accompanied by excess random signal variation, changing the spectral characteristics of the RSN. This may account for or contribute to the reported decreased functional connectivity within networks under anaesthesia.

Conclusion

The identification of temporally coherent signal fluctuations using ICA proved extremely valuable in the experiment reported in chapter 5 where, as illustrated in figures 6.1 and 6.2, decomposition of the data into independent components allowed those components which were clearly not related to neuronal function to be removed. This improved the signal to noise ratio and reduced the impact of physiological and other fluctuations on the BOLD signal of interest. Given the complexity of interactions between hypercapnia, propofol, respiratory excursion and BOLD signal changes, these would have been impossible to accurately model and the data-driven ICA approach was preferable.

Further exploration of resting state functional data using ICA decomposition in this chapter has shown that spatiotemporal coherence in the resting state was identifiable in this dataset and *is* sustained, at least to some extent, during anaesthesia. The spatial extent and temporal nature of the correlated fluctuations does appear to change with the addition of propofol, consistent with published studies.

Application of the ICA technique to fMRI data gathered during stimulation identified a network subserving a specific function in the awake state, auditory processing, which showed sustained within-network connectivity as subjects became unresponsive, and this was associated with a change in the temporal dynamics of the network despite ongoing stimulation. The behaviour of this network suggests that perhaps the slow fluctuations seen in RSN may be the default behaviour of functionally connected networks when they are not engaged in signal processing, akin to the alpha waves of the Berger rhythm, only on a timescale four orders of magnitude slower.

This data exploration was a preliminary one. Mathematical tools to allow statistical comparisons of RSN at group level in different conditions are improving and it is envisaged that this dataset and planned further experiments on RSN during anaesthesia may yield as much if not more information as stimulus-based experiments about changing interactions between brain regions.

Chapter 7: Concluding remarks

The motivation for the work in this thesis was the desire to better understand what happens within the brain when consciousness is therapeutically manipulated. Understanding the way that anaesthetic drugs affect the cardiovascular, renal and respiratory systems is central to ensuring good cardiovascular, renal and respiratory outcomes for patients. It is only sensible therefore to expect that good neurological outcomes, including post-anaesthesia recovery, post-operative cognitive function, appropriate sedation management during intensive care and effective neuroprotection, depend on a comprehensive understanding of the way these drugs affect central nervous system function itself, not just the observed behaviour.

Pharmacologically induced unconsciousness cannot and should not be considered as a phenomenon in isolation. Physiological sleep and pathological disorders of consciousness are inextricably linked to each other and to anaesthesia. Research within each of these three fields has been mutually informative. Throughout this thesis therefore, each observation has been considered with reference not only to what is known about anaesthesia, but also in the context of related observations in sleep and DOC.

It is increasingly becoming apparent that, rather than imposing an artificial state on the central nervous system, as was hypothesised in the early days of anaesthesia, at least some anaesthetic drugs exploit native sleep-wake physiology, in much the same way as inotropic drugs exploit native catecholamine physiology. By tipping the balance of native systems in the desired direction, through pharmacological rather than physiological changes in chemical messages, the desired outcome, such as unconsciousness or augmented cardiac output, can be achieved. Since sleep is beneficial, and sleep deprivation detrimental, promotion of homeostasis within the CNS, through the active processes of sleep, may be an important target in the optimisation of neurological outcomes, just as physiological homeostasis is in other systems.

One of the more compelling arguments for the physiological (rather than simply behavioural) similarities between sleep and anaesthesia comes from the discovery that fatigue is ameliorated by anaesthesia. More specifically, that the need for specific components of sleep is satisfied by certain types of anaesthetic drugs. Tung and colleagues discovered that rats sedated with propofol during their normal sleep period showed no subsequent signs of sleep deprivation [38]. Sleep-deprived rats were later found to have the same rate of recovery during the first six hours after sleep deprivation, whether during that period they were sedated with propofol or

allowed to sleep naturally [39]. Propofol anaesthesia appears to satisfy the homeostatic need for both REM and NREM sleep. If volatile anaesthetics rather than propofol are administered after sleep deprivation, NREM sleep debt is discharged but not REM sleep debt [40,375,376]. This raises two important points. The first is that slow waves during anaesthesia may serve the same metabolic function as those seen in sleep. The second is that slow waves during anaesthesia may therefore be an important clinical endpoint. While this may be a minor concern during brief procedures, it could become a more pressing issue during long cases or when managing sedation in ICU.

While absolute sleep deprivation is recognised to be deleterious, the potential for inadequate attention to the specific homeostatic role of slow wave activity to impact upon cognitive function may be underestimatied. Intriguing work by van der Werf and colleagues illustrates this point[377,378]. Rather than applying a simple sleep deprivation protocol, this group selectively reduced slow wave sleep in healthy volunteers, while maintaining sleep architecture and total sleep time. In the experimental condition, when SWA was detected, it was interrupted by playing auditory beeps, increasing in volume until SWA dropped below a specified threshold. In the control condition subjects slept with the same EEG equipment on but SWA was not interrupted. The subjects not only reported feeling unrefreshed by sleep that was deficient in SWA (van der Werf, personal communication), but were found to have significantly impaired vigilance and declarative memory the following morning. This was associated with a reduction in hippocampal activation on fMRI during memory task performance. In light of this and a wealth of emerging work emphasising the functional role of slow wave sleep, it would be interesting to relate the adequacy of slow wave sleep during intensive care to the development of cognitive dysfunction or delirium.

The experiments reported in this thesis aimed to translate a scientific understanding of the neurophysiology of sedation into useful clinical concepts which might contribute to better provision of targeted sedation and anaesthesia. The first experiment suggests a potential mechanism for the disintegration of perception during sedation with propofol. The second experiment reports the progressive changes in sleep-related oscillations during induction of and recovery from deeper sedation with propofol and the third experiment relates these changes to stepwise modulation of thalamocortical function. Finally, the behaviour of temporally correlated, spatially distributed activity in the brain in different conditions was explored as a prelude to future studies.
In the first experiment (reported in chapter 3) the functional connectivity between the striatum and a broad array of brain regions, including the thalamus, was found to be significantly and selectively reduced by relatively low

levels of propofol (no higher than the level required to eliminate the response to verbal stimulation). This occurred in the absence of any impairment of thalamocortical connectivity. The result, while novel in the context of sedation, is consistent with what is known about connections between the basal ganglia, intralaminar thalamic nuclei, cortical processing networks and brainstem arousal nuclei. Distortion of function within these co-ordinating circuits may provide a mechanistic basis for the cognitive unbinding to which impaired conscious perception has been attributed [16].

Interval timing is believed to be maintained by the basal ganglia circuitry [319]. There is interesting evidence from patients with Parkinson's disease (PD), in which dopaminergic nigrostriatal connections are lost, for the role of the basal ganglia in the maintenance of the brain's internal temporal dynamics [379]. Co-ordination of planned complex movements, rather than execution of the individual components of a movement, is impaired. This is associated with cognitive dysfunction and altered time perception. PD patients who can reliably reproduce a specified time interval when on levodopa and apomorphine fail to do so when untreated [318], and time perception deficits have been shown using fMRI to be associated with striatal dysfunction in these patients [380]. While it would be very difficult to objectively quantify, time perception is widely accepted to be distorted during sedation and anaesthesia [321]. It may be that the activity of propofol in the striatum leads to the failure of integration of information in distributed brain regions, relating to specific aspects of an experience, because re-entrant cortico-striato-thalamo-cortical loops no longer provide a robust temporal framework. While this study does not introduce any new measurements which could guide clinical practice, it is worth considering the distorting effect of sedation on patients' internal timing structure, as fragmented perception may exacerbate, rather than ameliorate, delirium during critical illness.

In the second experiment (reported in chapter 4) a very specific relationship between the characteristic electrophysiology of sleep and the depth of anaesthesia was established. It was shown that slow wave activity increases with increasing CNS concentrations of propofol until it reaches a plateau or saturation point. The explanation proposed here for this observation is that increasing power in the 0.5-1.5 Hz band reflects the involvement of increasing numbers of neurons in the slow waves as they travel across the cortex [283], and that this activity must therefore reach a maximum when no further neurons can be recruited and further dose increases lead only to burst suppression. This would be a useful endpoint for titration of anaesthesia.

In formulating this hypothesis, consideration must be given to the relationship between slow wave activity and the underlying metabolic demands which appear to drive it during physiological sleep. SWA reflects sleep need [29]. It is highest during the first sleep cycle and decreases thereafter until waking [381]. It is further increased during this first cycle if sleep is preceded a period of sleep deprivation [382], but is decreased by napping during the day [383]. The effect of prior neuronal activity on subsequent SWA is specific to the groups of neurons exercised. Transcranial magnetic stimulation prior to sleep increases subsequent SWA in the stimulated region [384]. Motor learning increases subsequent SWA in the motor cortex [385], while limb immobilisation decreases it [386]. These studies all provide compelling evidence for the synaptic homeostasis hypothesis of sleep [29,387], for which direct evidence has been reported in Drosophila [30]. Indeed, if sleep is delayed long enough, SWA occurs locally even if the rest of the brain is still awake [388].

If SWA power during anaesthesia is also determined by the synaptic homeostat, then it might be expected that with prolonged administration of propofol (beyond the brief period studied here) SWA power will wane. If on the other hand SWA during anaesthesia is sustained because it is driven exogenously (either directly through hyperpolarisation or indirectly through potentiation of inhibitory neurons) rather than endogenously (by a combination of processes C an S for example), it may prove to be an important clinical measure. Before exploring the possibility of SWA being monitored during anaesthesia, its stability over several hours or even longer must be studied.

In the third experiment, (reported in chapter 5), stepwise, modality-specific changes in thalamocortical responses to stimulation were found to be associated with specific behavioural and electrophysiological observations. The most important finding in this experiment was that after subjects become unresponsive, but before SWA becomes saturated, the thalamocortical system continues to respond to external stimulation, even after the loss of integrative functions across broader associative networks appears to preclude conscious perception. When SWA had reached saturation however, no further fMRI responses to external stimuli were detected. Instead, activation was identified in the precuneus, a brain region with connections to brainstem arousal nuclei and the first area to show an increase in metabolic activity during recovery from DOC following traumatic brain injury.

Finally, using a data-driven approach to fMRI analysis, the persistence of resting state networks during propofol anaesthesia was confirmed in humans. Furthermore, the nature of correlated signal changes within the auditory

network studied was seen to change with increasing levels of propofol from stimulus driven activity to slower synchronous fluctuations, spectrographically similar to the resting state when awake, despite ongoing stimulation. This supports the more recent interpretation of RSN as reflecting the intrinsic function and structure of neural networks rather than any internal process specific to consciousness.

Mircea Steriade maintained that the sleeping brain was not idle, but was instead exclusively engaged in processing internal, rather than external signals [284]. Similarly, as shown in this thesis, anaesthesia is also a highly active brain state. Internal signaling processes, spindles, slow waves, and resting state networks persist despite loss of consciousness and perception.

Appendices

Appendix A - Volunteer Documentation

Reference No: 09/H0605/57 University of Oxford/Nuffield Department of Anaesthetics 26 March 2009
Professor Irene Tracey Version 1.0
Dr. Róisín Ní Mhuircheartaigh

Volunteer Health Questionnaire

Study Title: Modulation of connectivity in the brain by propofol

Please answer the following questions as honestly as you can. You can speak to your investigator directly if there are any questions you do not wish to answer. No details will be written down or recorded against your wishes. The purpose of these questions and of those in the questionnaire about magnet safety is to ensure that your participation in the study is safe and comfortable.

	Yes	No
1. Do you have any chronic medical condition?	☐	☐
2. Do you take **any** regular medicines, prescription or over the counter?	☐	☐
3. Have you ever had an operation?	☐	☐
4. Have you or any of your family ever had a reaction to anaesthetics?	☐	☐
5. Are you allergic to any food or drug that you know of?	☐	☐
6. Specifically, are you allergic to eggs or egg proteins?	☐	☐
7. Have you any loose teeth or dental implants?	☐	☐
8. Do you snore (that you know of)?	☐	☐
9. Do you smoke?	☐	☐
10. Do you drink more than 14 units of alcohol in an average week?	☐	☐
11. Is there any possibility that you could be pregnant? If you are not certain we will provide you with a pregnancy test.	☐	☐
12. Will there be somebody at home with you on the night after you participate in the study?	☐	☐

If you use recreational drugs please inform the investigator as it may affect the study, Thank You

Volunteer Instruction Checklist

Study Title: Modulation of connectivity in the brain by propfol

Thank you for agreeing to take part in this study. This page contains a list of things you need to remember in preparation for your study day. If you have any questions that are not adequately answered here, please to not hesitate to contact Róisín by e mail (roisin@fmrib.ox.ac.uk) or phone (07518366282).

1. Please come to FMRIB at 8 am on .....
2. Please do not drink any caffeinated drinks on the day of the study.
3. You should have a good meal on the evening before and drink plenty of clear fluids (e.g. water, herbal tea). Do try to have a good night's sleep. You must not have any food or drink after 4 am on the morning of your study session.
4. Please wear comfortable, loose fitting clothes to the study session. Tracksuit bottoms/sweatpants and a t-shirt would be suitable. It is difficult if you get too warm during the study but we will provide you with a blanket if you feel cold.
5. We will arrange for your transport home by taxi so please do not cycle to the study session. If you need to take a taxi to get to the lab, please get a receipt and we will re-imburse you.
6. Please ensure that you will have somebody with you at home on the evening after your study session. We will not go ahead with the study if you will be alone that evening.
7. Remember that you are asked not to drive, use machinery, drink alcohol or engage in sporting activities on the evening after your study session. There are no restrictions from the following morning onwards.

Appendix B - Physiological noise components

The following figure contains examples of spatial maps in which temporally coherent signals were identified when the datasets were decomposed into independent components using ICA. This technique was used for two different purposes in the experiments reported. In the figure below, the top row shows examples of components that were attributable to cardiorespiratory artifact, motion or vascular pulsations. The bottom row shows examples of components of functional origin.

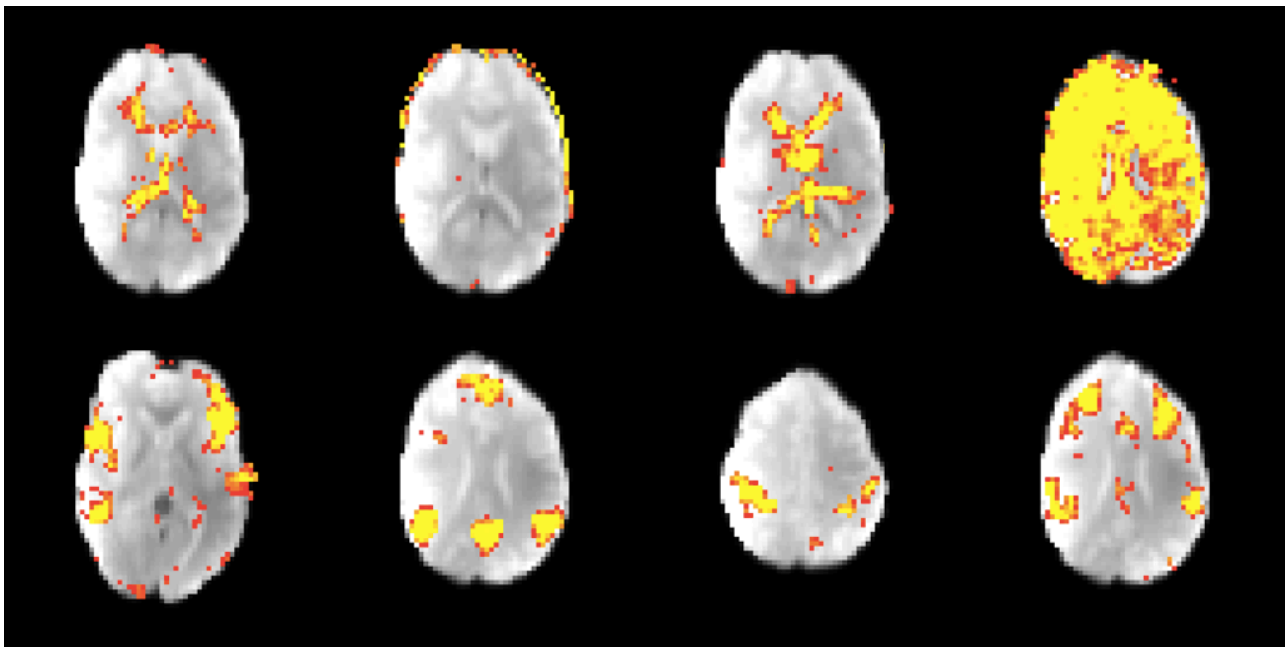

Appendix C - Permutation entropy algorithm

The following is the algorithm published by Olofsen and colleagues for the estimation of permutation entropy, a measure of complexity in the electroencephalogram.

```
function [epei, pe1, pe2, p1tie, p2tie, pk12]=cpei(y,epz)


%Permutation Entropy - order set at 3
%Input timeseries y and noise threshold epz
%Output all combinations of entropies for tau1 vs tau2 (lags)

%Set epz to zero for no ties

%check data and initialise variables

ord=3;
sd=std(y);
pe1=0; pe2=0; epei=0; pk12=0;

if sd==0; %returns if nonsense data
   return;
end

%check and turn y vector to correct direction
csize=size(y);
if csize(2)==1;
   y=y';
end

ly=length(y);

%calculate PE for tau= 1 and 2 and threshold=epz

e1=[]; e2=[]; p1=[]; p2=[];
permlist=perms(1:ord);
ctie1=0;
ctie2=0; %initial ties bin
ct1(1:length(permlist))=0; %initialise tau=1 bins
ct2(1:length(permlist))=0; %initialise tau=2 bins

for j=3:ly-2;
   seg=y(j-2:j+2); %total segment
   seg1=[seg(2),seg(3),seg(4)];  %seg for tau=1
   seg2=[seg(1),seg(3),seg(5)];  %seg for tau=2
   [a,iv]=sort(seg);             %sorts ordsize of seg
   [a1,iv1]=sort(seg1);          %sorts ordsize of seg1
   [a2,iv2]=sort(seg2);          %sorts ordsize of seg2

   %gets bins -epz and 6 other motifs for PE tau=1

   da1=abs(diff(a1));            %find difference between points in motif
   if(min(da1))<epz;             %if < threshold add to 7th bin
      ctie1=ctie1+1;
   else
      for jj=1:length(permlist);
         if permlist(jj,:)-iv1==0;
            ct1(jj)=ct1(jj)+1;%accumulates into the correct bin
         end
      end
   end                           %if min da1

   %repeats for tau=2

   da2=abs(diff(a2));            %find difference between points in motif
   if(min(da2))<epz;             %if < threshold add to 7th bin
      ctie2=ctie2+1;
```

```
    else
        for jj=1:length(permlist);
            if permlist(jj,:)-iv2==0;
                ct2(jj)=ct2(jj)+1;%accumulates into the correct bin
            end
        end
    end                             %if min da2
end
    lenn=ly-5;                      %effective length
    p1=ct1/(lenn);                  %normalises to total area
    p2=ct2/(lenn);
    ptie1=ctie1/(lenn);
    ptie2=ctie2/(lenn);

    ziz=find(p1>0);                 %handle p*log(p)=0
    e1=-sum(p1(ziz).*log(p1(ziz)));

    ziz=find(p2>0);
    e2=-sum(p2(ziz).*log(p2(ziz)));

    if ptie1>0;
        etie1=-ptie1.*log(ptie1);
    else
        etie1=0;
    end

    if ptie2>0;
        etie2=-ptie2.*log(ptie2);
    else
        etie2=0;
    end

    p1tie=etie1;
    p2tie=etie2;
    pe1=(e1+etie1)/log(7);
    pe2=(e2+etie2)/log(7);
    epei=(e1+e2+etie1+etie2)/log(49);
    pk12=-sum(pe2.*log(pe2./pe1));
    return;
```

Appendix D - Spindle prevalence estimation algorithm

The following is a modification of the algorithm published by Sleigh and colleagues for the estimation of spindle prevalence in the electroencephalogram. The modification was introduced to allow the detection of spindles at different frequencies within the alpha band

```
function [p]=roisin_spindles_2(y,f,amp)

%finds number of order six spindles in EEG segment
%Inputs:
% y – the segment of EEG for analysis (3 second epochs ususally)
% f – the frequency of the spindles being sought
% amp – the minumum amplitude threshold
    %Outputs:
% p – the proportion of points in an epoch which are part of a spindle
%This all assumes that the sampling rate is 500Hz

ord=12; % this is the number of 'lag' intervals that define a spindle
lenn=length(y);
if f==9;
    lag=13;
elseif f==10;
    lag=12;
elseif f==11;
    lag=11;
elseif f==12;
    lag=10;
elseif f==14;
    lag=9;
elseif f==16;
    lag=8;
end

%pass the spindle pattern over y:

cs=0;   %initialise variable for a number of spindes
i=1;
while i<lenn-lag*ord+1;   %move along the eeg until there isn't enough segment left
    yy=y(i:lag:i+ord*lag);    %yy is a sample from the eeg, from i, in ord steps of lag
    da=diff(yy);              %% da is the set of first differences of y

if((da(1)>0)&&(da(2)<=0)&&(da(3)<=0)&&(da(4)>=0)&&(da(5)>=0)&&(da(6)<=0)&&(da(7)<=0)&&(da(8)>=0)&&...
        (da(9)>=0)&&(da(10)<=0)&&(da(11)<=0)&&(da(12)>=0)&&(abs(min(da))>=amp))...
        ||((da(1)<0)&&(da(2)>=0)&&(da(3)>=0)&&(da(4)<=0)&&(da(5)<=0)&&(da(6)>=0)&&(da(7)>=0)&&(da(8)<=0)...
        &&(da(9)<=0)&&(da(10)>=0)&&(da(11)>=0)&&(da(12)<=0)&&(abs(min(da))>=amp));

    %i.e. 0-1-0 pattern /¥/¥/¥/ with three peaks and three troughs
    %starting with either a positive or a negative deflection

    cs=cs+(lag*ord);
    i=i+lag*ord-1;      %jump beyond the end of the spindle

end
i=i+1;
end
p=cs/lenn;
return
```

Appendix E - Motion correction parameters during the wake up scan

The motion correction parameters measured during the wake up scan for some of the subjects are shown in the figure below. Head movement around the time of return of responses can be clearly seen. This caused an additional non-fMRI artifact to appear in the EEG and also rendered fMRI data unusable from this time point on.

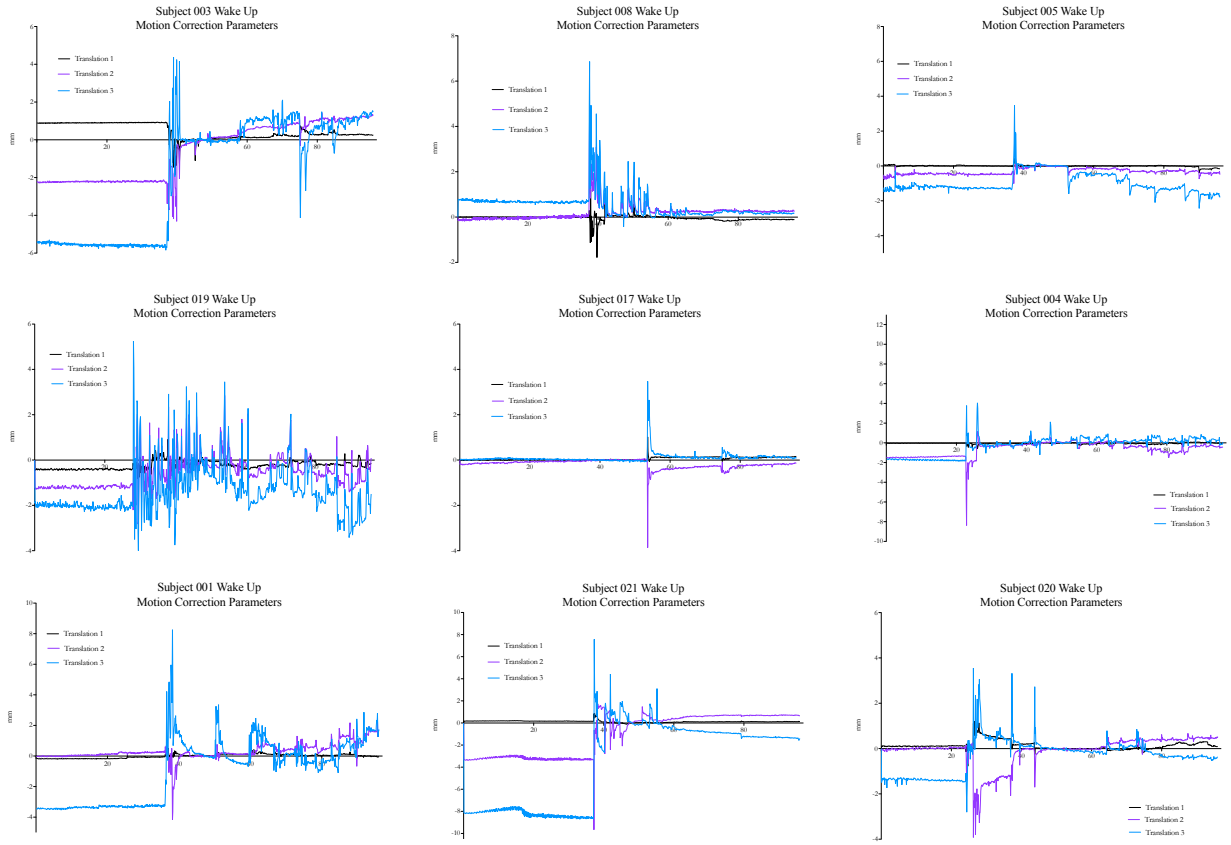

Bibliography

1. Looking back on the millennium in medicine. *New England Journal of Medicine* **342**, 42–49 (2000).
2. Sanchez, G. M. & Burridge, A. L. Decision making in head injury management in the Edwin Smith Papyrus. *Neurosurg Focus* **23**, E5 (2007).
3. Karenberg, A. Headache in magical and medical papyri of Ancient Egypt - Karenberg - 2002 - Cephalalgia - Wiley Online Library. *Cephalalgia* (2001).
4. Demertzi, A., Liew, C., Ledoux, D., Bruno, M.-A., Sharpe, M., Laureys, S. & Zeman, A. Dualism persists in the science of mind. *Ann N Y Acad Sci* **1157**, 1–9 (2009).
5. James, W. & McDermott, J. J. *The Writings of William James*. 858 (University Of Chicago Press: 1977).
6. Molyneaux, B. J., Arlotta, P., Menezes, J. R. L. & Macklis, J. D. Neuronal subtype specification in the cerebral cortex. *Nat. Rev. Neurosci.* **8**, 427–437 (2007).
7. Bolton, J. A contribution to the localization of cerebral function based on the clinico-pathological study of mental disease. *Brain* **33**, 143–148 (1910).
8. Campbell, A. W. *Histological studies on the localisation of cerebral function*. 360 (1905).
9. Douglas, R. Neuronal circuits of the neocortex - Annual Review of Neuroscience, 27(1):419. *Annu. Rev. Neurosci.* (2004).
10. Mountcastle, V. The columnar organization of the neocortex. *Brain* (1997).
11. Buzsáki, G., Kaila, K. & Raichle, M. Inhibition and brain work. *Neuron* **56**, 771–783 (2007).
12. Mody, I. & Pearce, R. A. Diversity of inhibitory neurotransmission through GABA(A) receptors. *Trends Neurosci.* **27**, 569–575 (2004).
13. Buzsáki, G. *Rhythms of the brain - G. Buzsáki*. (2006).
14. Watts, D. J. & Strogatz, S. H. Collective dynamics of "small-world" networks. *Nature* **393**, 440–442 (1998).
15. Galambos, R., Makeig, S. & Talmachoff, P. J. A 40-Hz auditory potential recorded from the human scalp. *Proc Natl Acad Sci USA* **78**, 2643–2647 (1981).
16. Mashour, G. A. Cognitive unbinding in sleep and anesthesia. *Science* **310**, 1768–9; author reply 1768–9 (2005).
17. Jan, J. E., Reiter, R. J., Bax, M. C. O., Ribary, U., Freeman, R. D. & Wasdell, M. B. Long-term sleep disturbances in children: a cause of neuronal loss. *Eur. J. Paediatr. Neurol.* **14**, 380–390 (2010).
18. Cirelli, C. Cellular consequences of sleep deprivation in the brain. *Sleep Med Rev* **10**, 307–321 (2006).

19. Kirsch, D. B. There and back again: a current history of sleep medicine. *Chest* **139**, 939–946 (2011).

20. Coriat, I. H. The nature of sleep. *The Journal of Abnormal Psychology* **6**, 329–367 (1911).

21. Loomis, A. L., Harvey, E. N. & Hobart, G. Further observations on the potential rhythms of the cerebral cortex during sleep. *Science* **82**, 198–200 (1935).

22. Loomis, A. L., Harvey, E. N. & Hobart, G. Potential rhythms of the cerebral cortex during sleep. *Science* **81**, 597–598 (1935).

23. Davis, H., Davis, P. A., Loomis, A. L., Harvey, E. N. & Hobart, G. Changes in human brain potentials during the onset of sleep. *Science* **86**, 448–450 (1937).

24. Aserinsky, E. & Kleitman, N. Regularly occurring periods of eye motility, and concomitant phenomena, during sleep. *Science* **118**, 273–274 (1953).

25. Walker, A. J. & Mashour, G. A. A brief history of sleep and anesthesia. *Int Anesthesiol Clin* **46**, 1–10 (2008).

26. Moruzzi, G. & Magoun, H. W. Brain stem reticular formation and activation of the EEG. *Electroencephalogr Clin Neurophysiol* **1**, 455–473 (1949).

27. Nelson, L. E., Lu, J., Guo, T., Saper, C. B., Franks, N. P. & Maze, M. The alpha2-adrenoceptor agonist dexmedetomidine converges on an endogenous sleep-promoting pathway to exert its sedative effects. *Anesthesiology* **98**, 428–436 (2003).

28. Rétey, J. V., Adam, M., Honegger, E., Khatami, R., Luhmann, U. F. O., Jung, H. H., Berger, W. & Landolt, H.-P. A functional genetic variation of adenosine deaminase affects the duration and intensity of deep sleep in humans. *Proc Natl Acad Sci USA* **102**, 15676–15681 (2005).

29. Tononi, G. & Cirelli, C. Sleep and synaptic homeostasis: a hypothesis. *Brain Res. Bull.* **62**, 143–150 (2003).

30. Bushey, D., Tononi, G. & Cirelli, C. Sleep and synaptic homeostasis: structural evidence in Drosophila. *Science* **332**, 1576–1581 (2011).

31. Vyazovskiy, V. V., Cirelli, C., Pfister-Genskow, M., Faraguna, U. & Tononi, G. Molecular and electrophysiological evidence for net synaptic potentiation in wake and depression in sleep. *Nat Neurosci* **11**, 200–208 (2008).

32. Braun, A. R., Balkin, T. J., Wesenten, N. J., Carson, R. E., Varga, M., Baldwin, P., Selbie, S., Belenky, G. & Herscovitch, P. Regional cerebral blood flow throughout the sleep-wake cycle. An H2(15)O PET study. *Brain* **120 (Pt 7)**, 1173–1197 (1997).

33. Faraguna, U., Vyazovskiy, V. V., Nelson, A. B., Tononi, G. & Cirelli, C. A causal role for brain-derived neurotrophic factor in the homeostatic regulation of sleep. *J Neurosci* **28**, 4088–4095 (2008).

34. Lu, J., Nelson, L. E., Franks, N., Maze, M., Chamberlin, N. L. & Saper, C. B. Role of endogenous sleep-wake and analgesic systems in anesthesia. *J. Comp. Neurol.* **508**, 648–662 (2008).

35. Franks, N. P. & Zecharia, A. Y. Sleep and general anesthesia. *Can J Anaesth* **58**, 139–148 (2011).

36. Schiff, N. D., Giacino, J. T., Kalmar, K., Victor, J. D., Baker, K., Gerber, M., Fritz, B., Eisenberg, B., Biondi, T., O'Connor, J., Kobylarz, E. J., Farris, S., Machado, A., McCagg, C., Plum, F., Fins, J. J. & Rezai, A. R. *Behavioural improvements with thalamic stimulation after severe traumatic brain injury*. *Nature* **448**, 600–603 (2007).

37. Shah, S. A. & Schiff, N. D. Central thalamic deep brain stimulation for cognitive neuromodulation - a review of proposed mechanisms and investigational studies. *Eur J Neurosci* **32**, 1135–1144 (2010).

38. Tung, A., Lynch, J. P. & Mendelson, W. B. Prolonged sedation with propofol in the rat does not result in sleep deprivation. *Anesth Analg* **92**, 1232–1236 (2001).

39. Tung, A., Bergmann, B. M., Herrera, S., Cao, D. & Mendelson, W. B. Recovery from sleep deprivation occurs during propofol anesthesia. *Anesthesiology* **100**, 1419–1426 (2004).

40. Mashour, G. A., Lipinski, W. J., Matlen, L. B., Walker, A. J., Turner, A. M., Schoen, W., Lee, U. & Poe, G. R. Isoflurane anesthesia does not satisfy the homeostatic need for rapid eye movement sleep. *Anesth. Analg.* **110**, 1283–1289 (2010).

41. Evans, B. M. & Bartlett, J. R. Prediction of outcome in severe head injury based on recognition of sleep related activity in the polygraphic electroencephalogram. *J. Neurol. Neurosurg. Psychiatr.* **59**, 17–25 (1995).

42. Valente, M., Placidi, F., Oliveira, A. J., Bigagli, A., Morghen, I., Proietti, R. & Gigli, G. L. Sleep organization pattern as a prognostic marker at the subacute stage of post-traumatic coma. *Clin Neurophysiol* **113**, 1798–1805 (2002).

43. Cuvillon, P., Nouvellon, E., Marret, E., Albaladejo, P., Fortier, L.-P., Fabbro-Perray, P., Malinovsky, J.-M. & Ripart, J. American Society of Anesthesiologists' physical status system: a multicentre Francophone study to analyse reasons for classification disagreement. *Eur J Anaesthesiol* **28**, 742–747 (2011).

44. Sebel, P. S., Bowdle, T. A., Ghoneim, M. M., Rampil, I. J., Padilla, R. E., Gan, T. J. & Domino, K. B. The incidence of awareness during anesthesia: a multicenter United States study. *Anesth. Analg.* **99**, 833–9, table of contents (2004).

45. Sandin, R. H., Enlund, G., Samuelsson, P. & Lennmarken, C. Awareness during anaesthesia: a prospective case study. *The Lancet* **355**, 707–711 (2000).

46. Ghoneim, M., Block, R. & Haffarnan, M. Awareness During Anesthesia: Risk Factors, Causes and Sequelae: A Review of Reported Cases in the Literature. *Anesth. Analg.* (2009).

47. McCleane, G. The nature of pre-operative anxiety - McCleane - 2007 - Anaesthesia - Wiley Online Library. *Anaesthesia* (1990).

48. Davydow, D. S., Gifford, J. M., Desai, S. V., Needham, D. M. & Bienvenu, O. J. Posttraumatic stress disorder in general intensive care unit survivors: a systematic review. *General Hospital Psychiatry* **30**, 421–434 (2008).

49. Ballard, N., Robley, L., Barrett, D. & Fraser, D. Patients' recollections of therapeutic paralysis in the intensive care unit. *American Journal of Critical Care* (2006).

50. Sessler, C., Gosnell, M. & Grap, M. The Richmond Agitation–Sedation Scale. *Am. J. Respir. Crit. Care Med.* (2002).

51. Payen, J.-F., Chanques, G., Mantz, J., Hercule, C., Auriant, I., Leguillou, J.-L., Binhas, M., Genty, C., Rolland, C. & Bosson, J.-L. Current practices in sedation and analgesia for mechanically ventilated critically ill patients: a prospective multicenter patient-based study. *Anesthesiology* **106**, 687–95; quiz 891–2 (2007).

52. Bienvenu, O. J. & Neufeld, K. J. Post-traumatic stress disorder in medical settings: focus on the critically ill. *Curr Psychiatry Rep* **13**, 3–9 (2011).

53. Jubran, A., Lawm, G., Duffner, L. A., Collins, E. G., Lanuza, D. M., Hoffman, L. A. & Tobin, M. J. Post-traumatic stress disorder after weaning from prolonged mechanical ventilation. *Intensive Care Med* **36**, 2030–2037 (2010).

54. Bolton, C. Neuromuscular manifestations of critical illness - Bolton - 2005 - Muscle & Nerve - Wiley Online Library. *Muscle & nerve* (2005).

55. Posner, J. & Plum, F. *The diagnosis of stupor and coma.* (Philadelphia: FA Davis Company: 1966).

56. Jennett, B. & Plum, F. Persistent vegetative state after brain damage. A syndrome in search of a name. *The Lancet* **1**, 734–737 (1972).

57. Plum, F. & Posner, J. B. The diagnosis of stupor and coma. *Contemp Neurol Ser* **10**, 1–286 (1972).

58. Kinney, H., Korein, J. & Panigrahy, A. Neuropathological findings in the brain of Karen Ann Quinlan--the role of the thalamus in the persistent vegetative state. *New England Journal of Medicine* (1994).

59. Quill, T. Terri Schiavo — A Tragedy Compounded. *New England Journal of Medicine* (2005).

60. Smedira, N., Evans, B. & Grais, L. Withholding and Withdrawal of Life Support from the Critically Ill. *New England Journal of Medicine* (1990).

61. Andrews, K., Murphy, L., Munday, R. & Littlewood, C. Misdiagnosis of the vegetative state: retrospective study in a rehabilitation unit. *BMJ* **313**, 13–16 (1996).

62. Childs, N. & Mercer, W. Accuracy of diagnosis of persistent vegetative state. *Neurology* (1993).

63. Schnakers, C., Vanhaudenhuyse, A., Giacino, J., Ventura, M., Boly, M., Majerus, S., Moonen, G. & Laureys, S. Diagnostic accuracy of the vegetative and minimally conscious state: clinical consensus versus standardized neurobehavioral assessment. *BMC Neurol* **9**, 35 (2009).

64. Giacino, J. T., Ashwal, S., Childs, N., Cranford, R., Jennett, B., Katz, D. I., Kelly, J. P., Rosenberg, J. H., Whyte, J., Zafonte, R. D. & Zasler, N. D. The minimally conscious state: definition and diagnostic criteria. *Neurology* **58**, 349–353 (2002).

65. Wijdicks, E. Minimally Conscious State vs Persistent Vegetative State: The Case of Terry (Wallis) vs the Case of Terri (Schiavo). *Mayo Clinic Proceedings* (2006).

66. Owen, A. M. Detecting Awareness in the Vegetative State. *Science* **313**, 1402–1402 (2006).

67. Plourde, G., Belin, P., Chartrand, D., Fiset, P., Backman, S. B., Xie, G. & Zatorre, R. J. Cortical processing of complex auditory stimuli during alterations of consciousness with the general anesthetic propofol. *Anesthesiology* **104**, 448–457 (2006).

68. Giacino, J. T., Kalmar, K. & Whyte, J. The JFK Coma Recovery Scale-Revised: Measurement characteristics and diagnostic utility. *Arch Phys Med Rehabil* **85**, 2020–2029 (2004).

69. Monti, M. M., Vanhaudenhuyse, A., Coleman, M. R., Boly, M., Pickard, J. D., Tshibanda, L., Owen, A. M. & Laureys, S. Willful Modulation of Brain Activity in Disorders of Consciousness. *The New England Journal of Medicine* **362**, 579–589 (2010).

70. Meyer, H. *Meyer: Zur theorie der alkolnarkose - Google Scholar.* (Naunyn Schmied Arch Exp Path Pharmakol: 1901).

71. Overton, E. *Studien uber die Narkose.* (Fischer: 1901).

72. Trudell, J. R., Hubbell, W. L., Cohen, E. N. & Kendig, J. J. Pressure reversal of anesthesia: the extent of small-molecule exclusion from spin-labeled phospholipid model membranes. *Anesthesiology* **38**, 207–211 (1973).

73. Ueda, I. & Kamaya, H. Kinetic and thermodynamic aspects of the mechanism of general anesthesia in a model system of firefly luminescence in vitro. *Anesthesiology* **38**, 425–436 (1973).

74. Franks, N. P. & Lieb, W. R. Do general anaesthetics act by competitive binding to specific receptors? *Nature* **310**, 599–601 (1984).

75. Franks, N. P. & Lieb, W. R. Seeing the light: protein theories of general anesthesia. 1984. *Anesthesiology* **101**, 235–237 (2004).

76. Gruner, S. M. & Shyamsunder, E. Is the mechanism of general anesthesia related to lipid membrane spontaneous curvature? *Ann N Y Acad Sci* **625**, 685–697 (1991).

77. Franks, N. P., Jenkins, A., Conti, E., Lieb, W. R. & Brick, P. Structural basis for the inhibition of firefly luciferase by a general anesthetic. *Biophys. J.* **75**, 2205–2211 (1998).

78. Patel, A. J., Honoré, E., Lesage, F., Fink, M., Romey, G. & Lazdunski, M. Inhalational anesthetics activate two-pore-domain background K+ channels. *Nat Neurosci* **2**, 422–426 (1999).

79. Franks, N. P. General anaesthesia: from molecular targets to neuronal pathways of sleep and arousal. *Nat. Rev. Neurosci.* **9**, 370–386 (2008).

80. Yeh, J. Z., Quandt, F. N., Tanguy, J., Nakahiro, M., Narahashi, T. & Brunner, E. A. General anesthetic action on gamma-aminobutyric acid-activated channels. *Ann N Y Acad Sci* **625**, 155–173 (1991).

81. MacDonald, R. L., Rogers, C. J. & Twyman, R. E. Barbiturate regulation of kinetic properties of the GABAA receptor channel of mouse spinal neurones in culture. *J Physiol (Lond)* **417**, 483–500 (1989).

82. Hales, T. G. & Lambert, J. J. The actions of propofol on inhibitory amino acid receptors of bovine adrenomedullary chromaffin cells and rodent central neurones. *Br. J. Pharmacol.* **104**, 619–628 (1991).

83. Krasowski, M. D., Jenkins, A., Flood, P., Kung, A. Y., Hopfinger, A. J. & Harrison, N. L. General anesthetic potencies of a series of propofol analogs correlate with potency for potentiation of gamma-aminobutyric acid (GABA) current at the GABA(A) receptor but not with lipid solubility. *J. Pharmacol. Exp. Ther.* **297**, 338–351 (2001).

84. Devor, M. & Zalkind, V. Reversible analgesia, atonia, and loss of consciousness on bilateral intracerebral microinjection of pentobarbital. *Pain* **94**, 101–112 (2001).

85. Sukhotinsky, I., Hopkins, D. A., Lu, J., Saper, C. B. & Devor, M. Movement suppression during anesthesia: neural projections from the mesopontine tegmentum to areas involved in motor control. *J. Comp. Neurol.* **489**, 425–448 (2005).

86. Antognini, J. F. & Schwartz, K. Exaggerated anesthetic requirements in the preferentially anesthetized brain. *Anesthesiology* **79**, 1244–1249 (1993).

87. Antognini, J. F., Carstens, E. & Atherley, R. Does the immobilizing effect of thiopental in brain exceed that of halothane? *Anesthesiology* **96**, 980–986 (2002).

88. Sukhotinsky, I., Zalkind, V., Lu, J., Hopkins, D. A., Saper, C. B. & Devor, M. Neural pathways associated with loss of consciousness caused by intracerebral microinjection of GABA A-active anesthetics. *Eur J Neurosci* **25**, 1417–1436 (2007).

89. Vanini, G., Watson, C. J., Lydic, R. & Baghdoyan, H. A. Gamma-aminobutyric acid-mediated neurotransmission in the pontine reticular formation modulates hypnosis, immobility, and breathing during isoflurane anesthesia. *Anesthesiology* **109**, 978–988 (2008).

90. Alkire, M. T., Haier, R. J. & Fallon, J. H. Toward a unified theory of narcosis: brain imaging evidence for a thalamocortical switch as the neurophysiologic basis of anesthetic-induced unconsciousness. *Consciousness and cognition* **9**, 370–386 (2000).

91. Alkire, M. T., Pomfrett, C. J., Haier, R. J., Gianzero, M. V., Chan, C. M., Jacobsen, B. P. & Fallon, J. H. Functional brain imaging during anesthesia in humans: effects of halothane on global and regional cerebral glucose metabolism. *Anesthesiology* **90**, 701–709 (1999).

92. Kaisti, K. K., Metsähonkala, L., Teräs, M., Oikonen, V., Aalto, S., Jääskeläinen, S., Hinkka, S. & Scheinin, H. Effects of surgical levels of propofol and sevoflurane anesthesia on cerebral blood flow in healthy subjects studied with positron emission tomography. *Anesthesiology* **96**, 1358–1370 (2002).

93. White, N. S. & Alkire, M. T. Impaired thalamocortical connectivity in humans during general-anesthetic-induced unconsciousness. *Neuroimage* **19**, 402–411 (2003).

94. Zhou, J., Liu, X., Song, W., Yang, Y., Zhao, Z., Ling, F., Hudetz, A. G. & Li, S.-J. Specific and nonspecific thalamocortical functional connectivity in normal and vegetative states. *Consciousness and cognition* **20**, 257–268 (2011).

95. Imas, O. A., Ropella, K. M., Ward, B. D., Wood, J. D. & Hudetz, A. G. Volatile anesthetics disrupt frontal-posterior recurrent information transfer at gamma frequencies in rat. *Neurosci Lett* **387**, 145–150 (2005).

96. Massimini, M. Breakdown of Cortical Effective Connectivity During Sleep. *Science* **309**, 2228–2232 (2005).

97. Ferrarelli, F., Massimini, M., Sarasso, S., Casali, A., Riedner, B. A., Angelini, G., Tononi, G. & Pearce, R. A. *Breakdown in cortical effective connectivity during midazolam-induced loss of consciousness. Proc Natl Acad Sci USA* **107**, 2681–2686 (2010).

98. Massimini, M., Ferrarelli, F., Murphy, M. J., Huber, R., Riedner, B. A., Casarotto, S. & Tononi, G. Cortical reactivity and effective connectivity during REM sleep in humans. *Cogn Neurosci* **1**, 176–183 (2010).

99. Boveroux, P., Vanhaudenhuyse, A., Bruno, M.-A., Noirhomme, Q., Lauwick, S., Luxen, A., Degueldre, C., Plenevaux, A., Schnakers, C., Phillips, C., Brichant, J.-F., Bonhomme, V., Maquet, P., Greicius, M. D., Laureys, S. & Boly, M. Breakdown of within- and between-network resting state functional magnetic resonance imaging connectivity during propofol-induced loss of consciousness. *Anesthesiology* **113**, 1038–1053 (2010).

100. Lyamin, O. I., Manger, P. R., Ridgway, S. H., Mukhametov, L. M. & Siegel, J. M. Cetacean sleep: an unusual form of mammalian sleep. *Neurosci Biobehav Rev* **32**, 1451–1484 (2008).

101. Zimmerman, J. E., Naidoo, N., Raizen, D. M. & Pack, A. I. Conservation of sleep: insights from non-mammalian model systems. *Trends Neurosci.* **31**, 371–376 (2008).

102. Humphrey, J. A., Sedensky, M. M. & Morgan, P. G. Understanding anesthesia: making genetic sense of the absence of senses. *Hum. Mol. Genet.* **11**, 1241–1249 (2002).

103. Franks, N. P. Molecular targets underlying general anaesthesia. *Br. J. Pharmacol.* **147 Suppl 1**, S72–81 (2006).

104. Simons, P. J., Cockshott, I. D., Douglas, E. J., Gordon, E. A., Hopkins, K. & Rowland, M. Disposition in male volunteers of a subanaesthetic intravenous dose of an oil in water emulsion of 14C-propofol. *Xenobiotica* **18**, 429–440 (1988).

105. Gepts, E., Camu, F., Cockshott, I. D. & Douglas, E. J. Disposition of propofol administered as constant rate intravenous infusions in humans. *Anesth. Analg.* **66**, 1256–1263 (1987).

106. Struys, M. M., De Smet, T., Depoorter, B., Versichelen, L. F., Mortier, E. P., Dumortier, F. J., Shafer, S. L. & Rolly, G. Comparison of plasma compartment versus two methods for effect compartment--controlled target-controlled infusion for propofol. *Anesthesiology* **92**, 399–406 (2000).

107. White, M., Schenkels, M. J., Engbers, F. H., Vletter, A., Burm, A. G., Bovill, J. G. & Kenny, G. N. Effect-site modelling of propofol using auditory evoked potentials. *Br J Anaesth* **82**, 333–339 (1999).

108. Sundman, E., Witt, H., Sandin, R., Kuylenstierna, R., Bodén, K., Ekberg, O. & Eriksson, L. I. Pharyngeal function and airway protection during subhypnotic concentrations of propofol, isoflurane, and sevoflurane: volunteers examined by pharyngeal videoradiography and simultaneous manometry. *Anesthesiology* **95**, 1125–1132 (2001).

109. Kodaka, M., Okamoto, Y., Handa, F., Kawasaki, J. & Miyao, H. Relation between fentanyl dose and predicted EC50 of propofol for laryngeal mask insertion. *Br J Anaesth* **92**, 238–241 (2004).

110. Davidson, J. A., Macleod, A. D., Howie, J. C., White, M. & Kenny, G. N. Effective concentration 50 for propofol with and without 67% nitrous oxide. *Acta Anaesthesiol Scand* **37**, 458–464 (1993).

111. Milne, S. E., Troy, A., Irwin, M. G. & Kenny, G. N. C. Relationship between bispectral index, auditory evoked potential index and effect-site EC50 for propofol at two clinical end-points. *Br J Anaesth* **90**, 127–131 (2003).

112. Kheterpal, S., Martin, L., Shanks, A. M. & Tremper, K. K. Prediction and outcomes of impossible mask ventilation: a review of 50,000 anesthetics. *Anesthesiology* **110**, 891–897 (2009).

113. Westbrook, C., Roth, C. K. & Talbot, J. *MRI in Practice*. 456 (Wiley-Blackwell: 2011).

114. Jezzard, P., Matthews, P. M. & Smith, S. M. *Functional MRI*. 390 (Oxford University Press, USA: 2001).

115. Logothetis, N. K. The underpinnings of the BOLD functional magnetic resonance imaging signal. *J Neurosci* **23**, 3963–3971 (2003).

116. Heeger, D. J. & Ress, D. What does fMRI tell us about neuronal activity? *Nat. Rev. Neurosci.* **3**, 142–151 (2002).

117. Ogawa, S., Lee, T. M., Kay, A. R. & Tank, D. W. Brain magnetic resonance imaging with contrast dependent on blood oxygenation. *Proc Natl Acad Sci USA* **87**, 9868–9872 (1990).

118. Kwong, K. K., Belliveau, J. W., Chesler, D. A., Goldberg, I. E., Weisskoff, R. M., Poncelet, B. P., Kennedy, D. N., Hoppel, B. E., Cohen, M. S. & Turner, R. Dynamic magnetic resonance imaging of human brain activity during primary sensory stimulation. *Proc Natl Acad Sci USA* **89**, 5675–5679 (1992).

119. Logothetis, N. K., Guggenberger, H., Peled, S. & Pauls, J. Functional imaging of the monkey brain. *Nat Neurosci* **2**, 555–562 (1999).

120. Buxton, R. B., Wong, E. C. & Frank, L. R. Dynamics of blood flow and oxygenation changes during brain activation: the balloon model. *Magn Reson Med* **39**, 855–864 (1998).

121. Dagal, A. & Lam, A. M. Cerebral autoregulation and anesthesia. *Curr Opin Anaesthesiol* **22**, 547–552 (2009).

122. MacIntosh, B. J., Pattinson, K. T. S., Gallichan, D., Ahmad, I., Miller, K. L., Feinberg, D. A., Wise, R. G. & Jezzard, P. Measuring the effects of remifentanil on cerebral blood flow and arterial arrival time using 3D GRASE MRI with pulsed arterial spin labelling. *J Cereb Blood Flow Metab* **28**, 1514–1522 (2008).

123. LASSEN, N. A. Cerebral blood flow and oxygen consumption in man. *Physiol Rev* **39**, 183–238 (1959).

124. Strebel, S., Lam, A. M., Matta, B., Mayberg, T. S., Aaslid, R. & Newell, D. W. Dynamic and static cerebral autoregulation during isoflurane, desflurane, and propofol anesthesia. *Anesthesiology* **83**, 66–76 (1995).

125. Aaslid, R., Lindegaard, K. F., Sorteberg, W. & Nornes, H. Cerebral autoregulation dynamics in humans. *Stroke* **20**, 45–52 (1989).

126. McCulloch, T. J., Thompson, C. L. & Turner, M. J. A randomized crossover comparison of the effects of propofol and sevoflurane on cerebral hemodynamics during carotid endarterectomy. *Anesthesiology* **106**, 56–64 (2007).

127. Enlund, M., Andersson, J., Hartvig, P., Valtysson, J. & Wiklund, L. Cerebral normoxia in the rhesus monkey during isoflurane- or propofol-induced hypotension and hypocapnia, despite disparate blood-flow patterns. A positron emission tomography study. *Acta Anaesthesiol Scand* **41**, 1002–1010 (1997).

128. Eng, C., Lam, A. M., Mayberg, T. S., Lee, C. & Mathisen, T. The influence of propofol with and without nitrous oxide on cerebral blood flow velocity and CO2 reactivity in humans. *Anesthesiology* **77**, 872–879 (1992).

129. Strebel, S., Kaufmann, M., Guardiola, P. M. & Schaefer, H. G. Cerebral vasomotor responsiveness to carbon dioxide is preserved during propofol and midazolam anesthesia in humans. *Anesth. Analg.* **78**, 884–888 (1994).

130. Alkire, M. T., Haier, R. J., Barker, S. J., Shah, N. K., Wu, J. C. & Kao, Y. J. Cerebral metabolism during propofol anesthesia in humans studied with positron emission tomography. *Anesthesiology* **82**, 393–403; discussion 27A (1995).

131. Fiset, P., Paus, T., Daloze, T., Plourde, G., Meuret, P., Bonhomme, V., Hajj-Ali, N., Backman, S. B. & Evans, A. C. Brain mechanisms of propofol-induced loss of consciousness in humans: a positron emission tomographic study. *J Neurosci* **19**, 5506–5513 (1999).

132. Kaisti, K. K., Långsjö, J. W., Aalto, S., Oikonen, V., Sipilä, H., Teräs, M., Hinkka, S., Metsähonkala, L. & Scheinin, H. Effects of sevoflurane, propofol, and adjunct nitrous oxide on regional cerebral blood flow, oxygen consumption, and blood volume in humans. *Anesthesiology* **99**, 603–613 (2003).

133. Mintun, M. A., Lundstrom, B. N., Snyder, A. Z., Vlassenko, A. G., Shulman, G. L. & Raichle, M. E. Blood flow and oxygen delivery to human brain during functional activity: theoretical modeling and experimental data. *Proc Natl Acad Sci USA* **98**, 6859–6864 (2001).

134. Lindauer, U., Leithner, C., Kaasch, H., Rohrer, B., Foddis, M., Füchtemeier, M., Offenhauser, N., Steinbrink, J., Royl, G., Kohl-Bareis, M. & Dirnagl, U. Neurovascular coupling in rat brain operates independent of hemoglobin deoxygenation. *J Cereb Blood Flow Metab* **30**, 757–768 (2010).

135. Powers, W. J., Hirsch, I. B. & Cryer, P. E. Effect of stepped hypoglycemia on regional cerebral blood flow response to physiological brain activation. *Am. J. Physiol.* **270**, H554–9 (1996).

136. Piknova, B., Kocharyan, A., Schechter, A. N. & Silva, A. C. The role of nitrite in neurovascular coupling. *Brain Research* **1407**, 62–68 (2011).

137. Busija, D. W., Bari, F., Domoki, F. & Louis, T. Mechanisms involved in the cerebrovascular dilator effects of N-methyl-d-aspartate in cerebral cortex. *Brain Research Reviews* **56**, 89–100 (2007).

138. Attwell, D. & Iadecola, C. The neural basis of functional brain imaging signals. *Trends Neurosci.* **25**, 621–625 (2002).

139. Franceschini, M. A., Radhakrishnan, H., Thakur, K., Wu, W., Ruvinskaya, S., Carp, S. & Boas, D. A. The effect of different anesthetics on neurovascular coupling. *Neuroimage* 1–42 (2010).doi:10.1016/j.neuroimage.2010.03.060

140. Chen, J. J. & Pike, G. B. MRI measurement of the BOLD-specific flow-volume relationship during hypercapnia and hypocapnia in humans. *Neuroimage* **53**, 383–391 (2010).

141. Jenkinson, M., Bannister, P., Brady, M. & Smith, S. Improved optimization for the robust and accurate linear registration and motion correction of brain images. *Neuroimage* **17**, 825–841 (2002).

142. Jenkinson, M. Fast, automated, N-dimensional phase-unwrapping algorithm. *Magn Reson Med* **49**, 193–197 (2003).

143. Smith, S. M. Fast robust automated brain extraction. *Hum Brain Mapp* **17**, 143–155 (2002).

144. Beckmann, C. F. & Smith, S. M. Probabilistic independent component analysis for functional magnetic resonance imaging. *IEEE Trans Med Imaging* **23**, 137–152 (2004).

145. Smith, S. M., Jenkinson, M., Woolrich, M. W., Beckmann, C. F., Behrens, T. E. J., Johansen-Berg, H., Bannister, P. R., De Luca, M., Drobnjak, I., Flitney, D. E., Niazy, R. K., Saunders, J., Vickers, J., Zhang, Y., De Stefano, N., Brady, J. M. & Matthews, P. M. Advances in functional and structural MR image analysis and implementation as FSL. *Neuroimage* **23 Suppl 1**, S208–19 (2004).

146. Woolrich, M. W., Ripley, B. D., Brady, M. & Smith, S. M. Temporal autocorrelation in univariate linear modeling of FMRI data. *Neuroimage* **14**, 1370–1386 (2001).

147. Krakow, K., Allen, P. J., Symms, M. R., Lemieux, L., Josephs, O. & Fish, D. R. EEG recording during fMRI experiments: image quality. *Hum Brain Mapp* **10**, 10–15 (2000).

148. Mullinger, K., Debener, S., Coxon, R. & Bowtell, R. Effects of simultaneous EEG recording on MRI data quality at 1.5, 3 and 7 tesla. *Int J Psychophysiol* **67**, 178–188 (2008).

149. Dueck, M. H., Petzke, F., Gerbershagen, H. J., Paul, M., Hesselmann, V., Girnus, R., Krug, B., Sorger, B., Goebel, R., Lehrke, R., Sturm, V. & Boerner, U. Propofol attenuates responses of the auditory cortex to acoustic stimulation in a dose-dependent manner: a FMRI study. *Acta Anaesthesiol Scand* **49**, 784–791 (2005).

150. Kerssens, C., Hamann, S., Peltier, S., Hu, X. P., Byas-Smith, M. G. & Sebel, P. S. Attenuated brain response to auditory word stimulation with sevoflurane: a functional magnetic resonance imaging study in humans. *Anesthesiology* **103**, 11–19 (2005).

151. Heinke, W., Fiebach, C. J., Schwarzbauer, C., Meyer, M., Olthoff, D. & Alter, K. Sequential effects of propofol on functional brain activation induced by auditory language processing: an event-related functional magnetic resonance imaging study. *Br J Anaesth* **92**, 641–650 (2004).

152. Rasmusson, D. X., Bylsma, F. W. & Brandt, J. Stability of performance on the Hopkins Verbal Learning Test. *Arch Clin Neuropsychol* **10**, 21–26 (1995).

153. Gaab, N., Gabrieli, J. D. E. & Glover, G. H. Assessing the influence of scanner background noise on auditory processing. I. An fMRI study comparing three experimental designs with varying degrees of scanner noise. *Hum Brain Mapp* **28**, 703–720 (2007).

154. Bromm, B. & Treede, R. D. Nerve fibre discharges, cerebral potentials and sensations induced by CO2 laser stimulation. *Hum Neurobiol* **3**, 33–40 (1984).

155. Torebjörk, H. E. & Ochoa, J. L. Specific sensations evoked by activity in single identified sensory units in man. *Acta Physiol. Scand.* **110**, 445–447 (1980).

156. Perchet, C., Godinho, F., Mazza, S., Frot, M., Legrain, V., Magnin, M. & Garcia-Larrea, L. Evoked potentials to nociceptive stimuli delivered by CO2 or Nd:YAP lasers. *Clin Neurophysiol* **119**, 2615–2622 (2008).

157. Hepner, D. Anaphylaxis during the perioperative period. *Anesth. Analg.* (2003).

158. AAGBI Provision of Anaesthetic Services in Magnetic Resonance Units.

159. Deeprose, C., Andrade, J., Varma, S. & Edwards, N. Unconscious learning during surgery with propofol anaesthesia. *Br J Anaesth* **92**, 171–177 (2004).

160. Deeprose, C., Andrade, J., Harrison, D. & Edwards, N. Unconscious auditory priming during surgery with propofol and nitrous oxide anaesthesia: a replication. *Br J Anaesth* **94**, 57–62 (2005).

161. Münte, S., Schmidt, M., Meyer, M., Nager, W., Lüllwitz, E., Münte, T. F. & Piepenbrock, S. Implicit memory for words played during isoflurane- or propofol-based anesthesia: the lexical decision task. *Anesthesiology* **96**, 588–594 (2002).

162. Kerssens, C., Lubke, G. H., Klein, J., van der Woerd, A. & Bonke, B. Memory function during propofol and alfentanil anesthesia: predictive value of individual differences. *Anesthesiology* **97**, 382–389 (2002).

163. Bejjani, G., Lequeux, P.-Y., Schmartz, D., Engelman, E. & Barvais, L. No evidence of memory processing during propofol-remifentanil target-controlled infusion anesthesia with bispectral index monitoring in cardiac surgery. *J. Cardiothorac. Vasc. Anesth.* **23**, 175–181 (2009).

164. Hadzidiakos, D., Horn, N., Degener, R., Buchner, A. & Rehberg, B. Analysis of Memory Formation during General Anesthesia (Propofol/Remifentanil) for Elective Surgery Using the Process-dissociation Procedure. *Anesthesiology* **111**, 293–301 (2009).

165. Yppärilä, H., Karhu, J., Westerén-Punnonen, S., Musialowicz, T. & Partanen, J. Evidence of auditory processing during postoperative propofol sedation. *Clin Neurophysiol* **113**, 1357–1364 (2002).

166. Anker-Møller, E., Spangsberg, N., Arendt-Nielsen, L., Schultz, P., Kristensen, M. S. & Bjerring, P. Subhypnotic doses of thiopentone and propofol cause analgesia to experimentally induced acute pain. *Br J Anaesth* **66**, 185–188 (1991).

167. Frölich, M., Price, D., Robinson, M. & Shuster, J. The effect of propofol on thermal pain perception. … *& Analgesia* (2005).

168. Yanagidani, T., Ota, K. & Collins, J. G. Complex effects of general anesthesia on sensory processing in the spinal dorsal horn. *Brain Research* **812**, 301–304 (1998).

169. Barter, L. S., Mark, L. O., Jinks, S. L., Carstens, E. E. & Antognini, J. F. Immobilizing doses of halothane, isoflurane or propofol, do not preferentially depress noxious heat-evoked responses of rat lumbar dorsal horn neurons with ascending projections. *Anesth. Analg.* **106**, 985–90, table of contents (2008).

170. The Wylie Report. Report of the Working Party on Training in Dental Anaesthesia. *Br Dent J* **151**, 385–388 (1981).

171. Friston, K. J. Functional and effective connectivity in neuroimaging: A synthesis. *Hum Brain Mapp* **2**, 56–78 (2004).

172. Tracey, I. & Mantyh, P. W. The cerebral signature for pain perception and its modulation. *Neuron* **55**, 377–391 (2007).

173. Wiech, K., Lin, C.-S., Brodersen, K. H., Bingel, U., Ploner, M. & Tracey, I. Anterior insula integrates information about salience into perceptual decisions about pain. *J Neurosci* **30**, 16324–16331 (2010).

174. Alkire, M. T., McReynolds, J. R., Hahn, E. L. & Trivedi, A. N. Thalamic microinjection of nicotine reverses sevoflurane-induced loss of righting reflex in the rat. *Anesthesiology* **107**, 264–272 (2007).

175. Tracey, I. & Johns, E. The pain matrix: Reloaded or reborn as we image tonic pain using arterial spin labelling. *Pain* **148**, 359–360 (2010).

176. TerRiet, M. F., Jacobs, J. S., Lewis, M. C. & DeSouza, G. J. Propofol and analgesia. *Anesth. Analg.* **90**, 1455 (2000).

177. Ploghaus, A., Becerra, L., Borras, C. & Borsook, D. Neural circuitry underlying pain modulation: expectation, hypnosis, placebo. *Trends Cogn. Sci. (Regul. Ed.)* **7**, 197–200 (2003).

178. Sonner, J. M., Antognini, J. F., Dutton, R. C., Flood, P., Gray, A. T., Harris, R. A., Homanics, G. E., Kendig, J., Orser, B., Raines, D. E., Rampil, I. J., Trudell, J., Vissel, B. & Eger, E. I. Inhaled anesthetics and immobility: mechanisms, mysteries, and minimum alveolar anesthetic concentration. *Anesth. Analg.* **97**, 718–740 (2003).

179. Antognini, J. F., Barter, L. & Carstens, E. Overview movement as an index of anesthetic depth in humans and experimental animals. *Comp. Med.* **55**, 413–418 (2005).

180. Kungys, G., Kim, J., Jinks, S. L., Atherley, R. J. & Antognini, J. F. Propofol produces immobility via action in the ventral horn of the spinal cord by a GABAergic mechanism. *Anesth. Analg.* **108**, 1531–1537 (2009).

181. Wood, A., Campagna, J. & Miller, K. Mechanisms of Actions of Inhaled Anesthetics — NEJM. *New England Journal …* (2003).

182. Maquet, P., Degueldre, C., Delfiore, G., Aerts, J., Péters, J. M., Luxen, A. & Franck, G. Functional neuroanatomy of human slow wave sleep. *J Neurosci* **17**, 2807–2812 (1997).

183. Volkow, N. D., Wang, G. J., Hitzemann, R., Fowler, J. S., Pappas, N., Lowrimore, P., Burr, G., Pascani, K., Overall, J. & Wolf, A. P. Depression of thalamic metabolism by lorazepam is associated with sleepiness. *Neuropsychopharmacology* **12**, 123–132 (1995).

184. Alkire, M. T., Haier, R. J., Shah, N. K. & Anderson, C. T. Positron emission tomography study of regional cerebral metabolism in humans during isoflurane anesthesia. *Anesthesiology* **86**, 549–557 (1997).

185. Laitio, R. M., Kaisti, K. K., Låangsjö, J. W., Aalto, S., Salmi, E., Maksimow, A., Aantaa, R., Oikonen, V., Sipilä, H., Parkkola, R. & Scheinin, H. Effects of xenon anesthesia on cerebral blood flow in humans: a positron emission tomography study. *Anesthesiology* **106**, 1128–1133 (2007).

186. Tononi, G. & Edelman, G. M. Consciousness and complexity. *Science* **282**, 1846–1851 (1998).

187. Lull, N., Noé, E., Lull, J. J., García-Panach, J., García-Martí, G., Chirivella, J., Ferri, J., Sopena, R., La Cueva, de, L. & Robles, M. [Thalamic metabolism and neurological outcome after traumatic brain injury. A voxel-based morphometric FDG-PET study]. *Neurologia* **25**, 174–180 (2010).

188. Lull, N., Noé, E., Lull, J. J., García-Panach, J., Chirivella, J., Ferri, J., López-Aznar, D., Sopena, P. & Robles, M. Voxel-based statistical analysis of thalamic glucose metabolism in traumatic brain injury: relationship with consciousness and cognition. *Brain Inj* **24**, 1098–1107 (2010).

189. Bonhomme, V., Fiset, P., Meuret, P., Backman, S., Plourde, G., Paus, T., Bushnell, M. C. & Evans, A. C. Propofol anesthesia and cerebral blood flow changes elicited by vibrotactile stimulation: a positron emission tomography study. *J Neurophysiol* **85**, 1299–1308 (2001).

190. Veselis, R. A., Reinsel, R. A., Beattie, B. J., Mawlawi, O. R., Feshchenko, V. A., DiResta, G. R., Larson, S. M. & Blasberg, R. G. Midazolam changes cerebral blood flow in discrete brain regions: an H2(15)O positron emission tomography study. *Anesthesiology* **87**, 1106–1117 (1997).

191. Silva, A., Cardoso-Cruz, H., Silva, F., Galhardo, V. & Antunes, L. Comparison of anesthetic depth indexes based on thalamocortical local field potentials in rats. *Anesthesiology* **112**, 355–363 (2010).

192. Weiskrantz, L., Warrington, E. K., Sanders, M. D. & Marshall, J. Visual capacity in the hemianopic field following a restricted occipital ablation. *Brain* **97**, 709–728 (1974).

193. Bridge, H., Thomas, O., Jbabdi, S. & Cowey, A. Changes in connectivity after visual cortical brain damage underlie altered visual function. *Brain* **131**, 1433–1444 (2008).

194. Herrero, M.-T., Barcia, C. & Navarro, J. M. Functional anatomy of thalamus and basal ganglia. *Childs Nerv Syst* **18**, 386–404 (2002).

195. Alexander, G. E., DeLong, M. R. & Strick, P. L. Parallel organization of functionally segregated circuits linking basal ganglia and cortex. *Annu. Rev. Neurosci.* **9**, 357–381 (1986).

196. Di Martino, A., Scheres, A., Margulies, D. S., Kelly, A. M. C., Uddin, L. Q., Shehzad, Z., Biswal, B., Walters, J. R., Castellanos, F. X. & Milham, M. P. Functional connectivity of human striatum: a resting state FMRI study. *Cereb Cortex* **18**, 2735–2747 (2008).

197. McHaffie, J. G., Stanford, T. R., Stein, B. E., Coizet, V. & Redgrave, P. Subcortical loops through the basal ganglia. *Trends Neurosci.* **28**, 401–407 (2005).

198. Mena-Segovia, J., Bolam, J. P. & Magill, P. J. Pedunculopontine nucleus and basal ganglia: distant relatives or part of the same family? *Trends Neurosci.* **27**, 585–588 (2004).

199. Mena-Segovia, J., Cintra, L., Prospéro-García, O. & Giordano, M. Changes in sleep-waking cycle after striatal excitotoxic lesions. *Behav Brain Res* **136**, 475–481 (2002).

200. Mahon, S., Deniau, J. M. & Charpier, S. Relationship between EEG potentials and intracellular activity of striatal and cortico-striatal neurons: an in vivo study under different anesthetics. *Cereb Cortex* **11**, 360–373 (2001).

201. Walder, B., Tramèr, M. R. & Seeck, M. Seizure-like phenomena and propofol: a systematic review. *Neurology* **58**, 1327–1332 (2002).

202. West, M. O. Anesthetics eliminate somatosensory-evoked discharges of neurons in the somatotopically organized sensorimotor striatum of the rat. *J Neurosci* **18**, 9055–9068 (1998).

203. Abulafia, R., Zalkind, V. & Devor, M. Cerebral Activity during the Anesthesia-Like State Induced by Mesopontine Microinjection of Pentobarbital. *J Neurosci* **29**, 7053–7064 (2009).

204. Jones, A. K., Brown, W. D., Friston, K. J., Qi, L. Y. & Frackowiak, R. S. Cortical and subcortical localization of response to pain in man using positron emission tomography. *Proc. Biol. Sci.* **244**, 39–44 (1991).

205. Casey, K. L., Minoshima, S., Berger, K. L., Koeppe, R. A., Morrow, T. J. & Frey, K. A. Positron emission tomographic analysis of cerebral structures activated specifically by repetitive noxious heat stimuli. *J Neurophysiol* **71**, 802–807 (1994).

206. Tracey, I., Becerra, L., Chang, I., Breiter, H., Jenkins, L., Borsook, D. & González, R. G. Noxious hot and cold stimulation produce common patterns of brain activation in humans: a functional magnetic resonance imaging study. *Neurosci Lett* **288**, 159–162 (2000).

207. Chudler, E. H. & Dong, W. K. The role of the basal ganglia in nociception and pain. *Pain* **60**, 3–38 (1995).

208. Upadhyay, J., Chudler, E. & Becerra, L. A key role of the basal ganglia in pain and analgesia-insights gained through human functional imaging. *Molecular pain* (2010).

209. Braz, J. M., Nassar, M. A., Wood, J. N. & Basbaum, A. I. Parallel "pain" pathways arise from subpopulations of primary afferent nociceptor. *Neuron* **47**, 787–793 (2005).

210. Hagelberg, N., Forssell, H., Aalto, S., Rinne, J. O., Scheinin, H., Taiminen, T., Någren, K., Eskola, O. & Jääskeläinen, S. K. Altered dopamine D2 receptor binding in atypical facial pain. *Pain* **106**, 43–48 (2003).

211. Hagelberg, N., Forssell, H., Rinne, J. O., Scheinin, H., Taiminen, T., Aalto, S., Luutonen, S., Någren, K. & Jääskeläinen, S. Striatal dopamine D1 and D2 receptors in burning mouth syndrome. *Pain* **101**, 149–154 (2003).

212. Schiff, N. D. & Plum, F. The role of arousal and "gating" systems in the neurology of impaired consciousness. *J Clin Neurophysiol* **17**, 438–452 (2000).

213. Castle, M., Aymerich, M. S., Sanchez-Escobar, C., Gonzalo, N., Obeso, J. A. & Lanciego, J. L. Thalamic innervation of the direct and indirect basal ganglia pathways in the rat: Ipsi- and contralateral projections. *J. Comp. Neurol.* **483**, 143–153 (2005).

214. Schiff, N. Central Thalamic Contributions to Arousal Regulation and Neurological Disorders of Consciousness - Schiff - 2008 - Annals of the New York Academy of Sciences - Wiley Online Library. *Ann N Y Acad Sci* (2008).

215. Behrens, T. E. J., Johansen-Berg, H., Woolrich, M. W., Smith, S. M., Wheeler-Kingshott, C. A. M., Boulby, P. A., Barker, G. J., Sillery, E. L., Sheehan, K., Ciccarelli, O., Thompson, A. J., Brady, J. M. & Matthews, P. M. Non-invasive mapping of connections between human thalamus and cortex using diffusion imaging. *Nat Neurosci* **6**, 750–757 (2003).

216. Fountas, K. N., Smith, J. R., Robinson, J. S., Tamburrini, G., Pietrini, D. & Di Rocco, C. Anatomical hemispherectomy. *Childs Nerv Syst* **22**, 982–991 (2006).

217. Baars, B. J. Tutorial commentary: surprisingly small subcortical structures are needed for the state of waking consciousness, while cortical projection areas seem to provide perceptual contents of consciousness. *Consciousness and cognition* **4**, 159–162 (1995).

218. Steyn-Ross, M. L., Steyn-Ross, D. A. & Sleigh, J. W. Modelling general anaesthesia as a first-order phase transition in the cortex. *Prog. Biophys. Mol. Biol.* **85**, 369–385 (2004).

219. McKay, I. D. H., Voss, L. J., Sleigh, J. W., Barnard, J. P. & Johannsen, E. K. Pharmacokinetic-pharmacodynamic modeling the hypnotic effect of sevoflurane using the spectral entropy of the electroencephalogram. *Anesth. Analg.* **102**, 91–97 (2006).

220. Friedman, E. B., Sun, Y., Moore, J. T., Hung, H.-T., Meng, Q. C., Perera, P., Joiner, W. J., Thomas, S. A., Eckenhoff, R. G., Sehgal, A. & Kelz, M. B. A conserved behavioral state barrier impedes transitions between anesthetic-induced unconsciousness and wakefulness: evidence for neural inertia. *PLoS ONE* **5**, e11903 (2010).

221. Kelz, M. B., Sun, Y., Chen, J., Cheng Meng, Q., Moore, J. T., Veasey, S. C., Dixon, S., Thornton, M., Funato, H. & Yanagisawa, M. An essential role for orexins in emergence from general anesthesia. *Proc Natl Acad Sci USA* **105**, 1309–1314 (2008).

222. Delorme, A. & Makeig, S. EEGLAB: an open source toolbox for analysis of single-trial EEG dynamics including independent component analysis. *J Neurosci Methods* **134**, 9–21 (2004).

223. Bandt, C. & Pompe, B. Permutation entropy: a natural complexity measure for time series. *Phys. Rev. Lett.* **88**, 174102 (2002).

224. Olofsen, E., Sleigh, J. W. & Dahan, A. Permutation entropy of the electroencephalogram: a measure of anaesthetic drug effect. *Br J Anaesth* **101**, 810–821 (2008).

225. Li, X., Cui, S. & Voss, L. J. Using permutation entropy to measure the electroencephalographic effects of sevoflurane. *Anesthesiology* **109**, 448–456 (2008).

226. Jordan, D., Stockmanns, G., Kochs, E. F., Pilge, S. & Schneider, G. Electroencephalographic order pattern analysis for the separation of consciousness and unconsciousness: an analysis of approximate entropy, permutation entropy, recurrence rate, and phase coupling of order recurrence plots. *Anesthesiology* **109**, 1014–1022 (2008).

227. Zeitlhofer, J., Gruber, G., Anderer, P., Asenbaum, S., Schimicek, P. & Saletu, B. *Topographic distribution of sleep spindles in young healthy subjects*. *J Sleep Res* **6**, 149–155 (1997).

228. Urakami, Y. Relationships between sleep spindles and activities of cerebral cortex as determined by simultaneous EEG and MEG recording. *J Clin Neurophysiol* **25**, 13–24 (2008).

229. Zygierewicz, J., Blinowska, K. J., Durka, P. J., Szelenberger, W., Niemcewicz, S. & Androsiuk, W. High resolution study of sleep spindles. *Clin Neurophysiol* **110**, 2136–2147 (1999).

230. MacKay, E. C., Sleigh, J. W., Voss, L. J. & Barnard, J. P. Episodic waveforms in the electroencephalogram during general anaesthesia: a study of patterns of response to noxious stimuli. *Anaesth Intensive Care* **38**, 102–112 (2010).

231. Mitra, P. & Bokil, H. *Observed brain dynamics*. 381 (Oxford University Press, USA: 2008).

232. Bokil, H., Andrews, P., Kulkarni, J. E., Mehta, S. & Mitra, P. P. Chronux: a platform for analyzing neural signals. *J Neurosci Methods* **192**, 146–151 (2010).

233. Bastuji, H., Perchet, C., Legrain, V., Montes, C. & Garcia-Larrea, L. Laser evoked responses to painful stimulation persist during sleep and predict subsequent arousals. *Pain* **137**, 589–599 (2008).

234. Mesa, A., Diaz, A. P. & Frosth, M. Narcolepsy and anesthesia. *Anesthesiology* **92**, 1194–1196 (2000).

235. Burrow, B., Burkle, C., Warner, D. O. & Chini, E. N. Postoperative outcome of patients with narcolepsy. A retrospective analysis. *J Clin Anesth* **17**, 21–25 (2005).

236. Archer, D. P., Ewen, A., Froelich, J., Roth, S. H. & Samanani, N. Thiopentone induced enhancement of somatic motor responses to noxious stimulation: influence of GABAA receptor modulation. *Can J Anaesth* **43**, 503–510 (1996).

237. Matta, J. A., Cornett, P. M., Miyares, R. L., Abe, K., Sahibzada, N. & Ahern, G. P. General anesthetics activate a nociceptive ion channel to enhance pain and inflammation. *Proc Natl Acad Sci USA* **105**, 8784–8789 (2008).

238. Bandschapp, O., Filitz, J., Ihmsen, H., Berset, A., Urwyler, A., Koppert, W. & Ruppen, W. Analgesic and antihyperalgesic properties of propofol in a human pain model. *Anesthesiology* **113**, 421–428 (2010).

239. Mobascher, A., Brinkmeyer, J., Warbrick, T., Musso, F., Schlemper, V., Wittsack, H. J., Saleh, A., Schnitzler, A. & Winterer, G. Brain activation patterns underlying fast habituation to painful laser stimuli. *Int J Psychophysiol* **75**, 16–24 (2010).

240. Flor, H., Diers, M. & Birbaumer, N. Peripheral and electrocortical responses to painful and non-painful stimulation in chronic pain patients, tension headache patients and healthy controls. *Neurosci Lett* **361**, 147–150 (2004).

241. Kortelainen, J., Koskinen, M., Mustola, S. & Seppänen, T. EEG frequency progression during induction of anesthesia: from start of infusion to onset of burst suppression pattern. *Conf Proc IEEE Eng Med Biol Soc* **2007**, 1570–1573 (2007).

242. John, E. R., Prichep, L. S., Kox, W., Valdés-Sosa, P., Bosch-Bayard, J., Aubert, E., Tom, M., di Michele, F., Gugino, L. D. & diMichele, F. Invariant reversible QEEG effects of anesthetics. *Consciousness and cognition* **10**, 165–183 (2001).

243. Kishimoto, T., Kadoya, C., Sneyd, R., Samra, S. K. & Domino, E. F. Topographic electroencephalogram of propofol-induced conscious sedation. *Clin Pharmacol Ther* **58**, 666–674 (1995).

244. Veselis, R. A., Reinsel, R., Alagesan, R., Heino, R. & Bedford, R. F. The EEG as a monitor of midazolam amnesia: changes in power and topography as a function of amnesic state. *Anesthesiology* **74**, 866–874 (1991).

245. Veselis, R. A. & Reinsel, R. A. Electroencephalographic effects of sedative hypnotics. *Anesthesiology* **77**, 837–838 (1992).

246. Roman-Liu, D. & Konarska, M. Characteristics of power spectrum density function of EMG during muscle contraction below 30%MVC. *J Electromyogr Kinesiol* **19**, 864–874 (2009).

247. De Luca, C. J., Gilmore, L. D., Kuznetsov, M. & Roy, S. H. Filtering the surface EMG signal: Movement artifact and baseline noise contamination. *J Biomech* **43**, 1573–1579 (2010).

248. Rampil, I. J. A primer for EEG signal processing in anesthesia. *Anesthesiology* **89**, 980–1002 (1998).

249. Gugino, L. D., Chabot, R. J., Prichep, L. S., John, E. R., Formanek, V. & Aglio, L. S. Quantitative EEG changes associated with loss and return of consciousness in healthy adult volunteers anaesthetized with propofol or sevoflurane. *Br J Anaesth* **87**, 421–428 (2001).

250. Fulton, S. A. & Mullen, K. D. Completion of upper endoscopic procedures despite paradoxical reaction to midazolam: a role for flumazenil? *Am. J. Gastroenterol.* **95**, 809–811 (2000).

251. Kent, E. A., Bacon, D. R., Harrison, P. & Lema, M. J. Sexual illusions and propofol sedation. *Anesthesiology* **77**, 1037–1038 (1992).

252. McCarthy, M. M., Brown, E. N. & Kopell, N. Potential network mechanisms mediating electroencephalographic beta rhythm changes during propofol-induced paradoxical excitation. *J Neurosci* **28**, 13488–13504 (2008).

253. Brown, P. Abnormal oscillatory synchronisation in the motor system leads to impaired movement. *Curr Opin Neurobiol* **17**, 656–664 (2007).

254. Gilbertson, T., Lalo, E., Doyle, L., Di Lazzaro, V., Cioni, B. & Brown, P. Existing motor state is favored at the expense of new movement during 13-35 Hz oscillatory synchrony in the human corticospinal system. *J Neurosci* **25**, 7771–7779 (2005).

255. Jenkinson, N. & Brown, P. New insights into the relationship between dopamine, beta oscillations and motor function. *Trends Neurosci.* (2011).doi:10.1016/j.tins.2011.09.003

256. Cruikshank, L. C., Singhal, A. & Caplan, J. B. Theta oscillations reflect a putative neural mechanism for human sensorimotor integration. *J Neurophysiol* (2011).doi:10.1152/jn.00893.2010

257. Cantero, J. L., Atienza, M., Stickgold, R., Kahana, M. J., Madsen, J. R. & Kocsis, B. Sleep-dependent theta oscillations in the human hippocampus and neocortex. *J Neurosci* **23**, 10897–10903 (2003).

258. Caplan, J. B., Madsen, J. R., Schulze-Bonhage, A., Aschenbrenner-Scheibe, R., Newman, E. L. & Kahana, M. J. Human theta oscillations related to sensorimotor integration and spatial learning. *J Neurosci* **23**, 4726–4736 (2003).

259. Karbowski, K. *Hans Berger (1873-1941). J. Neurol.* **249**, 1130–1131 (2002).

260. Anderer, P., Gruber, G., Parapatics, S. & Dorffner, G. Automatic sleep classification according to Rechtschaffen and Kales. *Conf Proc IEEE Eng Med Biol Soc* **2007**, 3994–3997 (2007).

261. Andersen, P., Andersson, S. A. & Lomo, T. Some factors involved in the thalamic control of spontaneous barbiturate spindles. *J Physiol (Lond)* **192**, 257–281 (1967).

262. Andersen, P., Andersson, S. A. & Lomo, T. Nature of thalamo-cortical relations during spontaneous barbiturate spindle activity. *J Physiol (Lond)* **192**, 283–307 (1967).

263. Contreras, D., Curró Dossi, R. & Steriade, M. Electrophysiological properties of cat reticular thalamic neurones in vivo. *J Physiol (Lond)* **470**, 273–294 (1993).

264. Mackenzie, L., Pope, K. J. & Willoughby, J. O. Physiological and pathological spindling phenomena have similar regional EEG power distributions. *Brain Research* **1008**, 92–106 (2004).

265. Contreras, D. & Steriade, M. Spindle oscillation in cats: the role of corticothalamic feedback in a thalamically generated rhythm. *J Physiol (Lond)* **490 (Pt 1)**, 159–179 (1996).

266. Steriade, M., Domich, L., Oakson, G. & Deschênes, M. The deafferented reticular thalamic nucleus generates spindle rhythmicity. *J Neurophysiol* **57**, 260–273 (1987).

267. Llinás, R. R. & Steriade, M. Bursting of thalamic neurons and states of vigilance. *J Neurophysiol* **95**, 3297–3308 (2006).

268. Contreras, D., Destexhe, A., Sejnowski, T. J. & Steriade, M. Spatiotemporal patterns of spindle oscillations in cortex and thalamus. *J Neurosci* **17**, 1179–1196 (1997).

269. Steriade, M. The GABAergic reticular nucleus: a preferential target of corticothalamic projections. *Proc Natl Acad Sci USA* **98**, 3625–3627 (2001).

270. Bonjean, M., Baker, T., Lemieux, M., Timofeev, I., Sejnowski, T. & Bazhenov, M. Corticothalamic feedback controls sleep spindle duration in vivo. *J Neurosci* **31**, 9124–9134 (2011).

271. Keifer, J. C., Baghdoyan, H. A., Becker, L. & Lydic, R. Halothane decreases pontine acetylcholine release and increases EEG spindles. *Neuroreport* **5**, 577–580 (1994).

272. Huotari, A.-M., Koskinen, M., Suominen, K., Alahuhta, S., Remes, R., Hartikainen, K. M. & Jäntti, V. Evoked EEG patterns during burst suppression with propofol. *Br J Anaesth* **92**, 18–24 (2004).

273. Wolter, S., Friedel, C., Böhler, K., Hartmann, U., Kox, W. J. & Hensel, M. Presence of 14Hz spindle oscillations in the human EEG during deep anesthesia. *Clin Neurophysiol* **117**, 157–168 (2006).

274. Ferenets, R., Lipping, T., Suominen, P., Turunen, J., Puumala, P., Jäntti, V., Himanen, S.-L. & Huotari, A.-M. Comparison of the properties of EEG spindles in sleep and propofol anesthesia. *Conf Proc IEEE Eng Med Biol Soc* **1**, 6356–6359 (2006).

275. Rosanova, M., Casali, A., Bellina, V., Resta, F., Mariotti, M. & Massimini, M. Natural frequencies of human corticothalamic circuits. *J Neurosci* **29**, 7679–7685 (2009).

276. Feshchenko, V. A., Veselis, R. A. & Reinsel, R. A. Propofol-induced alpha rhythm. *Neuropsychobiology* **50**, 257–266 (2004).

277. Werth, E., Achermann, P., Dijk, D. J. & Borbély, A. A. Spindle frequency activity in the sleep EEG: individual differences and topographic distribution. *Electroencephalogr Clin Neurophysiol* **103**, 535–542 (1997).

278. Steriade, M., Nuñez, A. & Amzica, F. A novel slow (. *J Neurosci* **13**, 3252–3265 (1993).

279. Steriade, M., Nuñez, A. & Amzica, F. Intracellular analysis of relations between the slow (< 1Hz) neocortical oscillation and other sleep rhythms of the electroencephalogram. *J Neurosci* **13**, 3266–3283 (1993).

280. Steriade, M., Contreras, D., Curró Dossi, R. & Nuñez, A. The slow (<1Hz) Oscillation in reticular thalamic and thalamocortical neurons: scnario of sleep generation in interacting thalamic and neocortical networks. *J Neurosci* **13**, 3284–3299 (1993).

281. Steriade, M., Amzica, F. & Nuñez, A. Cholinergic and noradrenergic modulation of the slow (approximately 0.3 Hz) oscillation in neocortical cells. *J Neurophysiol* **70**, 1385–1400 (1993).

282. Contreras, D. & Steriade, M. Cellular basis of EEG slow rhythms: a study of dynamic corticothalamic relationships. *J Neurosci* **15**, 604–622 (1995).

283. Massimini, M., Huber, R., Ferrarelli, F., Hill, S. & Tononi, G. The sleep slow oscillation as a traveling wave. *J Neurosci* **24**, 6862–6870 (2004).

284. Steriade, M., Timofeev, I. & Grenier, F. Natural waking and sleep states: a view from inside neocortical neurons. *J Neurophysiol* **85**, 1969–1985 (2001).

285. Murphy, M., Riedner, B. A., Huber, R., Massimini, M., Ferrarelli, F. & Tononi, G. Source modeling sleep slow waves. *Proc Natl Acad Sci USA* **106**, 1608–1613 (2009).

286. Picton, T. W., Hillyard, S. A., Krausz, H. I. & Galambos, R. Human auditory evoked potentials. I. Evaluation of components. *Electroencephalogr Clin Neurophysiol* **36**, 179–190 (1974).

287. Plourde, G. & Picton, T. W. Long-latency auditory evoked potentials during general anesthesia: N1 and P3 components. *Anesth. Analg.* **72**, 342–350 (1991).

288. Qiu, Y., Inui, K., Wang, X., Tran, T. D. & Kakigi, R. Effects of attention, distraction and sleep on CO(2) laser evoked potentials related to C-fibers in humans. *Clin Neurophysiol* **113**, 1579–1585 (2002).

289. Baumgärtner, U., Tiede, W., Treede, R.-D. & Craig, A. D. B. Laser-evoked potentials are graded and somatotopically organized anteroposteriorly in the operculoinsular cortex of anesthetized monkeys. *J Neurophysiol* **96**, 2802–2808 (2006).

290. Shaw, F. Z., Chen, R. F. & Yen, C. T. Dynamic changes of touch- and laser heat-evoked field potentials of primary somatosensory cortex in awake and pentobarbital-anesthetized rats. *Brain Research* **911**, 105–115 (2001).

291. Ujszászi, J. & Halász, P. Late component variants of single auditory evoked responses during NREM sleep stage 2 in man. *Electroencephalogr Clin Neurophysiol* **64**, 260–268 (1986).

292. Amzica, F. & Steriade, M. Cellular substrates and laminar profile of sleep K-complex. *Neuroscience* **82**, 671–686 (1998).

293. Amzica, F. & Steriade, M. The functional significance of K-complexes. *Sleep Med Rev* **6**, 139–149 (2002).

294. Bastien, C. & Campbell, K. The evoked K-complex: all-or-none phenomenon? *Sleep* **15**, 236–245 (1992).

295. Cornwall, J., Cooper, J. D. & Phillipson, O. T. Afferent and efferent connections of the laterodorsal tegmental nucleus in the rat. *Brain Res. Bull.* **25**, 271–284 (1990).

296. Schofield, B. R. Projections from auditory cortex to midbrain cholinergic neurons that project to the inferior colliculus. *Neuroscience* **166**, 231–240 (2010).

297. Schoedel, A. L. A., Zimmermann, K., Handwerker, H. O. & Forster, C. The influence of simultaneous ratings on cortical BOLD effects during painful and non-painful stimulation. *Pain* **135**, 131–141 (2008).

298. Stamatakis, E. A., Adapa, R. M., Absalom, A. R. & Menon, D. K. Changes in resting neural connectivity during propofol sedation. *PLoS ONE* **5**, e14224 (2010).

299. Schrouff, J., Perlbarg, V., Boly, M., Marrelec, G., Boveroux, P., Vanhaudenhuyse, A., Bruno, M.-A., Laureys, S., Phillips, C., Pélégrini-Issac, M., Maquet, P. & Benali, H. Brain functional integration decreases during propofol-induced loss of consciousness. *Neuroimage* **57**, 198–205 (2011).

300. Purdon, P. L., Pierce, E. T., Bonmassar, G., Walsh, J., Harrell, P. G., Kwo, J., Deschler, D., Barlow, M., Merhar, R. C., Lamus, C., Mullaly, C. M., Sullivan, M., Maginnis, S., Skoniecki, D., Higgins, H.-A. & Brown, E. N. Simultaneous electroencephalography and functional magnetic resonance imaging of general anesthesia. *Ann N Y Acad Sci* **1157**, 61–70 (2009).

301. Mitchell, J. Recommendations for standards of monitoring during anaesthesia and recovery. *Anaesthesia* **56**, 488–488 (2001).

302. Mayrovitz, H. N., Sims, N. & Dribin, L. Heel skin hyperaemia: direct compression versus vascular occlusion. *Clin Physiol Funct Imaging* **23**, 354–359 (2003).

303. Glover, G. H., Li, T. Q. & Ress, D. Image-based method for retrospective correction of physiological motion effects in fMRI: RETROICOR. *Magn Reson Med* **44**, 162–167 (2000).

304. Cheng, H. & Li, Y. Respiratory noise correction using phase information. *Magn Reson Imaging* **28**, 574–582 (2010).

305. Melzack, R. From the gate to the neuromatrix. *Pain* **Suppl 6**, S121–6 (1999).

306. Lauter, J. L., Herscovitch, P., Formby, C. & Raichle, M. E. Tonotopic organization in human auditory cortex revealed by positron emission tomography. *HEARING RESEARCH* **20**, 199–205 (1985).

307. Brooks, J. C. W., Zambreanu, L., Godinez, A., Craig, A. D. B. & Tracey, I. *Somatotopic organisation of the human insula to painful heat studied with high resolution functional imaging*. *Neuroimage* **27**, 201–209 (2005).

308. Frot, M., Garcia-Larrea, L., Guénot, M. & Mauguiere, F. Responses of the supra-sylvian (SII) cortex in humans to painful and innocuous stimuli. A study using intra-cerebral recordings. *Pain* **94**, 65–73 (2001).

309. Frot, M., Magnin, M., Mauguiere, F. & Garcia-Larrea, L. Human SII and Posterior Insula Differently Encode Thermal Laser Stimuli. *Cereb Cortex* **17**, 610–620 (2006).

310. Greenspan, J. D., Lee, R. R. & Lenz, F. A. Pain sensitivity alterations as a function of lesion location in the parasylvian cortex. *Pain* **81**, 273–282 (1999).

311. Chen, T. L., Babiloni, C., Ferretti, A., Perrucci, M. G., Romani, G. L., Rossini, P. M., Tartaro, A. & Del Gratta, C. Human secondary somatosensory cortex is involved in the processing of somatosensory rare stimuli: an fMRI study. *Neuroimage* **40**, 1765–1771 (2008).

312. Wertheimer, M. *Studies in the theory of Gestalt Psychology*. (Psychol. Forsch.: 1923).

313. Huberle, E. & Karnath, H.-O. The role of temporo-parietal junction (TPJ) in global Gestalt perception. *Brain Struct Funct* (2011).doi:10.1007/s00429-011-0369-y

314. Karnath, H.-O., Himmelbach, M. & Küker, W. The cortical substrate of visual extinction. *Neuroreport* **14**, 437–442 (2003).

315. Meister, I. G., Wienemann, M., Buelte, D., Grünewald, C., Sparing, R., Dambeck, N. & Boroojerdi, B. Hemiextinction induced by transcranial magnetic stimulation over the right temporo-parietal junction. *Neuroscience* **142**, 119–123 (2006).

316. Davis, B., Christie, J. & Rorden, C. Temporal order judgments activate temporal parietal junction. *J Neurosci* **29**, 3182–3188 (2009).

317. Spierer, L., Bernasconi, F. & Grivel, J. The temporoparietal junction as a part of the "when" pathway. *J Neurosci* **29**, 8630–8632 (2009).

318. Malapani, C., Rakitin, B., Levy, R., Meck, W. H., Deweer, B., Dubois, B. & Gibbon, J. Coupled temporal memories in Parkinson's disease: a dopamine-related dysfunction. *Journal of Cognitive Neuroscience* **10**, 316–331 (1998).

319. Buhusi, C. V. & Meck, W. H. What makes us tick? Functional and neural mechanisms of interval timing. *Nat. Rev. Neurosci.* **6**, 755–765 (2005).

320. Mhuircheartaigh, R. N., Rosenorn-Lanng, D., Wise, R., Jbabdi, S., Rogers, R. & Tracey, I. Cortical and subcortical connectivity changes during decreasing levels of consciousness in humans: a functional magnetic resonance imaging study using propofol. *J Neurosci* **30**, 9095–9102 (2010).

321. Joseph T Daley, M. B. K. Time in General Anesthesia: Depriving the Homeostat? *Sleep* **33**, 1583–1584 (2010).

322. Veselis, R. A., Pryor, K. O., Reinsel, R. A., Mehta, M., Pan, H. & Johnson, R. Low-dose propofol-induced amnesia is not due to a failure of encoding: left inferior prefrontal cortex is still active. *Anesthesiology* **109**, 213–224 (2008).

323. Aho, A. J., Lyytikäinen, L.-P., Yli-Hankala, A., Kamata, K. & Jäntti, V. Explaining Entropy responses after a noxious stimulus, with or without neuromuscular blocking agents, by means of the raw electroencephalographic and electromyographic characteristics. *Br J Anaesth* **106**, 69–76 (2011).

324. Sandin, M., Thörn, S.-E., Dahlqvist, A., Wattwil, L., Axelsson, K. & Wattwil, M. Effects of pain stimulation on bispectral index, heart rate and blood pressure at different minimal alveolar concentration values of sevoflurane. *Acta Anaesthesiol Scand* **52**, 420–426 (2008).

325. Peschanski, M. & Besson, J. M. A spino-reticulo-thalamic pathway in the rat: an anatomical study with reference to pain transmission. *Neuroscience* **12**, 165–178 (1984).

326. Panousis, P., Heller, A. R., Koch, T. & Litz, R. J. Epidural ropivacaine concentrations for intraoperative analgesia during major upper abdominal surgery: a prospective, randomized, double-blinded, placebo-controlled study. *Anesth. Analg.* **108**, 1971–1976 (2009).

327. Fox, M. D., Snyder, A. Z., Vincent, J. L., Corbetta, M., Van Essen, D. C. & Raichle, M. E. The human brain is intrinsically organized into dynamic, anticorrelated functional networks. *Proc Natl Acad Sci USA* **102**, 9673–9678 (2005).

328. Cavanna, A. E. & Trimble, M. R. The precuneus: a review of its functional anatomy and behavioural correlates. *Brain* **129**, 564–583 (2006).

329. Gusnard, D. A., Raichle, M. E. & Raichle, M. E. Searching for a baseline: functional imaging and the resting human brain. *Nat. Rev. Neurosci.* **2**, 685–694 (2001).

330. Raichle, M. E., MacLeod, A. M., Snyder, A. Z., Powers, W. J., Gusnard, D. A. & Shulman, G. L. A default mode of brain function. *Proc Natl Acad Sci USA* **98**, 676–682 (2001).

331. Maquet, P. Functional neuroimaging of normal human sleep by positron emission tomography. *J Sleep Res* **9**, 207–231 (2000).

332. Alkire, M. T. & Miller, J. General anesthesia and the neural correlates of consciousness. *Prog. Brain Res.* **150**, 229–244 (2005).

333. De Volder, A. G., Michel, C., Guérit, J. M., Bol, A., Georges, B., de Barsy, T. & Laterre, C. Brain glucose metabolism in postanoxic syndrome due to cardiac arrest. *Acta Neurol Belg* **94**, 183–189 (1994).

334. Laureys, S., Owen, A. M. & Schiff, N. D. Brain function in coma, vegetative state, and related disorders. *The Lancet Neurology* **3**, 537–546 (2004).

335. Silva, S., Alacoque, X., Fourcade, O., Samii, K., Marque, P., Woods, R., Mazziotta, J., Chollet, F. & Loubinoux, I. Wakefulness and loss of awareness: brain and brainstem interaction in the vegetative state. *Neurology* **74**, 313–320 (2010).

336. Laureys, S., Lemaire, C., Maquet, P., Phillips, C. & Franck, G. Cerebral metabolism during vegetative state and after recovery to consciousness. *J. Neurol. Neurosurg. Psychiatr.* **67**, 121–122 (1999).

337. Cavanna, A. E. The precuneus and consciousness. *CNS Spectr* **12**, 545–552 (2007).

338. Xie, G., Deschamps, A., Backman, S. B., Fiset, P., Chartrand, D., Dagher, A. & Plourde, G. Critical involvement of the thalamus and precuneus during restoration of consciousness with physostigmine in humans during propofol anaesthesia: a positron emission tomography study. *Br J Anaesth* **106**, 548–557 (2011).

339. Biswal, B., Yetkin, F. Z., Haughton, V. M. & Hyde, J. S. Functional connectivity in the motor cortex of resting human brain using echo-planar MRI. *Magn Reson Med* **34**, 537–541 (1995).

340. Lowe, M. J., Mock, B. J. & Sorenson, J. A. Functional connectivity in single and multislice echoplanar imaging using resting-state fluctuations. *Neuroimage* **7**, 119–132 (1998).

341. Cordes, D., Haughton, V. M., Arfanakis, K., Wendt, G. J., Turski, P. A., Moritz, C. H., Quigley, M. A. & Meyerand, M. E. Mapping functionally related regions of brain with functional connectivity MR imaging. *AJNR Am J Neuroradiol* **21**, 1636–1644 (2000).

342. Waites, A. B., Stanislavsky, A., Abbott, D. F. & Jackson, G. D. Effect of prior cognitive state on resting state networks measured with functional connectivity. *Hum Brain Mapp* **24**, 59–68 (2005).

343. Vahdat, S., Darainy, M., Milner, T. E. & Ostry, D. J. Functionally specific changes in resting-state sensorimotor networks after motor learning. *J Neurosci* **31**, 16907–16915 (2011).

344. Greicius, M. D., Srivastava, G., Reiss, A. L. & Menon, V. Default-mode network activity distinguishes Alzheimer's disease from healthy aging: evidence from functional MRI. *Proc Natl Acad Sci USA* **101**, 4637–4642 (2004).

345. Uddin, L. Q., Mooshagian, E., Zaidel, E., Scheres, A., Margulies, D. S., Kelly, A. M. C., Shehzad, Z., Adelstein, J. S., Castellanos, F. X., Biswal, B. B. & Milham, M. P. Residual functional connectivity in the split-brain revealed with resting-state functional MRI. *Neuroreport* **19**, 703–709 (2008).

346. Pizoli, C. E., Shah, M. N., Snyder, A. Z., Shimony, J. S., Limbrick, D. D., Raichle, M. E., Schlaggar, B. L. & Smyth, M. D. Resting-state activity in development and maintenance of normal brain function. *Proc Natl Acad Sci USA* **108**, 11638–11643 (2011).

347. Binder, J. R., Frost, J. A., Hammeke, T. A., Bellgowan, P. S., Rao, S. M. & Cox, R. W. Conceptual processing during the conscious resting state. A functional MRI study. *Journal of Cognitive Neuroscience* **11**, 80–95 (1999).

348. Mazoyer, B., Zago, L., Mellet, E., Bricogne, S., Etard, O., Houdé, O., Crivello, F., Joliot, M., Petit, L. & Tzourio-Mazoyer, N. Cortical networks for working memory and executive functions sustain the conscious resting state in man. *Brain Res. Bull.* **54**, 287–298 (2001).

349. De Luca, M., Beckmann, C. F., De Stefano, N., Matthews, P. M. & Smith, S. M. fMRI resting state networks define distinct modes of long-distance interactions in the human brain. *Neuroimage* **29**, 1359–1367 (2006).

350. Fransson, P. Spontaneous low-frequency BOLD signal fluctuations: an fMRI investigation of the resting-state default mode of brain function hypothesis. *Hum Brain Mapp* **26**, 15–29 (2005).

351. Fransson, P., Skiöld, B., Horsch, S., Nordell, A., Blennow, M., Lagercrantz, H. & Aden, U. Resting-state networks in the infant brain. *Proc Natl Acad Sci USA* **104**, 15531–15536 (2007).

352. Fransson, P., Skiöld, B., Engström, M., Hallberg, B., Mosskin, M., Aden, U., Lagercrantz, H. & Blennow, M. Spontaneous brain activity in the newborn brain during natural sleep--an fMRI study in infants born at full term. *Pediatr. Res.* **66**, 301–305 (2009).

353. Doria, V., Beckmann, C. F., Arichi, T., Merchant, N., Groppo, M., Turkheimer, F. E., Counsell, S. J., Murgasova, M., Aljabar, P., Nunes, R. G., Larkman, D. J., Rees, G. & Edwards, A. D. Emergence of resting state networks in the preterm human brain. *Proc Natl Acad Sci USA* **107**, 20015–20020 (2010).

354. Smyser, C. D., Inder, T. E., Shimony, J. S., Hill, J. E., Degnan, A. J., Snyder, A. Z. & Neil, J. J. Longitudinal analysis of neural network development in preterm infants. *Cereb Cortex* **20**, 2852–2862 (2010).

355. Schöpf, V., Kasprian, G., Brugger, P. C. & Prayer, D. Watching the fetal brain at 'rest'. *Int. J. Dev. Neurosci.* **30**, 11–17 (2012).

356. Thomason, M. E., Dennis, E. L., Joshi, A. A., Joshi, S. H., Dinov, I. D., Chang, C., Henry, M. L., Johnson, R. F., Thompson, P. M., Toga, A. W., Glover, G. H., Van Horn, J. D. & Gotlib, I. H. Resting-state fMRI can reliably map neural networks in children. *Neuroimage* **55**, 165–175 (2011).

357. Rombouts, S. A. R. B., Barkhof, F., Goekoop, R., Stam, C. J. & Scheltens, P. Altered resting state networks in mild cognitive impairment and mild Alzheimer's disease: an fMRI study. *Hum Brain Mapp* **26**, 231–239 (2005).

358. Sorg, C., Riedl, V., Mühlau, M., Calhoun, V. D., Eichele, T., Läer, L., Drzezga, A., Förstl, H., Kurz, A., Zimmer, C. & Wohlschläger, A. M. Selective changes of resting-state networks in individuals at risk for Alzheimer's disease. *Proc Natl Acad Sci USA* **104**, 18760–18765 (2007).

359. Bluhm, R. L., Miller, J., Lanius, R. A., Osuch, E. A., Boksman, K., Neufeld, R. W. J., Théberge, J., Schaefer, B. & Williamson, P. Spontaneous low-frequency fluctuations in the BOLD signal in schizophrenic patients: anomalies in the default network. *Schizophr Bull* **33**, 1004–1012 (2007).

360. Sharp, D. J., Beckmann, C. F., Greenwood, R., Kinnunen, K. M., Bonnelle, V., De Boissezon, X., Powell, J. H., Counsell, S. J., Patel, M. C. & Leech, R. Default mode network functional and structural connectivity after traumatic brain injury. *Brain* **134**, 2233–2247 (2011).

361. Hillary, F. G., Slocomb, J., Hills, E. C., Fitzpatrick, N. M., Medaglia, J. D., Wang, J., Good, D. C. & Wylie, G. R. Changes in resting connectivity during recovery from severe traumatic brain injury. *Int J Psychophysiol* **82**, 115–123 (2011).

362. Boly, M., Tshibanda, L., Vanhaudenhuyse, A., Noirhomme, Q., Schnakers, C., Ledoux, D., Boveroux, P., Garweg, C., Lambermont, B., Phillips, C., Luxen, A., Moonen, G., Bassetti, C., Maquet, P. & Laureys, S.

Functional connectivity in the default network during resting state is preserved in a vegetative but not in a brain dead patient. *Hum Brain Mapp* **30**, 2393–2400 (2009).

363. Pawela, C. P., Biswal, B. B., Cho, Y. R., Kao, D. S., Li, R., Jones, S. R., Schulte, M. L., Matloub, H. S., Hudetz, A. G. & Hyde, J. S. Resting-state functional connectivity of the rat brain. *Magn Reson Med* **59**, 1021–1029 (2008).

364. Becerra, L., Pendse, G., Chang, P.-C., Bishop, J. & Borsook, D. Robust reproducible resting state networks in the awake rodent brain. *PLoS ONE* **6**, e25701 (2011).

365. Hutchison, R. M., Leung, L. S., Mirsattari, S. M., Gati, J. S., Menon, R. S. & Everling, S. Resting-state networks in the macaque at 7 T. *Neuroimage* **56**, 1546–1555 (2011).

366. Vincent, J. L., Patel, G. H., Fox, M. D., Snyder, A. Z., Baker, J. T., Van Essen, D. C., Zempel, J. M., Snyder, L. H., Corbetta, M. & Raichle, M. E. Intrinsic functional architecture in the anaesthetized monkey brain. *Nature* **447**, 83–86 (2007).

367. Greene, J. D., Sommerville, R. B., Nystrom, L. E., Darley, J. M. & Cohen, J. D. An fMRI investigation of emotional engagement in moral judgment. *Science* **293**, 2105–2108 (2001).

368. Liang, Z., King, J. & Zhang, N. Anticorrelated resting-state functional connectivity in awake rat brain. *Neuroimage* **59**, 1190–1199 (2012).

369. Peltier, S. J., Kerssens, C., Hamann, S. B., Sebel, P. S., Byas-Smith, M. & Hu, X. Functional connectivity changes with concentration of sevoflurane anesthesia. *Neuroreport* **16**, 285–288 (2005).

370. Martuzzi, R., Ramani, R., Qiu, M., Rajeevan, N. & Constable, R. T. Functional connectivity and alterations in baseline brain state in humans. *Neuroimage* **49**, 823–834 (2010).

371. Deshpande, G., Kerssens, C., Sebel, P. S. & Hu, X. Altered local coherence in the default mode network due to sevoflurane anesthesia. *Brain Research* **1318**, 110–121 (2010).

372. Horovitz, S. G., Braun, A. R., Carr, W. S., Picchioni, D., Balkin, T. J., Fukunaga, M. & Duyn, J. H. Decoupling of the brain's default mode network during deep sleep. *Proc Natl Acad Sci USA* **106**, 11376–11381 (2009).

373. Horovitz, S. G., Fukunaga, M., de Zwart, J. A., van Gelderen, P., Fulton, S. C., Balkin, T. J. & Duyn, J. H. Low frequency BOLD fluctuations during resting wakefulness and light sleep: a simultaneous EEG-fMRI study. *Hum Brain Mapp* **29**, 671–682 (2008).

374. Cole, D. M., Smith, S. M. & Beckmann, C. F. Advances and pitfalls in the analysis and interpretation of resting-state FMRI data. *Front Syst Neurosci* **4**, 8 (2010).

375. Nelson, A. B., Faraguna, U., Tononi, G. & Cirelli, C. Effects of anesthesia on the response to sleep deprivation. *Sleep* **33**, 1659–1667 (2010).

376. Pal, D., Lipinski, W. J., Walker, A. J., Turner, A. M. & Mashour, G. A. State-specific effects of sevoflurane anesthesia on sleep homeostasis: selective recovery of slow wave but not rapid eye movement sleep. *Anesthesiology* **114**, 302–310 (2011).

377. Van der Werf, Y. D., Altena, E., Schoonheim, M. M., Sanz-Arigita, E. J., Vis, J. C., De Rijke, W. & Van Someren, E. J. W. Sleep benefits subsequent hippocampal functioning. *Nat Neurosci* **12**, 122–123 (2009).

378. Van Someren, E. J. W., Van Der Werf, Y. D., Roelfsema, P. R., Mansvelder, H. D. & da Silva, F. H. L. Slow brain oscillations of sleep, resting state, and vigilance. *Prog. Brain Res.* **193**, 3–15 (2011).

379. Matell, M. S. & Meck, W. H. Cortico-striatal circuits and interval timing: coincidence detection of oscillatory processes. *Brain Res Cogn Brain Res* **21**, 139–170 (2004).

380. Harrington, D. L., Castillo, G. N., Greenberg, P. A., Song, D. D., Lessig, S., Lee, R. R. & Rao, S. M. Neurobehavioral mechanisms of temporal processing deficits in Parkinson's disease. *PLoS ONE* **6**, e17461 (2011).

381. Finelli, L. A., Baumann, H., Borbély, A. A. & Achermann, P. Dual electroencephalogram markers of human sleep homeostasis: correlation between theta activity in waking and slow-wave activity in sleep. *Neuroscience* **101**, 523–529 (2000).

382. Tobler, I. & Borbély, A. A. Sleep EEG in the rat as a function of prior waking. *Electroencephalogr Clin Neurophysiol* **64**, 74–76 (1986).

383. Werth, E., Dijk, D. J., Achermann, P. & Borbély, A. A. Dynamics of the sleep EEG after an early evening nap: experimental data and simulations. *Am. J. Physiol.* **271**, R501–10 (1996).

384. Huber, R., Esser, S. K., Ferrarelli, F., Massimini, M., Peterson, M. J. & Tononi, G. TMS-induced cortical potentiation during wakefulness locally increases slow wave activity during sleep. *PLoS ONE* **2**, e276 (2007).

385. Hanlon, E. C., Faraguna, U., Vyazovskiy, V. V., Tononi, G. & Cirelli, C. Effects of skilled training on sleep slow wave activity and cortical gene expression in the rat. *Sleep* **32**, 719–729 (2009).

386. Huber, R., Ghilardi, M. F., Massimini, M., Ferrarelli, F., Riedner, B. A., Peterson, M. J. & Tononi, G. Arm immobilization causes cortical plastic changes and locally decreases sleep slow wave activity. *Nat Neurosci* **9**, 1169–1176 (2006).

387. Tononi, G. & Cirelli, C. Sleep function and synaptic homeostasis. *Sleep Med Rev* **10**, 49–62 (2006).

388. Vyazovskiy, V. V., Olcese, U., Hanlon, E. C., Nir, Y., Cirelli, C. & Tononi, G. Local sleep in awake rats. *Nature* **472**, 443–447 (2011).